universität wien

Dissertation

Titel der Dissertation

”Heavy metal attack”

Stress response analyses of *Saccharomyces cerevisiae*

Verfasserin

Mag[a]. rer. nat. Dagmar Hosiner

Angestrebter akademischer Grad

Doktorin der Naturwissenschaften (Dr. rer. nat.)

Wien, 2012

Studienkennzahl:	A 091 441
Dissertationsgebiet:	Dr.-Studium der Naturwissenschaften (Genetik – Mikrobiologie)
Betreuer:	P.Doz. Dr. Christoph Schüller

„Das Ganze ist mehr als die Summe seiner Teile.“

Aristoteles

Table of Contents

1. INTRODUCTION

Metals such as calcium, magnesium, and iron, besides others, are an integral part of all living organisms and thus indispensable for life. In small quantities they serve as essential micronutrients from prokaryotes to humans and are even used as therapeutic agents to treat diseases like dermatitis or cancer (Ertekin *et al.*, 2004; Wu *et al.*, 2011). Even though biologically relevant metals play important roles in the cell´s metabolism, they become toxic at higher concentrations. Metals with no biological role, like cadmium or mercury, may already lead to severe cell damage at very low doses. Metal contaminations accumulate in the environment such as in the food chain, potable water, soil, or air and are well established today to threaten human health (Nash, 2005).

Over the last century metal homeostasis has been intensively explored, but little is yet known about the impact of metals on detoxification pathways and their fundamental regulatory mechanisms. The aim of this study was to identify cellular metal stress targets as well as common transcriptional regulatory networks, and to explore detoxification strategies that take part in the cellular response to early metal stress. For this purpose mRNA profiles were used to examine the genome-wide transcriptional response of the baker´s yeast, *Saccharomyces cerevisiae*, to metal exposure. For microarray analyses we selected a total of 10 metal cations: the transition metals silver (Ag^{2+}), cadmium (Cd^{2+}), cobalt (Co^{2+}), mercury (Hg^{2+}), manganese (Mn^{2+}), nickel (Ni^{2+}), vanadium (V^{3+}), and zinc (Zn^{2+}), the metalloid arsenic (As^{3+}), and the post-transition metal aluminium (Al^{3+}). These were chosen because of a link to human metal exposure pathologies (chapter 1.7.3 Table 1).

The following chapters provide an overview of the definition and the biological relevance of metals. These include the cellular uptake mechanisms of metals, their toxic potential on cell homeostasis, as well as detoxification mechanisms in response to metal impact.

In the following text the term “metal” is used in a comprehensive way and refers to transition metals, metalloids or post-transition metals.

1.1 Definition of metals and their biological relevance

The sun and the milky way galaxy are composed of roughly 74% hydrogen, 24% helium, and 2% "metals", which were primarily produced by nucleosynthesis in stars or supernovae (Sparke and Gallagher, 2000). Nucleosynthesis is the process of creating new atomic nuclei from pre-existing nucleons (protons and neutrons). Generally, metals are defined as chemical elements that are characterized by high electrical and heat conductivity, as well as high chemical reactivity. For instance, they can replace the hydrogens of acids to form a number of crystalline metal salts. In organisms metals are part and parcel of various complex compounds that play structurally and functionally important roles in biochemical and physiological cell reactions, e.g. nucleic acid and protein synthesis, enzymatic reactions, oxidative phosphorylation, antioxidative activities, etc. (Nies, 1999; Fraga, 2005; Kaluarachchi *et al.*, 2010).

The primary determinant of an element's chemical properties is its electron configuration, which describes the arrangement of electrons in the shells and the subshells of an atom. An electron shell is termed as an orbit followed by electrons around an atomic nucleus. Each shell is filled with a fixed number of electrons from innermost to outermost. The electrons of the valence shell ultimately affect how the atom reacts chemically with other atoms (Figure 1).

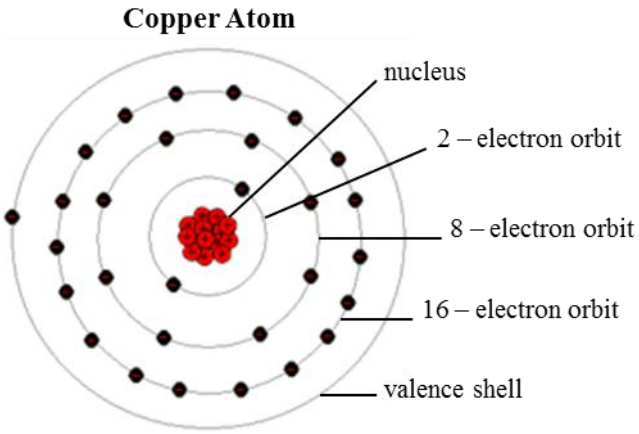

Figure 1: Electron configuration of a copper atom.

For main group elements, which comprise group 1, 2, and 13 to 18 of the periodic table (Figure 2), only the outermost electrons are valence electrons. In transition metals, covering group 3 to 12 of the periodic table, some inner-shell electrons are also valence electrons.

Atoms with a complete shell of valence electrons tend to be chemically inert, which means that they are chemically not reactive. Most of the biologically relevant metals are transition elements. In common oxidation states they exhibit an incompletely filled inner electron shell that enables them to form ionic bonds with non-metals. The three elements of group 12, zinc, cadmium, and mercury are exceptions as these elements have a filled d-subshell.

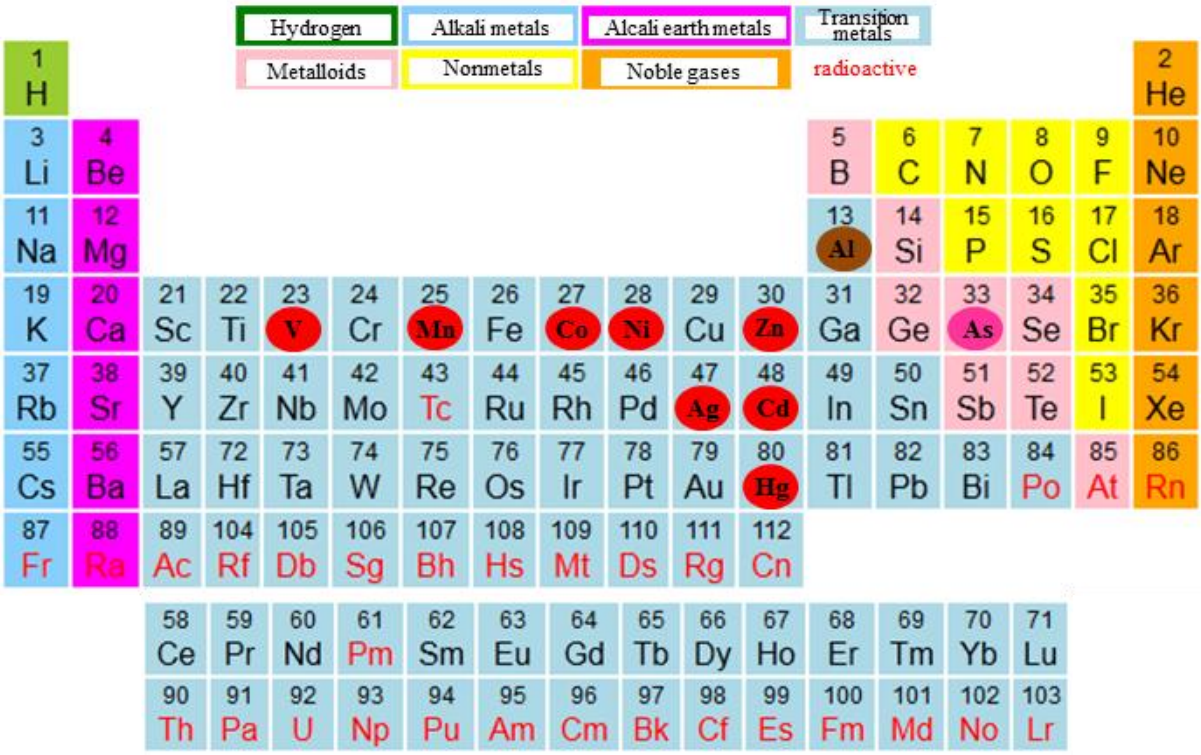

Figure 2: The periodic table of the chemical elements. Metals used in this study are highlighted in red (transition metals), pink (metalloid), and brown (post-transition metal of the boron group).

Biologically relevant metals (in humans) are also called trace elements and include arsenic, calcium, chromium, cobalt, copper, iron, magnesium, manganese, molybdenum, potassium, selenium, sodium, and zinc. For other organisms aluminium, cadmium, nickel, silicon, tin, and vanadium, may also be vital. Hence, in different uni- and multicellular organisms different metals are essential in very small quantities. Because micronutrients are metabolically consumed in living cells, all organisms replenish them by the uptake from environment.

1.2 Cellular uptake of metals

Organisms have evolved various mechanisms for the uptake of nutrients across the plasma membrane (Figure 3). In general, metal uptake occurs through the combined action of active and passive transport. Adenosine-triphosphate (ATP) driven metal transporters are only induced by the cell in times of need. On the other hand, constitutively expressed low affinity membrane channels utilize electrochemical gradients as driving force and passively transport metals and other substances. Besides vital metal ions, metals with no biological role also enter the cell on the basis of molecular mimicry or by several unspecific uptake systems.

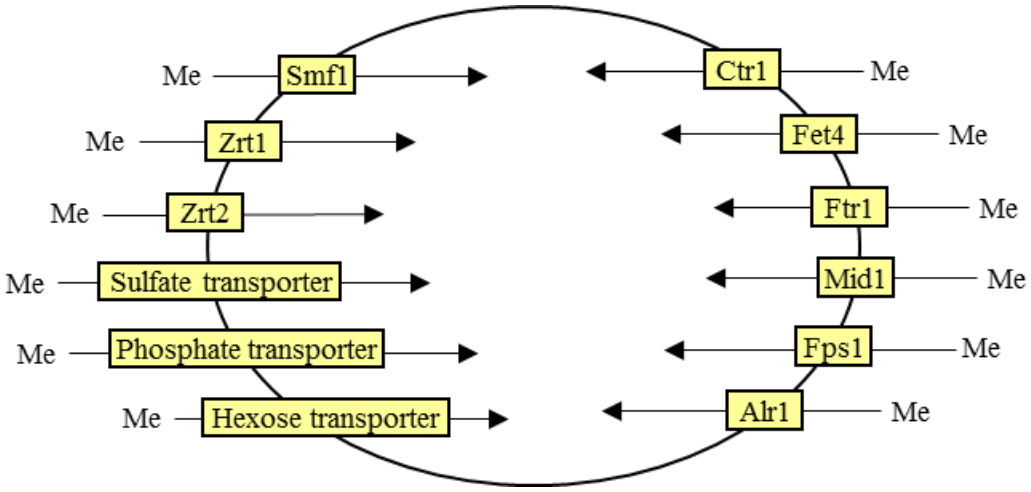

Figure 3: Yeast plasma membrane systems mediating metal uptake. See text for detailed explanation concerning transport proteins and metals. Me – metal;

With the aid of molecular and genetic techniques a number of gene families involved in metal transport processes through the plasma membrane have been identified (Paulsen *et al.*, 1998; Nelson, 1999). These primarily include the eukaryotic SLC31 or Ctr family of Cu^{2+} transporters (Petris, 2004) such as the yeast Ctr1 (Dancis *et al.*, 1994), and the ZIP (ZRT- and IRT-like protein) family involving the yeast Zn^{2+} transporters Zrt1 and Zrt2, or IRT1 in plants (Zhao *et al.*, 1998; Korshunova *et al.*, 1999). Further examples are the NRAMP (natural resistance-associated macrophage protein) metal transporters such as the yeast Mn^{2+} transporter Smf1 (Supek *et al.*, 1996) and the DMT1 (divalent metal ion transporter 1) transporters that are highly conserved from bacteria to humans (Au *et al.*, 2008). NRAMP and DMT1 transporters make up the SLC11 gene family that is energized by the H^{+}-electrochemical gradient (Mackenzie and Hediger, 2004).

The mammalian DMT1 for instance primarily internalizes iron, but also mediates the transport of various toxic metals (Gunshin *et al.*, 1997; Conrad *et al.,* 1999). Yeast cells especially import iron via the low-affinity Fet4 transporter (Dix *et al.*, 1994) and the high-affinity Ftr1 permease (Stearman *et al.*, 1996). In unicellular organisms one major uptake route for metals such as Co^{2+}, Mn^{2+}, Ni^{2+}, and Zn^{2+} arises via the constitutively expressed CorA-Mrs2-Alr1 superfamily of Mg^{2+} transporters including the bacterial CorA and the yeast Alr1 Mg^{2+} transporter (Smith and Maguire, 1995; Graschopf *et al.,* 2001). In addition, the yeast Mid1 forms a channel, which internalizes Ca^{2+} (Iida *et al.*, 1994).

From bacteria to humans metal ions like As^{3+}, Cd^{2+}, Co^{2+}, Mn^{2+}, V^{3+}, and Zn^{2+} also enter cells through highly conserved unspecific phosphate transporters involving the yeast Pho84, Pho86, Pho87, or Pho88 proteins (Mahanty *et al.*, 1991; Bun-ya *et al.*, 1996; Yompakdee *et al.*, 1996; Lau *et al.*, 2000; Jensen *et al.*, 2003) or aquaglyceroporins like the bacterial GlpF, Fps1 in yeast or the human AQP7 and AQP9 (Wysocki *et al.*, 2001; Liu *et al.*, 2002; Meng *et al.*, 2004; Bhattacharjee *et al.,* 2004; Rosen and Tamas, 2010). Moreover, metal uptake was demonstrated for bacterial and fungal sulfate transporters and yeast hexose permeases (Smith *et al.*, 1995; Aguilar-Barajas *et al.*, 2001; Liu *et al.*, 2004). Mutations of these plasma membrane transport systems impair metal uptake into the cell and therefore lead to increased metal tolerance.

1.3 How metals exert their toxic potential on cellular homeostasis

Once nutrients as well as trace metals have entered the cell across the plasma membrane they are transported to their final intracellular destination. The biological activity of metals is related to their strictly regulated physicochemical interaction with metabolic receptors, whereas nonessential metals generally lack the homeostasis control (Ballatori, 2002). Most metals, also including the toxic ones, tend to link to binding sites of proteins like phosphates, porphyrins, pteridines, purines, and cysteinyl as well as histidyl side chains (Hartwig, 2001; Thilakaraj *et al.*, 2007). Unlike toxic organic compounds metals cannot be degraded or modified. They form unspecific complex compounds which accordingly interfere with the cellular metabolic pathways and lead to various toxic effects outlined as follows:

Nonessential metals may compete for binding sites for essential metals, thereby disrupting the normal biochemical functions of proteins. Hg^{2+}, for instance, was shown to replace Se^{+4} in the

Se-dependent glutathione peroxidase (Se-GPx) in human haemocytes which was compensated by increased selenium substitution (Chatziargyriou and Dailianis, 2010). Cd^{2+} and Co^{2+} are suggested to displace the zinc ion in zinc finger transcription factors, which creates severe regulatory disorders (Hartwig, 2001). Toxic metal ions may also compete with essential metals for shared uptake systems as shown for Cd^{2+}, which inhibits the uptake of Ca^{2+} in crabs and conversely Ca^{2+} preventing Cd^{2+} uptake in bivalves (Rainbow and Black, 2005; Qiu *et al.,* 2005). Furthermore, excess Mg^{2+} was demonstrated to compete with Al^{3+}, Cd^{2+}, and Ni^{2+} in yeast (MacDiarmid and Gardner, 1998; Kern *et al.,* 2005; Sarikaya *et al.,* 2006).

One of the main negative characteristics with metals like As^{3+}, Cd^{2+}, or Hg^{2+} is their high affinity to thiol (-SH) groups which play a decisive role in the function of several cellular components including enzymes, transcription factors and membrane proteins (Chrestensen *et al.,* 2000; Khanna *et al.,* 2011; Hassinen *et al.,* 2011). Thus, these metal ions bound to the ubiquitous antioxidant glutathione and other proteins are supposed to indirectly cause oxidative stress by depletion of glutathione or altering enzyme activities (Stohs and Bagchi, 1995; Chrestensen *et al.,* 2000; Ercal *et al.,* 2001; Westwater *et al.,* 2002; Shekar *et al.,* 2006; Han *et al.,* 2008).

Redox active metals such as Co^{2+}, Cu^{2+}, and Fe^{2+} may also directly cause oxidative stress by generating reactive oxygen species (ROS) in Fenton-like reactions (Halliwell and Gutteridge, 1984; Leonard *et al.,* 1998 and 2004; Jomova and Valko, 2011; Figure 4). ROS include peroxides (e.g. hydrogen peroxide H_2O_2) and free radicals (e.g. superoxide $.O_2^-$ and hydroxyl OH^- radicals) with unpaired electrons making them extremely reactive. ROS production is mainly associated with mitochondria, microsomes and peroxisomes under standard conditions (Milczarek *et al.,* 2007; Soares *et al.,* 2008; Yu *et al.,* 2009; Piao *et al.,* 2011). Arsenic species may cause the release of iron from ferritin and thereby indirectly lead to the generation of iron-dependent ROS (Ahmad *et al.,* 2000).

$$Fe^{2+} + H_2O_2 \longrightarrow Fe^{3+} + .OH - OH^-$$

$$Fe^{3+} + H_2O_2 \longrightarrow Fe^{2+} + .OOH + H^+$$

Figure 4: Fenton reaction. In 1894 H.J.H Fenton discovered that several metal ions obtain a strong catalytic power to generate highly reactive hydroxyl radicals: Ferrous iron(II) is oxidized by hydrogen peroxide to ferric iron(III), a hydroxyl radical, and a hydroxyl anion. Thereafter Fe^{3+} is reduced back to Fe^{2+}, a peroxide radical, and a proton by the same hydrogen peroxide.

Another cause of metal toxicity is based on the molecular mimicry of endogenous molecules (Ballatori, 2002). Oxyanions like arsenate and vanadate resemble phosphate and have the property to partly substitute in phosphoryl transfer reactions causing alterations in protein phosphorylation (Kanik-Ennulat and Neff, 1990; Valko *et al.*, 2005). Similarly, chromate, selenate, and molybdate can interfere with the metabolism of sulphate (Aguilar-Barajas *et al.*, 2011). As a consequence, reduction of the damaging metal oxyanions via NADPH-dependent electron transfer results in the production of ROS (Lynn *et al.*, 2000; Flora, 2011).

Taken together, the determinative mechanisms of metal toxicity are primarily based on the alteration of protein and enzyme function along with the generation and accumulation of intracellular ROSs that lead to oxidative stress and cause diverse mutagenic and carcinogenic effects (Chen and Shi, 2002; Dizdaroglu *et al.*, 2002; Valko *et al.*, 2006; Beyersmann and Hartwig, 2008).

1.4 Detoxification mechanisms in response to metal stress

Organisms maintain metal homeostasis through tightly regulated processes of metal sensing, uptake across the plasma membrane, distribution to the appropriate subcellular compartments, as well as detoxification of excess metals. To prevent the damaging effects of toxic metals, the intracellular balance between essential and toxic levels of metals has to be maintained. For this purpose cells have to respond rapidly with the induction of cellular defense programs on transcriptional level, thereby adapting to the hazard potential of the metals (Mager and De Krujiff, 1995; Gash *et al.*, 2000). The overall detoxification principles of metals involve metal chelation via glutathiones, metallothioneins, or phytochelatins followed by sequestration and storage in cellular compartments. Further detoxification mechanisms comprise reduction and active extrusion of toxic metals, restriction of metal uptake, degradation of damaged protein complexes, and the participation of low molecular weight organic molecules in cellular metal defense processes. The main metal defense strategies are illustrated in Figure 5.

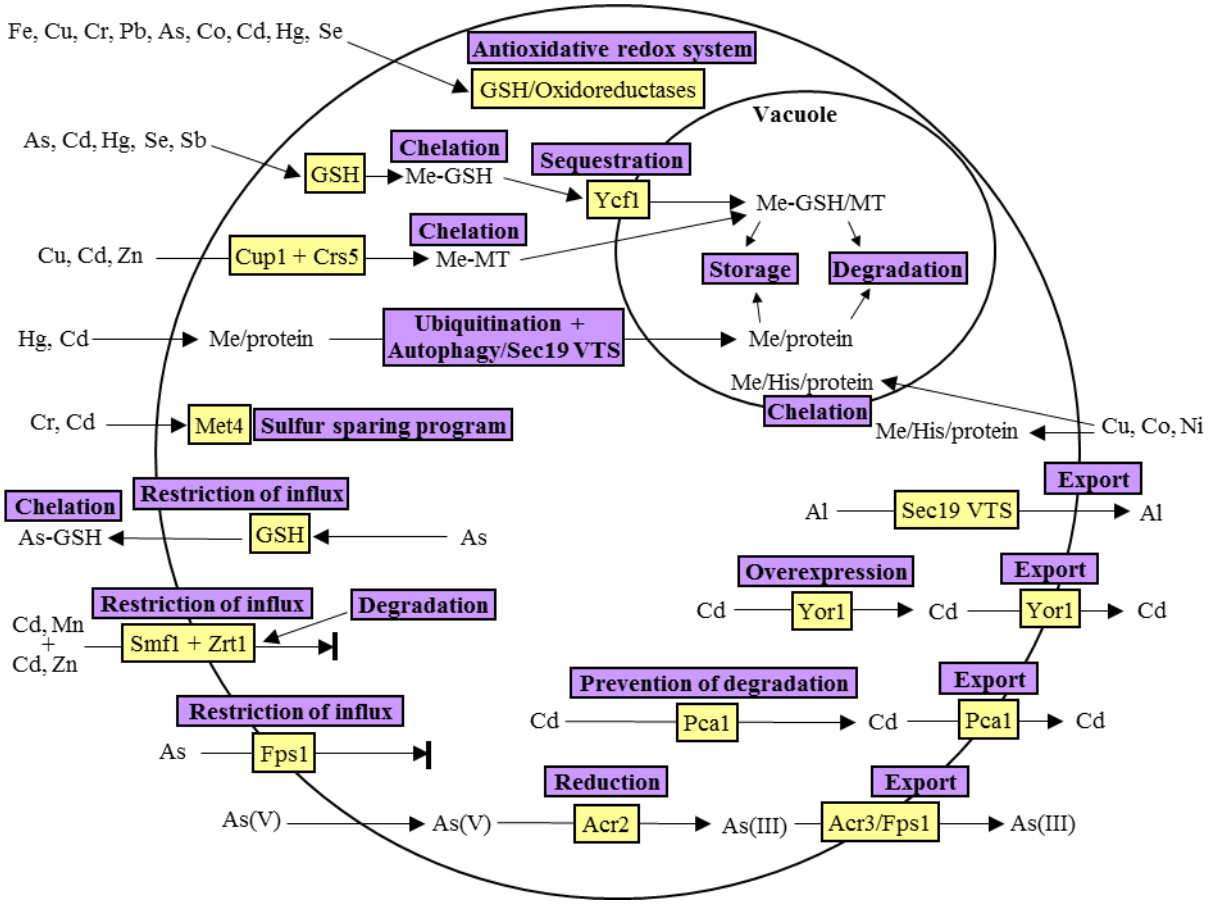

Figure 5: Metal detoxification strategies in *S. cerevisiae*. In response to metal stress a number of defense pathways are activated in yeast cells. See text for detailed explanation of the particular metal detoxification mechanisms. Me – metal, GSH – glutathione, MT – metallothionein;

1.4.1 Chelation and sequestration of nonessential metals

Eukaryotic cells mainly dispose of toxic metals by chelation with glutathiones (Momose and Iwahashi, 2001; Klein *et al.*, 2002; Haugen *et al.*, 2004; Pocsi *et al.*, 2004; Preveral *et al.*, 2009; Khan *et al.*, 2011; Jan *et al.*, 2011), phytochelatins (Zenk, 1996; Hall, 2002; Cobbett and Goldsbrough, 2002; Vatamaniuk *et al.*, 2005; Sookska-Nguan *et al.*, 2009; Tennstedt *et al.*, 2009), and metallothioneins (Ecker *et al.*, 1986; Culotta *et al.*, 1994; Jensen *et al.*, 1996; Tohoyama *et al.*, 2001; Weinlich *et al.*, 2006; Ramesh *et al.*, 2009). This means, they take advantage of the preference of metals for thiol-groups, which are an essential part of all three metal chelate binder. The chelates are subsequently sequestrated into vacuoles or lysosomes, where the metals get stored and the proteins immediately degraded by resident hydrolases and other enzymes.

The *S. cerevisiae* genome only encodes metallothioneins and glutathione but no phytochelatins. Cup1 and Crs5, the two types of yeast metallothioneins, are known to be involved in the chelation of copper, cadmium, and zinc (Wine *et al.*, 1985; Gross *et al.*, 2000; Pagani *et al.*, 2007a). The yeast sulfur/glutathione (GSH) pathway serves several cellular functions such as extra- and intracellular chelation of toxic metals, chelation of proteins (protein glutathionylation) to protect them from metal- and oxidative damage, and direct protection against metal-induced oxidation (Grant, 2001; Wysocki and Tamas, 2010).

Sequestration of metal-glutathione conjugates primarily occurs via the vacuolar ABC transporter of the multidrug resistance-associated protein subfamily (MRP) yeast cadmium factor 1 Ycf1 (Szczypka *et al.*, 1994; Li *et al.*, 1996 and 1997; Ghosh *et al.*, 1999; Gueldry *et al.*, 2003; Preveral *et al.*, 2006; Mielniczki-Pereira *et al.*, 2008; Lazard *et al.*, 2011). But it becomes the rate-limiting step of metal tolerance when an intracellular overdose of metals leads to the gradual depletion of glutathione (Wang and Ballatori, 1998). To avoid this bottleneck cells further adapt to an increased GSH requirement by globally modifying their proteome to reduce the production of abundant sulfur-rich proteins. This allows saving of up to 30% of overall sulfur amino acid supporting increased glutathione production (Fauchon *et al.*, 2002; Lafaye *et al.*, 2005). In humans a direct correlation persists with aging and intracellular glutathione levels: during aging, the levels of GSH drop concurrently with the ability to detoxify metals or free radicals (Fulle *et al.*, 2005; Tchaikovskaya *et al.*, 2005; Robillard *et al.*, 2011).

1.4.2 Oxidative cell defense

To maintain proteins and other cellular components in an active state for metabolism, the induction of the antioxidative system constitutes a ubiquitous defense mechanism against metal-induced oxidative stress (Vido *et al.*, 2000; Hansen *et al.*, 2006; Thorsen *et al.*, 2007 and 2009). Organisms, from bacteria to humans, exhibit complex systems of multiple types of antioxidants. Highly conserved NADPH-dependent glutaredoxins, thioredoxins, and the mitochondrial peroxiredoxins are the key oxidoreductases of the glutathione/thiol redox system by using glutathione or thioredoxin as electron donor for reduction of ROS (Greetham *et al.*, 2009 and 2010). Further important antioxidant defense enzymes constitute superoxide dismutase (SOD) and catalase. SOD especially catalyzes superoxide (O_2^-) to O_2 and H_2O_2, whereas catalase reduces hydrogen peroxide (H_2O_2) to less reactive O_2 and H_2O molecules (Grant *et al.*, 1998; Dziadkowiec *et al.*, 2007). An additional enzymatic defense relies on the

pentose phosphate pathway which produces the major amount of NADPH for the cellular redox system (Thorpe *et al.* 2004). Moreover, vitamins like vitamin C and vitamin E are also known to act as antioxidants (Padayatty *et al.*, 2003; Ayed-Boussema *et al.*, 2011). Together, all these different types of antioxidants regulate the intracellular accumulation of ROSs.

1.4.3 Reduction and active extrusion of metals

The efflux of metal cations from cells provides an efficient detoxification mechanism. In bacteria, for instance, metal expulsion is mediated through resistance-nodulation cell division (RND) driven transenvelope exporters, cation diffusion facilitators (CDF), and P-type ATPases such as the ArsB family of transporters (Rosen, 1999; Nies, 2003; Grass *et al.*, 2005; Blaha *et al.*, 2011). In eukaryotes active extrusion of metals is primarily carried out by transport systems involving MRP-type (Multidrug Resistance Proteins) ABC transporter such as the mammalian MRP1 pump (Lorico *et al.*, 2002), the zebrafish MRP5 (Long *et al.*, 2011), ABCB6 in mice and humans (Paterson *et al.*, 2007; Chavan *et al.*, 2011), and the yeast Yor1 (Nagy *et al.*, 2006). Furthermore, metals are exported by ATPases including the yeast Pca1 and the human ATP7A and ATP7B (Shiraishi *et al.*, 2000; La Fontaine and Mercer, 2007; Adle *et al.*, 2007). Generally, these transporters are regulated by transcriptional activation in times of excess metals.

A “negatively” regulated metal extrusion system in yeast constitutes the prevention of Pca1 degradation via the endoplasmic reticulum-associated degradation (ERAD) system and its subsequent accumulation in the plasma membrane under excess Cd^{2+} to overcome intracellular cadmium levels. Under normal conditions, when there is no need of Cd^{2+} efflux, this ATPase is constitutively expressed but posttranscriptionally ubiquitinated and degraded before reaching the plasma membrane (Adle *et al.*, 2008 and 2009).

Reduction of metal ions into less toxic forms and active extrusion of toxic metal complexes additionally decrease the toxicity of metals like Hg^{2+}, As^{5+}, or V^{5+} (Macara *et al.*, 1980; Walsh *et al.*, 1988; Tamas and Wysocki, 2001; Ledwidge *et al.*, 2005; Crans *et al.*, 2010). Arsenate, for instance, is reduced to arsenite by the reductase Acr2 and is then released from the cell via the plasma membrane arsenite efflux transporter Acr3 (Silver, 1996; Ghosh *et al.*, 1999; Bouganim *et al.*, 2001; Menezes *et al.*, 2004; Wysocki *et al.*, 2004). Aqueous arsenical salts, such as found in contaminated drinking water, are usually in the form of arsenate. Because only arsenite can be recognized by the cellular expulsion system, reduction of

arsenate is the first step of arsenic detoxification (Mukhopadhyay *et al.*, 2000). Efflux through Acr2/Acr3 is regulated by Yap8 (Wysocki *et al.*, 2004) and represents the primary As defense mechanism, whereas cells lacking an efflux system depend on the sulfur/GSH-mediated detoxification system (Thorsen *et al.*, 2007).

1.4.4 Restriction of metal uptake

The most efficient mechanism to prevent the toxic consequences of metals inside the cell is the restriction of metal uptake. Because of the continued transport of nutrients into the cell, a selective limitation for all toxic substances would be extremely energy-consuming. Nevertheless some interesting mechanisms have been detected like the secretion of malate or citrate in plants, which increases aluminium tolerance by chelating Al^{3+} ions to nonphytotoxic Al^{3+} complexes and prevents them from entering the cell (Sasaki *et al.*, 2004; Suzuki *et al.*, 2007; Furukawa *et al.*, 2007; Han *et al.*, 2009). Strikingly, in yeast GSH was suggested to be exported upon arsenic stress to extracellularly chelate As(III) and prevent its uptake into the cell (Wysocki and Tamas, 2010).

One further example for restriction of sustained metal uptake in yeast is the Rsp5-dependent ubiquitination of the general plasma membrane NRAMP manganese transporter Smf1. In response to elevated manganese and cadmium levels Rsp5 is recruited by the Bsd2/Tre1/Tre2 complex to provoke the vacuolar degradation of Smf1 (Eguez *et al.*, 2004; Stimpson *et al.*, 2006; Nikko *et al.*, 2008; Jensen *et al.*, 2009). Another transporter that is ubiquitinated and degraded in the face of zinc and cadmium toxicity constitutes the yeast zinc transporter Zrt1 (Gitan *et al.*, 2000 and 2003).

Recently, restriction of Fps1-dependent arsenic uptake mediated by the mitogen-activated protein kinase (MAPK) Hog1 was described as one new metal detoxification pathway (Thorsen *et al.*, 2006). *FPS1* encodes a glycerol channel and represents the main entrance route of arsenic and antimonite in *S. cerevisiae* (Wysocki *et al.*, 2001). However, Fps1 is a bidirectional arsenite channel that was also shown to mediate As^{3+}-efflux in concert with Acr3 (Maciaszczyk *et al.*, 2010). Besides Fps1, arsenic influx in yeast is additionally managed by hexose permeases (Liu *et al.*, 2004). In this regard, repression of genes encoding carbohydrate transporters upon metal stress might serve as an additional metal detoxification mechanism (Jin *et al.*, 2008).

1.4.5 Degradation of damaged protein complexes

As a result of indirect oxidative stress in response to excess metals protein degradation via the Rpn4-regulated 26S proteasome occurs in order to remove the ROS-inactivated proteins, which otherwise interfere with various cellular enzyme systems (Xie and Varshavsky, 2001; Owsianik *et al.,* 2002; Haugen *et al.,* 2004). Ubiquitin-conjugating enzymes like Cdc34 and Ubc4 play important roles in the selective ubiquitination of proteins involved in metal homeostasis, thereby accelerating degradation and conferring resistance to metals like Hg^{2+} or Cd^{2+} (Furuchi *et al.,* 2002; Hwang *et al.,* 2008).

In addition, yeast cells employ the catabolic process of autophagy to degrade damaged organelles and proteins. During this process structures targeted for destruction are sequestered into large double-membrane vesicles called autophagosomes and then delivered into vacuoles or lysosomes, where they are subsequently degraded. In this regard, the yeast Sec19 vesicle transport system (VTS), which is normally required for autophagy and vesicular transport between ER and Golgi, was also suggested to function in an efflux of cytoplasmic aluminium (Ezaki *et al.,* 2005).

1.4.6 Further metal detoxification processes

Besides the major and ubiquitously used cellular detoxification principles, various species-specific metal defense processes have evolved. One of these mechanisms is the ability of the human H-chain ferritin to attenuate hydroxyl radical production by the Fenton reaction (Orino *et al.,* 2001; Chiancone *et al.,* 2004; Zhao *et al.,* 2006). Human ferritins are globular proteins that keep up to thousands of iron atoms in a non-toxic form.

Low molecular weight organic molecules, like amino acids (histidine, serine, or cysteine) and their derivatives, also are suggested to take part in metal homeostasis by forming complexes with metal ions, thereby preventing the interaction of the metals with physiologically important cellular proteins (Gachot *et al.,* 1991; Tandon *et al.,* 2002; Barbier *et al.,* 2005; Ali *et al.,* 2009). Histidine for instance, is known to bind to metal ions and seems to alleviate the toxicity of Co^{2+}, Cu^{2+}, and Ni^{2+} (Pearce and Sherman, 1999). Moreover, several proteins with histidine- or glutamine-rich domains have special properties to bind metal ions (esp. Ni^{2+}), thus serving roles in intracellular binding/storage and detoxification of excess metals (Benini *et al.,* 1996; Hara *et al.,* 2005; Zeng *et al.,* 2008; Schauer *et al.,* 2010).

In plants intracellular detoxification of Al^{3+} occurs via the formation of nontoxic Al^{3+} complexes with organic acids or other chelators and sequestration in the vacuole (Ma *et al.*, 2001; Shen *et al.*, 2002). DNA repair mechanisms upon metal toxicity also constitute an important part of the cellular metal defense system including enzymes of the RAD family like Rad27, besides several others (Pagani *et al.*, 2007b; Ruotolo *et al.*, 2008). After all, the activation of heat shock proteins (HSPs) with chaperone activities is an integral part of the mammalian stress response to metal ions (Han *et al.*, 2005). Chaperones are mainly responsible for the recycling, refolding, and prevention of hydrophobic aggregation of misfolded or damaged proteins. In connection with dermatitis-causing concentrations of Ni^{2+}, human keratinocytes and fibroblasts were shown to accumulate key stress chaperones like Hsp90, Hsp72, and Hsp73 in the nucleus (Carroll and Wood, 2000). Another HSP, the secreted *S. cerevisiae* Hsp150, was shown to play a role in Al^{3+} tolerance (Ezaki *et al.*, 1998).

With regard to the multitude of detoxification strategies in organisms, metal resistance may be considered as the result of variable levels of defense systems with overlapping substrate specificities but unique functions.

1.5 Cellular and systemic implications of metal toxicity

Due to continued metal uptake that surpasses the detoxification and antioxidant capacity of the cell metabolism defective cell components and intracellular ROS levels increase and subsequently generate severe cell damage. This includes cleavage of DNA and RNA molecules (Sirover *et al.*, 1976; Serero *et al.*, 2008; Wurtmann and Wolin, 2009), impairment of DNA repair mechanisms (Dally and Hartwig, 1997; Jin *et al.*, 2003; Banerjee and Flores-Rozas, 2005; Chen *et al.*, 2010), protein crosslinking (Xie *et al.*, 2007; Kennett *et al.*, 2010), altered calcium- and sulfhydryl-homeostasis (Nilius *et al.*, 2004; McElnea *et al.*, 2011), and alteration of the epigenetic state of chromatin in terms of increased histone methylation and ubiquitination, as well as decreased histone acetylation (Lee *et al.*, 1995; Broday *et al.*, 2000; Zoroddu *et al.*, 2002; Karaczyn *et al.*, 2005; Chen *et al.*, 2006; Ke *et al.*, 2006). Moreover, enhanced lipid peroxidation occurs e.g. resulting in disruption of mitochondrial membrane potential and mitochondrial swelling with the release of cytochrome c and apoptosis (Aubrecht *et al.*, 1998; Shi *et al.*, 2004; Liu *et al.*, 2005; Tuszynska, 2006; Vujcic *et al.*, 2007; Roess *et al.*, 2008).

In multicellular organisms metal toxicity causes systemic defects (Table 1) involving cancer, cardiovascular diseases, diabetes, atherosclerosis, neurological disorders, chronic inflammation, and others. More precisely, the particular metal stress effects comprise damaged or reduced mental and central nervous functions, lower energy levels, as well as damage to blood composition, kidneys, liver, lungs, and other vital organs (Hussain *et al.*, 1987; Shibasaki *et al.*, 1993; Wong *et al.*, 2005; Satarug *et al.*, 2006; Wolf and Baynes, 2006). In this regard, it has for instance been reported that metals like Cd^{2+}, Hg^{2+}, or Pb^{2+} interact with a number of renal transporters and ion channels, thereby exerting a blocking effect, which leads to decreased reabsorption of the physiological metals (Gachot *et al.*, 1991; Barbier *et al.*, 2005).

Long-term metal exposure may result in slowly progressing physical, muscular, and neurological degenerative processes that mimic Alzheimers´s disease, Parkinson´s disease, muscular dystrophy, and multiple sclerosis (Basun *et al.*, 1991; Cornett *et al.*, 1998; Figueiredo-Pereira *et al.*, 1998; Mutter *et al.*, 2004; Olanow, 2004; Uriu-Adams and Keen, 2005; Bolin *et al.*, 2006). Allergies, in response to repeated long-term contact with metals or their compounds (esp. Cu^{2+}, Co^{2+}, Ni^{2+}, Al^{3+}, Hg^{2+}, and Cr^{2+}) are of growing significance today and are counted among the major health impacts in response to metal exposure (Basketter *et al.*, 1993; Costa *et al.*, 2001; Kasprzak *et al.*, 1995 and 2003; Forte *et al.*, 2008; Castelain, 2011).

1.6 Regulatory mechanisms under metal stress

The cellular defense response to metal exposition is associated with both, macromolecular damage and adaptive changes in gene expression. The overall extent of such genetic changes comprises hundreds to thousands of genes in microorganisms, plants, or humans and is still not well understood. Generally, early stress-activated genes in yeast are notably involved in plasma membrane and active transport processes, which are primarily Yap1- and Pdr1-controlled (Gounalaki and Thireos, 1994; Lucau-Danila *et al.*, 2004). But Yap1 also cooperates with other transcription factors such as Skn7 to regulate the thiol redox system (Lee *et al.*, 1999) and Met4 in concert with the Met28-Met31-Met32-Cbf1 complex to regulate glutathione biosynthesis and sulfur assimilation (Thomas and Surdin-Kerjan, 1997; Dormer *et al.*, 2000; Wheeler *et al.*, 2003). Yap1 is able to sense hydrogen peroxide through reversible disulfide linkage between cysteine residues (Delaunay *et al.*, 2000). In higher

eukaryotes regulatory functions during oxidative stress responses have been verified for the zinc finger protein Zat12 in *A. thaliana*, the apoptosis controlling p53 in human carcinoma cells, the p38 MAP kinase in human intestinal epithelial cells, or the nuclear factor κB (NF-κB) in human neutrophils, besides others (Vogt and Rossman, 2001; Dandrea *et al.*, 2004; Davletova *et al.*, 2005; Ivison *et al.*, 2010; Freitas *et al.*, 2010).

Though, the main strategy that yeast cells use to protect the internal system from severe environmental stress impacts is the initiation of a common gene expression program. This program includes approximately 900 genes and is termed as "environmental stress response" (ESR; Gasch *et al.*, 2000). The ESR is characterized by a simultaneous repression of *de novo* protein synthesis which is suggested to allow energy to be diverted to the increased expression of genes involved in general defense as well as specific detoxification mechanisms. The major players of this highly sophisticated stress-response network vary due to the particular stress conditions and include transcription factors such as Yap1, Msn2, Msn4, Hsf1, Gcn4, Rpn4, Sfp1, Fhl1, or Rap1 which have partly also been shown to participate under metal stress (Klein *et al.*, 1994; Natarajan *et al.*, 2001; Rohde and Cardenas, 2003; Haugen *et al.*, 2004; Ferguson *et al.*, 2004; Martin *et al.*, 2004). However, the main cross reactions between the pathways of signal transduction are not entirely clear yet.

1.7 Analysis of transcriptional expression patterns upon metal stress

In the field of metal homeostasis, toxicity, and detoxification numerous questions especially concerning the complex network of metal stress defense pathways and their respective regulatory associations at the molecular level as well as the molecular mechanisms linking metal toxicity to human pathologies are still unresolved. Accordingly, the studies already carried out until today investigating these issues provide a solid basis and starting point for further research of metal stress.

1.7.1 What distinguishes yeast as a model organism?

One recently generated As- and Cd- sensitive yeast gene set of in total 106 genes has been reported to exhibit about 41% human orthologues indicating that both organisms may use similar mechanisms to prevent metal toxicity and carcinogenesis (Thorsen *et al.*, 2009). In this regard S*accharomyces cerevisiae* appeared as a suitable model organism to study the

molecular details of metal action based on whole-genome expression analyses of metal-exposed yeast cells in order to enlarge the global view of the genetic basis of metal stress. Besides the high degree of evolutionary conservation between yeast and higher eukaryotes, the most particular advantages of yeast as a genetic model organism are its short generation times, its unproblematic experimental treatment and the availability of a wide range of techniques in classic and molecular genetics.

It is well known that yeast cells rapidly respond with alterations of whole-genome gene expression patterns as well as in fundamental regulatory processes on the post-translational level to cope with sudden stressful environmental changes (Mager and de Kruijff, 1995; Gash *et al.*, 2000; Causton *et al.*, 2001; Jin *et al.*, 2008). The capacity to adapt to the new environmental condition is critical to the survival of all organisms. Global technologies including transcriptomics, large-scale proteomics as well as metabolomics have enabled an integrated view of the remarkable ability of yeast and other organisms to deal successfully with stressful impacts (Ideker *et al.*, 2001; Begley *et al.*, 2002; Lafaye *et al.*, 2005). This present study particularly investigated the effects of metal toxicity in *S. cerevisiae* cells on a transcriptional level by using high-throughput DNA microarray technology.

1.7.2 cDNA microarray technique

Since microarray technique constituted the experimental basis of my studies I present a short overview of this experimental method (Figure 6): Biological samples for microarray analysis are prepared by extracting mRNA and labelling cDNA with different fluorescent dyes by reverse transcription. The labelled cDNAs are then hybridized to their complementary DNA sequence fragments spotted on the microarray. In a subsequent procedure of purification all non-specific and unbound samples are washed off. Thus, only strongly paired strands remain hybridized and generate a fluorescent signal that in its strength depends upon the amount of sample cDNAs. For every spot the intensity of this signal is detected by light scanning with a high precision microarray scanner. The ratio of the fluorescent light emission between the two different wavelengths serves as a direct measure of the relative gene transcript expression level. For quality assurance a so called "dye-swap" step is inevitable to identify possible false data. In this experimental design all conditions remain the same except for the labeling of the samples which is switched. Following accurate preprocessing of the expressional raw data, a decisive step to enable the proper biological interpretation of the detected genes is their consistent annotation to unique metadata of corresponding databases.

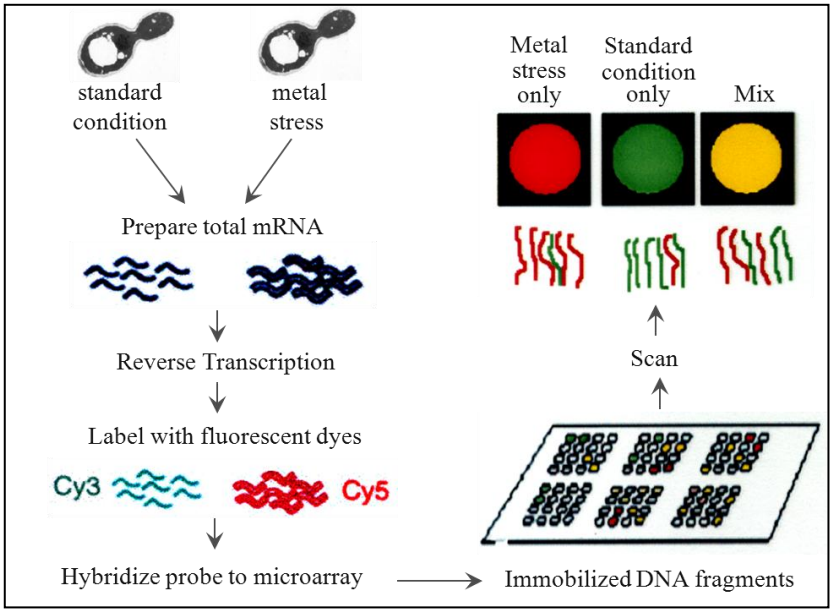

Figure 6: cDNA microarray technique. Biological samples are prepared by isolating RNA from yeast cell cultures, labeling of the probes by reverse transcription, and hybridizing to a microarray. The image is scanned and signal intensities are detected. Spots, whose mRNAs are present at a higher level in one of the two samples, show up as predominantly red or green. Yellow spots are generated by roughly equal amounts of bound cDNA from each sample (red + green = yellow).

1.7.3 Selection criteria of the metals used for transcript profiling

Expression profiles were generated in response to overall 10 metal salts: aluminium chloride ($AlCl_3$), silver nitrate ($AgNO_3$), arsenic chloride ($AsCl_3$), cadmium chloride ($CdCl_2$), cobalt chloride ($CoCl_2$), mercury chloride ($HgCl_2$), manganese chloride ($MnCl_2$), nickel sulphate ($NiSO_4$), vanadium chloride (VCl_3), and zinc chloride ($ZnCl_2$); These metals were primarily selected to be hazardous to human health when abundant (Table 1). Another important selection criterion was the relevance of human exposure to the metals in everyday life (clarified in Table 1 under the general term “biotechnological uses”). The content of Table 1 was generated by using various internet sources (as indicated in the legend), besides scientific references.

Metals	Biological role	Biotechnological uses	Health risks
TRANSITION METALS:			
Ag	no biological role;	dental amalgam, antibacterial agent, jewelry, photography, electrical contacts, batteries, silverware, used in mirror production, coinage metal;	most Ag-salts are toxic (esp. to lower organisms), skin irritation; renal and reproductive disorders; hemolysis; nervous system impairment;
Cd	no biological role in higher organisms; plays a necessary role in rats and marine diatoms;	fungicides, insecticides, marijuana, rubber, seafood (oyster, tuna), coffee, mushrooms, cigarettes, liver, instant dental alloys, paints, ceramics, batteries, PVC plastics, motor oil, exhaust, sludge;	highly toxic and carcinogenic (e.g. lung and prostate cancer); cumulative poison; causes renal failure and blood pressure problems; neurological disorders; gastrointestinal symptoms; respiratory and reproductive problems;
Co	essential trace element (coenzymes – cobalamins; e.g. vitamin B_{12}); deficiencies of cobalt lead to pernicious anemia;	radio therapeutic, alloys (jet engines and turbine engines), in magnet steels and stainless steels, used in electroplating; ceramics, glass, pottery, batteries, paints;	most components are toxic, some are considered carcinogenic; causes contact dermatitis; cardiovascular and respiratory difficulties; developmental problems; overproduction of red blood cells (erythropoiesis);
Hg	no biological role;	widespread in biosphere and food chain (esp. fish), childhood vaccines, antiseptic creams, dental amalgams, contact lens solutions, pesticides and antifouling paint, thermometers, batteries;	extremely toxic; dreadful poison; nervous and digestive disorders; developmental disorders; allergies; infertility; ocular and renal problems;
Mn	essential trace element (enzymes); deficiencies lead to infertility, metabolic weakness, pancreas and enzyme problems;	important in the utilization of vitamin B_1, oxidizing agent, medicine, nuts, seeds, whole-grain products, beans, peas, ginger, coffee, tea, wheat germ;	highly toxic; possibly carcinogenic (higher risk for several cancers e.g. fibroid tumors); nervous and cardiovascular disorders; respiratory problems; osteoporosis; liver disease; diabetes:
Ni	essential trace element for many species (bacteria, plants); deficiencies in rats and chicks lead to liver problems;	peanut butter, hydrogenated vegetable oils, margarine, herring, oysters, cigarette smoking, tea, alloys, coinage metal, in glasses (green color), catalyst, batteries, electroplating, jewelry;	toxic (esp. for plants); carcinogenic (esp. lung); skin allergies or dermatitis; dizziness; digestive and respiratory disorders; apathy; vertigo; cardiac symptoms (Ni interferes with vitamin E activity); immunological problems; kidney damage;
V	essential trace element for some species (e.g. rats, chicks); deficiencies result in reduced growth and impaired reproduction;	in some industrial smoke pollution, vegetable oils, olives, black pepper, seafood, spinach, fats, in diesel fuels, in nuclear applications, bonding agent, ceramics, catalyst, plastics;	highly toxic; may be carcinogenic (esp. lung); arthritis, cardiovascular and renal problems; weakened immune system; gastrointestinal and respiratory problems; reproductive disorders;
Zn	essential trace element (enzymes); deficiencies result in skin, hair and nail problems, depression, stunted growth and male infertility, immune deficiency, hypothyroidism,	pollution from industrial smoke, cosmetics, pharmaceuticals, dry batteries, in lightweight coins, used in the manufacture of paints, rubber and dyes, plastics, textiles and electrical equipments, fluorescent lights;	some compounds are carcinogens (lung disease); skin irritant; affects the balance of other nutrients (e.g. Ni, Ca, vitamin A, B1, C); gastrointestinal and respiratory problems; hematological disorders; muscle spasms; interstitial nephritis;
METALLOID:			
As	necessary ultra-trace element for humans (and other organisms); deficiencies result in inhibited growth;	rat poisoning, fungicides, pesticides, coal combustion, table salt, drinking water, beer, paints, bronzing, pyrotechnics, wood preservatives, chemicals and glasses;	very poisonous to plants and animals; carcinogenic; renal, gastrointestinal and respiratory problems; neurological, hepatic and reproductive disorders;
POST-TRANSITION METAL:			
Al	no biological role; may be involved in the action of some enzymes (e.g. succinic dehydrogenase);	antacids, buffered aspirin, nasal sprays, antiperspirants, cans and foils, kitchen utensils, industrial applications, electrical transmissions, alloys, coatings, automobile exhaust, tobacco smoke;	toxic; its toxicity can be traced to deposition in bone and the central nervous system; linked to Alzheimer´s disease; nervous + digestive disorders; may increase the risk of breast cancer; musculoskeletal + respiratory problems;

Table 1: Biological role, biotechnical uses, and health risks of the metals used in this study: Selected metals: silver (Ag), cadmium (Cd), cobalt (Co), mercury (Hg), manganese (Mn), nickel (Ni), vanadium (V), zinc (Zn), arsenic (As), and aluminium (Al); Used internet sources: Rutherford – Lexikon der Elemente (http://www.uniterra.de/); Web Elements – The Periodic Table (http://www.webelements.com/); Wikipedia, the free encyclopedia (http://www.wikipedia.org/); ATSDR – Agency for Toxic Substances and Disease Registry (http://www.atsdr.cdc.gov/); See also the classification of metals in the periodic table in Figure 2;

1.8 Analysis workflows

The source of the manuscripts introduced in chapters 1.8.2, 1.8.3, and 1.8.4 is the transcriptional expression analysis in response to the 10 selected metals summarized in chapter 1.8.1 in the manuscript entitled "Transcript profiling analysis of acute metal stress response of *Saccharomyces cerevisiae*", which in the course of examination led to the more detailed research of some interesting aspects. In particular they include the regulatory role of the target of rapamycin complex 1 (TORC1) and PKA kinase under arsenic stress, the participation of the transcription factor Stb5 in the transcriptional yeast response to short-term and chronic mercury exposure, and the characterization of the plasma membrane protein Pun1 in response to excess manganese.

1.8.1 Ad "Transcript profiling analysis of acute metal stress response of *Saccharomyces cerevisiae*"

In order to enlarge the global knowledge of metal stress, this primary study focuses on a comparative view of transcriptional stress responses upon silver, aluminium, arsenic, cadmium, cobalt, mercury, manganese, nickel, vanadium, and zinc. *S. cerevisiae* cells were treated with metal solutions for 30min and the expression patterns were analysed by cDNA microarray technique. To properly compare the stress responses of all ten metals, transcriptomes were produced by using one specific yeast strain cultivated under consistent growth conditions, approximately equi-toxic metal concentrations to cause moderate metal stress, as well as standard protocols for total RNA extraction, microarray technique, and data analyses.

We particularly investigated the early-on effects of the selected metals including the major pathways that have been differentially expressed and their respective regulatory associations. We searched for transporters and detoxification strategies that to date had not been described for the distinct metal stress conditions and analyzed similarities between and unique effects in the expression patterns of the particular metal data sets. To prove the uniqueness of our findings, we finally compared our compendium (30min) with previously generated metal stress data comprising prolonged metal treatment up to 2h.

1.8.2 Ad "Arsenic toxicity to *Saccharomyces cerevisiae* is a consequence of inhibition of the TORC1 kinase combined with a chronic stress response"

Examination of the metal stress profiles revealed arsenic as the most significant inducer of general stress genes, besides the strongest down-regulator of genes encoding ribosomal proteins (RP; Supplemental Figure 1). This is consistent with literature describing arsenic and many of its compounds as notoriously poisonous and cancerogenic. The highly toxic effects of arsenic are even linked to epigenetic changes (Mandal and Suzuki, 2002; Chu and Crawford-Brown, 2006; Baccarelli and Bollati, 2009). However, arsenic trioxide is still used for the treatment of cancer, most commonly for patients with acute promyelocytic leukemia (Antman, 2001; Hu, 2011). And arsenic poisoning from naturally occurring trivalent arsenite in drinking water remains a problem in many parts of the world (Lamm *et al.,* 2006; Knobeloch *et al.,* 2006). In regard to the actuality of the arsenic threat to human health and the obscurities concerning the molecular mechanisms of arsenic toxicity, we decided to investigate the regulatory associations of the above mentioned transcriptional yeast response to arsenic stress.

Previous studies have implicated important transcription factors like Msn2, Msn4, or Sfp1 in the yeast response to environmental impacts (Martinez-Pastor *et al.,* 1996; Fingerman *et al.,* 2003; Marion *et al.,* 2004). In this regard, we searched for a possible participation of these regulators under metal exposure via GFP-localization studies and indeed found them involved (Supplemental Figure 2 and 3). Thereupon, we concentrated on the signaling pathways controlling these factors.

The highly conserved nutrient signaling protein kinase Target Of Rapamycin Complex 1 (TORC1) has been described as a direct negative regulator of Msn2/4 (Beck and Hall, 1999). TORC1 was shown to partly act through the protein kinase Sch9, which down-regulates several Msn2/4 target genes as well as RP genes (Urban *et al.,* 2007). Protein kinase A (PKA) and TORC1 kinase have further been verified to regulate Sfp1 in response to nutrients and rapamycin treatment, respectively (Jorgensen *et al.,* 2004; Marion *et al.,* 2004; Wullschleger *et al.,* 2006). Accordingly, we examined the TORC1 and PKA signaling pathways and their downstream targets Msn2/4, Sfp1, and Sch9 as potential arsenic targets, especially in regard to RP gene repression and Msn2/4-dependent activation of stress-related genes.

1.8.3 Ad "Stb5 participates in the adaptation of *Saccharomyces cerevisiae* to acute and chronic mercury stress"

In the course of growth assays with deletion strains on metal-supplemented solid plates we observed a severe growth defect of the *stb5*Δ mutant upon all tested metal ions including mercury, arsenic, aluminium, and vanadium, besides others. The zinc finger transcription factor Stb5 has been previously reported to play an important role during oxidative stress (Larochelle *et al.,* 2006), which is in line with the established fact that most metals are capable to induce oxidative stress (Valko *et al.,* 2005). To this effect we determined to investigate a potential participation of Stb5 in the yeast metal defense.

Mercury and its compounds have been used in medicine as ingredient in dental amalgams, preservatives in vaccines, diuretics, or topical disinfectants. Today, mercury is known as extremely toxic and is one of the major environmental pollutants especially harming humans by eating mercury-contaminated seafood (Yorifuji *et al.,* 2009; Ruelas-Inzunza *et al.,* 2011; Al-Saleh and Al-Sedairi, 2011). Mercury primarily affects the neurological system (Moen *et al.,* 2008; Montgomery *et al.,* 2008) but little is known about its exact toxicity mechanisms.

To gain new insights into the cellular defense mechanisms against mercury toxicity, we analyzed short-term (15min and 30min), sustained (2h), and chronic (24h) mercury stress in wild-type and *STB5* deletion strains by cDNA microarray technique. We additionally performed a systematic query for sequence signature motifs in the upstream sequences of the detected significantly differentially expressed genes to examine the respective regulatory networks.

1.8.4 Ad "Pun1 is a metal ion-inducible, calcineurin/Crz1p-regulated plasma membrane protein required for cell wall integrity"

In search of potential transmembrane metal transporters we found the uncharacterized yeast gene *YLR414C* (*PUN1*) as significantly up-regulated especially upon manganese and to a lesser degree in response to silver stress (Supplemental Figure 4). Manganese is both nutritionally essential for utilization of vitamin B and potentially toxic (Keen *et al.,* 1999). It plays an important role in a number of physiological processes as constituent or activator of multiple enzymes like the mitochondrial superoxide dismutase (Mn-SOD), which is the main antioxidant enzyme of nearly all organisms living in the presence of oxygen (Wedler, 1994).

However, chronic exposure to high levels of manganese in occupational or environmental settings can lead to its accumulation in the brain resulting in neurological disorders partly mimicking those of Parkinson's disease (Roels *et al.*, 1987; Aschner and Aschner, 1991). Excess manganese has also been shown to interfere with the absorption of iron, therefore resulting in iron-deficiency anemia (Finley, 1999; Fitsanakis *et al.*, 2009). Regarding these pathological effects of manganese and its participation under oxidative stress, we decided to investigate a putative role of Pun1 under manganese stress in more detail.

Phenotypic growth analyses with *pun1*Δ mutants on solid medium supplemented with metals confirmed the importance of Pun1 to attain tolerance to metal stress (Supplemental Figure 5). Surprisingly, sequence analyses of *PUN1* displayed similarities to mammalian claudins, the major components of plasma membrane tight junctions (Furuse *et al.*, 1998; Morita *et al.*, 1999). In view of the biological importance of these highly selective diffusion barriers, we explored whether yeast Pun1 shares evolutionary conserved structural and functional properties with human claudins. We therefore analyzed the subcellular localization of Pun1 and the transcriptional regulation of *PUN1* upon metal treatment. Moreover, we investigated the oligomerization and self-interaction capacity of Pun1 to prove whether Pun1 has the property to form homo-oligomers like mammalian claudins. Regarding a morphological defect of the *PUN1* deletion strain under optimal growth conditions, we examined the cell wall morphology of *pun1*Δ and its sensitivity to zymolyase, manganese as well as other metals to provide indication of Pun1 function during metal stress.

2. PUBLICATIONS

2.1 Transcript profiling analysis of acute metal stress response in *Saccharomyces cerevisiae*

Dagmar Hosiner[6 *], Susanne Gerber[2,5 *], Hella Lichtenberg-Fraté[3], Walter Glaser[4], Edda Klipp[5] and Christoph Schüller[1 ¶)]

[1] Department of Applied Genetics and Cell Biology UFT-Campus Tulln, University of Natural Resources and Life Sciences (BOKU), Vienna

[2] AG Computational Time Series Analysis, Institute of Computational Science, Faculty of Informatics, Università della Svizzera italiana, Lugano

[3] AG Molekulare Bioenergetik, IZMB, Rheinische-Friedrich-Wilhelms-Universität Bonn

[4] Institute of Medical Biochemistry, MFPL, Medical University of Vienna, Vienna

[5] Theoretical Biophysics Humboldt-Universität Berlin

[6] Department of Genetics, MFPL, University of Vienna, Vienna

***** Both authors contributed equally to this work

¶) To whom correspondence should be addressed

The author's contribution

Dagmar Hosiner	- conceived the study, microarray analyses, writing
Susanne Gerber	- conceived the study, microarray analyses, writing
Walter Glaser	- microarray analyses
Hella Lichtenberg-Fraté	- writing, advices
Edda Klipp	- writing, advices
Christoph Schüller	- correspondence, writing, advices

Transcript profiling analysis of acute metal stress response in *Saccharomyces cerevisiae*

Abstract

We compared the early-on effects of Ag^{+}, Al^{3+}, As^{3+}, Cd^{2+}, Co^{2+}, Hg^{2+}, Mn^{2+}, Ni^{2+}, V^{3+}, and Zn^{2+} to *Saccharomyces cerevisiae*. We show that activation of metal-specific oxidative detoxification and protein catabolic strategies along with the repression of RP/Ribi genes are the primary defense pathways against acute metal stress. Moreover, we indicate chaperon activity and chelation of metal ions via siderophores and amino acids as additional important detoxification mechanisms. Finally, we substantiate that there is no general homeostatic defense pathway against metals in yeast. However, we also provide evidence for distinct metal clusters evoking similar metal detoxification strategies with shared predicted regulatory associations.

Introduction

Metals are an integral part of our environment and all living organisms are exposed to metals in their natural habitat or through anthropogenic sources. Hence, metals and metalloids with biological as well as toxic relevance are widespread in nature and can locally reach fairly high concentrations following for instance metal pollution or extensive use of some metals and metal compounds as fungicides and disinfectants. Some metals are intrinsically toxic like cadmium, arsenic, antimony, and mercury while others such as copper, manganese, zinc, or cobalt are needed in trace amounts for essential cellular functions but become toxic in excess quantities. Many metals are essential nutrients, and a large number of proteins require metals for catalytic activity or for maintaining structural properties [1].

The term “heavy metal” comprises a loosely-defined subset of elements that exhibit metallic properties. It mainly includes the transition metals, some metalloids, lanthanides, and actinides. Biologically relevant metals are mostly the so called "transition metals/elements" including groups 3 to 12 on the periodic table. However, their valence electrons which are those that may combine with other elements, are present in more than one shell so these elements often exhibit several common oxidation states such as iron. Since zinc, cadmium, and mercury have no incomplete d shell in the oxidation state +2, they are also classified as “soft” transition metals.

Metals cannot be degraded or modified like toxic organic compounds. They form unspecific complex compounds in the cells, which lead to various toxic effects [2]. Metal toxicity results from oxidative stress [3,4,5,6], alteration of enzyme and protein function [7,8,9,10,11], and impaired DNA repair leading to several pathological effects on cellular and organismal level such as defects in cell cycle progression, deregulation of proliferation processes, apoptosis, or various age-related diseases [12,13,14,15].

To preserve the balance between essential and toxic levels of metal ions, cells utilize sophisticated metabolic mechanisms for regulating uptake, sequestration to the sub-cellular compartments and complexes, as well as detoxification [16,17]. Because no dedicated sensors exist for most metal ions, exposed cells respond with alterations in gene expression due to secondary induced damage [18,19]. *S. cerevisiae* senses and responds to a variety of qualitatively different stressors like nutrient depletion, temperature, osmo- and oxidative stress, and a number of toxicants [18,19,20]. In recent years a considerable amount of information concerning the exposure of yeast cells to toxic metals and metalloids accumulated [21]. However, several molecular details of metal toxicity and detoxification mechanisms still have to be clarified. In this regard *S. cerevisiae* is a suitable experimental model organism to explore metal sensing, toxicity, and detoxification strategies.

In order to gain new insights into the immediate adaptation to metal stress, we investigated early gene expression changes of *S. cerevisiae* exposed to selected metals. We focused on short-term exposition to moderate and intermediate metal ion concentrations and examined expression profiles obtained after 30 min exposure of yeast cells to the (heavy) metal ions Ag^{+}, Al^{3+}, As^{3+}, Cd^{2+}, Co^{2+}, Hg^{2+}, Mn^{2+}, Ni^{2+}, V^{3+}, and Zn^{2+}. The significantly differentially expressed genes were investigated for similarities between and uniqueness within the distinct transcript profiles and revealed a rather general stress response among the highly toxic metal cluster Ag^{+}, As^{3+}, Cd^{2+}, and Hg^{2+}. Expression patterns were further analyzed by cluster and network analysis for associations to significantly shared GO terms and showed characteristic common and metal specific cross reactions. We especially observed varying antioxidative and protein degradation strategies as the main immediate defense mechanisms against acute metal stress. Moreover, analyses of the regulatory network architecture revealed discrete metal clusters with shared putative transcriptional regulators. Finally, we compared our compendium of acute metal stress (30min) with previously generated metal stress data comprising prolonged metal treatment up to 2h and illustrate the significant distinction between both metal stress states indicating adaptation of yeast cells to continued metal exposure.

Results and Discussion

Metal toxicity analyses

To test the toxicity of metal salts on cells of the yeast *Saccharomyces cerevisiae*, we performed two types of analyses. First, we checked for the minimal inhibitory concentration (MIC) of ten biologically relevant metal ions. Second, we measured the metal ion concentrations causing 50 percent growth inhibition (50% GI) in the yeast cultures. Both are presented as the quantity determined to reduce growth to 5 (MIC) and 50% (GI) of the mean growth of the control cultures (Table 1). We defined Cd^{2+} as the most toxic metal ion with a MIC of 1µM and a 50% GI of 10µM, whereas Mn^{2+}, Ni^{2+}, and Zn^{2+} showed the highest MIC with 1mM and V^{3+} the highest 50% GI with 4mM.

Metal	MIC	50% GI	EP	NR
$AgNO_3$	20µM	100µM	40µM	4
$AlCl_3$	400µM	3mM	500µM	3
$AsCl_3$	50µM	500µM	200µM	3
$CdCl_2$	1µM	10µM	2µM	3
$CoCl_2$	100µM	400µM	100µM	3
$HgCl_2$	20µM	75µM	30µM	3
$MnCl_2$	1mM	1,75mM	1,5mM	3
$NiSO_4$	1mM	2mM	1,5mM	3
VCl_3	200µM	4mM	500µM	3
$ZnCl_2$	1mM	2,5mM	1,5mM	3

Table 1. Metal toxicity assays in *S. cerevisiae*. Toxicity assays carried out in liquid-YPD (2% yeast-extract, 1% polypeptone, 2% glucose, pH 6.4); MICs (minimal inhibitory concentration), 50% GI (50% growth inhibition), *de facto* concentration for EP (expression profiling), NR (number of replicates) for expression profiling;

In order to induce moderate metal stress for expression profiling (EP) these values were taken as upper and lower threshold to derive the experimental concentrations (Table 1) for yeast cell culture treatments. Exposure for 30min with low doses of these 10 metal salts ensured detection of early responses. Microarrays were conducted according to MIAME [22] standards.

Expression profiles under conditions of moderate metal stress

Gene expression after treatment with metal ions for 30min was taken as changed significant when at least a 50% deviation from the untreated control condition was detected. In total 740 genes were up-regulated, which corresponds to 11.8% of the yeast genome and 283 genes were down-regulated corresponding to 4.5% of the entire *S. cerevisiae* genome (Figure 1).

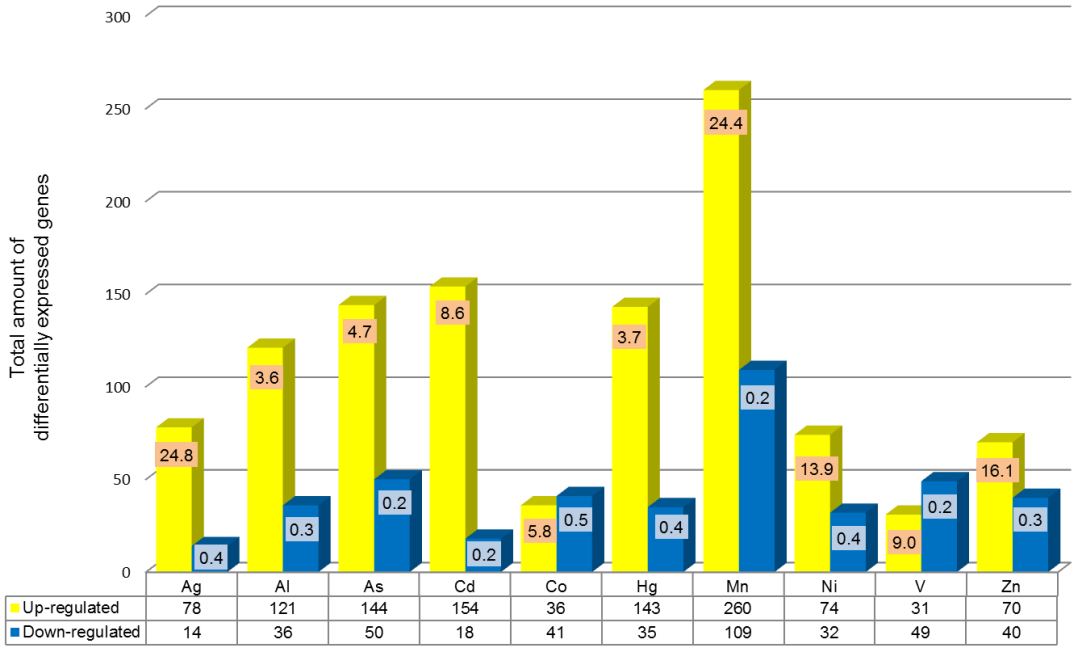

	Ag	Al	As	Cd	Co	Hg	Mn	Ni	V	Zn
Up-regulated	78	121	144	154	36	143	260	74	31	70
Down-regulated	14	36	50	18	41	35	109	32	49	40

Figure 1. Total number of differentially expressed genes. Descriptive summary of the total number of genes differentially expressed by a factor greater +50% (yellow) or minor -50% (blue) upon treatment with indicated concentrations of metal ions compared to the untreated control; total numbers of up- and down-regulated genes upon the distinct metal stress conditions are indicated in the figure. The numbers on top of the bars represent the maximum response (fold change of up- and down-regulated genes) measured for each condition.

Manganese induced the maximal response with 260 (4.2%) up- and 109 (1.7%) down-regulated genes and caused the second highest individual expression induction with a 24.4-fold change compared to the untreated control. This was followed by cadmium with 154 (2.5%) up- and 18 (0.3%) down-regulated genes and a maximal induction of 8.6-fold change. Cobalt exhibited the lowest response with 36 (0.57 %) up- and 41 (0.65 %) down-regulated genes. Silver treatment resulted in the up-regulation of 78 (1.24 %) genes, comparable to nickel and zinc and the lowest number of down-regulated genes, namely 14 (0.22 %). At the same time silver induced the maximal individual induction rate by a 24.8-fold change (Figure 1).

Ag^{+}, As^{3+}, Cd^{2+}, and Hg^{2+} constitute a tight metal cluster

In order to identify similarities in the expression patterns all possible overlaps between the transcriptional profiles were computed. First, the expression patterns upon different metal stresses were subjected to cluster analysis as explained in Materials and Methods. Genes with similar expression patterns across the experimental setup are likely to be functionally related. They might be co-regulated in biological processes, function in the same biochemical pathways, share regulatory sequence motives, or respond to the same regulatory control mechanisms [23,24].

Via pair-wise comparison of all experiments we first determined the number of shared (overlapping) genes (Table 2). The diagonal line in figure 2 summarizes the total amount of significantly up- and down-regulated genes upon the distinct experimental condition. Metals with the lowest MICs, in fact cadmium, mercury, silver, and arsenic caused the most overlaps of up- and down-regulated genes with other metal stress conditions. For instance, silver exposition generated a moderate response of in total 78 up- and 14 down-regulated genes with most of them being also expressed upon arsenic, cadmium, mercury, manganese, and nickel treatment. It is of note that the transcript profile upon nickel exposition also displayed considerable gene overlaps especially with the expression patterns under arsenic and silver stress, although toxicity assays with nickel in yeast cells showed the second weakest toxicity level of all tested metals. And it is interesting that aluminum and manganese, despite a high number of individually up-regulated genes, appear to induce specific expression patterns with only limited overlap to other stressors.

	Ag	**Al**	**As**	**Cd**	**Co**	**Hg**	**Mn**	**Ni**	**V**	**Zn**
Ag	78/-14	1	28	32	1	34	42	29	3	6
Al	-3	121/-36	7	4	1	7	1	2	3	5
As	-7	-1	144/-50	53	3	35	28	27	2	8
Cd	-5	-1	-9	154/-18	7	56	35	23	1	6
Co	-2	-1	-1	-1	36/-41	1	12	8	1	9
Hg	-8	-1	-17	-11	-1	143/-36	50	24	2	5
Mn	-7	-5	-17	-8	-4	-20	260/-109	21	0	10
Ni	-5	-1	-10	-5	-7	-9	-5	74/-32	1	10
V	-2	-16	-4	-3	-3	-4	-5	-3	31/-49	7
Zn	-1	-8	-1	-1	-5	-1	-4	-2	-12	70/-40

Table 2. Pair-wise comparison of 10 metal stress conditions. Matrix on the number of shared (overlapping) genes after pair-wise comparison of all differentially expressed genes upon 10 metal expositions. The diagonal line illustrates the total amount of genes significantly differentially expressed in response to the particular metals (up/down-regulated).

The results of the pair-wise similarity comparisons were transformed into Jaccard (Tanimoto) similarity indices [25], and are plotted in Figure 2 as a heat map with two dendrograms representing the outcome of hierarchical clustering. Cluster analysis revealed four unique clusters for up-regulated genes with a tight clustering of vanadium with aluminum and zinc with cobalt (Figure 2A). A separate group comprised the nodes connecting nickel with silver and mercury with cadmium separated by arsenic and, rather distinct manganese. For the down-regulated genes in total three unique tight clusters were obtained (Figure 2B). Strikingly, cobalt clustered to none of these groups. Similar to the up-regulated genes, vanadium clustered with aluminum and, more distinctly zinc, nickel clustered with arsenic and mercury with cadmium and more distinctly silver in the second large group. Manganese obtained a rather distant status.

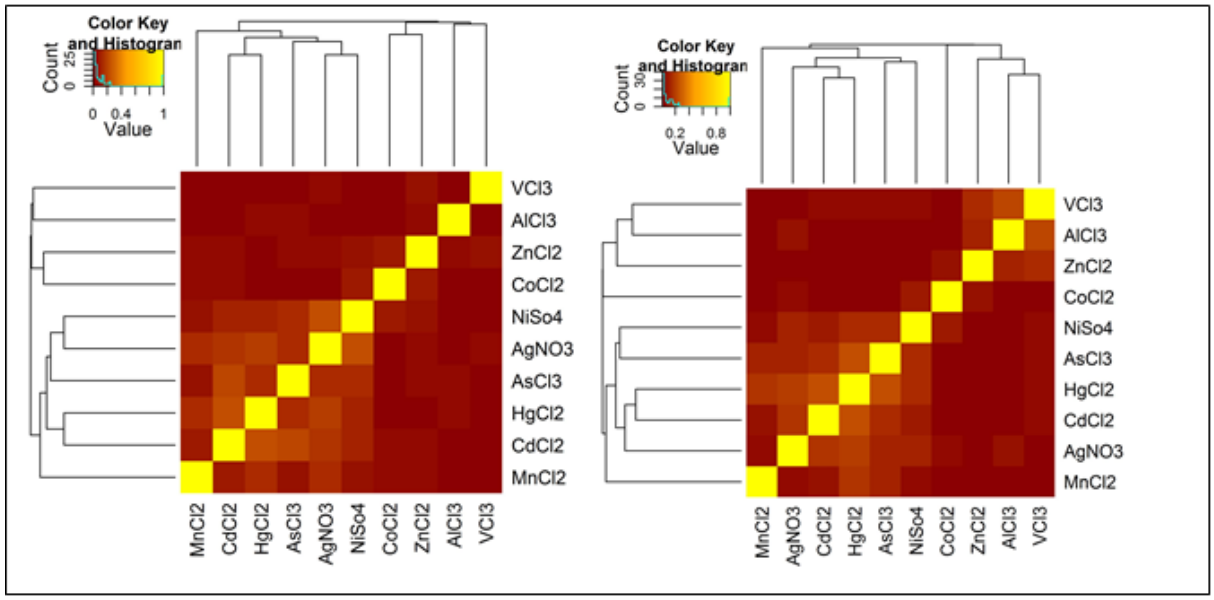

Figure 2. Jaccard heatmap. Unsupervised hierarchical clustering was applied to visualize the degree of pair wise similarity comparisons of the particular metal stress responses via dendrograms for up- regulated genes, **2A**) and down-regulated genes, **2B**). The heatmap refers to the data in Table 2 and was generated by transformation of the intersect counts into Jaccard (Tanimoto) similarity indices, which are correlation coefficients for determination of the similarity between two bit-vectors. The size of the intersection becomes divided by the size of the entire sample sets. The figure clearly illustrates a large size difference of the sample sets (see diagonal in Table 2). The more yellow the color the higher is the similarity between the two samples, yellow means both conditions are identical.

Next, we tested genes that were solely differentially expressed under one metal stress condition (Table 3). Aluminum treatment caused a total response of 121 genes of which 100 genes were uniquely expressed. This was the most specific systemic response (83%) upon all applied metals followed by vanadium (71%). Among the 260 genes that were up-regulated upon manganese treatment 158 were unique and thus 61% of the entire spectrum specific. Arsenic, cadmium, and mercury as the most toxic metal ions specifically activated 53 genes (of totally altered 144 genes = 37%), 46 genes (of totally altered 154 genes = 30%), and 37 genes (of totally altered 143 genes = 26%). Gene expression in response to silver showed the lowest specificity with 14%.

	Ag	**Al**	**As**	**Cd**	**Co**	**Hg**	**Mn**	**Ni**	**V**	**Zn**
Up-reg.	11	100	53	46	18	37	158	24	22	42
% induced	14%	83%	37%	30%	50%	26%	61%	32%	71%	60%
Down- reg.	0	15	19	6	28	4	64	13	19	20
% repressed	0%	42%	38%	33%	68%	11%	59%	41%	39%	50%

Table 3. Analysis of uniquely expressed genes under the 10 metal stress conditions. Numbers of up- or down-regulated genes that were specifically ex- or repressed under the distinct metals; percentage referred to the total numbers of differentially ex- or repressed genes provided in Figure 1.

Taken together, the comparisons of transcript profiles (Figure 2, Table 2 and 3) revealed a series of unspecific and specific responses to different metal ions and clearly illustrated distinct overlaps of expression patterns upon metal stress groups. In particular, a cluster of the highly toxic metal ions Ag^{+}, As^{3+}, Cd^{2+}, and Hg^{2+} was observed to generate the most overlaps of differentially expressed genes with other metal stressors. For example, the Ag^{+} response expression profile shared 66 genes with other metal stress responses, but showed only 11 specifically induced genes (not responding in any of the other conditions, Table 2 and 3). This is indicative for a less specific but rather general systemic stress response to these metal ions. On the other hand, less toxic metals such as Al^{+}, V^{3+}, and Mn^{2+} generated the highest number of individually expressed genes.

Absence of a common metal detoxification mechanism

Aiming at putative mutual detoxification strategies upon metal stress, we investigated which genes were the most commonly observed in our experimental setup. Strikingly, we found no gene that was induced under all 10 metal stress conditions (Table 4). 17 up-regulated and 4 down-regulated genes out of the in total 1023 differentially expressed genes were changed under at least five treatments. *TRX2* encoding an oxidoreductase of the thioredoxin system which protects cells against oxidative stress was observed as the most frequently up-regulated gene (upon Ag^{+}, As^{3+}, Cd^{2+}, Hg^{2+}, Mn^{2+}, Ni^{2+}, and Zn^{2+}). In turn, *NSR1* coding for a protein involved in ribosomal biogenesis was the most frequently down-regulated gene (upon Ag^{+}, As^{3+}, Cd^{2+}, Hg^{2+}, Mn^{2+}, and Ni^{2+}). Thus, the gene expression patterns were partly similar for distinct metal groups but are largely specific for the particular metals. This clearly indicates that there is no common metal detoxification pathway in yeast.

Counts	SN	GN	Conditions	Up/Down
7	YGR209C	TRX2	Ag-As-Cd-Hg-Mn-Ni-Zn	Up
6	YMR251W-A	HOR7	Ag-As-Hg-Mn-Ni-Zn	Up
6	YML100W	TSL1	Ag-As-Cd-Hg-Mn-Ni	Up
6	YLR303W	MET17	Ag-As-Cd-Hg-Mn-Ni	Up
6	YKL103C	LAP4	Ag-As-Cd-Hg-Mn-Ni	Up
6	YEL060C	PRB1	Ag-As-Cd-Hg-Mn-Ni	Up
6	YDL124W	NA	Ag-As-Cd-Hg-Mn-Ni	Up
6	YGR159C	NSR1	Ag-As-Cd-Hg-Mn-Ni	Down
5	YHL040C	ARN1	Cd-Co-Mn-Ni-Zn	Up
5	YPL154C	PEP4	Ag-As-Hg-Mn-Ni	Up
5	YNL160W	YGP1	Ag-As-Cd-Hg-Ni	Up
5	YMR173W	DDR48	Ag-As-Cd-Hg-Mn	Up
5	YHR071W	PCL5	Ag-Cd-Hg-Mn-Ni	Up
5	YDL022W	GPD1	Ag-As-Cd-Mn-Ni	Up
5	YCL040W	GLK1	Ag-As-Cd-Hg-Mn	Up
5	YNL208W	NA	Ag-Cd-Hg-Mn-Ni	Up
5	YNL134C	NA	Ag-As-Cd-Hg-Mn	Up
5	YCL042W	NA	Ag-As-Cd-Hg-Ni	Up
5	YPR124W	CTR1	As-Cd-Hg-Ni-V	Down
5	YML056C	IMD4	As-Cd-Hg-Mn-Ni	Down
5	YLR175W	CBF5	Ag-As-Cd-Hg-Mn	Down

Table 4. Analysis of genes expressed or repressed in at least five metal stress conditions. Genes that were identified as significantly up- or down-regulated (Up/Down) in at least 5 of the 10 experimental metal stress conditions after computational analysis of all expression profiles; "Counts" is the total number of conditions under which the respective gene was differentially expressed; SN (systematic name), GN (gene name); "Conditions" declare the combinations of experimental conditions under which the respective gene showed response;

T Profiler revealed metal clusters with shared putative TFs under acute metal stress

To decipher the regulatory network involved in metal stress, T-profiler was used for prediction of potential transcription factors (TFs). These predictions are based on our gene expression data (1023 significantly differentially expressed genes) and TF binding motifs in the promoter region of the corresponding genes (http://www.t-profiler.org/; [26,27]) and resulted in significant t-values for the particular TFs (Table 5). Accordingly, T Profiler generated four metal clusters with shared transcriptional regulators.

The largest cluster comprised arsenic, cadmium, mercury, and silver with the predicted stress response TFs Msn2, Msn4, Yap1, Rpn4, Yap1 homologues (Yap7, Yap6, and Cad1), and the heat shock TF Hsf1. This result is consistent with the aforementioned similarity analyses of the expression profiles and previous studies [19,28,29], wherein these TFs were identified as key regulators of the yeast stress response. In addition, the sulfur amino acid regulatory network Met4-Cbf1-Met31-Met32, which has been reported to play an important role in the stress response to cadmium [30,31,32], was also detected to participate in the response to silver stress.

TF	As	Cd	Hg	Ag	Ni	Mn	Co	V	Zn	Al
Msn2	9,78	6,46	9,62	3,39	4,47	4,26	2,63	3,56		
Msn4	9,93	6,09	8,2	2,54				3,91		
Yap1	9,39	5,57	7,01	3,18		2,1		2,58		
Yap7	10,6	5,69	9,02	4,91		3,7				
Cad1	4,46	3,14	4,47	4,87						
Yap6	4,05	2,34	3,22							
Hsf1	14,03	6,21		4,3			2,48	2,66		2,97
Met4		8,61		3,92				2,86		2,42
Met32		14,49	2,48	7,47		2,49				
Met31		6,22		2,19					2,2	2,16
Cbf1		5,96						2,49	3,09	
Rpn4	9,73	5,59	2,22				2,78			
Rph1	5,56			3,75	3,31					
Pho2	4,04			2,02						
Gcr2					4,95			2,65	2,75	
Ace2	3,32			2,37	4,68					
Leu3			7,31							2,2
Skn7			5,36	3,4						
Gln3			3,35			11				
Gcn4		2,58	12,68	5,29		17,72				
Rtg3	2,69	2,61	3,17	4,55		4,95				
Put3					3,82	4,95	8,16	4,32		2,55
Aft1					3,61	4,93	6,88	2,98		
Aft2		2		2,72		3,46	4,59			2,38
Dal81		2,4				6,98				
Fhl1	-16,04	-8,47	-9,6	-13,04	-10,84			-6,15	-5,69	
Sfp1	-8,5	4,21	-5,32	-6,36	-5,53			-2,65		
Rap1	-10,09	-5,2	-5,94	-7,75	-5,66			-3,57		
Swi4						-4,21				
Mbp1						-4,35				
Hir1						-4,66				
Hir2						-6,48				
Hir3						-4,57				

Table 5. T Profiler analysis of TF binding motifs. Corresponding to TF binding motifs in the upstream region of the differentially expressed genes, putative TFs involved in positive (red fields) and negative (green fields) response to metal treatment were predicted by T-profiler. Light-colored fields are predictions with enhanced t-value but did not reach the significance level of E-value < 0.05.

Mercury, silver, and manganese form a smaller cluster which involved regulators such as Rtg3 and Gcn4 in the yeast stress response. Rtg3, a leucine zipper TF, mediates mitochondrion degradation, whereas Gcn4 is a regulator of amino acid metabolism in response to nutrient limitation [33,34] and the nitrogen catabolite repression regulatory (NCR) network [35]. Another transcriptional activator of genes regulated by NCR, Gln3, was predicted by T Profiler for only Hg^{2+} and Mn^{2+}. Together, it appears that the nitrogen/amino acid biosynthesis is especially regulated by Gcn4 and Gln3 in response to Hg^{2+} and Mn^{2+}.

Nickel, manganese, cobalt, and vanadium constitute a third rather loose metal group, which was predicted to cause induction of Put3, a TF regulating proline metabolism, and the iron homeostasis TFs Aft1 and Aft2. In addition, all three subunits of the HIR complex, a nucleosome assembly complex involved in regulation of histone gene transcription and in position-dependent gene silencing, were found to be significant (in terms of their t-values) for

Mn^{2+}. This is interesting since a bulk of genes (*HHF1+1, HHT1+2, HTA1+2, HTB1+2*) in our data set encoding core histone proteins was significantly down-regulated in response to manganese treatment. These genes encode core histone proteins required for chromatin assembly and chromosome function. Inhibition of histone genes might therefore indicate severe disaggregation of yeast chromatin under acute Mn^{2+} exposure.

Finally, the TFs predicted to be involved in the regulation of the repressed genes under As^{3+}, Cd^{2+}, Hg^{2+}, Ag^{+}, Ni^{2+}, and V^{3+} were the regulators of ribosomal protein transcription Fhl1 and Sfp1 [28,36,37,38] and Rap1, a repressor/activator-protein involved in silencing of telomeric repeats and activation of glycolytic and RP genes [39]. Accordingly, repression of ribosome biogenesis seems to constitute a main mechanism of metal stress response.

Differential expression of transcription factors under metal stress

In addition to T Profiler analysis for prediction of putative regulators, we investigated TFs that were differentially expressed upon at least two metal stress conditions (Table 6). In this regard, we found induction of *HOT1*, encoding a regulator required for the transient induction of the glycerol biosynthetic genes *GPD1* and *GPP2* upon Ag^{+}, Cd^{2+}, and Hg^{2+}. Two further transcriptionally activated TFs involved in cellular amino acid metabolism were Arg80 under Ni^{2+} and Al^{3+} and Met28 under Cd^{2+} and Mn^{2+}. Transcription of *STB5* participating in multidrug resistance and the oxidative stress response was significantly elevated in response to As^{3+} and Cd^{2+}. Moreover, the mRNA levels encoding Gat1 involved in nitrogen catabolite repression, and the glucose-responsive TF Rgt1 regulating expression of glucose transporters were differentially expressed. Transcription of *HIR1* was inhibited upon Mn^{2+} and induced upon Zn^{2+}, respectively. Interestingly, Hir1 was also analyzed by T Profiler to play a role under Mn^{2+} stress. On the other hand, the mRNA levels of Cha4 involved in amino acid catabolism were significantly repressed in cells treated with Al^{3+} and V^{3+}. Together, these findings point to the participation of further regulators in long term response to metal exposure.

TF	Ag	As	Cd	Hg	Ni	V	Mn	Co	Zn	Al
Arg80					1					1
Hot1	1		1	1						
Met28			1				1			
Stb5		1	1							
Gat1								-1		1
Hir1							-1		1	
Rgt1			1					-1		
Cha4						-1				-1

Table 6. Differential expression of TFs under metal stress. TFs that were found to be significantly up- (1) or down- (-1) regulated in at least two of the ten metal stress responses.

Metabolic network under acute metal stress

To associate the significantly differentially expressed genes (greater/minor than 2-fold) of the particular metal stress responses to common GO terms, we used GO Term Finder (http://www.yeastgenome.org/cgibin/GO/ goTermFinder.pl; Table 7). Notably, we observed no significant GO terms for the down-regulated genes, which might be due to their weak repression under the relatively low metal concentrations used in this study.

We noted that Al^{3+} induced a group of genes involved in RNA-mediated transposition. Similar to retroviral genes, these ubiquitous retrotransposon genes are transcribed into RNA, then reverse-transcribed into cDNA which at last integrates into new sites in the nuclear genome thereby generating mutations or genome rearrangements [40]. Ag^{+} and V^{3+} primarily activated the expression of metallothionein (MT) genes (As^{3+} and Zn^{2+} caused a weaker response), whereas Co^{2+} and Zn^{2+} especially induced siderophore iron homeostasis genes. As^{3+}, Cd^{2+}, and Hg^{2+} caused the activation of a variety of stress response genes encoding proteins involved in protein folding and aldehyde metabolism (As^{3+}), in sulfur compound metabolism (Cd^{2+}), and in the oxidative stress defense (Cd^{2+} and Hg^{2+}). Hg^{2+} and Mn^{2+} led to the up-regulation of a bulk of genes associated with amino acid metabolism, which might be regulated by Gcn4 and Gln3 as predicted by T Profiler analyses. Ni^{2+} generated a weak response lacking a significantly associated GO term.

Metals	GO terms	Gene names
Al	RNA-mediated transposition	YAR010C,YBL005W-A,YCL020W,YJR026W,YJR028W,YML040W,YML045W
Ag	Metal chelation	CUP1-1,CUP1-2
As	Protein folding	SSA1,HSP26,SSA4,SSC1,SSA2,HSP104,CPR6,HSP60,HSC82,YDJ1,STI1,HSP82
	Aldehyde metabolism	AAD3,AAD6,AAD16,AAD10,ADH6,AAD14,AAD15
Cd	Sulfur compound metabolism	CYS3,SAM2, MET2,MET3,MET5,MET6,MET14, MET16,MET17
	Response to oxidative stress	YBL055C,PRX1,YDL124W,AHP1,ZWF1
Co	Iron ion homeostasis	ARN1,ARN2,FET3,ENB1,FIT2
Hg	Amino acid metabolism	ARG1,ARG4,CPA2,HIS3,HIS4,LEU1,LEU2,LEU4,FMT1,ARO3,HOM2,HOM3,MET17
	Response to oxidative stress	YBL055C,PRX1,GPX2,YDL124W,TRR1,GRX2,TRX2,CCP1,AHP1,TSA1
	Response to stress	ATG8,PCL5,CCP1,DDR48
Mn	Amino acid metabolism	ARG1,ARG4,CPA2,HIS1,HIS3,HIS4,HIS5,HIS7,LEU4,LYS1,LYS9,LYS21,LYS20, BAT2,ACO1,ORT1,ARO3,TRP2,TRP3,TRP5,TRP4,ILV6,HOM2,MET17,MET22, SAM1,PRO2,GLN1,ASN1,CIT2,IDP1
	Siderophore iron transport	ARN1,ARN2,ENB1,FIT2
Ni	Amide metabolism	No significant GO term
V	Metal chelation	CUP1-1,CUP1-2
Zn	Siderophore iron transport	FIT1,TIS11,FIT2,FIT3

Table 7. Significant GO terms associated to the particular metal stress conditions. Genes differentially expressed greater than 2-fold in response to metal stress associated to significant GO terms by GO Term Finder;

Moreover, we enlarged the analysis spectrum and compared all genes differentially expressed upon at least two of the in total 10 metal stress conditions using K-means clustering. We annotated the gene clusters with significant GO terms using the Term Finder tool. The median fold induction/repression values of the GO terms were calculated and visualized to highlight

their significance (Figure 3). Analyses of transcriptional networks were in large part consistent with the findings in table 7 and revealed activation of metal-specific oxidative and general stress defense mechanisms, protein degradation, activation of nitrogen/amino acid biosynthesis, and iron ion homeostasis along with repression of ribosomal biogenesis and translation as the main response mechanisms of yeast cells upon acute metal stress.

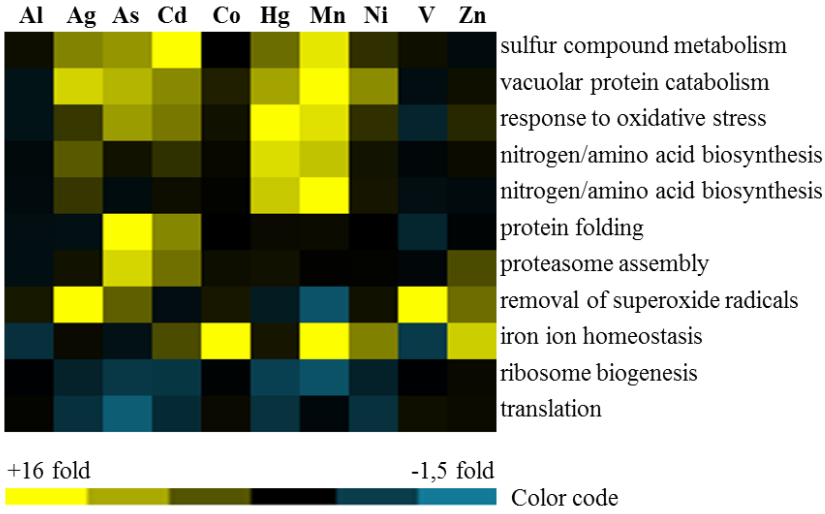

Figure 3. Transcript profile of acute metal stress. The results of the transcriptional metal stress responses following K-means clustering and association to significantly shared GO terms via the Term Finder tool were visualized using Java TreeView. Variations in transcript abundance for each GO pathway under the particular metal stress conditions were calculated as medial fold inductions and repressions, respectively, and depicted by means of color code in which shades of yellow represent increases and shades of blue decreases in mRNA levels, relative to the unstressed control culture. Black colors indicate an undetectable change in transcript level.

Figure 4 summarizes these findings in a hierarchical phylogram illustrating one bigger cluster with tight clustering of arsenic with cadmium and mercury with silver. Nickel and manganese clustered in proximate vicinity, whereas aluminium grouped together with vanadium in one separate cluster and cobalt and zinc clustered rather distinct.

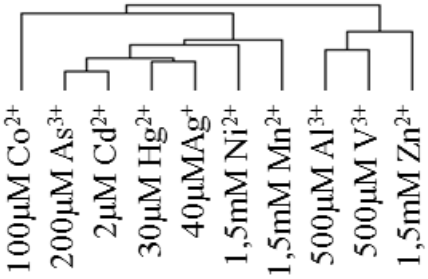

Figure 4. Hierarchical cluster analysis of acute metal stress responses. Metals were clustered due to similar expression patterns of the detected genes using cluster3 and the cluster result was visualized with TreeView.

Oxidative defense is the main detoxification response

Since several metal ions are known to induce oxidative stress, stimulation of the sulfur/GSH pathway and the thiol redox system (glutathione, thioredoxin) appear to be of a general nature for cellular defense against metal stress [41,42,43,44]. In this regard we observed variable oxidative defense responses against particular metal ions. Upon Ag^{+}, As^{3+}, Cd^{2+}, Hg^{2+}, and Mn^{2+} exposure we found significant induction of genes involved in the sulfur compound metabolism (e.g. *MET28*, *MET5*, *MET17*, *LAP3*, and *MET16*). This is consistent with recent studies in yeast, documenting the conversion of sulfur assimilates into glutathione as a result of arsenic and cadmium exposure [28,45]. Glutathione acts as a first line of defense against several stresses by sequestering and forming complexes with toxic metalloids [17,41,42,46]. Recently, vanadate (at higher concentrations than in this study) was shown to be converted to the less toxic vanadyl by cellular glutathione and other reducing components (e.g. cysteines) in the cell [47,48,49]. This substantiates the importance of reduction for detoxification of a broad range of metal ions.

Genes encoding proteins with antioxidative functions such as the glutathione peroxidase gene *GRX2* or the thioredoxin reductases *TRR1*, *TRR2*, and the above-mentioned *TRX2*, were significatly up-regulated by Hg^{2+} and Mn^{2+} and to a lesser degree by As^{3+} and Cd^{2+} (for *TRX2* also by Ag^{+}, Ni^{2+}, and Zn^{2+}; Table 4). Accordingly, we found oxidative stress responses upon all tested metal ions except aluminum, cobalt, and vanadium. This appears to be due to the low metal concentrations used in this study, because at higher concentrations aluminium and vanadium were shown to induce oxidative stress response as well [50,51]. Hence, our results indicate that metals generate oxidative stress in yeast cells and highlight the importance of oxidative defense mechanisms as the primary detoxification strategy against short-term metal exposure.

Metal chelation via siderophores may be an additional detoxification mechanism

In response to Co^{2+}, Mn^{2+}, $Ni,^{2+}$ and Zn^{2+} we observed significant induction of iron ion homeostasis genes, especially involved in high-affinity iron transport (*FET3* and *FTR1*) and siderophore iron transport (*ARN1*, *ARN2*, *SIT1/ARN3*, *ENB1/ARN4*, *FIT2*, and *FIT3*). Recent studies have shown that metals such as vanadium, aluminium, cobalt, nickel, and zinc interfere with iron homeostasis by competing with iron for iron-binding sites of transporters, enzymes, or diverse other iron-containing cellular proteins [52,53,54,55,56,57]. Iron depletion appears to be a common feature of several toxic metals. As a compensatory mechanism of resulting iron deprivation, iron uptake is activated by the iron-responsive TF Aft1 [58,59,60]. But increased iron uptake upon metal exposure was also suggested to serve a protective role by outpacing toxic metal ions [54]. This protective function might apply to the induction of the high affinity iron uptake system as above mentioned (Figure 5).

Moreover, we indicate that induction of the siderophore transport system of the Fit and Arn family might serve as an additional detoxification mechanism by chelating extracellular metal

ions to prevent their uptake (Figure 5). To that effect, vanadium has been reported to form complexes with siderophores of *Pseudomonas aeruginosa*, albeit internalization of the chelate complexes has not been shown [61]. However, a direct participation of the siderophore-mediated iron uptake system in metal detoxification still has to be proven.

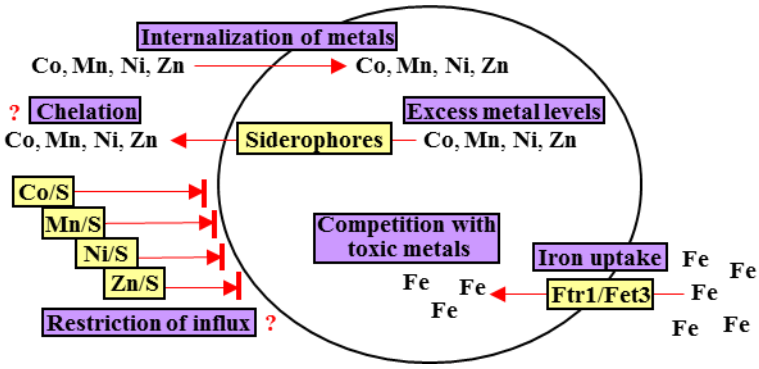

Figure 5. Hypothetic participation of the iron regulon under metal stress. Metals enter the cell and generate intracellular damage of proteins when they are in excess. The high-affinity iron uptake system is induced to internalize iron which intracellularly competes with toxic metals for protein binding sites. Simultaneously, transcription of siderophores (S) is activated. The siderophores are excreted and chelate toxic metals to prevent their uptake.

Protein degradation facilitates metal detoxification

Our transcript profiles revealed a strong induction of vacuolar protein catabolism genes (*PRB1*, *LAP4*, and *PEP4*) in response to Ag^{+}, As^{3+}, Cd^{2+}, and Mn^{2+} and to a lesser degree to Hg^{2+}, and Ni^{2+}. Genes (*RPN2*, *IRC25*, *HSP82*, and *PRE2*) involved in the assembly of the 26S proteasome that is responsible for non-vacuolar degradation of cellular proteins [62] were significantly activated under As^{3+} and Cd^{2+} exposition. Moreover, we observed a considerable induction of the protein folding pathway (*YDJ1*, *SSA1*, *SSA2*, *SSA3*, *SSA4*, *SSE1*, *HSP60*, *HSP104*, *CPR6*, *STI1*, and *HSP82*) as another important metal detoxification mechanism under As^{3+} and Cd^{2+} exposure. These genes encode proteins involved in the formation and activation of chaperone complexes functioning in folding and refolding of proteins [63,64], suppression and rescue of protein aggregates [65,66], and degradation of aberrant proteins [67].

Some further genes encoding proteins involved in catabolic processes were induced under particular metal stress conditions. For instance *SEC17* in response to Hg^{2+} and to a lesser degree to Al^{3+} and Cd^{2+} coding for a membrane protein required for vesicular transport between ER and Golgi, homotypic vacuole fusion, and autophagy. Yeast cells employ the catabolic process of autophagy to degrade damaged or obsolete organelles and proteins. Our results are in agreement with a previous study reporting that the yeast Sec19 vesicle transport system accounts for increased metal tolerance [68]. Finally, we found *VPS27* involved in ubiquitin-dependent protein catabolism in the vacuole up-regulated by Al^{3+}. In conclusion,

besides activation of oxidative defense mechanisms, degradation of damaged proteins appears to be the second main cellular detoxification mechanism under acute metal stress.

Histidine and other amino acids as putative metal scavengers upon Mn^{2+} and Hg^{2+}

We detected significant up-regulation of nitrogen/amino acid biosynthesis genes mainly including arginine (*ARG1*, *ARG4*, *CPA1*, and *CPA2*) and histidine (*HIS1*, *HIS3*, *HIS4*, and *HIS5*) in response to Mn^{2+} and Hg^{2+} (Table 7). For *S. cerevisiae* it has been shown that the accumulation of histidine in the vacuole decreases the toxicity of copper, cobalt and nickel [69]. Although the exact process of vacuolar sequestration via histidine remains unclear, histidine and histidine-rich proteins were suggested to form complexes with toxic metal ions to prevent them to interact with physiologically important cellular proteins [70]. The remarkably increased synthesis of gene products involved in arginine biosynthesis besides histidine suggests that this amino acid may play similar roles in conferring resistance to metal ions and in attenuating metal toxicity.

Restriction of protein synthesis diverts homeostatic energy to enhanced metal detoxification

The majority of repressed genes upon Ag^{+}, As^{3+}, Cd^{2+}, Hg^{2+}, Mn^{2+}, and Ni^{2+} exposure were involved in growth-related processes such as ribosomal biogenesis and translation. This appears to be a general feature of metal stress and has been noted and discussed in previous studies [19,38,71]. Ribosome biogenesis requires the activity of all three RNA polymerases, which are suggested to be coordinated by the evolutionarily conserved target of rapamycin (TOR)-PKA pathway. This pathway is a major signaling network mediating growth regulation in eukaryotes [72,73,74].

Recently, we substantiated that As^{3+}, Cd^{2+}, and Ni^{2+} stress deactivate Sfp1 a TOR complex 1 (TORC1) kinase regulated transcriptional activator. Sfp1 deactivation leads to dissociation of Sfp1 from chromatin, relocation of Sfp1 from nucleus to cytosol, and subsequent reduction of ribosomal protein (RP) gene transcription [36]. We further proved that Ag^{2+}, Cd^{2+}, Co^{2+}, and Mn^{2+} did not affect Sfp1 activity (data not shown) suggesting the participation of further regulators apart from Sfp1. Previous reports also implicated Rap1 and Fhl1 in the regulation of ribosomal biogenesis [28,36,75]. This is in line with T Profiler analysis (Table 6) which predicted all three TFs (Fhl1, Rap1, and Sfp1) as negative regulators upon almost all metals (Ag^{+}-, As^{3+}-, Cd^{2+}-, Hg^{2+}-, Ni^{2+}-, and V^{3+} except Mn^{2+}). Though, a direct effect of these TFs on the repression of RP biosynthesis remains to be determined in response to the particular metal stress conditions.

In rapidly growing yeast cells RP mRNAs contribute to nearly 30% of the total mRNAs and therefore constitute major consumers of cellular resources [76,77,78]. In this regard, restriction of ribosome biogenesis might serve the purpose as energy saving during the cellular metal defense. The decrease (with increasing metal concentrations) of *de novo RP* biosynthesis and growth reduction under acute metal stress may allow energy to be diverted to

the increased expression of genes involved in stress response and specific detoxification mechanisms.

Yeast cells appear to adapt to sustained metal stress (up to 2h)

To prove the uniqueness of our results we compared our transcriptional data (40µM Ag^{+}, 200µM As^{3+}, 2µM Cd^{2+}, 30µM Hg^{2+}, and 1,5mM Zn^{2+}) of acute metal stress (30min) with those of sustained metal stress (2h) of one recent study (20µM Ag^{+}, 400µM As^{3+}, 5µM Cd^{2+}, 19µM Hg^{2+}, and 1mM Zn^{2+}; [20]). We selected genes differentially expressed greater/minor than 1.5-fold and found a total of 456 genes (338 up- and 118 down-regulated) in the data set of this study, whereas the Jin data set revealed a total of 1090 genes (538 up- and 552 down-regulated).

In comparison of the particular metal stress conditions of both data sets we observed a surprisingly small overlap of 37% of the genes detected under acute metal stress with 5% of the genes detected under sustained metal stress. The minimal overlap of simultaneously expressed genes (greater/minor than 1.2-fold) was found upon Ag^{+} and Zn^{2+} (18 genes), followed by Hg^{2+} (30), Cd^{2+} (38), and As^{3+} (64; Figure 6A). Notably, another recent study also revealed relatively poor overlaps in terms of mutants between differently published genome-wide phenotypic screens which were based on similar metal sensitivity data. But despite the discrepancy of the largely non-overlapping gene sets these screens revealed different mutants encoding proteins in the same homeostatic pathway [44]. Therefore, comparisons between inconsistent expression data sets might similarily provide relevant indication of effective biological processes.

In this regard, we associated the detected genes to significant GO terms by GO Term Finder as well as by T Profiler (Figure 6B and C) and investigated the affected pathways. The overlapping genes of both data sets coded for proteins involved in the oxidative and general stress response, in the sulfur compound and amino acid metabolism, in transport processes, and in iron homeostasis (Figure 6B). These metabolic pathways appear to include the essential stress response of yeast cells under acute and sustained metal exposure.

The uniquely induced genes were 3- (Cd^{2+}, Hg^{2+}) to 7-fold (Zn^{2+}) and the uniquely repressed genes 7- (As^{3+}) to 59-fold (Ag^{+}) increased under sustained compared to acute metal exposure (Figure 6A). In this context, the early-on effects of metal stress (30min) mainly comprised the induction of specific oxidative and general stress response strategies, cell wall organization, amino acid biosynthesis, chaperon complex activities, proteolytic processes, and aldehyde metabolism along with the repression of translation and ribosome biogenesis. Sustained metal treatment of yeast cells up to 2h primarily evoked the up-regulation of specific iron homeostasis and sulfur compound metabolism genes, ribosome biogenesis, and nucleic acid metabolism along with the down-regulation of energy generation processes, cellular respiration as well as glycine and glutamate metabolism (Figure 6C).

Taken together, these results indicate a certain stress release and adaptation to sustained metal exposure via effective metal detoxification. One indication is the activation of additional detoxification pathways in response to acute metal stress, which were not detectable at 2h. Moreover, growth-related processes that were initially repressed were reactivated upon continued metal treatment (except under 1250µM As^{3+}; [20]). However, whether yeast cells indeed adapt to sustained metal stress by generating similar expression patterns, still needs to be proven by means of a consistent experimental setup.

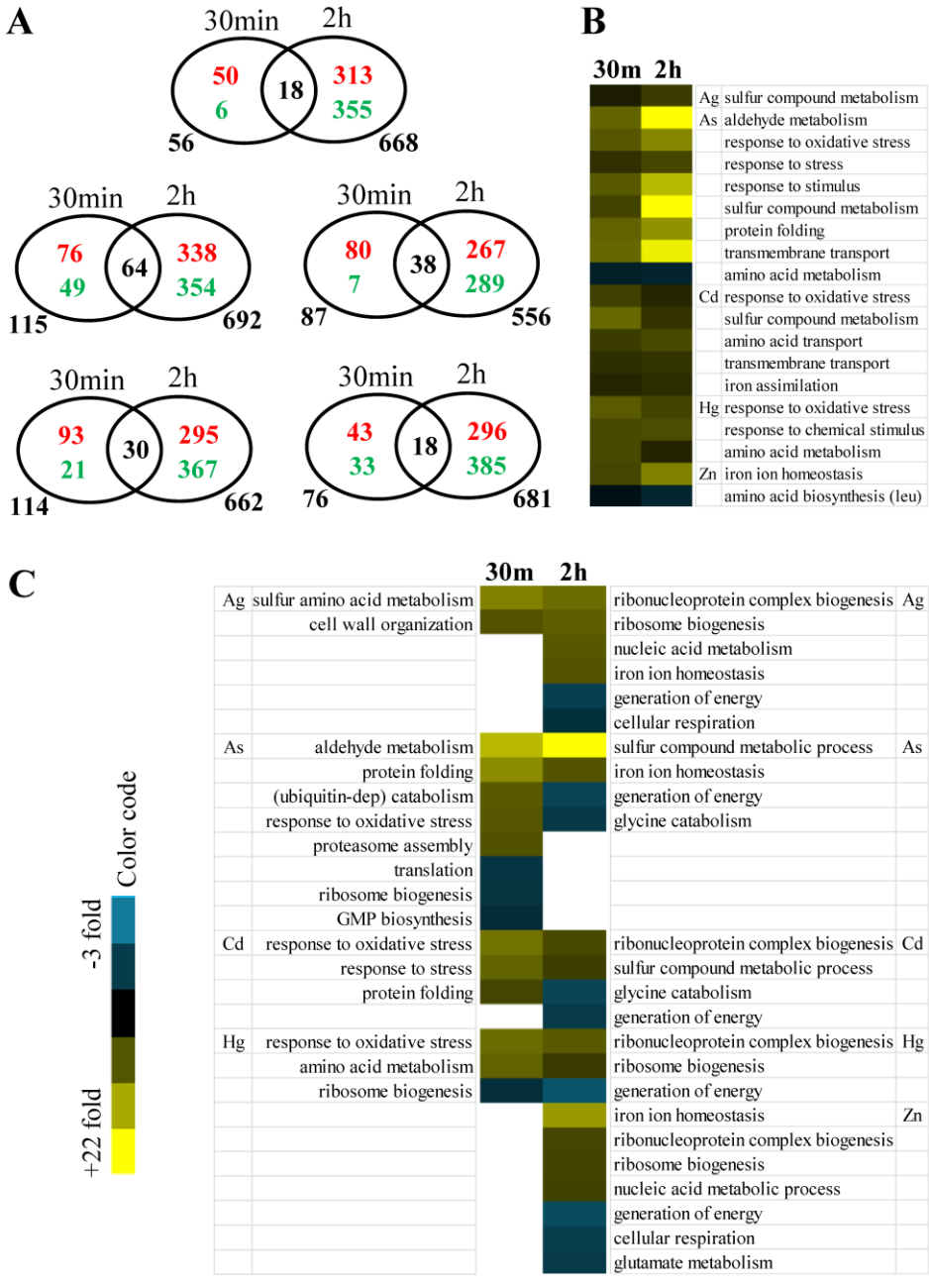

Figure 6. Comparison of transcript profiles upon acute and sustained metal stress. A) Venn diagrams illustrate the distribution of transcriptionally up-regulated (red) and down-regulated (green) genes from metal-stressed BY*wt* cells (30min and 2h). **B)** Gene expression overlaps between both data sets and **C)** individually expressed genes in both data sets associated to significant GO terms by GO Term Finder and T Profiler;

Conclusions

We investigated the early stress response of logarithmically growing *S. cerevisiae* cells upon ten biologically relevant metal ions with Cd^{2+} as the most toxic one, followed by Hg^{2+}, Ag^{+}, As^{3+}, Co^{2+}, Al^{3+}, V^{+}, Ni^{2+}, Mn^{2+}, and Zn^{2+}. In total 1023 genes were significantly differentially expressed by a factor greater/minor than ±50% corresponding to 16.5% of the entire yeast genome. With the aid of similarity analyses between the transcript profiles we provided evidence that yeast cells do not have a common detoxification mechanism for metal ions but respond highly specifically. However, As^{3+}, Cd^{2+}, Hg^{2+}, and Ag^{+} induced similar detoxification mechanisms with shared predicted regulatory associations such as the stress response TFs Msn2, Msn4, Rpn4, Hsf1, Met4, Yap1, and Yap1 homologues. Other smaller cluster included Hg^{2+} and Mn^{2+} with the putative regulators Gcn4 and Gln3, or Ni^{2+}, Mn^{2+}, Co^{2+}, and V^{3+} which were indicated to evoke activation of Aft1 and Aft2), .

For all metal ions tested the primary transcriptional response to acute metal stress was activation of oxidative defense strategies and protein degradation processes, most likely to remove damaged cellular components (Table 8). We detected antioxidant activity effected by the glutathione/thioredoxin system in response to Ag^{+}, As^{3+}, Cd^{2+}, Hg^{2+}, Mn^{2+}, and Ni^{2+} and by metallothionein chelation upon Ag^{+}, As^{3+}, V^{3+}, and Zn^{2+}. Moreover, we suggested chelation of metal ions via siderophores upon Co^{2+}, Mn^{2+}, Ni^{2+}, and Zn^{2+} as an additional detoxification mechanism. We also observed expression responses pointing to chelation with histidine and other amino acids like arginine in response to Hg^{2+} and Mn^{2+}. The most prominent transcriptional induction of catabolic strategies during immediate metal stress comprised vacuolar protein degradation upon Ag^{+}, As^{3+}, Cd^{2+}, Hg^{2+}, Mn^{2+}, and Ni^{2+}, 26S proteasomal proteolysis and chaperone complex activities upon As^{3+} and Cd^{2+}), as well as Sec19 vesicle transport upon Al^{3+}, Cd^{2+}, and Hg^{2+}.

Metal detoxification strategies	Ag	Al	As	Cd	Co	Hg	Mn	Ni	V	Zn
Antioxidant activity										
Glutathione/thioredoxin system	+		+	+		+	+	+		
Metallothionein chelation	+		+						+	+
Catabolic processes										
Vacuolar protein catabolism	+	+	+	+		+	+	+		
Non-vacuolar 26S proteolysis			+	+						
Chaperone complex formation			+	+						
Sec19 vesicle transport		+		+		+				
Siderophore iron homeostasis					+		+	+		+
Histidine and other aa biosynthesis						+	+			

Table 8. Summary of metal detoxification strategies under acute metal stress. Based on Cluster analyses, up-regulation of the indicated metal detoxification strategies upon the distinct metal stress conditions is assigned by "+" in the table.

On the other hand, we observed reduction of ribosomal biogenesis and translation as the main common gene repression effect under acute Ag^{+}, As^{3+}, Cd^{2+}, Hg^{2+}, Mn^{2+}, and Ni^{2+} exposure. T profiler analysis predicted the involved genes to be regulated by Fhl1, Rap1, and Sfp1. Restriction of growth-related processes was suggested to save cellular energy for diverting it to the increased induction of metal detoxification processes. Finally, we compared our gene expression analysis data with a recently generated metal stress response data set and provided indication of transcriptional adaptation of yeast cells to sustained metal stress. In contrast to acute metal stress we delineated reactivation of ribosomal biogenesis and translation along with reduction of metal detoxification pathways under sustained metal exposure. However, this assumption has to be proven by a consistent time course analysis upon metal stress.

Materials and Methods

Metal Toxicity Assays

For determination of the Minimal Inhibitory Concentration (MIC) and the 50% growth inhibition upon heavy metal treatment in *S. cerevisiae*, the effect of 10 biologically relevant metal ions (Ag^{+}, Al^{3+} , As^{3+} , Cd^{2+} , Co^{2+} , Hg^{2+} , Mn^{2+} , Ni^{2+} , V^{+} , and Zn^{2+}) on yeast growth was examined. BY-4741 overnight cultures (MATa leu2 ura3 his3 met15 can1) were diluted in liquid YPD (2% yeast-extract, 1% polypeptone, 2% glucose, pH 6.4) to an optical density OD_{600} of ~0.15 and grown to ~0.8 at 30°C. The cultures were then supplemented with increasing concentrations of dissolved metal ions and incubated at 30°C. Yeast growth was monitored via optical density. Each metal toxicity analysis consisted of one control and up to 5 test concentrations with growth inhibition scored between >0% and <100%. For each tested metal ion at least three replicate tests were carried out on different days. The Minimal Inhibitory Concentration (MIC) was set as lower threshold inducing 5% growth inhibition and the 50% growth inhibition (GI) as upper threshold compared to the mean growth of the control cultures. Based on these values (Table 1) the concentrations for expression profiling were chosen.

Preparation of Yeast RNA

Over-night cultures were diluted with 50ml fresh liquid YPD medium to an OD_{600} of ~0.15 as start inoculum, grown to OD_{600}~0.8, and treated with the indicated concentrations of dissolved metal salts (EP in Table 1), incubated for 30min at 30°C, harvested at 3000 rpm, washed in 1ml ice-cold DEPC-H_2O, reharvested and frozen at -80°C. Total RNA was prepared by hot acidic phenol extraction according to Ausubel et al. (1997) with three chloroform extractions.

Microarrays

Fluorescently labeled cDNA was synthesized from 15µg of total RNA by oligo dT-primed polymerization using 200 U Superscript II (Invitrogen, Carlsbad, CA) and Cy3-CTP or Cy5-CTP (GE Healthcare, Waukesha, WI). Labeled cDNAs were pooled and RNA was hydrolyzed for 20min in 10N NaOH at 65°C, neutralized with 5M acetic acid, and purified by the Cy Scribe GFX purification kit (GE Healthcare). Microarrays (obtained from Microarray Centre Toronto, Ontario, CAN) containing PCR fragments of 6144 predicted *S. cerevisiae* open-reading-frames (ORFs) spotted in duplicates were used for expression profiling. Hybridization was performed for 14-18h in DigEasyHyb solution (Roche Diagnostics, Basel, Switzerland) with 0,1mg/ml salmon sperm DNA (Sigma, St Louis, MO) as a carrier solution at 37°C. After hybridization, microarrays were washed three times in 1×SSC, and 0,1% SDS at 50°C for 10min, followed by 1min in 1×SSC and 0,1%×SSC at RT and a 5min 500rpm spin to dryness. All microarray experiments were performed in triplicate including the necessary dye swap. In total 31 images of slides were used for further evaluation.

Microarray Reading Analysis

The microarrays were scanned using an Axon GenePix 4000B scanner (Molecular Devices, Sunnyvale, CA). The image data were quantified using the GenePix Pro4.1 software (Molecular Devices) that returns quantitative intensities for each spot. Raw data are available under the ArrayExpress (http://www.ebi.ac.uk/arrayexpress/) accession nos. E-MEXP-2985 and E-MEXP-2987.

Computational processing and data analysis

The data preprocessing and the differential expression tests have been performed by using the R computing environment and several software packages from the Bioconductor project (http://www.bioconductor.org), particular the Limma package [79]. For the present evaluations the background correction method “normexp” developed by Ritchie et al. [80] was applied. With this method a convolution of normal and exponential distributions is fitted to the foreground intensities by using the ambient signal as a covariate. The expected signal given by the observed foreground becomes the corrected intensity. An offset-value (numeric value to add to intensities) of 50 was chosen as is recommended [80,81]. This approach resulted in a smooth monotonic transformation of the already background corrected intensities. Typical problems such as negative corrected intensities and high variability of low intensity log-ratios were thus avoided [80,81].

All spots with missing values as well as "bad"-spots with illegal shape were zero weight allocated for all further normalization and analysis steps. The corrected intensities were used to form the log-ratio and the average log-intensity for each spot. Normalization was performed using the robust spline normalization [82] which is an empirical Bayes

compromise between Print-tip and Global Loess normalization with 5-parameter regression splines used in place of the Loess curves.

Afterwards a quantile normalization [83] between all arrays ensured that the average intensities show the same empirical distribution across arrays and across channels. The quantile normalization approach first ranked data on each array and substituted data of the same rank across all arrays by the mean of the data.

The moderate t-statistic to a multidimensional case (generalized and implemented in the Bioconductor package Limma by Smyth et al. [79,84]) was used to detect differentially expressed genes as follows: For each gene six data points were available arising from the three performed experimental replicates (independent arrays) where each of the replicates contained two spots with the same probe. A linear model was fitted to the expression of each probe [79,84]. Replications of the same treatment were merged in the calculation due to the consideration of dye-swaps. Duplicated spots within a single array were evaluated using a pooled correlation method to make full use of the information [84]. The p-value adjustment method from Benjamini and Hochberg was chosen to control the false discovery rate, which is the expected proportion of false discoveries amongst the rejected hypotheses [85]. Genes were ranked in order of evidence for differential expression of the stressed samples in comparison to the reference sample in each experiment. All genes that appeared significantly differentially expressed after the normalization process (showing at least a +/- 50% deviation from normal conditions) were taken into account for further analysis and a descriptive statistic approach. The identification of commonly expressed genes was performed using the R script "overlapper.r" (http://faculty.ucr.edu/~tgirke/Documents/R_BioCond/My_R_Scripts/overLapper.R).

Cluster analysis [86,87] were performed using the cluster3 and visualized with TreeView [88]. For further data evaluation, clustering algorithms using the Matlab Bioinformatics toolbox were applied to identify groups of genes with similar expression profiles for the time point "30 minutes" after metal exposition. Significant associations to gene ontology (GO)-terms and regulatory associations were obtained by GO Term Finder provided by SGD (http://www.yeastgenome.org/cgibin/GO/goTermFinder.pl) and T Profiler (http://www.t-profiler.org/).

Acknowledgments

This work was supported by the the German Ministry for Eduction and Research (BMBF grant for the SysMO project Translucent), by the Swiss HP2C-initiative "Swiss Platform for High-Performance and High-Productivity Computing", and the Austrian science fund

FWFgrant P23355 (to CS). And we wish to thank Rudolf J. Schweyen, who passed away in 2009, for fruitful discussions and general support.

References

1. Waldron KJ, Rutherford JC, Ford D, Robinson NJ (2009) Metalloproteins and metal sensing. Nature 460: 823-830.
2. Ballatori N (2002) Transport of toxic metals by molecular mimicry. Environ Health Perspect 110 Suppl 5: 689-694.
3. Halliwell B, Gutteridge JM (1984) Oxygen toxicity, oxygen radicals, transition metals and disease. Biochem J 219: 1-14.
4. Leonard S, Gannett PM, Rojanasakul Y, Schwegler-Berry D, Castranova V, et al. (1998) Cobalt-mediated generation of reactive oxygen species and its possible mechanism. J Inorg Biochem 70: 239-244.
5. Ercal N, Gurer-Orhan H, Aykin-Burns N (2001) Toxic metals and oxidative stress part I: mechanisms involved in metal-induced oxidative damage. Curr Top Med Chem 1: 529-539.
6. Valko M, Morris H, Cronin MT (2005) Metals, toxicity and oxidative stress. Curr Med Chem 12: 1161-1208.
7. Porwol T, Ehleben W, Zierold K, Fandrey J, Acker H (1998) The influence of nickel and cobalt on putative members of the oxygen-sensing pathway of erythropoietin-producing HepG2 cells. Eur J Biochem 256: 16-23.
8. Chrestensen CA, Starke DW, Mieyal JJ (2000) Acute cadmium exposure inactivates thioltransferase (Glutaredoxin), inhibits intracellular reduction of protein-glutathionyl-mixed disulfides, and initiates apoptosis. J Biol Chem 275: 26556-26565.
9. Westwater J, McLaren NF, Dormer UH, Jamieson DJ (2002) The adaptive response of *Saccharomyces cerevisiae* to mercury exposure. Yeast 19: 233-239.
10. Qiu JW, Xie ZC, Wang WX (2005) Effects of calcium on the uptake and elimination of cadmium and zinc in Asiatic clams. Arch Environ Contam Toxicol 48: 278-287.
11. Belcastro M, Marino T, Russo N, Toscano M (2005) Interaction of cysteine with Cu^{2+} and group IIb (Zn^{2+}, Cd^{2+}, Hg^{2+}) metal cations: a theoretical study. J Mass Spectrom 40: 300-306.
12. Stohs SJ (1995) The role of free radicals in toxicity and disease. J Basic Clin Physiol Pharmacol 6: 205-228.
13. Chen F, Shi X (2002) Intracellular signal transduction of cells in response to carcinogenic metals. Crit Rev Oncol Hematol 42: 105-121.
14. Dandrea T, Hellmold H, Jonsson C, Zhivotovsky B, Hofer T, et al. (2004) The transcriptosomal response of human A549 lung cells to a hydrogen peroxide-generating system: relationship to DNA damage, cell cycle arrest, and caspase activation. Free Radic Biol Med 36: 881-896.
15. Beyersmann D, Hartwig A (2008) Carcinogenic metal compounds: recent insight into molecular and cellular mechanisms. Arch Toxicol 82: 493-512.
16. Nies DH (1999) Microbial heavy-metal resistance. Appl Microbiol Biotechnol 51: 730-750.

17. Rosen BP (2002) Transport and detoxification systems for transition metals, heavy metals and metalloids in eukaryotic and prokaryotic microbes. Comp Biochem Physiol A Mol Integr Physiol 133: 689-693.
18. Mager WH, De Kruijff AJ (1995) Stress-induced transcriptional activation. Microbiol Rev 59: 506-531.
19. Gasch AP, Spellman PT, Kao CM, Carmel-Harel O, Eisen MB, et al. (2000) Genomic expression programs in the response of yeast cells to environmental changes. Mol Biol Cell 11: 4241-4257.
20. Jin YH, Dunlap PE, McBride SJ, Al-Refai H, Bushel PR, et al. (2008) Global transcriptome and deletome profiles of yeast exposed to transition metals. PLoS Genet 4: e1000053.
21. Wysocki R, Tamas MJ How *Saccharomyces cerevisiae* copes with toxic metals and metalloids. FEMS Microbiol Rev 34: 925-951.
22. Brazma A, Hingamp P, Quackenbush J, Sherlock G, Spellman P, et al. (2001) Minimum information about a microarray experiment (MIAME)-toward standards for microarray data. Nat Genet 29: 365-371.
23. McLachlan GJ, Do K-A, Ambroise C (2004) Analyzing microarray gene expression data. Hoboken, N.J.: Wiley-Interscience. xx, 320 p. p.
24. Tavazoie S, Hughes JD, Campbell MJ, Cho RJ, Church GM (1999) Systematic determination of genetic network architecture. Nat Genet 22: 281-285.
25. Jaccard P (1912) The distribution of flora in the alpine zone *New Phytologist* 11: 37-50.
26. Harbison CT, Gordon DB, Lee TI, Rinaldi NJ, Macisaac KD, et al. (2004) Transcriptional regulatory code of a eukaryotic genome. Nature 431: 99-104.
27. Boorsma A, Foat BC, Vis D, Klis F, Bussemaker HJ (2005) T-profiler: scoring the activity of predefined groups of genes using gene expression data. Nucleic Acids Res 33: W592-595.
28. Haugen AC, Kelley R, Collins JB, Tucker CJ, Deng C, et al. (2004) Integrating phenotypic and expression profiles to map arsenic-response networks. Genome Biol 5: R95.
29. Jelinsky SA, Estep P, Church GM, Samson LD (2000) Regulatory networks revealed by transcriptional profiling of damaged *Saccharomyces cerevisiae* cells: Rpn4 links base excision repair with proteasomes. Mol Cell Biol 20: 8157-8167.
30. Wheeler GL, Trotter EW, Dawes IW, Grant CM (2003) Coupling of the transcriptional regulation of glutathione biosynthesis to the availability of glutathione and methionine via the Met4 and Yap1 transcription factors. J Biol Chem 278: 49920-49928.
31. Su NY, Ouni I, Papagiannis CV, Kaiser P (2008) A dominant suppressor mutation of the met30 cell cycle defect suggests regulation of the *Saccharomyces cerevisiae* Met4-Cbf1 transcription complex by Met32. J Biol Chem 283: 11615-11624.
32. Dormer UH, Westwater J, McLaren NF, Kent NA, Mellor J, et al. (2000) Cadmium-inducible expression of the yeast *GSH1* gene requires a functional sulfur-amino acid regulatory network. J Biol Chem 275: 32611-32616.
33. Mueller PP, Hinnebusch AG (1986) Multiple upstream AUG codons mediate translational control of *GCN4*. Cell 45: 201-207.
34. Natarajan K, Meyer MR, Jackson BM, Slade D, Roberts C, et al. (2001) Transcriptional profiling shows that Gcn4p is a master regulator of gene expression during amino acid starvation in yeast. Mol Cell Biol 21: 4347-4368.
35. Sosa E, Aranda C, Riego L, Valenzuela L, DeLuna A, et al. (2003) Gcn4 negatively regulates expression of genes subjected to nitrogen catabolite repression. Biochem Biophys Res Commun 310: 1175-1180.

36. Martin DE, Soulard A, Hall MN (2004) TOR regulates ribosomal protein gene expression via PKA and the Forkhead transcription factor *FHL1*. Cell 119: 969-979.
37. Cipollina C, van den Brink J, Daran-Lapujade P, Pronk JT, Porro D, et al. (2008) *Saccharomyces cerevisiae SFP1*: at the crossroads of central metabolism and ribosome biogenesis. Microbiology 154: 1686-1699.
38. Hosiner D, Lempiainen H, Reiter W, Urban J, Loewith R, et al. (2009) Arsenic toxicity to *Saccharomyces cerevisiae* is a consequence of inhibition of the TORC1 kinase combined with a chronic stress response. Mol Biol Cell 20: 1048-1057.
39. Miyoshi K, Shirai C, Mizuta K (2003) Transcription of genes encoding trans-acting factors required for rRNA maturation/ribosomal subunit assembly is coordinately regulated with ribosomal protein genes and involves Rap1 in *Saccharomyces cerevisiae*. Nucleic Acids Res 31: 1969-1973.
40. Boeke JD, S.B. S (1991) Yeast transposable elements. The molecular and cellular biology of the yeast *Saccharomyces*, eds Broach J, Jones E, Pringle J(Cold Spring Harbor Laboratory Press, Cold Spring Harbor, NY) 1: 193–261.
41. Vido K, Spector D, Lagniel G, Lopez S, Toledano MB, et al. (2001) A proteome analysis of the cadmium response in *Saccharomyces cerevisiae*. J Biol Chem 276: 8469-8474.
42. Momose Y, Iwahashi H (2001) Bioassay of cadmium using a DNA microarray: genome-wide expression patterns of *Saccharomyces cerevisiae* response to cadmium. Environ Toxicol Chem 20: 2353-2360.
43. Thorsen M, Lagniel G, Kristiansson E, Junot C, Nerman O, et al. (2007) Quantitative transcriptome, proteome, and sulfur metabolite profiling of the *Saccharomyces cerevisiae* response to arsenite. Physiol Genomics 30: 35-43.
44. Thorsen M, Perrone GG, Kristiansson E, Traini M, Ye T, et al. (2009) Genetic basis of arsenite and cadmium tolerance in *Saccharomyces cerevisiae*. BMC Genomics 10: 105.
45. Fauchon M, Lagniel G, Aude JC, Lombardia L, Soularue P, et al. (2002) Sulfur sparing in the yeast proteome in response to sulfur demand. Mol Cell 9: 713-723.
46. Tamas MJ, Wysocki R (2001) Mechanisms involved in metalloid transport and tolerance acquisition. Curr Genet 40: 2-12.
47. Macara IG, Kustin K, Cantley LC, Jr. (1980) Glutathione reduces cytoplasmic vanadate. Mechanism and physiological implications. Biochim Biophys Acta 629: 95-106.
48. Willsky GR, Leung JO, Offermann PV, Jr., Plotnick EK, Dosch SF (1985) Isolation and characterization of vanadate-resistant mutants of *Saccharomyces cerevisiae*. J Bacteriol 164: 611-617.
49. Crans DC, Zhang B, Gaidamauskas E, Keramidas AD, Willsky GR, et al. (2010) Is vanadate reduced by thiols under biological conditions? Changing the redox potential of V(V)/V(IV) by complexation in aqueous solution. Inorg Chem 49: 4245-4256.
50. Richards KD, Schott EJ, Sharma YK, Davis KR, Gardner RC (1998) Aluminum induces oxidative stress genes in *Arabidopsis thaliana*. Plant Physiol 116: 409-418.
51. Soares SS, Martins H, Gutiérrez-Merino C, Aureliano M (2008) Vanadium and cadmium in vivo effects in teleost cardiac muscle: metal accumulation and oxidative stress markers. Comp Biochem Physiol C Toxicol Pharmacol 147:168-178.
52. Saponja JA, Vogel HJ (1996) Metal-ion binding properties of the transferrins: a vanadium-51 NMR study. J Inorg Biochem 62: 253-270.
53. Ward RJ, Zhang Y, Crichton RR (2001) Aluminium toxicity and iron homeostasis. J Inorg Biochem 87: 9-14.
54. Stadler JA, Schweyen RJ (2002) The yeast iron regulon is induced upon cobalt stress and crucial for cobalt tolerance. J Biol Chem 277: 39649-39654.

55. Chen H, Davidson T, Singleton S, Garrick MD, Costa M (2005) Nickel decreases cellular iron level and converts cytosolic aconitase to iron-regulatory protein 1 in A549 cells. Toxicol Appl Pharmacol 206: 275-287.
56. Pagani MA, Casamayor A, Serrano R, Atrian S, Arino J (2007) Disruption of iron homeostasis in *Saccharomyces cerevisiae* by high zinc levels: a genome-wide study. Mol Microbiol 65: 521-537.
57. Ruotolo R, Marchini G, Ottonello S (2008) Membrane transporters and protein traffic networks differentially affecting metal tolerance: a genomic phenotyping study in yeast. Genome Biol 9: R67.
58. Yamaguchi-Iwai Y, Dancis A, Klausner RD (1995) *AFT1*: a mediator of iron regulated transcriptional control in *Saccharomyces cerevisiae*. EMBO J 14: 1231-1239.
59. Rutherford JC, Ojeda L, Balk J, Muhlenhoff U, Lill R, et al. (2005) Activation of the iron regulon by the yeast Aft1/Aft2 transcription factors depends on mitochondrial but not cytosolic iron-sulfur protein biogenesis. J Biol Chem 280: 10135-10140.
60. Philpott CC, Protchenko O (2008) Response to iron deprivation in *Saccharomyces cerevisiae*. Eukaryot Cell 7: 20-27.
61. Baysse C, De Vos D, Naudet Y, Vandermonde A, Ochsner U, et al. (2000) Vanadium interferes with siderophore-mediated iron uptake in *Pseudomonas aeruginosa*. Microbiology 146 (Pt 10): 2425-2434.
62. Hochstrasser M (1996) Ubiquitin-dependent protein degradation. Annu Rev Genet 30: 405-439.
63. Nathan DF, Vos MH, Lindquist S (1997) In vivo functions of the *Saccharomyces cerevisiae* Hsp90 chaperone. Proc Natl Acad Sci U S A 94: 12949-12956.
64. Kim S, Schilke B, Craig EA, Horwich AL (1998) Folding in vivo of a newly translated yeast cytosolic enzyme is mediated by the SSA class of cytosolic yeast Hsp70 proteins. Proc Natl Acad Sci U S A 95: 12860-12865.
65. Glover JR, Lindquist S (1998) Hsp104, Hsp70, and Hsp40: a novel chaperone system that rescues previously aggregated proteins. Cell 94: 73-82.
66. Abbas-Terki T, Donze O, Briand PA, Picard D (2001) Hsp104 interacts with Hsp90 cochaperones in respiring yeast. Mol Cell Biol 21: 7569-7575.
67. Lee DH, Sherman MY, Goldberg AL (1996) Involvement of the molecular chaperone Ydj1 in the ubiquitin-dependent degradation of short-lived and abnormal proteins in *Saccharomyces cerevisiae*. Mol Cell Biol 16: 4773-4781.
68. Ezaki B, Sasaki K, Matsumoto H, Nakashima S (2005) Functions of two genes in aluminium (Al) stress resistance: repression of oxidative damage by the *AtBCB* gene and promotion of efflux of Al ions by the *NtGDI1*gene. J Exp Bot 56: 2661-2671.
69. Pearce DA, Sherman F (1999) Toxicity of copper, cobalt, and nickel salts is dependent on histidine metabolism in the yeast *Saccharomyces cerevisiae*. J Bacteriol 181: 4774-4779.
70. Farcasanu IC, Mizunuma M, Nishiyama F, Miyakawa T (2005) Role of L-histidine in conferring tolerance to Ni^{2+} in *Sacchromyces cerevisiae* cells. Biosci Biotechnol Biochem 69: 2343-2348.
71. Wu LF, Hughes TR, Davierwala AP, Robinson MD, Stoughton R, et al. (2002) Large-scale prediction of *Saccharomyces cerevisiae* gene function using overlapping transcriptional clusters. Nat Genet 31: 255-265.
72. Loewith R, Jacinto E, Wullschleger S, Lorberg A, Crespo JL, et al. (2002) Two TOR complexes, only one of which is rapamycin sensitive, have distinct roles in cell growth control. Mol Cell 10: 457-468.

73. Schmelzle T, Beck T, Martin DE, Hall MN (2004) Activation of the RAS/cyclic AMP pathway suppresses a TOR deficiency in yeast. Mol Cell Biol 24: 338-351.
74. Wullschleger S, Loewith R, Hall MN (2006) TOR signaling in growth and metabolism. Cell 124: 471-484.
75. Li B, Nierras CR, Warner JR (1999) Transcriptional elements involved in the repression of ribosomal protein synthesis. Mol Cell Biol 19: 5393-5404.
76. Holstege FC, Jennings EG, Wyrick JJ, Lee TI, Hengartner CJ, et al. (1998) Dissecting the regulatory circuitry of a eukaryotic genome. Cell 95: 717-728.
77. Warner JR (1999) The economics of ribosome biosynthesis in yeast. Trends Biochem Sci 24: 437-440.
78. Grigull J, Mnaimneh S, Pootoolal J, Robinson MD, Hughes TR (2004) Genome-wide analysis of mRNA stability using transcription inhibitors and microarrays reveals posttranscriptional control of ribosome biogenesis factors. Mol Cell Biol 24: 5534-5547.
79. Smyth GK (2004) Linear models and empirical bayes methods for assessing differential expression in microarray experiments. Stat Appl Genet Mol Biol 3: Article3.
80. Ritchie ME, Silver J, Oshlack A, Holmes M, Diyagama D, et al. (2007) A comparison of background correction methods for two-colour microarrays. Bioinformatics 23: 2700-2707.
81. Silver JD, Ritchie ME, Smyth GK (2009) Microarray background correction: maximum likelihood estimation for the normal-exponential convolution. Biostatistics 10: 352-363.
82. Smyth GK, Speed T (2003) Normalization of cDNA microarray data. Methods 31: 265-273.
83. Bolstad BM, Irizarry RA, Astrand M, Speed TP (2003) A comparison of normalization methods for high density oligonucleotide array data based on variance and bias. Bioinformatics 19: 185-193.
84. Smyth GK, Gentleman R, Carey V, Dudoit S, Irizarry R, et al. (2005) Limma: linear models for microarray data. In: Bioinformatics and Computational Biology Solutions using R and Bioconductor *Springer, New York.*
85. Benjamini Y, Hochberg Y (1995) Controlling the false discovery rate: a practical and powerful approach to multiple testing *Journal of the Royal Statistical Society Series B* 57: 289-300.
86. Eisen MB, Spellman PT, Brown PO, Botstein D (1998) Cluster analysis and display of genome-wide expression patterns. Proc Natl Acad Sci U S A 95: 14863-14868.
87. Nadon R, Shoemaker J (2002) Statistical issues with microarrays: processing and analysis. Trends Genet 18: 265-271.
88. Saldanha AJ (2004) Java Treeview--extensible visualization of microarray data. Bioinformatics 20: 3246-3248.

2.2 Arsenic toxicity to *Saccharomyces cerevisiae* is a consequence of inhibition of the TORC1 kinase combined with a chronic stress response

Dagmar Hosiner †) ||), Harri Lempiäinen ‡) §) ||), Wolfgang Reiter *), Joerg Urban ‡), Robbie Loewith ‡), Gustav Ammerer *), Rudolf Schweyen †) David Shore ‡) §) ¶), and Christoph Schüller *) ¶)

*) Department of Biochemistry Max F. Perutz Laboratories, University of Vienna, A-1030 Vienna, Austria;

†) Department of Genetics Max F. Perutz Laboratories, University of Vienna A-1030 Vienna, Austria;

‡) Department of Molecular Biology and §) National Center for Competence in Research (NCCR) Program 'Frontiers in Genetics', University of Geneva, 30 quai Ernest-Ansermet, Geneva 4, 1211 Switzerland

||) These authors contributed equally to this work and are listed alphabetically

¶) To whom correspondence should be addressed

The author's contribution

Dagmar Hosiner	- microarray analyses, fluorescence microscopy, phenotypic analyses, writing
Harri Lempiäinen	- chromatin immunoprecipitation, chemical fragmentation, analysis of Sfp1 phosphorylation, phenotypic analyses, writing
Wolfgang Reiter	- analysis of Msn2 phosphorylation
Joerg Urban	- advice on Sfp1 phosphorylation
Robbie Loewith	- advice on Sfp1 phosphorylation
Gustav Ammerer	- advices
Rudolf Schweyen	- financer, advices
David Shore	- correspondence, financer, advices
Christoph Schüller	- conceived the study, microarray analyses, advices, writing

Published in: Molecular Biology of the Cell 2010 Feb; 20:1048-1057.

Arsenic Toxicity to *Saccharomyces cerevisiae* Is a Consequence of Inhibition of the TORC1 Kinase Combined with a Chronic Stress Response

Dagmar Hosiner,*† Harri Lempia¨inen,†§§ Wolfgang Reiter,‖ Joerg Urban,§ Robbie Loewith,§ Gustav Ammerer,‖ Rudolf Schweyen,* David Shore,§§ and Christoph Schu¨ller‖

‖Department of Biochemistry, and *Department of Genetics, Max F. Perutz Laboratories, University of Vienna, A-1030 Vienna, Austria; and ‡Department of Molecular Biology and §National Center for Competence in Research (NCCR) Program 'Frontiers in Genetics,' University of Geneva, Geneva 4, 1211 Switzerland

Submitted April 30, 2008; Revised November 25, 2008; Accepted December 1, 2008 Monitoring Editor: Charles Boone

The conserved Target Of Rapamycin (TOR) growth control signaling pathway is a major regulator of genes required for protein synthesis. The ubiquitous toxic metalloid arsenic, as well as mercury and nickel, are shown here to efficiently inhibit the rapamycin-sensitive TORC1 (TOR complex 1) protein kinase. This rapid inhibition of the TORC1 kinase is demonstrated in vivo by the dephosphorylation and inactivation of its downstream effector, the yeast S6 kinase homolog Sch9. Arsenic, mercury, and nickel cause reduction of transcription of ribosome biogenesis genes, which are under the control of Sfp1, a TORC1-regulated transcriptional activator. We report that arsenic stress deactivates Sfp1 as it becomes dephosphorylated, dissociates from chromatin, and exits the nucleus. Curiously, whereas loss of *SFP1* function leads to increased arsenic resistance, absence of *TOR1* or *SCH9* has the opposite effect suggesting that TORC1 has a role beyond down-regulation of Sfp1. Indeed, we show that arsenic activates the transcription factors Msn2 and Msn4 both of which are targets of TORC1 and protein kinase A (PKA). In contrast to TORC1, PKA activity is not repressed during acute arsenic stress. A normal level of PKA activity might serve to dampen the stress response since hyperactive Msn2 will decrease arsenic tolerance. Thus arsenic toxicity in yeast might be determined by the balance between chronic activation of general stress factors in combination with lowered TORC1 kinase activity.

INTRODUCTION

The transition metal arsenic has a long history of human exploitation as both a poison and a medicine. In more recent times Ehrlich's discovery of the antisyphilitic drug arsphenamine (also known as salvarsan) by systematic chemical modification of arsenic derivatives marked the beginning of modern pharmaceutical research. Arsenic trioxide (ATO) is used today in cancer treatment (Evens *et al.*, 2004; Lu *et al.*, 2007; Wang and Chen, 2008).

Exposure to arsenic evokes a broad spectrum of cellular reactions in *Saccharomyces cerevisiae* (Tamas and Wysocki, 2001; Haugen *et al.*, 2004; Jin, 2008; Thorsen *et al.*, 2007) and in higher eukaryotes (Salnikow and Zhitkovich, 2008). A number of mechanisms exist for detoxification, probably because arsenic has always been widespread in the environment. These involve reduction of influx through the aquaglyceroporin Fps1p (Wysocki *et al.*, 2001; Thorsen *et al.*, 2006); sequestration into the vacuole in the form of glutathione conjugates, metallothionein, and other metal/protein complexes; and active extrusion (Ghosh *et al.*, 1999). In yeast, genome-wide analysis of the transcription patterns in response to arsenic revealed a complex network of transcription factors controlling the expression of several hundred genes (Haugen *et al.*, 2004; Wysocki *et al.*, 2004; Thorsen *et al.*, 2007). Mitogen-activated protein kinases mediate protective responses involving AP-1- and AP-1-like transcription factors in higher eukaryotes and in fungi (Cavigelli *et al.*, 1996; Rodriguez-Gabriel and Russell, 2005; Thorsen *et al.*, 2006).

The mechanisms by which arsenic might influence signaling pathways other than MAP kinase systems are beginning to emerge. In addition to specific responses (e.g., oxidative stress), arsenic leads to the up-regulation of general stress genes, many of which are targets of the Msn2 and Msn4 transcriptional activators. Msn2 and Msn4 are partially redundant transcriptional activators responsible for the induction of genes in response to several types of stress (Martinez-Pastor *et al.*, 1996; Go¨rner *et al.*, 1998; Gasch, 2007). Activity and phosphorylation status of Msn2 is regulated by protein kinase A (PKA) as a crucial nutrient and carbon source mediator (Santangelo, 2006) and the action of phosphatase PP1. Interestingly however, among all adverse environmental conditions only acute glucose starvation causes dephosphorylation of Msn2 by inactivation of PKA and activation of PP1 (Go¨rner *et al.*, 1998, 2002; De Wever *et al.*, 2005; Garmendia-Torres *et al.*, 2007).

Arsenic also causes the rapid down-regulation of many genes that promote growth, a large number of which encode ribosomal proteins (RPs). Ribosome biogenesis is a major consumer of cellular energy and RNA polymerase II activity

This article was published online ahead of print in *MBC in Press* (http://www.molbiolcell.org/cgi/doi/10.1091/mbc.E08–04–0438) on December 10, 2008.

† These authors contributed equally to this work.

Address correspondence to: David Shore (david.shore@molbio. unige.ch) or Christoph Schu¨ller (christoph.schueller@univie.ac.at).

Table 1. Strains used in this study

Strain	Genotype	Source
BY-4741a	*MAT***a** *leu2 ura3 his3 met15 can1*	EUROSCARF
BY sfp1	*MAT***a** *sfp1::kanMX4*	EUROSCARF
BY-1541	*MAT***a** *SFP1-GFP::HIS3*	Marion *et al.* (2004)
RL285-16B (BYa)	*MAT***α** *LYS MET HIS ura3 LEU*	This study
YJU519 (BYa)	*MAT***α** *SCH9-2D3E; LYS MET HIS ura3 LEU*	This study
W303-1A	*MAT***a** *leu2 ura3 his3 trp1 ade2 can1*	K. Nasmyth (University of Oxford, United Kingdom)
DH303a	*MAT***a** *leu2 ura3 HIS3 TRP1 ade2 can1*	This study
DH303 msn2	*MAT***a** *msn2::HIS3 TRP1*	This study
DH303 msn4	*MAT***a** *msn4::TRP1 HIS3*	This study
W303 msn2msn4	*MAT***a** *msn2::HIS3 msn4::TRP1*	Görner *et al.* (1998)
W303 tpk123msn2msn4	*MAT***a** *tpk1::URA3 tpk2::HIS3 tpk3::TRP1 msn2::HIS3 msn4::TRP1*	Görner *et al.* (2002)
W303 bcy1	*MAT***a** *bcy1::LEU2*	Görner *et al.* (2002)
YHL38 (W303a)	*MAT***a** *SFP1-TAP::URA3*	This study
YHL69 (W303a)	*MAT***a** *tor1::natMX*	This study
YSS100 (W303a)	*MAT***a** *sfp1::HIS IFH1-13MYC::TRP1*	This study
YHL156 (W303a)	*MAT***a** *sfp1::HIS tor1::natMX IFH1-13MYC::TRP1*	This study
TB50a	*MAT***a** *leu2 ura3 rme1 trp1 his3*	M. Hall (University of Basel, Basel, Switzerland)
RL295-8B (TB50a)	*MAT***a** *SCH9-3E ura3 LEU2 TRP1 HIS3*	This study
YAS053-1 (TB50a)	*MAT***a** *sch9:kanMX4 gln3::KanMX gat1::HIS3*	Urban *et al.* (2007)
RL284-3D (TB50a)	*MAT***a** *TCO89-TAP::TRP1 TOR1-1*	This study
RL176-1C (TB50a)	*MAT***α** *TCO89-TAP::TRP1 mycTOR1KD*	This study

(Warner, 1999). Consequently, the regulation of ribosomal protein gene transcription constitutes a key mechanism by which protein synthesis and cell growth is regulated in response to the environment. Recent work has begun to reveal *trans*-acting factors involved in RP gene activation and regulation. The forkhead-like protein Fhl1 and an interacting factor Ifh1 constitute one axis of RP gene regulation (Martin *et al.*, 2004; Schawalder *et al.*, 2004; Wade *et al.*, 2004; Rudra *et al.*, 2005). A second regulator that localizes to RP gene promoters is the split Zn-finger transcription factor Sfp1 (Fingerman *et al.*, 2003; Jorgensen *et al.*, 2004; Marion *et al.*, 2004). RP gene expression is regulated by PKA through both Fhl1 (Martin *et al.*, 2004) and Sfp1 (Jorgensen *et al.*, 2004). Sfp1 is strongly regulated by the target of rapamycin (TOR) kinase, a conserved serine/threonine kinase of the phosphatidylinositol kinase–related kinase family that functions in all eukaryotes as a central growth regulator (Wullschleger *et al.*, 2006). Yeast and other eukaryotes have two TOR-containing complexes, TORC1 and TORC2, which have different targets and distinct physiological functions (Loewith *et al.*, 2002). Rapamycin inhibits TORC1 activity by the formation of a ternary complex with the peptidyl-prolyl *cis*-trans isomerase Fpr1 (FKBP12; Heitman *et al.*, 1991). Inhibition of TORC1 causes a loss of Sfp1 from RP gene promoters and its movement from the nucleus to the cytoplasm (Marion *et al.*, 2004). Furthermore, the Sch9 protein kinase, a yeast S6 kinase homolog, has been implicated as a major and direct downstream target of TORC1 for control of both stress- and growth-related transcription (Pedruzzi *et al.*, 2003; Jorgensen *et al.*, 2004; Kaeberlein *et al.*, 2005; Urban *et al.*, 2007), and indeed TOR activity has also been shown to modulate Msn2 intracellular localization (Beck and Hall, 1999; Santhanam *et al.*, 2004).

In this study we investigated the function of the TORC1 and PKA signaling pathways and their downstream targets Sfp1, Sch9, and Msn2/4, in the arsenic stress response of the budding yeast *S. cerevisiae*. We report that repression of RP genes after trivalent arsenic exposure is correlated with and most likely a consequence of rapid inactivation of TORC1 (within several minutes), whereas PKA activity is sustained. Inhibition of TORC1 leads to reduced Sfp1 activity and RP gene transcription, which nevertheless serves to promote cell growth under conditions of continuous low-level arsenic exposure. Conversely, our data suggest that a second consequence of reduced TORC1 activity, namely the chronic Msn2/4-dependent induction of stress-related genes, is a major contributor to arsenic toxicity.

MATERIALS AND METHODS

Plasmids and Yeast Strains

Strains used in this study are summarized in Table 1. To generate the DH303 isogenic series, fragments obtained by PstI digestion of pJJ246 containing the *TRP1* gene and EcoRI/SalI digestion from plasmid pJJ217 (Jones and Prakash, 1990) containing the *HIS3* genes were integrated by homologous recombination into DH303, DH303 *msn2*, and DH303 *msn4*.*pHSE2-LacZ* has been described previously (Sorger and Pelham, 1987).

RNA and DNA Methods

Fluorescently labeled cDNA was synthesized from 15 μg of total RNA and a T20VN primer using 200 U Superscript II (Invitrogen, Carlsbad, CA) and Cy3-CTP or Cy5-CTP (GE Healthcare, Waukesha, WI). Labeled cDNAs were pooled and RNA was hydrolyzed for 20 min in 10 N NaOH at 65°C, neutralized with acetic acid, and purified by the Cy Scribe GFX purification kit (GE Healthcare). Microarrays (obtained from Microarray Centre, Toronto, Ontario, CAN) had PCR fragments of 6144 predicted *S. cerevisiae* ORFs spotted in duplicate. Hybridization was performed for 14–16 h in DigEasyHyb solution (Roche Diagnostics, Basel, Switzerland) with 0.1 mg/ml salmon sperm DNA (Sigma, St. Louis, MO) as a carrier solution at 37°C. After hybridization, microarrays were washed three times in 1x SSC, and 0.1% SDS at 50°C for 10 min, followed by 1 min in 1x SSC and 0.1x SSC at RT and a 5-min 500 rpm spin to dryness. The microarrays were scanned using an Axon GenePix 4000B scanner (Molecular Devices, Sunnyvale, CA). The image data were quantified using the GenePix Pro4.1 software (Molecular Devices). Raw data are available under the ArrayExpress (http://www.ebi.ac.uk/arrayexpress/) accession no. E-MEXO-1075.

For individual microarrays the intensity of the two fluorescent channels were normalized to the mean of ratio of medians of all unflagged features using the Genepix Pro4.1 normalization option. Values of not found features were excluded from further analysis. Mean ratios were calculated for features with at least four values. Genes labeled as dubious ORFs in SGD were also removed from analysis. The remaining values were normalized. The filtered values used for further analysis are available as supplementary file.

Cluster analysis (Eisen *et al.*, 1998; Nadon and Shoemaker, 2002; http://rana.stanford.edu/software) was performed using the cluster3 and visualized with TreeView (Saldanha, 2004; http://jtreeview.sourceforge.net). Significant associations to either gene ontology (GO)-terms or transcription factors were obtained with the T-Profiler (http://www.t-profiler.org/; Boorsma *et al.*, 2005). Values of genes associated with the most significant terms were visualized by Cluster analysis using complete linkage and correlation as similarity metric. The hierarchical cluster results were confirmed by K-means clustering. For analysis of the effect of the absence of transcription factors for As(III) gene regulation the ratios of the wild type versus the mutant were calculated and the log2-transformed values and graphically included in the cluster analysis by setting their column weight value to zero.

Green Fluorescent Protein Fluorescence Microscopy

Green fluorescent protein (GFP) was visualized directly in living cells carrying plasmids p*ADH1MSN2*-GFP or p*ADH1MSN4*-GFP and EY*sfp1* Psfp1¯GFP without fixation on object slides (at 30°C). Stress conditions were applied as specified for individual experiments. DAPI (2 gg/ml) added 10 min before microscopy was used to localize nuclei. In living cells DAPI also stains other nucleic acids apart from nuclear DNA, resulting in a characteristic background. Images were recorded on a Zeiss Axioplan 2 fluorescence microscope (Thornwood, NY) with a Spot Pursuit camera (Visitron Systems, Puchheim, Germany). Quantification of Sfp1-GFP localization was done by counting —50 cells from three independent experiments ($p < 2 \times 10^{-4}$).

Chromatin Immunoprecipitation

For immunoprecipitations 20 gl rabbit IgG (Sigma, I5006) coupled magnetic Epoxy beads (Dynabeads M-270; Dynal Biotech, Invitrogen) was added, and tubes were rotated for 3 h at 4°C. Immunoprecipitates were washed with lysis buffer. Both an aliquot of sonicated cleared extract (input) and the immuno-precipitated material were de-cross-linked in TE (Tris-EDTA) plus 1% SDS for at least 8 h at 65°C. Quantitation of immunoprecipitated DNA was obtained by real-time PCR using SYBR Green detection (Bianchi *et al.*, 2004) on an Applied Biosystems ABI Prism 7700 machine (Foster City, CA). Primers used were RPL2B-5' (CAGAGAGGTCGTCCCAGTCT) and RPL2B-3' (GCA-GAATCCACCAGGAGTGT) for *RPL2B* promoter and HL228 (GAATT-GAGAGTTGCCCCAGA) and HL229 (AGAAGGCTGGAACGTTGAAA) for the *ACT1* gene. For each data point, results were obtained from at least two and up to four experiments.

Chemical Fragmentation

Chemical fragmentation analysis was performed as described (Urban *et al.*, 2007) with the following exceptions. Experiments were done in W303-1A strain background transformed with plasmid pRS416 containing *SCH9-5HA* (pJU676). Cultures were grown to midlog phase at 30°C in SC-Ura (pH 6.0, 2% glucose, and 0.2% Gln), inhibitors (or drug vehicles) were added for 30 min before harvesting. Antibody 12CA5 was used for the detection of SCH9-5HA.

Analysis of Sfp1 Phosphorylation

Overnight cultures of strain YHL89 (*SFP1*-TAP) were diluted in YPAD, grown to midlog phase, and harvested by centrifugation, and the pellets immediately frozen in liquid nitrogen. Pellets were resuspended in an equal volume of lysis buffer (100 mM HEPES-KOH, pH 8.0, 10% glycerol, 10 mM EGTA, 0.1 mM EDTA, 0.4% NP-40, 600 mM NaOAc,1 mM PMSF,1 mM DTT, 1x protease inhibitor cocktail [Roche, Indianapolis, IN] and 0.1x phosphatase inhibitor mix [PPi: 10 mM NaF, 10 mM NaN3, 10 mM *p*-nitrophenylphosphate, 10 mM $_{Na2P2O4,}$ and 10 mM 13-glycerophosphate]). Cells were lysed by vortexing two times for 1 min with zirconia/silica beads using a Minibeadbeater-8 machine (Biospec Products, Bartlesville, OK). Cell lysates were cleared by centrifugation (10 min, 3000 rpm, +4°C) and diluted with lysis buffer to a protein concentration of 5 mg/ml. For immunoprecipitations 40 gl rabbit IgG (Sigma, I5006) coupled magnetic Epoxy beads (Dynabeads M-270; Dynal Biotech, Invitrogen) were added, tubes were rotated for 3 h at 4°C, and then the beads were washed three times with lysis buffer. Proteins were eluted with 1x SDS-PAGE sample buffer and incubated at 65°C for 10 min and separated by SDS-PAGE. The quantitative ProQ Diamond Phosphoprotein Gel Stain (Invitrogen) and SYPRO Ruby protein stain (Bio-Rad, Hercules, CA) in-gel stains were used in accordance with the manufacturer's protocol. The fluorescent intensity of protein bands was visualized and quantified using an Ettan DIGE Imager (GE Healthcare) and accompanying ImageQuant TL software (GE Healthcare). For quantification, Sfp1 phosphoprotein levels were normalized to total Sfp1 protein levels and to the background on each lane and presented as relative phosphorylation normal-ized to untreated wild-type sample.

Phospho Msn2 Analysis

Phosphorylation status of Msn2 was determined by Western blots using a purified antiserum raised against phosphorylated peptides and loading of Msn2 was confirmed with an anti-Msn2 serum, both described by De Wever *et al.* (2005).

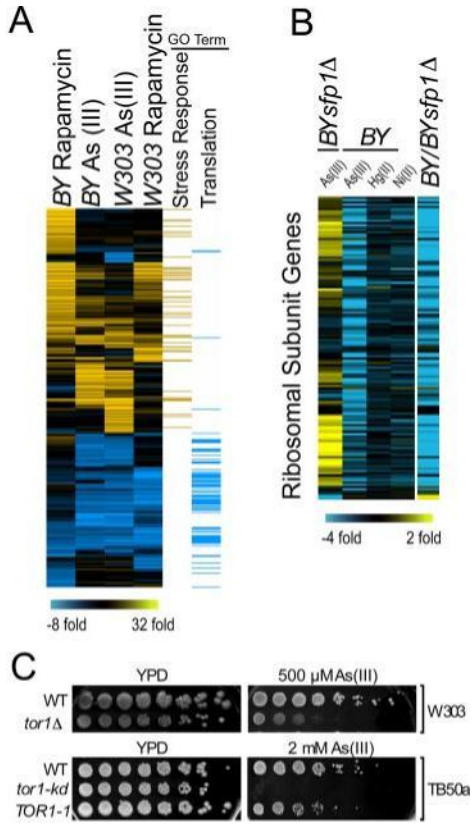

Figure 1. Transcript profile of arsenic stress. (A) Comparison of transcript profiles from arsenic-stressed (0.5 mM As(III) 30 min) BY4741 and W303-1A cells to rapamycin-treated cells (30 min, 200 ng/ml). Hierarchical clustering of those genes changed at least once <-4- or >4-fold. Right panel shows genes associated to GO terms "translation" and "response to stress". Supplemental Figure S2B shows a comparison of reported microarray data of rapamycintreated cells. (B) Regulation of 137 ribosomal protein genes by arsenic (0.5 mM As(III)), mercury (30 pM Hg(II)), and nickel (1.5 mM Ni(II)) in wild-type compared with *sfp1*Δ mutant cells; all treatments were for 30 min. The BY/BYsfp1 lane shows the color coded quotient of treated wild type and sfp1 mutant. Data to view clustering figures with TreeView are available as Supplemental Files. (C) Tor1 mutant strains have a growth defect during chronic arsenic stress. *tor1*Δ is a derivative from *W303-1A*, the kinase-dead *tor1*-KD and the rapamycin-insensitive *TOR1-1* are derivatives from TB50a. Growth was recorded after a 3-5-d incubation at 30°C.

RESULTS

A Role for TORC1 and Sfp1 in the Transcriptional Response to Arsenic Stress

Whole genome mRNA transcript profiles after treatment with trivalent arsenic [hereafter referred to as As(III)] were in some aspects, such as bulk repression of RP genes and classes of stress genes, similar to those from rapamycintreated cells both from reported profiles (Hardwick *et al.*, 1999) and our data. This result implicated the TOR nutrient-signaling pathway as a potential As(III) target. To further strengthen this interpretation arsenic stress profiles were generated after 30-min treatment with 0.5 mM As(III) and compared with those of 200 ng/ml rapamycin (Figure 1A). This concentration of As(III) caused only a slight increase in doubling time in exponential cultures. Transcript profiling experiments were done in the two strain backgrounds of the two isogenic sets used (see Table 1). Notably, BY4741 cells

Table 2. T-Profiler analysis (http://www.t-profiler.org/) of transcription factor–binding motifs from As(III)-treated cells

		W303				W303msn2msn4			
Motif	Name	t-value	E-value	Mean	ORFs	t-value	E-value	Mean	ORFs
GGTGGCRA	RPN4	5.83	8.10e-07	0.501	70	4.15	4.80e-03	0.396	62
AGGGG	MSN2-4	4.40	1.60e-03	0.086	643	1.08	1.00e+00	-0.028	569
CCCCT	MSN2-4	1.79	1.00e+00	0.013	662	-0.61	1.00e+00	-0.084	599
TTCTRGAA	HSF1	3.32	1.20e-01	0.214	104	2.74	5.90e-01	0.188	89
TTASTAA	YAP1	2.12	9.90e-01	0.038	432	1.13	1.00e+00	-0.017	378
ACGCGT	MBP1	0.78	1.00e+00	0.007	185	1.62	1.00e+00	0.04	176
CACGTK	PHO4	0.20	1.00e+00	-0.03	504	-5.11	4.70e-05	-0.346	231
CGATGAG	PAC	-3.43	<1.0e-15	-0.232	176	-2.29	9.60e-01	-0.231	139
AAAATTT	rRPe	-6.45	<1.0e-15	-0.181	891	-6.19	8.80e-08	-0.231	784
CCRTACA	RAP1	-8.87	<1.0e-15	-0.521	187	-9.14	<1.0e-15	-0.644	176

Raw data used for this analysis is available as supplementary files: W303_all.txt, W303_24_all.txt, and BY_all.txt, BY_sfp1_all.txt.

have a higher basal resistance against arsenic and gave a more pronounced response of induced genes (139 genes > 4-fold and 523 > 2-fold) than W303-1A (49 > 4-fold and 202 > 2-fold; see Figure 1A and Supplemental Files). In contrast, a similar number of genes was down-regulated in both strains (338 > 2-fold in BY4741 and 312 in W303-1A). T-Profiler analysis (Boorsma *et al.*, 2005) revealed significantly enriched GO terms (Tables 2 and 3), indicating the induction of regulons of the transcription factors Hsf1, Yap1, Rpn4, and Msn2/4, as well as repression of most ribosomal protein genes. The transcript patterns were also in agreement with previous studies (Haugen *et al.*, 2004; Thorsen *et al.*, 2007). Clustering analysis of our As(III) with rapamycin data further suggested similar regulation of genes associated with characteristic GO terms such as translation and stress response (Figure 1A, right panels). Significant GO terms were verified by GO-term enrichment (http://db.yeastgenome. org/cgi-bin/GO/goTermFinder.pl/; Supplemental Table ST1).

Inhibition of TORC1 by rapamycin causes dephosphorylation (H. Lempia¨inen and D. Shore, unpublished) and nuclear export of the transcription factor Sfp1 (Marion *et al.*, 2004). Inhibition of Sfp1 by arsenic stress was predicted previously based on the global repression of RP genes (Haugen *et al.*, 2004; Thorsen *et al.*, 2007). To verify this directly, we compared the mRNA profile of BY4741 wild-type cells to the corresponding BY*sfp1*A mutant cells. In stark contrast to the wild type, we found almost no down-regulation of RP genes in the *sfp1*A mutant strain (Figure 1B, compare *BY* to *BYsfp1*A). Changes of expression levels of genes coding for the large and small ribosomal subunit under arsenic treatment are shown in Figure 1B. Therefore, Sfp1 has a central role for down-regulation of RP gene transcription during arsenic stress.

From these profiles we noted that Sfp1 was also required for full induction of some genes. Strikingly, the levels of Hsf1-dependent heat shock genes were threefold reduced on average (Supplemental Figure S1A). However, Hsf1 function for heat stress signaling was not compromised in the *sfp1*A mutant. Thus, as predicted activity of a heat-shock element (HSE)-driven *lacZ* reporter under heat stress was unaffected by the absence of Sfp1, whereas induction by arsenic stress was abolished in the mutant (our unpublished results). Furthermore, we also noticed reduced induction of Yap1- and Rpn4-dependent genes in *sfp1*A mutant cells (Supplemental Figure S1, B and C, respectively). The mechanism(s) underlying these effects are at present unknown but could be specific to an arsenic stress signal or an indirect consequence of Sfp1 loss.

Because the microarray data suggested a role of TORC1 in the arsenic stress response, we looked at the survival of different Tor1 mutants using colony-forming ("drop") assays on plates containing As(III). We found that mutants lacking full Tor1 function either in a strain deleted for *TOR1* (W303 *tor1*A) or a *tor1-kDa* mutant with impaired kinase activity ($Tor1^{D2275A}$), had lower viability in the presence of As(III) (Figure 1C). In contrast, the *TOR1–1* allele, which confers rapamycin resistance, did not significantly change arsenic sensitivity. From this, one may conclude that TORC1 activity is necessary for an appropriate adaptive response to As(III).

Table 3. GO-enrichment analysis

Category	BY	BYsfp	W303	W303-msn2/4.
Heat shock protein activity	2.704	0.651	2.287	—
Aryl-alcohol dehydrogenase activity	2.596	1.927	2.447	2.15
Proteasome core complex	1.768	0.992	1.118	0.937
Endopeptidase activity	1.182	0.398	0.64	0.596
Protein folding	1.176	0.375	0.903	
Ribosome	-0.363	0.222	-1.192	-1.244
Structural constituent of ribosome	-0.523	0.224	-1.36	-1.342
Cytosolic ribosome (sensu Eukarya)	-0.588	0.296	-1.939	-1.787

Mean expression of genes associated to the respective terms. Restrictions: E-value of <0.05 and t-value <-4 or >4, values are log2 of normalized transcript differences (mean of ratios). —, overlaps with Msn2/4 regulon.

Arsenic Stress Promotes Sfp1 Chromatin Dissociation, Dephosphorylation, and Cytosolic Relocalization

In unstressed cells growing in nutrient rich medium Sfp1 is concentrated in the nucleus and is associated with RP gene promoters (Jorgensen *et al.*, 2002; Marion *et al.*, 2004). Inhibition of TORC1 kinase by rapamycin causes release of Sfp1 from promoters and its cytoplasmic redistribution (Marion *et al.*, 2004). We therefore investigated if As(III) exposure triggers a similar response. To follow Sfp1 localization, we used cells expressing a GFP-tagged version of Sfp1 from the endogenous *SFP1* locus. Within 20 min after arsenic addi-

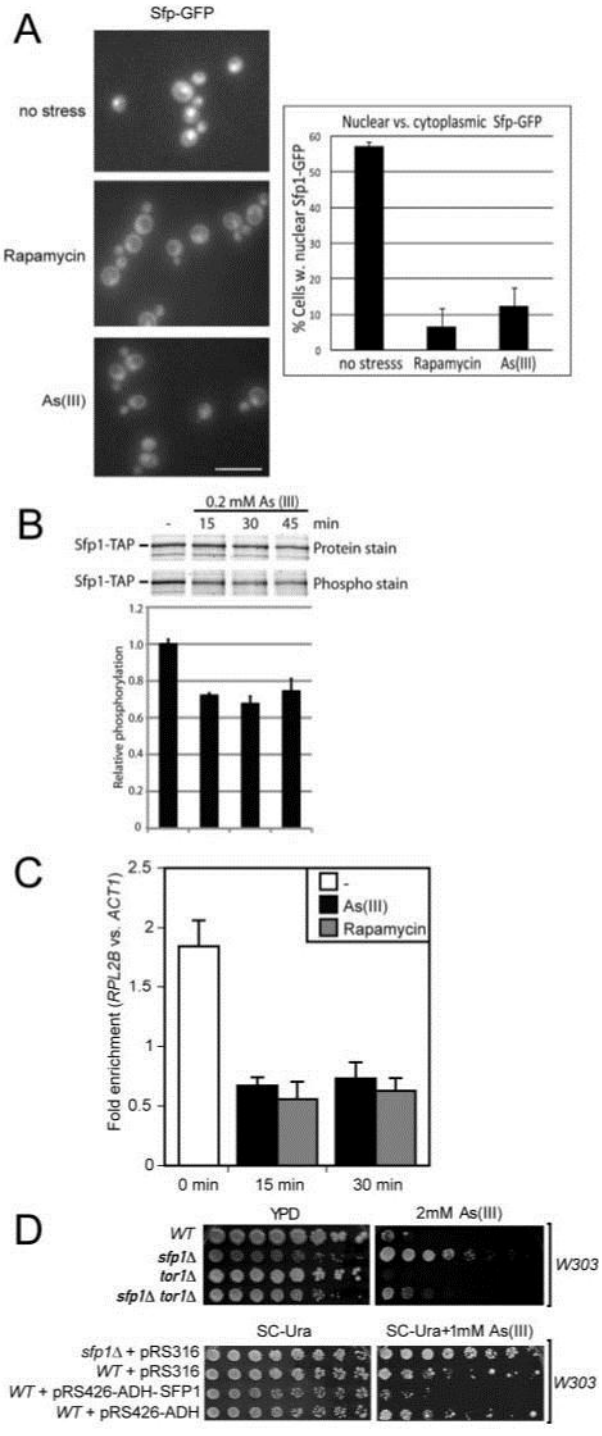

Figure 2. Regulation of Sfp1 by As(III) stress. (A) Localization of Sfp1-GFP. Cells carrying a *SFP1*-GFP genomic fusion gene were grown to exponential phase and treated with 0.5 mM As(III) and rapamycin (200 ng/ml) for 20 min. GFP-fluorescence images were taken from cells without fixation. Bar, 25 µm. Evaluation of Sfp1 GFP localization is indicated in the bar graph. (B) In-gel phosphoprotein stain of Sfp1 phosphorylation. Sfp1-TAP was purified and separated and stained as described in *Materials and Methods.* Bottom panel shows phosphorylation of Sfp1 normalized to Sfp1 protein levels at the indicated time points as an average of three independent experiments. (C) Binding of Sfp1 to RP gene promoter in As- and rapamycin-treated cells. Sfp1 recruitment to *RPL2B* promoter was analyzed by ChIP in a strain carrying a TAP-tagged endogenous allele of *SFP1*. Samples from unstressed cells (t = 0 min), from

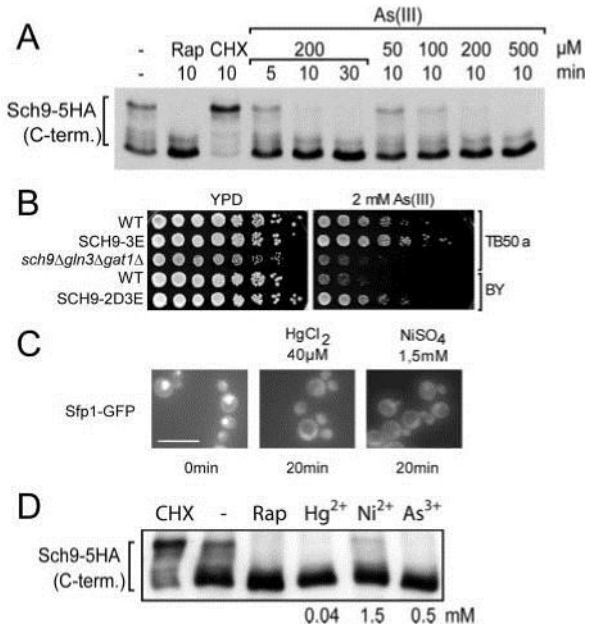

Figure 3. TORC1 kinase inhibition by arsenic. (A) Inhibition of TORC1 kinase activity by As(III). Chemical fragmentation analysis of the C-terminus of Sch9 demonstrates dephosphorylation in response to rapamycin (Rap, 200 ng/ml) and As (As(III), 200 or 500 µM) and hyperphosphorylation in response to cycloheximide (CHX, 25 µg/ml). Treatment times are indicated. (B) Growth properties of the indicated *SCH9* mutant strains, together with their isogenic parent wild-type strains on As(III) plates. The *sch9A* mutants were stabilized by the simultaneous deletion of *GLN3* and *GAT1*. Fivefold serial dilutions of overnight cultures were spotted onto containing the indicated amounts of As(III). Growth was recorded after a 3-5-d incubation at 30°C. Relevant strain backgrounds (W303-1A, BY4741) are indicated. (C) Sfp1-GFP localization of cells treated with 40 µM $HgCl_2$ and 1.5 mM $NiCl_2$ for 20 min. Bar, 25 µm. (D) Chemical fragmentation analysis of Sch9 after 20-min treatment at 30°C with to 40 µM $HgCl_2$ and 1.5 mM $NiCl_2$.

tion we observed a clear reduction of the nuclear fluorescence signal (Figure 2A and Supplemental Figure S2A). Quantification showed that arsenic and rapamycin caused a similar cytoplasmic accumulation of Sfp1-GFP. To address the Sfp1 phosphorylation status in vivo, we used an in-gel phosphoprotein stain to measure the phosphorylation of a partially purified Sfp1 TAP-tagged protein. Arsenic caused a clear reduction of Sfp1 phosphorylation to about —75% (Figure 2B, bottom), which was visible 15 min after arsenic addition and persisted for at least 30 min. Using chromatin immunoprecipitation (ChIP), we determined the association of a Sfp1 TAP-tag fusion protein with the *RPL2B* promoter. Arsenic treatment reduced the Sfp1-TAP ChIP signal within 15 min to levels similar to what was observed after rapamycin treatment (Figure 2C). Arsenic and rapamycin thus have similar effects both on chromatin binding and subcellular location of Sfp1.

We therefore tested the consequence of an *SFP1* deletion for cell viability during chronic As(III) exposure by drop

As(III)-(0.5 mM) and rapamycin-(200 ng/ml) treated cells at the indicated time points (t = 15 min or 30 min). (D) Growth properties of the indicated *SFP1* mutant strains, together with their isogenic parent wild-type strains on arsenic plates. Fivefold serial dilutions of overnight cultures were spotted onto rich (YPD) or synthetic medium (SC-URA) plates containing the indicated amounts of As(III). Growth was recorded after a 3-5-d incubation at 30°C.

assays on plates (Figure 2D). To our surprise we found that the *sfp1* mutation had the opposite effect compared with *tor1* mutations, rendering cells more resistant. However, the *tor1 sfp1* double mutant showed an intermediary phenotype. These genetic results point to a separate function of Tor1 during chronic As(III) stress apart from regulation of Sfp1. Additionally, high-level expression of Sfp1 reduced resistance (Figure 2D, bottom). Although, these genetic data are incompatible with a simple linear pathway connecting relationship of Tor1 and Sfp1 during arsenic stress, they do show that both are required for an optimal response.

TORC1 Kinase Is Inhibited by Arsenic

In an attempt to find an explanation for the apparently contradictory results obtained with *sfp1* and *tor1* deletion strains, we investigated whether the TORC1 kinase activity is changed by As(III) treatment. We measured the in vivo phosphorylation state of a C-terminal fragment of Sch9, which has been shown recently to be a bona fide TORC1 substrate (Urban *et al.*, 2007). Arsenic addition caused a rapid dephosphorylation of Sch9, similar to that observed after rapamycin treatment (Figure 3A). Although we cannot rule out the possibility that As(III) induces the activity of phosphatase(s) directed against Sch9, these data were consistent with the notion that As(III) causes a rapid inactivation of the TORC1 kinase pathway. Because Sch9 is a primary target of TORC1, we investigated its function during chronic arsenic stress (Urban *et al.*, 2007). Cells lacking Sch9 were sensitive to As(III) (Figure 3B). Significantly, two TORC1-independent "phospho-mimetic" mutants of Sch9 (SCH9-3E and SCH9-2D3E; Urban *et al.*, 2007) conferred resistance to As(III) (Figure 3B). The resistance phenotype of these mutants is consistent with a function of Tor1 separate from Sfp1 regulation during arsenic stress as shown above.

According to microarray data, mercury at a low concentration (0.04 mM) and nickel (at 1.5 mM) had an repressive effect comparable to As(III) (0.5 mM) on global RP gene transcription (Figure 1B and our unpublished results). We therefore tested if these metal ions also cause inhibition of TORC1. Under these same conditions Sfp1 rapidly accumulated in the cytoplasm within 20 min (Figure 3C), and TORC1 activity decreased, as judged by the phosphorylation status of Sch9 (Figure 3D). Therefore As(III) and certain other toxic metal ions cause repression of TORC1 activity, leading to Sfp1 dephosphorylation, loss of chromatin contact, cytoplasmic sequestration, and finally, reduction of ribosomal protein gene transcription.

Msn2 and Msn4 Are Activated by Arsenic Stress

Arsenic stress could also be an inhibitor of PKA activity, because Sfp1 is both TORC1 and PKA regulated (Jorgensen *et al.*, 2004; Marion *et al.*, 2004). Furthermore, the transcription factors Msn2 and Msn4 are also inhibited by PKA (Smith *et al.*, 1998), and both As(III) and rapamycin induce a cluster of Msn2/4 target genes (Figure 1A, Tables 2 and 3 and Supplemental Files). We confirmed this role of Msn2/4 for gene activation by transcript profiling of a *msn2*0*msn4*0 double deletion strain. Induction of 57 of the total 202 As(III)-induced genes was reduced by more than 1.4-fold in the *msn2*0*msn4*0 mutant (Figure 4A, compare *W303* with *W303m24*0). Twenty-four of these 57 genes ($P < —2 \times 10^{-16}$) were previously reported to be up-regulated by Msn2 overexpression (Chua *et al.*, 2006), indicating that many of these are direct target genes of Msn2/4. To test if Msn2/4 were directly activated by arsenic stress, we investigated the intracellular localization of Msn2- and Msn4-GFP fusion proteins. In unstressed cells both Msn2 and Msn4 are predominantly cytoplasmic, but both Msn2- and Msn4-GFP rapidly accumulated in the nucleus for at least 20 min after As(III) stress (Figure 4B), similar to other stress types (Go¨rner *et al.*, 1998).

Activation of Msn2 is either a consequence of reduced PKA activity or environmental stress (Durchschlag *et al.*, 2004). To differentiate between the two possibilities during As(III) stress, we determined the phosphorylation state of Msn2 using antibodies directed against PKA phosphorylation sites (serines 288, 582, 620; De Wever *et al.*, 2005; Figure 4C). Glucose starvation has been shown to cause a strong reduction of the phosphorylation status of the serine 620 PKA site in Msn2 (Go¨rner *et al.*, 2002). Because arsenate competes with phosphate for binding sites of glycolytic substrates, thereby inhibiting glycolysis (Jung and Rothstein, 1965), we suspected that arsenic stress might mimic aspects of glucose depletion. However, the signals obtained with phospho-specific antibodies indicated that As(III) stress leads to sustained phosphorylation of the tested sites (Figure 4C). Such an effect was also observed during heat stress (Go¨rner *et al.*, 2002 and W. Reiter, unpublished results). This sustained phosphorylation of Msn2 could result from continued PKA activity, the inactivation of one or more phosphatases, or both. In any case, these results indicated that As(III) stress, unlike acute glucose starvation, does not abolish PKA activity.

To analyze the importance of Msn2/4 for growth in the presence of arsenic, we tested mutants lacking Msn2, Msn4 or both (Figure 5A). Deletion of either *MSN2* or *MSN4* had no effect on sensitivity, whereas the *msn2*0*msn4*0 double mutant displayed increased tolerance. Therefore, Msn2/4 reduce growth during arsenic stress. This was supported by the enhanced arsenic sensitivity upon overexpression of either *MSN2* or *MSN4* under the control of the *ADH1* promoter. Mutants lacking the PKA regulatory subunit (*bcy1*0) have constitutively high PKA activity and low activity of Msn2/4. These mutants displayed higher resistance to arsenic. Comparing the arsenic resistance of the *msn2*0*msn4*0 double mutant strain to a mutant additionally lacking PKA activity (*tpk1*0*tpk2*0*tpk3*0 *msn2/4*0) demonstrates a role of PKA in parallel to its function as a regulator of Msn2/4 (Figure 5B). This might involve the inhibitory action of PKA on the Rim15 kinase and its downstream transcription factor Gis1 (Roosen *et al.*, 2005).

As shown above, TORC1 function for arsenic resistance is upstream of the Sch9 kinase and the Sfp1 transcription factor. Other TORC1 downstream targets may also play a role in arsenic resistance, among which might be the Msn2/4 stress response factors. Strikingly, we found that deletion of both *MSN2* and *MSN4* completely alleviates the arsenic sensitivity of *tor1*0 mutants (Figure 5C). The genetic interaction seen with these mutants displays clearly the connection between TORC1-based nutrient signaling and Msn2/4 stress signaling during a chronic stress.

DISCUSSION

Arsenic in the form of trivalent arsenite As(III) causes major metabolic adjustments and evokes a highly complex transcriptional response. We analyze here the contribution of the nutrient signaling protein kinases Target Of Rapamycin Complex 1 (TORC1) and PKA to the cellular arsenic response. We show rapid inactivation of TORC1 kinase but not of PKA. This effect modulates the activity of downstream factors such as Sch9, Sfp1, and Msn2/4 and has complex consequences for cell growth and survival in response to chronic arsenic exposure. Interestingly, our genetic data suggest that As(III) toxicity is caused in part by interference between signaling pathways.

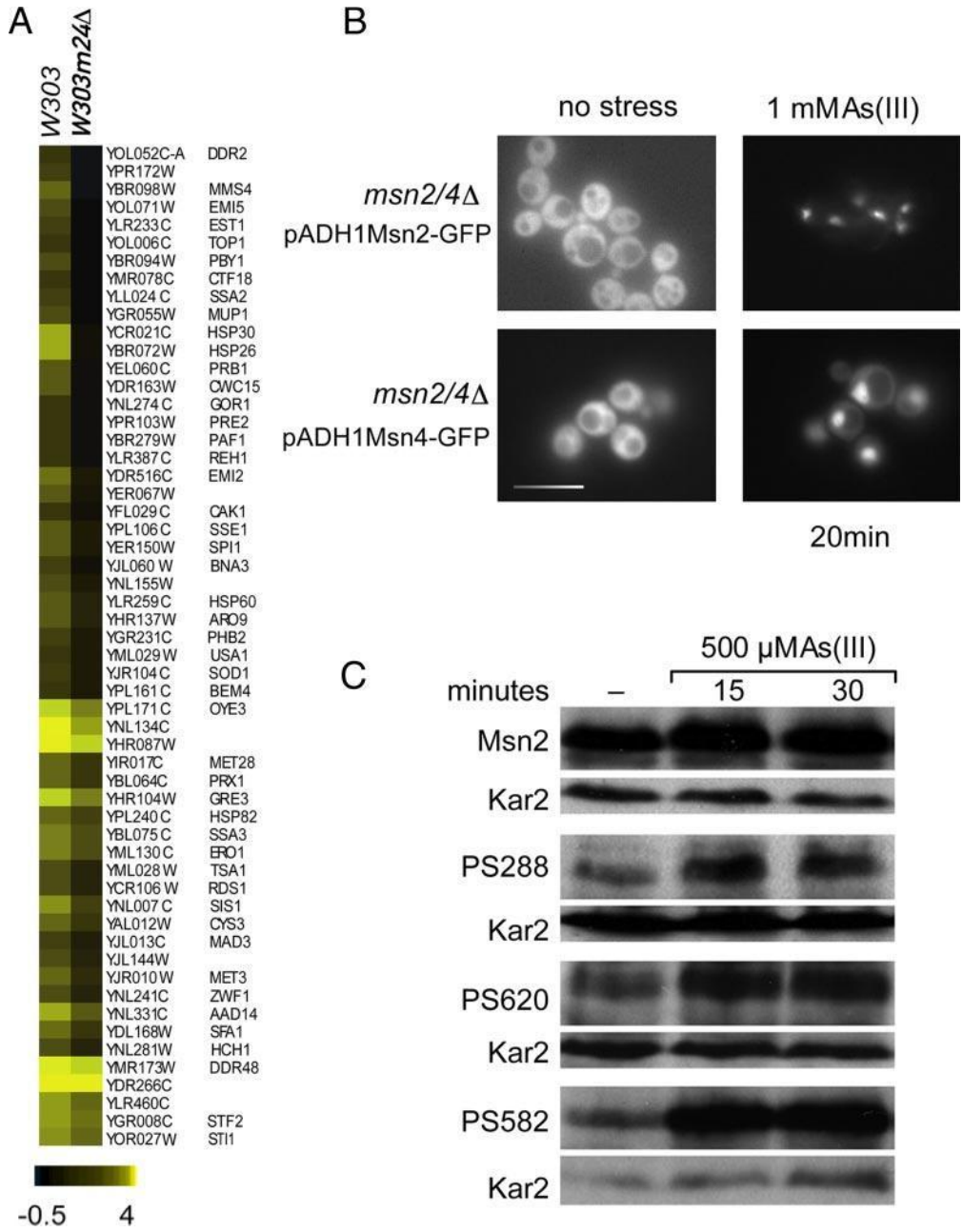

Figure 4. Function of Msn2/4 and the PKA pathway in arsenic response. (A) Hierarchical clustering (Eisen *et al.*, 1998) of 56 As(III)-induced genes, which were influenced more than 1.4-fold by the absence of Msn2 and Msn4 in the *msn2Amsn4A* double mutant strain. (B) Localization of Msn2-GFP in arsenic-stressed cells. W303 *msn2msn4* cells transformed with *pADH1-MSN2*-GFP and *pADH1-MSN4-GFP* were grown to exponential phase in synthetic medium and treated for 20 min with 1 mM As(III) at 30°C. GFP-fluorescence images were taken from cells without fixation. Bar, 25 μm. (C) Phosphorylation status of PKA sites of Msn2. W303-1A cells were grown in YPD medium to exponential phase and stressed by addition of 1 mM As(III). Samples for total protein extracts were taken at 15-min intervals and analyzed on Western blots with phosphorylation-specific antibodies directed against S620, S582, and S288. Msn2 and Kar2 levels served as a loading control.

Arsenic Inhibits TORC1

Our biochemical evidence indicates clearly that arsenic inhibits the rapamycin-sensitive TORC1 kinase. First, cells treated with rapamycin and the metalloid arsenic share a similar global transcriptional pattern. Second, interaction of the TORC1 mediator Sfp1 with a ribosomal protein gene promoter was reduced by As(III) to the same low level as observed after rapamycin treatment. Third, coincident with As(III) exposure, Sfp1 phosphorylation was decreased, and its localization was shifted from almost exclusively nuclear to a more cytoplasmic distribution. Fourth, we found that the phosphorylation status of Sch9, a bone fide in vivo target of TORC1 (Urban *et al.*, 2007), was rapidly reduced upon As(III) stress. Moreover, cells treated with mercury and nickel ions also displayed a similar shift of localization of Sfp1 and reduced Sch9 phosphorylation and RP gene repression, indicating that the response to arsenic observed here is part of a more general metal ion stress response.

The mechanism by which arsenic inhibits TORC1 activity is currently not known to us. Arsenic could, for example,

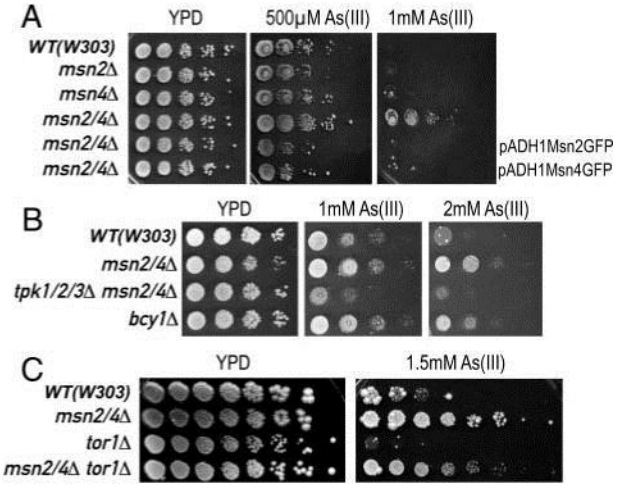

Figure 5. Growth of Msn2/4 mutants on As(III) solid medium representing chronic arsenic stress. Cultures were grown to saturation and spotted in 5- or 10-fold dilution series. (A) Comparison of DH303 series cells. (B) Hyperactive PKA (*bcy1*) confers resistance to As(III). PKA targets beside Msn2 are involved in As(III) resistance. (C) Double deletion of Msn2 and Msn4 alleviates the arsenic sensitivity of *tor1*A mutants. Plates were photographed after 2–4 d at 30°C.

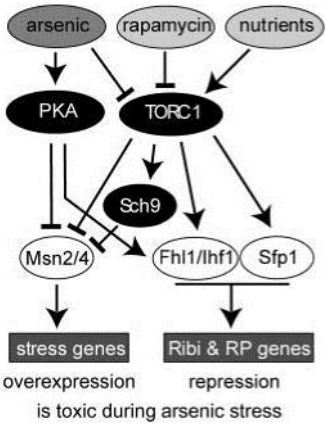

Figure 6. Schematic model of connections between signaling pathways and substrates.

affect the stability of the TORC1 complex and/or upstream signaling components. In *S. cerevisiae*, TOR signaling has been proposed to respond to metabolic signals originating from nitrogen and carbon sources (Schmidt *et al.*, 1998; Beck and Hall, 1999; Kuruvilla *et al.*, 2001; Crespo *et al.*, 2002). Glutamine deprivation inhibits TORC1 (Crespo *et al.*, 2002). Arsenic stress causes cells to channel sulfur into increased glutathione biosynthesis, as suggested by phenotypic profiling (Haugen *et al.*, 2004) and later by direct measurement (Thorsen *et al.*, 2007). The glutamate incorporated into glutathione is connected to glutamine pools by glutamate synthase (GOGAT) encoded by *GLT1*. It remains to be shown if increased glutathione consumption by the formation of $As(GS)_3$ conjugates results in a significant drop of glutamine levels. On the other hand, glutathione deprivation by arsenic might also cause other side effects such as oxidative stress, which also reduces TORC1 activity (Urban *et al.*, 2007).

The Complex Role of TORC1 in Arsenic Resistance

The down-regulation of RP gene expression signifies a major shift of cellular activity because it consumes a large proportion of the synthetic capacity of rapidly growing cells (Warner, 1999). Many different stress conditions cause reduction of RP gene synthesis (Jorgensen *et al.*, 2004; Marion *et al.*, 2004), presumably to save resources and to allow a shift of the gene transcription capacity of RNA Pol II to genes encoding proteins with protective functions, such as heat-shock proteins (HSPs). This was also observed earlier for arsenic (Chang *et al.*, 1989). The other side of the coin is that high RP gene transcription facilitates ribosome biogenesis, high capacity for protein synthesis and thus enhanced proliferation, when resources are available (Hartwell *et al.*, 1974; Hartwell and Unger, 1977; Warner, 1999; Jorgensen *et al.*, 2004). Therefore, dynamic control of RP gene transcription is important in a competitive environment. Our data indicate that inhibition of TORC1 by As(III) leads to the rapid inactivation of Sfp1 and a consequent reduction of RP gene expression. A similar loss of RP gene promoter binding is observed for Ifh1 upon As(III) treatment (data not shown), again paralleling the effect of rapamycin (Schawalder *et al.*, 2004). Interestingly, Sfp1 null mutants showed a higher capacity to survive under conditions of chronic arsenic stress. This result might be viewed as contradictory to the lower resistance seen with the *TOR1* null mutants. However, we see in microarrays that RP gene expression does not change in Sfp1 mutants. Therefore, these mutant cells are desensitized against RP gene repression. We speculate that in the wild-type strains chronic arsenic stress might drive many cells toward a terminal arrest condition caused in part by reduced RP gene expression. The arsenic sensitive phenotype of *tor1* mutant cells might be due to other targets of TORC1 such as Sch9. Furthermore, the transient inhibition of Sfp1 due to TORC1 inhibition as here reported with arsenic stress might be part of a general adaptive response. Consistent with this, overexpression of Sfp1 was detrimental to growth under arsenic stress. Nevertheless, increased survival of *SFP1* deletion mutants under chronic arsenic stress comes with the cost of a significantly reduced growth rate.

Unlike *SFP1* deletion, the absence of either Tor1 or Sch9 rendered cells more sensitive to arsenic. Consistent with an active role of the Tor1-Sch9 axis in counteracting As(III) stress, the phosphomimetic Sch9 mutants (*SCH9-3E*, *SCH9 2D3E*), whose activity is TORC1 independent, confer As(III) resistance. Because all three proteins (Sfp1, Tor1, and Sch9) function to activate RP genes, these observations indicate that Tor1 and Sch9 have function(s) related to the response to As(III) that are not shared with Sfp1. We suggest that one such function is the inhibition of Msn2/4, because deletion of these two genes completely reverses the As(III)-sensitivity phenotype of *tor1* cells (Figure 6). Consistent with this idea, previous work has implicated TORC1 as a negative regulator of Msn2/4 (Beck and Hall, 1999), at least partly acting through Sch9, which has recently been shown to down-regulate several Msn2/4 target genes (Urban *et al.*, 2007) and also directly regulates Rim15, a protein kinase involved in Msn2/4 regulation (Wanke *et al.*, 2008). TORC1 may well have other functions that promote growth in the presence of As(III). For example, TORC1 is involved in vacuolar-sorting functions (Aronova *et al.*, 2007) and might be important for vacuolar sequestration of glutathione conjugates resulting from As(III) exposure (Ghosh *et al.*, 1999). In any event, our genetic data indicate that inhibition of TORC1 signaling has two counteracting consequences regarding cell growth under conditions of chronic As(III) stress: inhibition of Sfp1 and de-repression of Msn2/4. Although the former promotes growth

at sublethal doses of As(III), continued expression of the stress factors Msn2/4 blocks growth. Moreover, arsenic might also trigger a general stress response, activating Msn2/4 and inactivating TORC1 in parallel. This scenario is in line with our genetic data showing that *msn2/4* and *tor1* mutants are independent. However, the fact that rapamycin as a rather specific inhibitor of TORC1 also activates Msn2, favors a sequential model in which TORC1 acts upstream to inactivate Msn2/4.

PKA and Arsenic Resistance

Arsenic-treated cells rapidly activated Msn2 and Msn4, raising the possibility that PKA becomes inhibited. This was also suggested recently (Jin *et al.*, 2008). Under optimal growth conditions PKA phosphorylates and inhibits both transcription factors, and inactivation of PKA is sufficient to activate Msn2 (Smith *et al.*, 1998). Furthermore, PKA activity is tightly regulated by short-term changes of glucose availability, with the presence of glucose resulting in high PKA activity. A connection between arsenite and PKA might be suggested by reduced glycolytic energy production similar to glucose depletion conditions (Jung and Rothstein, 1965). Acute glucose depletion triggers the rapid dephosphorylation of Msn2, whereas other Msn2 activating conditions such as heat stress do not lead to dephosphorylation (Go¨rner *et al.*, 2002; De Wever *et al.*, 2005). As(III) stress (similar to heat stress;Go¨rner *et al.*, 2002) slightly increased the Msn2 phosphorylation level on PKA sites. In principle this effect may also be the result of the inactivation of a phosphatase. In fact, PP2A was shown to be required for rapamycin- and stress-triggered nuclear retention of Msn2 (Santhanam *et al.*, 2004), which in turn is connected to TORC1 via its repressor Tap42 (Duvel *et al.*, 2003; Kuepfer *et al.*, 2007). PP2A is also involved in Msn2 regulation (W. Go¨rner and C. Schu¨ller, unpublished observations). Taken together, the phosphorylation status of Msn2 indicated sustained PKA activity and/or possibly reduced PP2A activity during As(III) stress.

In any case, PKA activity stays in a range that does not hinder down-regulation of RP genes. Hyperactive PKA prevents cytoplasmic accumulation of Sfp1 and also activates Fhl1/Ihf1, thus promoting RP gene transcription (Martin *et al.*, 2004; Schawalder *et al.*, 2004; Schmelzle *et al.*, 2004). Because in strains with zero PKA activity the shift of Sfp1 localization is not disturbed (Warner, 1999; Marion *et al.*, 2004), PKA activity below a threshold is most probably a precondition for inhibition of Sfp1. Sustained PKA activity is beneficial during chronic As(III) stress. It prevents hyperactivation of Msn2/4, which is detrimental for cell growth (Durchschlag *et al.*, 2004). This is supported by the increased As(III) resistance of mutants lacking Msn2 and Msn4. Second, additional repression of RP gene expression by reduced PKA activity through inactivation of Fhl1-Ifh1 might cause a pronounced shut-down of RP gene transcription, leading to irreversible stasis. In line with this notion, we find enhanced resistance of mutants with constitutive high PKA activity (*bcy10*) and increased arsenic stress sensitivity in cells with low (or no) PKA activity. Part of this phenotype can be attributed to inactivation of Msn2 and Msn4 by high PKA, but also to other targets, because its inactivation increases sensitivity in cells lacking Msn2 and Msn4 (*tpk1/2/30msn2/40* vs. *msn2/40*). In fact, PKA and TORC1 kinases also regulate the Rim15 kinase, which is required for entry into the stationary phase (Pedruzzi *et al.*, 2003).

Our results indicate a strong contribution of RP gene transcription in the arsenic stress response and a delicate balance of responses regulated by PKA and TOR (Figure 6). Dynamic regulation of RP gene expression has a role in the adaptation of growth and division according to environmental conditions. Arsenic seems to drive this response system into a dead-end situation where chronic activation of stress genes leads to severe growth inhibition. Our data indicate that although PKA may have an important influence on RP gene transcription under some conditions, TORC1 activity plays a key role even when PKA levels are high (Marion *et al.*, 2004; Zurita-Martinez and Cardenas, 2005; Chen and Powers, 2006), arguing against models in which PKA acts downstream of TOR to regulate ribosome biogenesis (Schmelzle *et al.*, 2004). One key question that remains is the mechanism by which arsenic inhibits TORC1. The answer to this may have important implications for understanding the effects of As(III) on humans, given the high degree of conservation of TORC1.

ACKNOWLEDGMENTS

We thank Peter W. Piper (University of Sheffield, Sheffield, United Kingdom) for the HSE-LacZ plasmid, Veerle de Wever for technical advice, and Nicolas Roggli for assistance with artwork. This work was supported by the Herzfelder Foundation (C.S.), the Austrian Science Fund (P19966-B12 to C.S.), the WWTF and SYSMO/Translucent (R.S.), the Swiss National Fund (31DY00-108708 to D.S.), the Canton of Geneva (R.L. and D.S.), the European Science Foundation EUROCORES program (03-DYNA-F-32 to D.S. and G.A.), and FP6-STREP QUASI (G.A.).

REFERENCES

Aronova, S., Wedaman, K., Anderson, S., Yates, J., 3rd, and Powers, T. (2007). Probing the membrane environment of the TOR kinases reveals functional interactions between TORC1, actin, and membrane trafficking in *Saccharomyces cerevisiae*. Mol. Biol. Cell *18*, 2779–2794.

Beck, T., and Hall, M. N. (1999). The TOR signalling pathway controls nuclear localization of nutrient-regulated transcription factors. Nature *402*, 689–692.

Bianchi, A., Negrini, S., and Shore, D. (2004). Delivery of yeast telomerase to a DNA break depends on the recruitment functions of Cdc13 and Est1. Mol. Cell *16*, 139–146.

Boorsma, A., Foat, B. C., Vis, D., Klis, F., and Bussemaker, H. J. (2005). T-profiler: scoring the activity of predefined groups of genes using gene expression data. Nucleic Acids Res. *33*, W592–W595.

Cavigelli, M., Li, W. W., Lin, A., Su, B., Yoshioka, K., and Karin, M. (1996). The tumor promoter arsenite stimulates AP-1 activity by inhibiting a JNK phosphatase. EMBO J. *15*, 6269–6279.

Chang, E. C., Kosman, D. J., and Willsky, G. R. (1989). Arsenic oxide-induced thermotolerance in *Saccharomyces cerevisiae*. J. Bacteriol. *171*, 6349–6352.

Chen, J. C., and Powers, T. (2006). Coordinate regulation of multiple and distinct biosynthetic pathways by TOR and PKA kinases in *S. cerevisiae*. Curr. Genet. *49*, 281–293.

Chua, G., Morris, Q. D., Sopko, R., Robinson, M. D., Ryan, O., Chan, E. T., Frey, B. J., Andrews, B. J., Boone, C., and Hughes, T. R. (2006). Identifying transcription factor functions and targets by phenotypic activation. Proc. Natl. Acad. Sci. USA *103*, 12045–12050.

Crespo, J. L., Powers, T., Fowler, B., and Hall, M. N. (2002). The TOR-controlled transcription activators GLN3, RTG1, and RTG3 are regulated in response to intracellular levels of glutamine. Proc. Natl. Acad. Sci. USA *99*, 6784–6789.

De Wever, V., Reiter, W., Ballarini, A., Ammerer, G., and Brocard, C. (2005). A dual role for PP1 in shaping the Msn2-dependent transcriptional response to glucose starvation. EMBO J. *24*, 4115–4123.

Durchschlag, E., Reiter, W., Ammerer, G., and Schu¨ller, C. (2004). Nuclear localization destabilizes the stress-regulated transcription factor Msn2. J. Biol. Chem. *279*, 55425–55432.

Duvel, K., Santhanam, A., Garrett, S., Schneper, L., and Broach, J. R. (2003). Multiple roles of Tap42 in mediating rapamycin-induced transcriptional changes in yeast. Mol. Cell *11*, 1467–1478.

Eisen, M. B., Spellman, P. T., Brown, P. O., and Botstein, D. (1998). Cluster analysis and display of genome-wide expression patterns. Proc. Natl. Acad. Sci. USA *95*, 14863–14868.

Evens, A. M., Tallman, M. S., and Gartenhaus, R. B. (2004). The potential of arsenic trioxide in the treatment of malignant disease: past, present, and future. Leuk. Res. *28*, 891–900.

Fingerman, I., Nagaraj, V., Norris, D., and Vershon, A. K. (2003). Sfp1 plays a key role in yeast ribosome biogenesis. Eukaryot. Cell *2*, 1061–1068.

Garmendia-Torres, C., Goldbeter, A., and Jacquet, M. (2007). Nucleocytoplasmic oscillations of the yeast transcription factor Msn2, evidence for periodic PKA activation. Curr. Biol. *17*, 1044–1049.

Gasch, A. P. (2007). Comparative genomics of the environmental stress response in ascomycete fungi. Yeast *24*, 961–976.

Ghosh, M., Shen, J., and Rosen, B. P. (1999). Pathways of As(III) detoxification in *Saccharomyces cerevisiae.* Proc. Natl. Acad. Sci. USA *96*, 5001–5006.

Go¨rner, W., Durchschlag, E., Martinez-Pastor, M. T., Estruch, F., Ammerer, G., Hamilton, B., Ruis, H., and Schu¨ller, C. (1998). Nuclear localization of the C2H2 zinc finger protein Msn2p is regulated by stress and protein kinase A activity. Genes Dev. *12*, 586–597.

Go¨rner, W., Durchschlag, E., Wolf, J., Brown, E. L., Ammerer, G., Ruis, H., and Schu¨ller, C. (2002). Acute glucose starvation activates the nuclear localization signal of a stress-specific yeast transcription factor. EMBO J. *21*, 135–144.

Hardwick, J. S., Kuruvilla, F. G., Tong, J. K., Shamji, A. F., and Schreiber, S. L. (1999). Rapamycin-modulated transcription defines the subset of nutrient-sensitive signaling pathways directly controlled by the Tor proteins. Proc. Natl. Acad. Sci. USA *96*, 14866–14870.

Hartwell, L. H., Culotti, J., Pringle, J. R., and Reid, B. J. (1974). Genetic control of the cell division cycle in yeast. Science *183*, 46–51.

Hartwell, L. H., and Unger, M. W. (1977). Unequal division in *Saccharomyces cerevisiae* and its implications for the control of cell division. J. Cell Biol. *75*, 422–435.

Haugen, A. C., Kelley, R., Collins, J. B., Tucker, C. J., Deng, C., Afshari, C. A., Brown, J. M., Ideker, T., and Van Houten, B. (2004). Integrating phenotypic and expression profiles to map arsenic-response networks. Genome Biol. *5*, R95.

Heitman, J., Movva, N. R., and Hall, M. N. (1991). Targets for cell cycle arrest by the immunosuppressant rapamycin in yeast. Science *253*, 905–909.

Jin, Y. H., Dunlap, P. E., McBride, S. J., Al-Refai, H., Bushel, P. R., and Freedman, J. H. (2008). Global transcriptome and deletome profiles of yeast exposed to transition metals. PLoS Genet *4*, e1000053.

Jones, J. S., and Prakash, L. (1990). Yeast *Saccharomyces cerevisiae* selectable markers in pUC18 polylinkers. Yeast *6*, 363–366.

Jorgensen, P., Nishikawa, J. L., Breitkreutz, B. J., and Tyers, M. (2002). Systematic identification of pathways that couple cell growth and division in yeast. Science *297*, 395–400.

Jorgensen, P., Rupes, I., Sharom, J. R., Schneper, L., Broach, J. R., and Tyers, M. (2004). A dynamic transcriptional network communicates growth potential to ribosome synthesis and critical cell size. Genes Dev. *18*, 2491–2505.

Jung, C., and Rothstein, A. (1965). Arsenate uptake and release in relation to the inhibition of transport and glycolysis in yeast. Biochem. Pharmacol. *14*, 1093–1112.

Kaeberlein, M., Powers, R. W., 3rd, Steffen, K. K., Westman, E. A., Hu, D., Dang, N., Kerr, E. O., Kirkland, K. T., Fields, S., and Kennedy, B. K. (2005). Regulation of yeast replicative life span by TOR and Sch9 in response to nutrients. Science *310*, 1193–1196.

Kuepfer, L., Peter, M., Sauer, U., and Stelling, J. (2007). Ensemble modeling for analysis of cell signaling dynamics. Nat. Biotechnol. *25*, 1001–1006.

Kuruvilla, F. G., Shamji, A. F., and Schreiber, S. L. (2001). Carbon- and nitrogen-quality signaling to translation are mediated by distinct GATA-type transcription factors. Proc. Natl. Acad. Sci. USA *98*, 7283–7288.

Loewith, R., Jacinto, E., Wullschleger, S., Lorberg, A., Crespo, J. L., Bonenfant, D., Oppliger, W., Jenoe, P., and Hall, M. N. (2002). Two TOR complexes, only one of which is rapamycin sensitive, have distinct roles in cell growth control. Mol. Cell *10*, 457–468.

Lu, J., Chew, E. H., and Holmgren, A. (2007). Targeting thioredoxin reductase is a basis for cancer therapy by arsenic trioxide. Proc. Natl. Acad. Sci. USA *104*, 12288–12293.

Marion, R. M., Regev, A., Segal, E., Barash, Y., Koller, D., Friedman, N., and O'Shea, E. K. (2004). Sfp1 is a stress- and nutrient-sensitive regulator of ribosomal protein gene expression. Proc. Natl. Acad. Sci. USA *101*, 14315–14322.

Martin, D. E., Soulard, A., and Hall, M. N. (2004). TOR regulates ribosomal protein gene expression via PKA and the Forkhead transcription factor FHL1. Cell *119*, 969–979.

Martinez-Pastor, M. T., Marchler, G., Schu¨ller, C., Marchler-Bauer, A., Ruis, H., and Estruch, F. (1996). The *Saccharomyces cerevisiae* zinc finger proteins Msn2p and Msn4p are required for transcriptional induction through the stress response element (STRE). EMBO J. *15*, 2227–2235.

Nadon, R., and Shoemaker, J. (2002). Statistical issues with microarrays: processing and analysis. Trends Genet. *18*, 265–271.

Pedruzzi, I., Dubouloz, F., Cameroni, E., Wanke, V., Roosen, J., Winderickx, J., and De Virgilio, C. (2003). TOR and PKA signaling pathways converge on the protein kinase Rim15 to control entry into G0. Mol. Cell *12*, 1607–1613.

Rodriguez-Gabriel, M. A., and Russell, P. (2005). Distinct signaling pathways respond to arsenite and reactive oxygen species in *Schizosaccharomyces pombe.* Eukaryot. Cell *4*, 1396–1402.

Roosen, J., Engelen, K., Marchal, K., Mathys, J., Griffioen, G., Cameroni, E., Thevelein, J. M., De Virgilio, C., De Moor, B., and Winderickx, J. (2005). PKA and Sch9 control a molecular switch important for the proper adaptation to nutrient availability. Mol. Microbiol. *55*, 862–880.

Rudra, D., Zhao, Y., and Warner, J. R. (2005). Central role of Ifh1p-Fhl1p interaction in the synthesis of yeast ribosomal proteins. EMBO J. *24*, 533–542.

Saldanha, A. J. (2004). Java Treeview—extensible visualization of microarray data. Bioinformatics *20*, 3246–3248.

Salnikow, K., and Zhitkovich, A. (2008). Genetic and epigenetic mechanisms in metal carcinogenesis and cocarcinogenesis: nickel, arsenic, and chromium. Chem. Res. Toxicol. *21*, 28–44.

Santangelo, G. M. (2006). Glucose signaling in *Saccharomyces cerevisiae.* Microbiol. Mol. Biol. Rev. *70*, 253–282.

Santhanam, A., Hartley, A., Duvel, K., Broach, J. R., and Garrett, S. (2004). PP2A phosphatase activity is required for stress and Tor kinase regulation of yeast stress response factor Msn2p. Eukaryot. Cell *3*, 1261–1271.

Schawalder, S. B., Kabani, M., Howald, I., Choudhury, U., Werner, M., and Shore, D. (2004). Growth-regulated recruitment of the essential yeast ribosomal protein gene activator Ifh1. Nature *432*, 1058–1061.

Schmelzle, T., Beck, T., Martin, D. E., and Hall, M. N. (2004). Activation of the RAS/cyclic AMP pathway suppresses a TOR deficiency in yeast. Mol. Cell. Biol. *24*, 338–351.

Schmidt, A., Beck, T., Koller, A., Kunz, J., and Hall, M. N. (1998). The TOR nutrient signalling pathway phosphorylates NPR1 and inhibits turnover of the tryptophan permease. EMBO J. *17*, 6924–6931.

Smith, A., Ward, M. P., and Garrett, S. (1998). Yeast PKA represses Msn2p/Msn4p-dependent gene expression to regulate growth, stress response and glycogen accumulation. EMBO J. *17*, 3556–3564.

Sorger, P. K., and Pelham, H. R. (1987). Purification and characterization of a heat-shock element binding protein from yeast. EMBO J. *6*, 3035–3041.

Tamas, M. J., and Wysocki, R. (2001). Mechanisms involved in metalloid transport and tolerance acquisition. Curr. Genet *40*, 2–12.

Thorsen, M., *et al.* (2006). The MAPK Hog1p modulates Fps1p-dependent arsenite uptake and tolerance in yeast. Mol. Biol. Cell *17*, 4400–4410.

Thorsen, M., Lagniel, G., Kristiansson, E., Junot, C., Nerman, O., Labarre, J., and Tamas, M. J. (2007). Quantitative transcriptome, proteome and sulfur metabolite profiling of the *Saccharomyces cerevisiae* response to arsenite. Physiol. Genomics *30*, 35–43.

Urban, J., *et al.* (2007). Sch9 is a major target of TORC1 in *Saccharomyces cerevisiae*. Mol. Cell *26*, 663–674.

Wade, J. T., Hall, D. B., and Struhl, K. (2004). The transcription factor Ifh1 is a key regulator of yeast ribosomal protein genes. Nature *432*, 1054–1058.

Wang, Z. Y., and Chen, Z. (2008). Acute promyelocytic leukemia: from highly fatal to highly curable. Blood *111*, 2505–2515.

Wanke, V., Cameroni, E., Uotila, A., Piccolis, M., Urban, J., Loewith, R., and De Virgilio, C. (2008). Caffeine extends yeast lifespan by targeting TORC1. Mol. Microbiol. *69*, 277–285.

Warner, J. R. (1999). The economics of ribosome biosynthesis in yeast. Trends Biochem. Sci. *24*, 437–440.

Wullschleger, S., Loewith, R., and Hall, M. N. (2006). TOR signaling in growth and metabolism. Cell *124*, 471–484.

Wysocki, R., Chery, C. C., Wawrzycka, D., Van Hulle, M., Cornelis, R., Thevelein, J. M., and Tamas, M. J. (2001). The glycerol channel Fps1p mediates the uptake of arsenite and antimonite in *Saccharomyces cerevisiae.* Mol. Microbiol. *40*, 1391–1401.

Wysocki, R., Fortier, P. K., Maciaszczyk, E., Thorsen, M., Leduc, A., Odhagen, A., Owsianik, G., Ulaszewski, S., Ramotar, D., and Tamas, M. J. (2004). Transcriptional activation of metalloid tolerance genes in *Saccharomyces cerevisiae* requires the AP-1-like proteins Yap1p and Yap8p. Mol. Biol. Cell *15*, 2049–2060.

Zurita-Martinez, S. A., and Cardenas, M. E. (2005). Tor and cyclic AMP-protein kinase A: two parallel pathways regulating expression of genes required for cell growth. Eukaryot. Cell *4*, 63–71.

Supplemental Figures ad "Arsenic toxicity to *Saccharomyces cerevisiae* is a consequence of inhibition of the TORC1 kinase combined with a chronic stress response"

Supplemental Figure 1: Influence of Sfp1 and Msn2/4 on different As(III) regulated signaling pathways. Hsf1-dependent genes (A), Yap1 dependent genes (B), and Rpn4 dependent genes (C) have a reduced response to As(III) in *sfp1Δ* but not in *msn2Δmsn4Δ* deletion mutant cells.

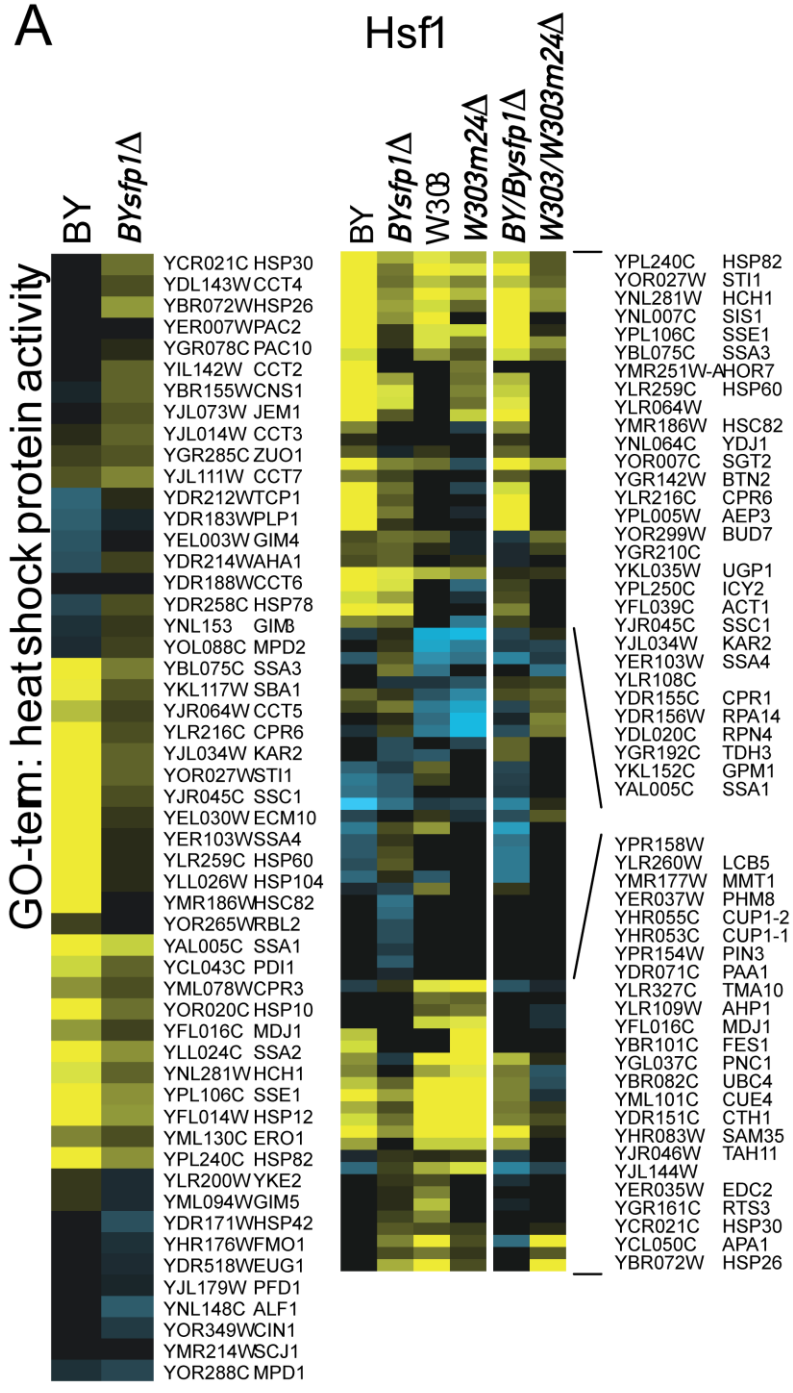

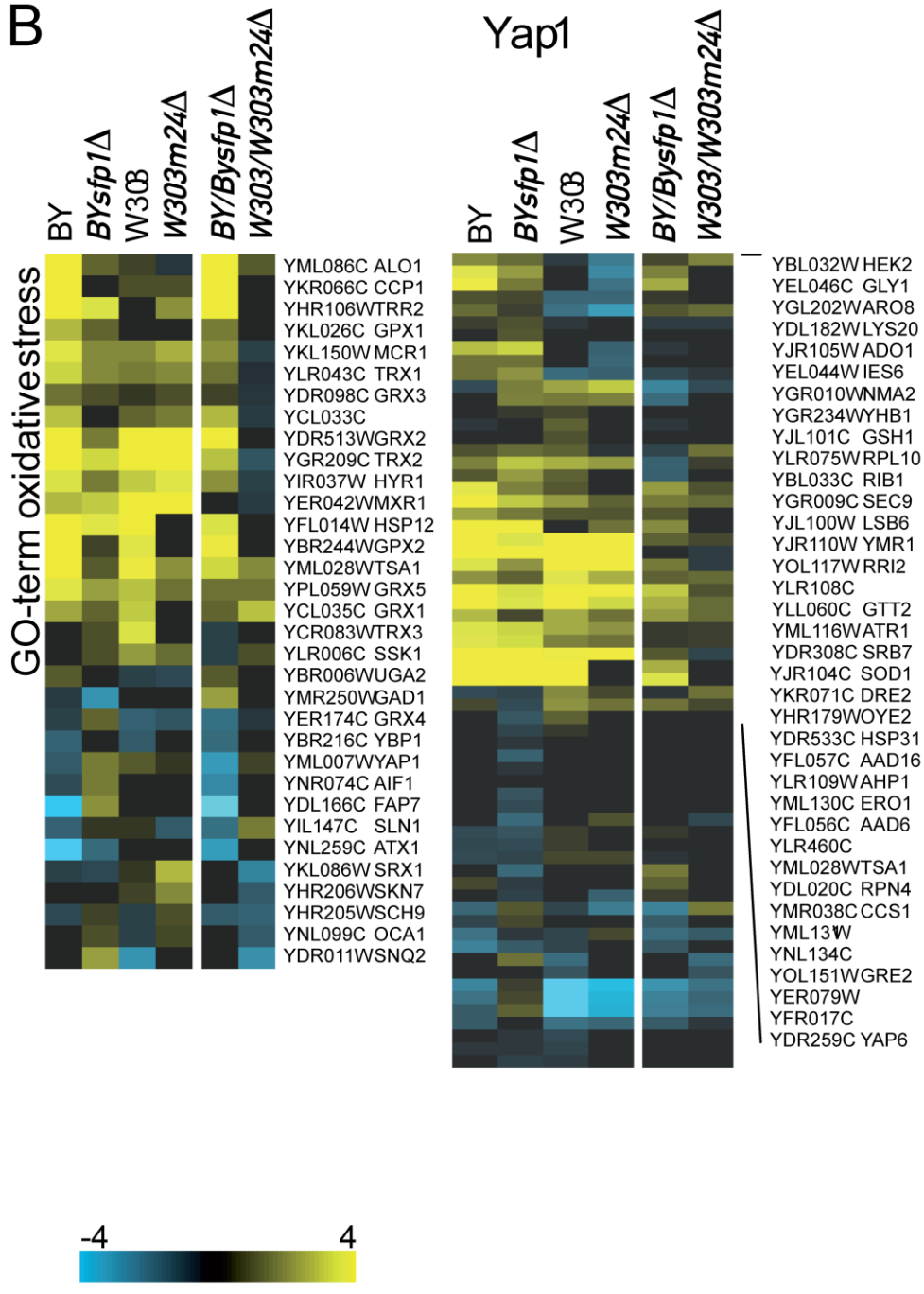
B
GO-term oxidativestress
BY
BYsfp1Δ
W303
W303m24Δ
BY/Bysfp1Δ
W303/W303m24Δ
YML086C ALO1
YKR066C CCP1
YHR106WTRR2
YKL026C GPX1
YKL150W MCR1
YLR043C TRX1
YDR098C GRX3
YCL033C
YDR513WGRX2
YGR209C TRX2
YIR037W HYR1
YER042WMXR1
YFL014W HSP12
YBR244WGPX2
YML028WTSA1
YPL059W GRX5
YCL035C GRX1
YCR083WTRX3
YLR006C SSK1
YBR006WUGA2
YMR250WGAD1
YER174C GRX4
YBR216C YBP1
YML007WYAP1
YNR074C AIF1
YDL166C FAP7
YIL147C SLN1
YNL259C ATX1
YKL086W SRX1
YHR206WSKN7
YHR205WSCH9
YNL099C OCA1
YDR011WSNQ2
Yap1
BY
BYsfp1Δ
W303
W303m24Δ
BY/Bysfp1Δ
W303/W303m24Δ
YBL032W HEK2
YEL046C GLY1
YGL202WARO8
YDL182W LYS20
YJR105W ADO1
YEL044W IES6
YGR010WNMA2
YGR234WYHB1
YJL101C GSH1
YLR075W RPL10
YBL033C RIB1
YGR009C SEC9
YJL100W LSB6
YJR110W YMR1
YOL117W RRI2
YLR108C
YLL060C GTT2
YML116WATR1
YDR308C SRB7
YJR104C SOD1
YKR071C DRE2
YHR179WOYE2
YDR533C HSP31
YFL057C AAD16
YLR109W AHP1
YML130C ERO1
YFL056C AAD6
YLR460C
YML028WTSA1
YDL020C RPN4
YMR038C CCS1
YML13?W
YNL134C
YOL151W GRE2
YER079W
YFR017C
YDR259C YAP6
-4
4

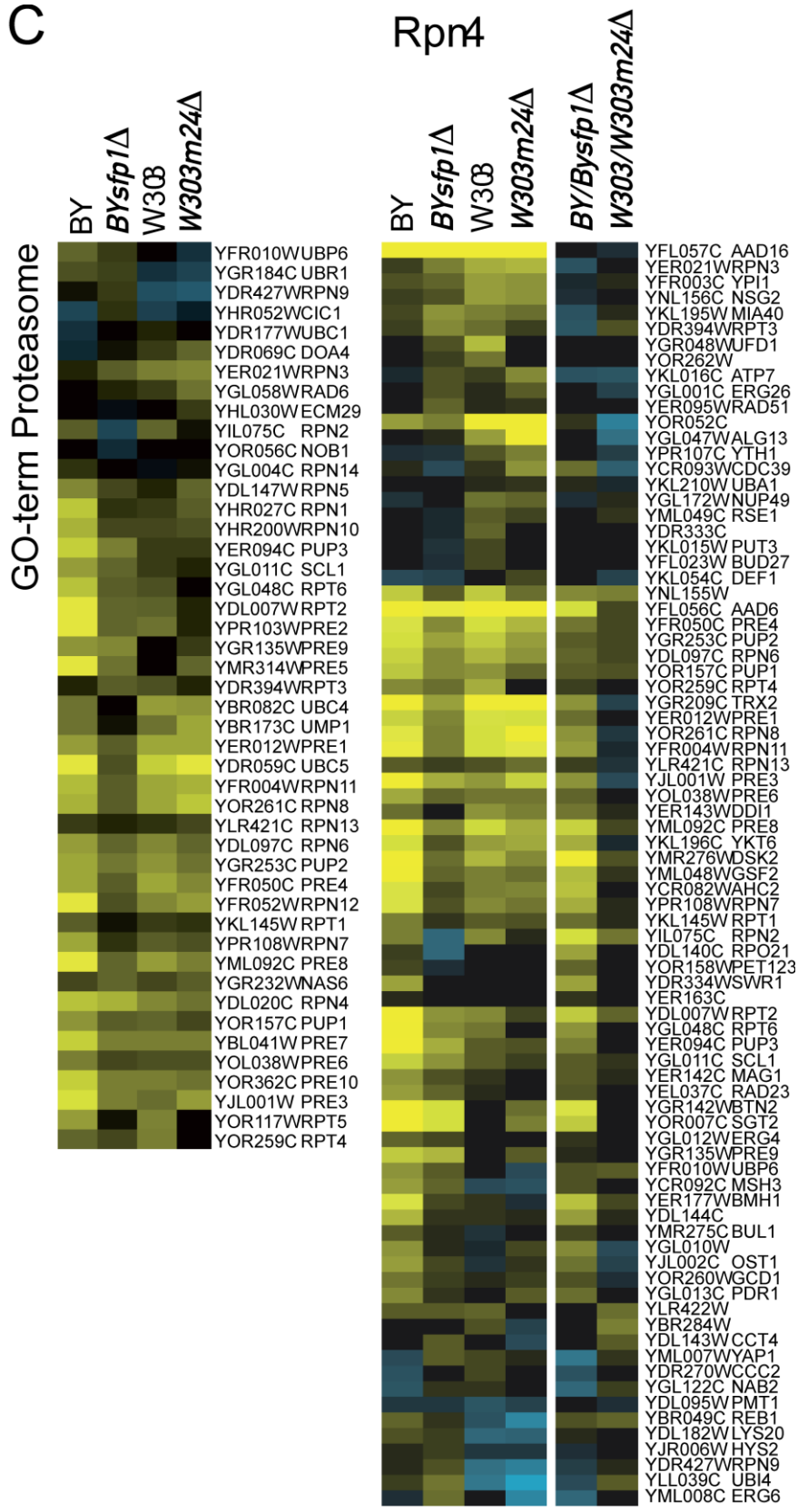
C
GO-term Proteasome
BY
BYsfp1Δ
W303
W303m24Δ
YFR010W UBP6
YGR184C UBR1
YDR427W RPN9
YHR052W CIC1
YDR177W UBC1
YDR069C DOA4
YER021W RPN3
YGL058W RAD6
YHL030W ECM29
YIL075C RPN2
YOR056C NOB1
YGL004C RPN14
YDL147W RPN5
YHR027C RPN1
YHR200W RPN10
YER094C PUP3
YGL011C SCL1
YGL048C RPT6
YDL007W RPT2
YPR103W PRE2
YGR135W PRE9
YMR314W PRE5
YDR394W RPT3
YBR082C UBC4
YBR173C UMP1
YER012W PRE1
YDR059C UBC5
YFR004W RPN11
YOR261C RPN8
YLR421C RPN13
YDL097C RPN6
YGR253C PUP2
YFR050C PRE4
YFR052W RPN12
YKL145W RPT1
YPR108W RPN7
YML092C PRE8
YGR232W NAS6
YDL020C RPN4
YOR157C PUP1
YBL041W PRE7
YOL038W PRE6
YOR362C PRE10
YJL001W PRE3
YOR117W RPT5
YOR259C RPT4
Rpn4
BY
BYsfp1Δ
W303
W303m24Δ
BY/Bysfp1Δ
W303/W303m24Δ
YFL057C AAD16
YER021W RPN3
YFR003C YPI1
YNL156C NSG2
YKL195W MIA40
YDR394W RPT3
YGR048W UFD1
YOR262W
YKL016C ATP7
YGL001C ERG26
YER095W RAD51
YOR052C
YGL047W ALG13
YPR107C YTH1
YCR093W CDC39
YKL210W UBA1
YGL172W NUP49
YML049C RSE1
YDR333C
YKL015W PUT3
YFL023W BUD27
YKL054C DEF1
YNL155W
YFL056C AAD6
YFR050C PRE4
YGR253C PUP2
YDL097C RPN6
YOR157C PUP1
YOR259C RPT4
YGR209C TRX2
YER012W PRE1
YOR261C RPN8
YFR004W RPN11
YLR421C RPN13
YJL001W PRE3
YOL038W PRE6
YER143W DDI1
YML092C PRE8
YKL196C YKT6
YMR276W DSK2
YML048W GSF2
YCR082W AHC2
YPR108W RPN7
YKL145W RPT1
YIL075C RPN2
YDL140C RPO21
YOR158W PET123
YDR334W SWR1
YER163C
YDL007W RPT2
YGL048C RPT6
YER094C PUP3
YGL011C SCL1
YER142C MAG1
YEL037C RAD23
YGR142W BTN2
YOR007C SGT2
YGL012W ERG4
YGR135W PRE9
YFR010W UBP6
YCR092C MSH3
YER177W BMH1
YDL144C
YMR275C BUL1
YGL010W
YJL002C OST1
YOR260W GCD1
YGL013C PDR1
YLR422W
YBR284W
YDL143W CCT4
YML007W YAP1
YDR270W CCC2
YGL122C NAB2
YDL095W PMT1
YBR049C REB1
YDL182W LYS20
YJR006W HYS2
YDR427W RPN9
YLL039C UBI4
YML008C ERG6

Supplemental Figure 2: A) Sfp1-GFP exits the nucleus upon arsenic stress. DAPI staining of living cells was done in parallel to mark the nucleus. **B)** Comparison of microarray data of rapamycin treated cells of Hardwick et al. 1999, (60 minutes time point) with data generated in this study. Ribosomal Protein (RP) genes are indicated.

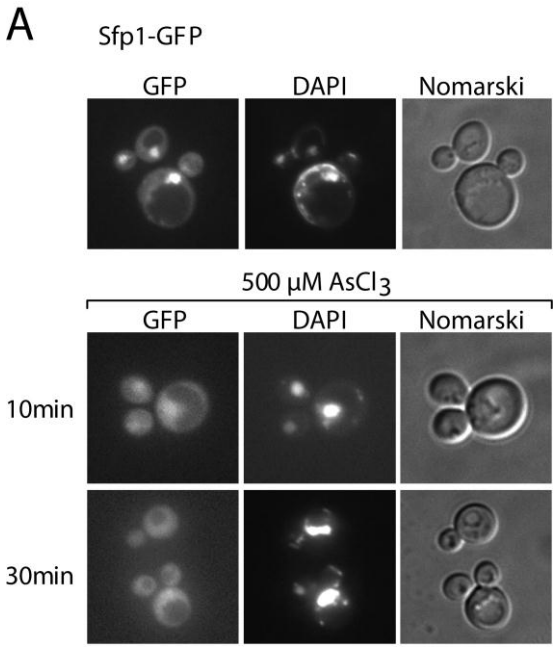

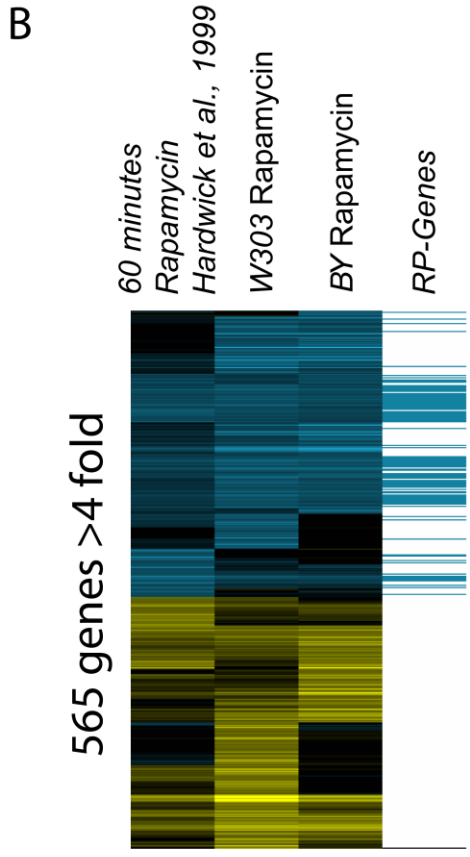

2.3 Stb5 participates in the adaptation of *Saccharomyces cerevisiae* to acute and chronic mercury stress

Dagmar Hosiner[5], Hella Lichtenberg-Fraté[2], Susanne Gerber[3,4], Edda Klipp[4] and Christoph Schüller[1] ¶)

[1] Department of Applied Genetics and Cell Biology UFT-Campus Tulln, University of Natural Resources and Life Sciences (BOKU), Vienna;

[2] AG Molekulare Bioenergetik, IZMB, Rheinische-Friedrich-Wilhelms-Universität Bonn

[3] AG Computational Time Series Analysis, Institute of Computational Science, Faculty of Informatics, Università della Svizzera italiana, Lugano

[4] Theoretical Biophysics Humboldt-Universität zu Berlin

[5] Department of Genetics, MFPL, University of Vienna, Vienna

¶) To whom correspondence should be addressed

The author's contribution

Dagmar Hosiner	- conceived the study, microarray analyses, phenotypic analyses, fluorescence microscopy, writing
Susanne Gerber	- microarray analyses, writing
Hella Lichtenberg-Fraté	- writing, advices
Edda Klipp	- advices
Christoph Schüller	- conceived the study, correspondence, writing, advices

Stb5 participates in the adaptation of *Saccharomyces cerevisiae* to acute and chronic mercury stress

Abstract

The *Saccharomyces cerevisiae* zinc finger transcription factor Stb5 is a regulator involved in response to oxidative stress. In this study, we provide evidence that Stb5 is also involved in the metal stress response. Aiming at the molecular function of Stb5 we investigated transcription profiles of wild-type cells under acute (15min and 30min), sustained (2h), and chronic (24h) mercury exposure in comparison with an *STB5* deletion strain. We demonstrated changes of yeast *wt* cells during adaptation to mercury treatment on the expression level and performed a detailed examination of further regulators involved in the mercury stress response. Although *stb5*Δ mutant cells also exhibited transcriptional adaptation to mercury stress we detected a considerably retarded growth phenotype. We indicated this effect to be due to enhanced oxidative stress in *stb5*Δ based on participation of Stb5 in the antioxidant system of yeast cells. In this regard we showed missing *MET17* expression and activation of cell aging genes in *stb5*Δ under acute mercury stress and significantly reduced production of high-energy compounds for oxidative defense along with selective activation of the oxidatively more resistant 20S proteasome in the mutant under chronic mercury treatment. In summary, we proved no direct function of Stb5 under mercury stress but place Stb5 important for the yeast metal defense.

Introduction

In former centuries mercury has been used as an essential part of cosmetics and pharmaceuticals such as antibacterial agents (antisyphilitics), diuretics, antiseptics, or laxatives. Despite diverse symptoms of poisoning (Maranzana, 1952; Waldron, 1983), mercury became popularly known as a health threatening metal not until the 1940s to the 1960s (Buckell *et al.*, 1946). Today mercury is accounted as one of the most toxic elements widespread in nature that still accumulates due to volcanic eruptions, which are responsible for approximately half of atmospheric mercury emissions. But mercury pollution is also generated by manmade sources including biomass combustion, gold mining and cement production as well as industrial waste disposal (Pacyna *et al.*, 2006; Cukrov *et al.*, 2010). Despite its toxicity, mercury is still used as ingredient in dental amalgams (Tedeschi, 1982; Ngim *et al.*, 1992; Moen *et al.*, 2008; Choy *et al.*, 2009; Al-Saleh and Al-Sedairi, 2011), fungicides, preservative in vaccines and or topical disinfectants (Clarkson and Magos, 2006; Clifton, 2007).

Ionic mercury and its highly reactive toxic compounds are well-known to cause irreversible damage upon peak or prolonged exposure in humans, plants and microorganisms. Mercury has the ability to cross the blood-brain as well as the placental barrier and primarily affects the neurological system but also inner organs as liver and kidneys (Liang *et al.*, 1993; Pathak and Bhowmik, 1998; Zalups, 2000a; Barbier *et al.*, 2005; Montgomery *et al.*, 2008; Fujimura *et al.*, 2009; Yorifuji *et al.*, 2009; Jan *et al.*, 2011). One of mercury´s most harmful properties is its high affinity for thiol or sulfhydryl groups. That attributes to its effects on structural and functional protein dysfunction and depletion of cellular antioxidants such as glutathione leading to intracellular accumulation of reactive oxygen species (ROS) and oxidative stress (Vallee and Ulmer, 1972; Stohs and Bagchi, 1995; Westwater *et al.*, 2002; Ballatori, 2002; Valko *et al.*, 2005; Mieiro *et al.*, 2010; Lushchak, 2010).

Basically cells respond to mercury exposure with chelation of mercury ions via antioxidants or metallothioneins and sequestration into vacuoles and lysosomes or active extrusion out of the cell (Nies, 1999; Zalups and Koropatnick, 2000; Westwater *et al.*, 2002; Brambila *et al.*, 2002; Liu *et al.*, 2003; Wolf and Baynes, 2007). In *S. cerevisiae* intracellular sequestration of mercury-chelates to vacuoles was so far described for the vacuolar ABC (ATP-binding cassette) transporter Ycf1 (Gueldry *et al.*, 2003). Ycf1 shares extensive homology with the human multidrug resistance-associated protein (MRP1), the rat canalicular MRP (cMRP), and the human cystic fibrosis transmembrane conductance regulator (hCFTR) also functioning in drug and ion transport (Szczypka *et al.*, 1994; Sugawara *et al.*, 1998; Gueldry *et al.*, 2003; Preveral *et al.*, 2006). These homologies may indicate that organisms use related metal detoxification mechanisms.

It was suggested that the early metal stress-activated genes are involved in plasma membrane and active transport processes of the PDR (pleiotropic or multidrug resistance) network, which are primarily Yap1/Pdr1-controlled (Gounalaki and Thireos, 1994; Jungwirth *et al.*, 2000; DeRisi *et al.*, 2000; Lucau-Danila *et al.*, 2005; Jungwirth and Kuchler, 2006; Fardeau *et al.*, 2007). Further transcription factors (TFs) involved in metal stress are Hsf1, Gcn4, Rpn4, Sfp1, and Rap1, besides others (Natarajan *et al.*, 2001; Moye-Rowley, 2003; Haugen *et al.*, 2004; Ferguson *et al.*, 2005). We found mRNAs of the zinc finger TF Stb5 increased under arsenic and cadmium stress (Hosiner *et al.*, 2012 in preparation). Stb5 is a regulator of multidrug resistance and oxidative stress response and was originally detected in a yeast two-hybrid screen as interacting factor with Sin3 (Kasten and Stillman, 1997; Akache and Turcotte, 2002; MacPherson *et al.*, 2006). Stb5 has been shown to bind to its own promoter, but also to form heterodimers with Pdr1 suggesting targetting of different genes (Harbison *et al.*, 2004; Akache *et al.*, 2004). Recently, Stb5 has been reported to bind almost exclusively without Pdr1 or Pdr3 to its target genes (100 of 108) and suggested as a key player in the control of NADPH production for resistance to oxidative stress (Larochelle *et al.*, 2006).

To investigate the role of Stb5 in response to mercury stress and to gain new insights into the cellular defense mechanisms against mercury, genome-wide time course expression analyses of sublethal mercury exposure of *S. cerevisiae* were performed. For this purpose the effects of

short- and long-term (15min, 30min, 2h, and 24h) mercury chloride ($HgCl_2$) treatment of *STB5* deletion mutants (*stb5*Δ) were compared with those of wild-type (*wt*) cells.

We show that Stb5 obtains an important role under acute as well as chronic mercury exposure. Transcriptional profiling revealed 640 differentially expressed (greater/minor than 1.5-fold) genes in *wt* and 576 differentially expressed genes in *stb5*Δ upon short-term (15min, 30min, and 2h) and 1207 genes in wild-type and 706 genes in the mutant in response to chronic (24h) mercury stress. These genes were used for further analyses comprising assignment to significant GO terms and regulatory associations and provide expressional evidence for adaptation of yeast cells to sustained mercury stress via establishment of detoxification strategies at a post-translational level. Similarity analyses between expression profiles present extensive overlaps between *wt* and *stb5*Δ and also show decisive deficiencies of the mutant during mercury stress compared to *wt*. The main findings especially include missing activation of *MET17* encoding a key enzyme for oxidant defense in yeast under acute mercury treatment. And we found decreased production of high-energy compounds for the antioxidant system and activation of the 20S proteasome in *stb5*Δ upon chronic mercury exposure, whereas genes of the 26S proteasome were expressed in *wt*.

Results and Discussion

Deletion of STB5 leads to increased metal ion sensitivity

The role of *STB5* deletion on cell growth upon metal stress was investigated by serial 10-fold dilutions of BY-4741 and BY*stb5*Δ cells on metal-ion containing agar plates ($AsCl_3$, $CdCl_2$, and $HgCl_2$) in comparison with a control plate (YPD). As shown in Figure 1 the *stb5*Δ mutant exhibited reduced growth upon the tested metal ions. Complementation with a centromeric *STB5* (+YCp111-*STB5*) plasmid restored the growth defect and proved that it was due to the absence of Stb5. Phenotypic analyses upon further metal ions ($CoCl_2$, $CuSO_4$, $MnCl_2$, $NiSO_4$, VCl_3, and $ZnCl_2$) resulted in similar growth deficiencies of *stb5*Δ (Supplemental Figure 1) indicating a central role for Stb5 in the systemic defense of yeast cells against metal exposure.

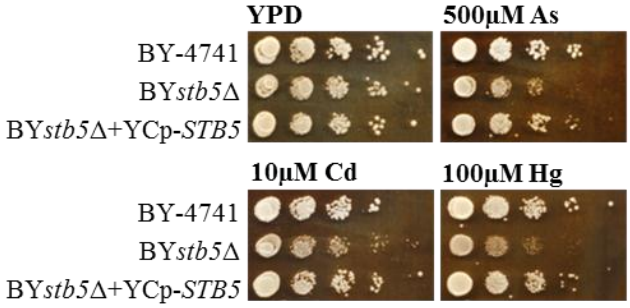

Figure 1. Growth assays on metal-containing solid medium. Serial 10-fold dilutions of BY-4741, BY*stb5*Δ, and BY*stb5*Δ+YCp/*STB5* were spotted onto YPD plates supplemented with $AsCl_3$, $CdCl_2$, and $HgCl_2$ (concentrations as indicated) and scored after 48h. Complementation of BY*stb5*Δ with YCp/*STB5* restored the growth defect of the mutant upon all tested metals.

The effect of mercury on yeast growth was also examined in liquid culture by exposition of logarithmically growing yeast cells (*wt*, *stb5*Δ) to increasing concentrations of $HgCl_2$ in YPD medium. Cell growth was monitored by determination of the optical density (OD) A_{600} 30°C for 12h. Cells lacking *STB5* nearly ceased growth at an Hg^{2+}-concentration of 30 to 40µM while the wild-type cells stopped growth not until 50µM $HgCl_2$ (Figure 2A and B). Accordingly, deletion of *STB5* increased mercury sensitivity of *stb5*Δ by 10 to 20µM compared to *wt*.

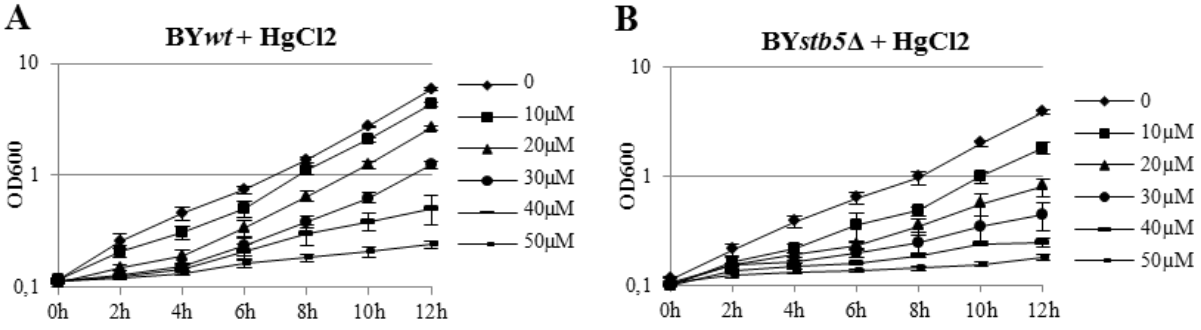

Figure 2. Toxicity assays of $HgCl_2$ in BY-4741 and BY*stb5*Δ. Mercury chloride was added to exponentially growing yeast cells, BY-4741 **(A)** and BY*stb5*Δ **(B)**, in liquid YPD at concentrations indicated in the figure and OD_{600} was measured every 2h up to 12h.

Next, we determined the critical concentration of $HgCl_2$ leading to the observed growth discrepancy between *wt* and *stb5*Δ during adaptation to mercury exposure. We cultivated over-night cultures of *wt* and *stb5*Δ in liquid YPD containing 30µM, 40µM, and 50µM $HgCl_2$ at 30°C starting from an OD_{600} ~ 0.1. After 18h the cells were recultivated in fresh Hg-containing YPD at an OD_{600} ~ 0.1 and incubated for 12 hours at 30°C by measuring OD_{600} every 4 hours. The growth rates of *wt* and *stb5*Δ showed no difference upon 30µM but stagnated upon 50µM

$HgCl_2$. At 40µM $HgCl_2$ the growth rate of the deletion strain was considerably decreased by about 60% in comparison with the wild-type (Figure 3).

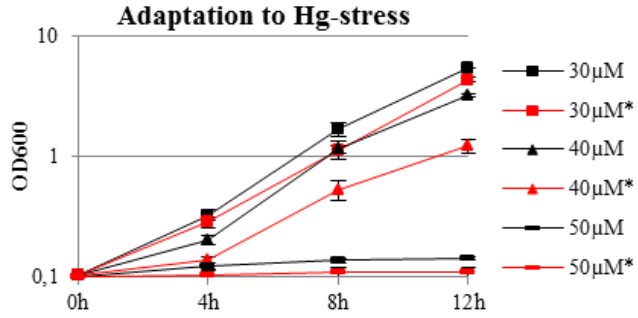

Figure 3. Adaptation of BY-4741 and BY*stb5*Δ to $HgCl_2$. Overnight cultures (BY-4741 in black, BY*stb5** in red) were grown for 18h in liquid YPD supplemented with 30µM, 40µM, and 50µM $HgCl_2$ and recultivated in fresh Hg-containing YPD. OD_{600} was measured after 0h, 4h, 8h, and 12h to follow adaptation of *wt* and *stb5*Δ to mercury exposure.

STB5 is localized to the nucleus

Subcellular localization studies of Stb5 were performed by fluorescence microscopy of GFP-tagged Stb5 in living cells. Cells were exposed to 40µM mercury chloride in liquid YPD for 30min at 30°C and the Stb5 localization was determined in comparison with untreated cells. GFP-fluorescence showed that Stb5 was localized in the nucleus under both conditions (Supplemental Figure 2). According to the obtained result Stb5 appears to belong to the category of Zn-cluster proteins that is constitutively present in the nucleus.

Global expression profiles upon 40µM mercury exposition

Transcriptional expression analyses were performed by exposing exponentially growing yeast cells (*wt*, *stb5*Δ) in liquid YPD medium supplemented with 40µM $HgCl_2$. To examine transcription differences during transient mercury exposure *wt* and *stb5*Δ cells (OD_{600} ~ 0.8) were exposed for 15min, 30min and 2h at 30°C. For investigation of chronic mercury stress the strains were grown in the presence of 40µM $HgCl_2$ for 18h at 30°C, re-cultivated in fresh $HgCl_2$ medium at an OD_{600} ~ 0.1 and grown to an OD_{600} ~ 0.8 at 30°C. In all cases total RNAs of stressed and control cells were prepared and assessed by cDNA microarrays. Genes with ratios of hybridization values (treated versus control) greater than 1.5 and minor than 0.66 (correlating to a 1.5-fold induction/repression) were considered to be significantly differentially expressed and subjected to further analysis.

Quantitatively, the expression profiles of wild-type and mutant differed significantly under all tested mercury exposure periods. The Venn diagrams in figure 4 illustrate detailed breakdowns

of the detected genes in *wt* and *stb5*Δ after short- (15min, 30min, and 2h) and long- (24h) term mercury treatment and display significant overlaps between wild-type and mutant genes. However, a considerable number of genes were also uniquely expressed in *wt* and *stb5*Δ.

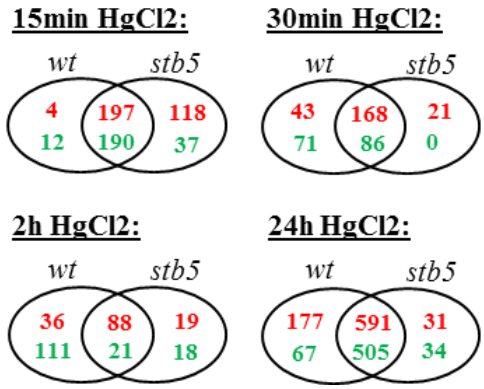

Figure 4. Identification of gene expression overlaps between BY*wt* and BY*stb5*Δ under mercury exposure. Venn diagram illustrates transcriptionally up-regulated (red) and down-regulated (green) genes from mercury-stressed (40µM $HgCl_2$ 15min, 30min, 2h, and 24h) BY*wt* to BY*stb5Δ* cells. Figure shows the number of simultaneously expressed genes (greater/minor than 1.5-fold in *wt* and/or *stb5*Δ) in response to the particular mercury incubation periods of *wt* and *stb5*Δ as well as the differentially expressed genes in *wt* and *stb5*Δ.

Regulatory associations upon $HgCl_2$ treatment

A systematic query for sequence signature motifs in the upstream sequences of the significantly differentially expressed genes was performed using YEASTRACT (Yeast Search for Transcriptional Regulators And Consensus Tracking; Teixeira *et al.*, 2006; Abdulrehman *et al.*, 2011) and T Profiler (http://www.t-profiler.org/; Table 1) to predict putative TFs involved in the transcriptional response to mercury. Accordingly, the most probable TFs for acute mercury treatment (15 and 30min) were the oxidative stress response activators Yap1 and Skn7, the Yap1 homologues Yap7, Cin5/Yap4, and Cad1/Yap2, the heat shock response activator Hsf1, the proteasomal gene activator Rpn4, and the regulators of cellular respiration Hap1 and Hap4. Besides these TFs, the iron-responsive TFs Aft1 and Aft2 as well as the activator of proline catabolism Put3 additionally appeared to play probable roles under chronic mercury stress (24h). These findings were in large part consistent with previous studies (Gasch *et al.*, 2000; Ferguson *et al.*, 2005; Fardeau *et al.*, 2007). It is of note that all above-mentioned activators are regulators of transcription from RNA polymerase II promoter. Finally, the most probable predicted TFs of the down-regulated genes were the regulators of ribosomal biogenesis Sfp1 and Fhl1 as well as the chromatin silencing protein Rap1. This is in agreement with the down-regulation of ribosome biogenesis genes in our data sets and also with literature (Wade *et al.*, 2004; Marion *et al.*, 2004; Hosiner *et al.*, 2009).

TF	*wt* 15m	*stb5* 15m	*wt* 30m	*stb5* 30m	*wt* 2h	*stb5* 2h	*wt* 24h	*stb5* 24h
MSN2	10,51	8,94	10,76	13,87	4,70	6,13	4,78	5,69
MSN4	10,58	7,91	9,82	12,00	4,31	6,22	4,94	5,96
YAP1	10,62	8,39	9,81	13,90	5,38	6,20	4,95	5,71
YAP7	12,10	9,88	11,04	14,69	4,37	4,91		4,93
RPN4	6,25	7,19	4,13	11,13	3,91		5,11	
YAP2	8,30	6,92	7,33	11,13		4,03		4,45
SKN7	5,60	4,87	5,05	4,56		4,44		5,14
HAP1	4,68	4,12			8,10	5,88	5,65	6,08
HSF1	7,93	5,51	4,53	5,02			4,50	6,93
YAP4	3,93			4,45				
HAP4	4,54							
MAL33							4,64	
AFT1								6,02
AFT2							4,99	7,05
YAP6				4,88				
SWI5						4,02		
PUT3							5,54	9,24
RAP1		-4,22		-5,59	-5,70	-5,20	-9,45	-7,64
FHL1	-4,08	-6,37		-9,78	-8,50	-8,35	-16,29	-12,88
SFP1				-4,93	-4,84	-5,30	-8,87	-7,44
BAS1						-4,05		

Table 1. Transcriptional regulation of mercury response. T Profiler prediction of TFs involved in positive (red fields) and negative (green fields) yeast response to short- and long-term mercury treatment; BY*wt* and BY*stb5*Δ cells were treated with 40µM $HgCl_2$ for 15min, 30min, 2h, and 24h. Gene expression was evaluated by microarray analyses.

We confirmed the functional importance of *YAP1*, *AFT1*, *RPN4*, and *SFP1* under metal stress (Ag^{+}, As^{3+}, Cd^{2+}, Co^{2+}, Cu^{2+}, Hg^{2+}, Mn^{2+}, Ni^{2+}, V^{3+}, and Zn^{2+}) by deletion mutant screening. Although Msn2 and Msn4 also were indicated as putative TFs with a role in the yeast mercury stress response, we found that *msn2/4*Δ mutants had no detrimental growth effect on metal-supplemented solid medium (Table 2) and showed no activation in response to mercury stress (Supplemental Figure 3A). On the other hand, we found inhibition of Sfp1 under acute mercury exposure (Supplemental Figure 3B), whereas it was not predicted by T Profiler. The same was true for the activators of the sulfur compound/GSH metabolism, Met4 and Cbf1, which were not detected by T Profiler, but *met4*Δ and *cbf1*Δ mutants caused significantly increased sensitivity to metal stress (Table 2).

SN	GN	Ag	As	Cd	Co	Cu	Hg	Mn	Ni	Zn
YGL071W	AFT1	-3	-2	-3	-3	-3	-3	-3	-3	-3
YJR060W	CBF1	-3	-3	-2	-3	-2	-3	-3	-3	-2
YNL103W	MET4	-3	-3	-3	-1	-3	-3	-3	-1	-3
YHR178W	STB5	-2	-2	-2	-2	-2	-2	-2	-1	-3
YDL020C	RPN4		-3	-3	-3		-2	-1		
YML007W	YAP1		-3	-3	-3		-2	-1		
YLR403W	SFP1	-1	1		-2	-1	-2	-1		
YMR037C	MSN2		-1	-1	-1	1		-1	1	-1
YKL062W	MSN4			1	1	2		-1		
YPL202C	AFT2			-1				-1		
YLR303W	MET17									

Table 2 Phenotypic growth assays. EUROSCARF disruptants were grown on solid YPD supplemented with metal ions (as indicated in the table) and growth was tested after 48h. Severe (-3) to marginal (-1) growth reduction; increased tolerance to metal ions (1); SN (systematic name); GN (gene name);

Gene ontology mapping of the mercury response

To create an overview of transient and chronic mercury stress induced transcripts, we identified the significantly represented GO terms (GO Term Finder - http://www.yeastgenome.org/cgi-bin/GO/goTermFinder.pl; T Profiler - http://www.t-profiler.org/; and K Means Clustering). The median fold induction and fold repression values of the differentially expressed genes were visualized as a heat map (Figure 5). We observed activated regulation of cell redox homeostasis as the main defense mechanism against mercury treatment. Further important metabolic pathways induced by transient mercury stress comprised protein folding and catabolism, aldehyde metabolism, energy generation, ergosterol and lipid biosynthesis, and alcohol metabolism along with the repression of ribosomal biogenesis, translation, and transcription from polymerase I and III promoter (Figure 5A). Transcriptional inhibition from polymerase I and III promoters is in line with T Profiler analysis, which revealed activity of regulators from polymerase II promoters. Under chronic mercury treatment genes encoding functions in siderochrome transport, glucose metabolism, proteolysis and peptidolysis were additionally up-regulated (Figure 5B).

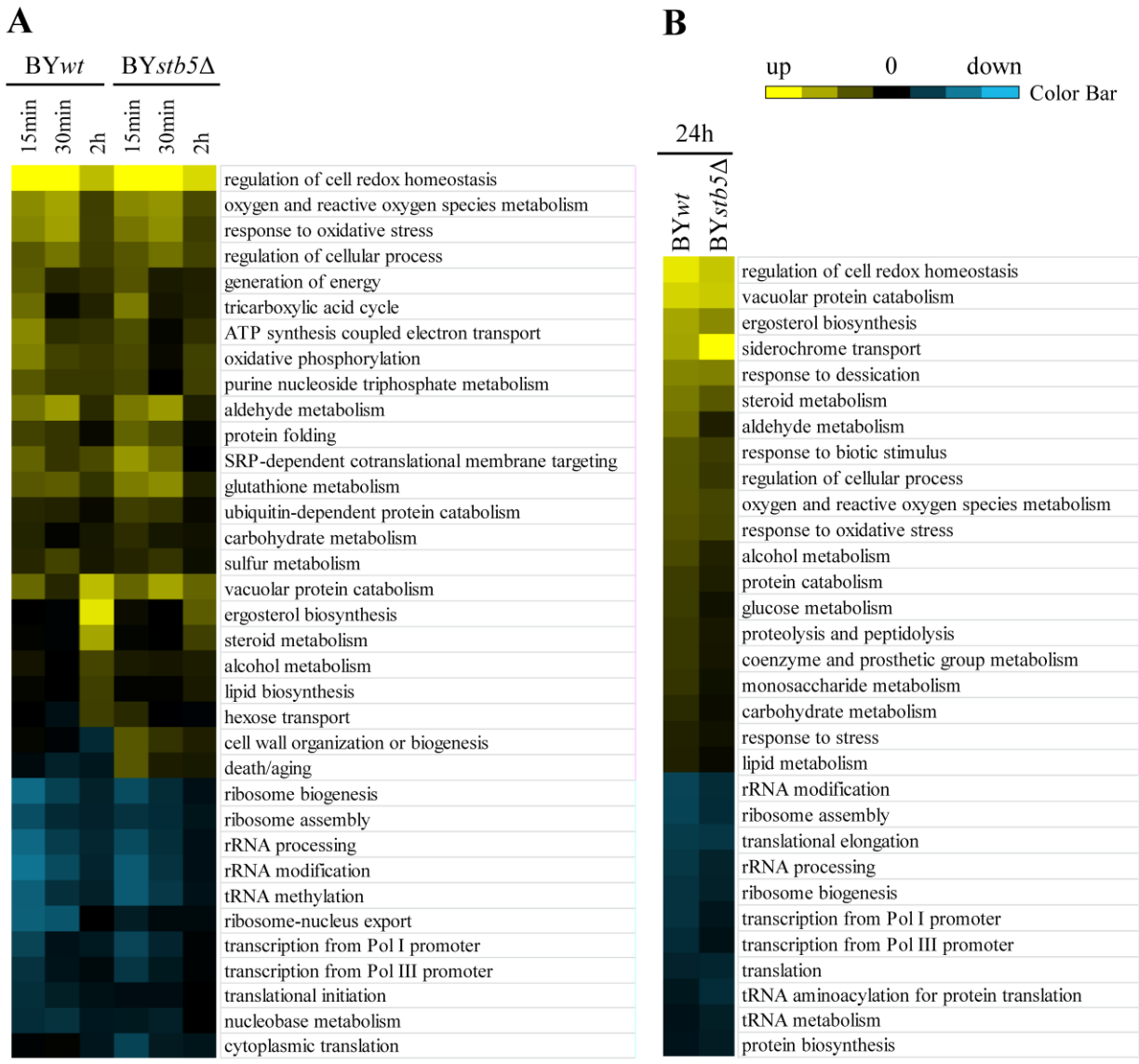

Figure 5. Global Gene Ontology mapping of Hg^{2+} response in BY*wt* and BY*stb5*Δ. K Means clustering, GO Term Finder, and T Profiler analyses of expression profiles upon 40µM $HgCl_2$ treatment (15min, 30min, 2h, and 24h) were used to associate the detected genes to significant GO terms. Variations in transcript abundance for the distinct GO pathways under transient **A)** and chronic mercury stress **B)** were calculated as medial fold inductions and repressions, respectively, and depicted by means of color code in which shades of yellow represent increases and shades of blue decreases in mRNA levels, relative to the unstressed control culture.

Analysis of acute mercury stress response (15 and 30min)

The cell wall is the primary mercury target

The yeast cell wall was shown to play an important role in the protection against Hg^{2+} ions by acting as a kind of adsorption filter. Mercury is suggested to bind to SH groups of cell wall components and to penetrate the cell membrane by a diffusion process, thereby increasing

cellular permeability and generating severe damage (Kaplan, 1965; Murray and Kidby, 1975; Ono *et al.*, 1988; Zhang and Crow, 2001). Interestingly, we observed a cluster of genes involved in cell wall and membrane organization (*ECM21*, *ROT2*, *ARP2*, *LRG1*, *UTH1*, *TUS1*, *ECM30*, *RRT12*, and *CRR1*) as strongly induced in the mutant after 15min up to 2h mercury treatment but not in *wt* (Figure 5A). Accordingly, wild-type cells seem to deal with cell wall stress better than the *stb5*Δ mutant indicating participation of Stb5 in the maintenance of cell wall integrity in the yeast response to acute mercury stress.

*Enhanced early oxidative stress response in stb5*Δ

Activation of the thiol redox system (thioredoxin, glutathione) for oxidative defense is the central detoxification mechanism upon mercury exposition in yeast cells (Figure 5). We primarily detected significantly activated genes involved in the regulation of cell redox homeostasis (*SOD1*, *AHP1*, *TRX2*, *PRX1*, *TSA2*, *TRR1*, *GRX1*, *TSA1*, and *TRX1*; Figure 5A). This corresponds to the known fact that Hg^{2+} and other metals cause intracellular oxidative stress (Valko *et al.*, 2005; Hansen *et al.*, 2006; Verlecar *et al.*, 2008; Hosiner *et al.*, 2012 in preparation). Previous studies proved that the redox system is regulated by the TFs Yap1, Met4, Met31, Met32, and Cbf1 (Mountain *et al.*, 1993, Dormer *et al.*, 2000; Wheeler *et al.*, 2003). We confirmed these findings for Yap1, Met4, and Cbf1 via growth assays of the corresponding disruptants on metal-supplemented medium, whereas deletion of *MET31* and *MET32* resulted in an unaltered growth phenotype in comparison with a wild-type strain (Table 2).

Moreover, we observed the induction of genes involved in glutathione biosynthesis (*GSH1*, *GSH2*, *GTT1*, *GTT2*, and *GLO1*; Figure 6) in *wt* and *stb5*Δ in response to all tested mercury stress conditions. Glutathione (GSH) is an essential antioxidant that serves for chelation of toxic metals via its sulfhydryl moiety as well as for direct protection against metal-induced oxidation (Allen *et al.*, 1988; Grant, 2001; Westwater *et al.*, 2002; Brambila *et al.*, 2002; Jan *et al.*, 2011). Interestingly, under acute mercury exposition *GSH1* and *GLR1*, encoding the glutathione reductase that regenerates GSH, were almost 2-fold stronger induced in *stb5*Δ than in *wt* indicating intensified oxidative stress defense in the mutant. This was consistent with the additional transiently stronger up-regulation of the vacuolar ABC transporter gene *YCF1* in *stb5*Δ. Ycf1 sequestrates glutathione/metal chelates into the yeast vacuole to prevent intracellular Hg^{2+} accumulation and subsequent oxidative stress (Gueldry *et al.*, 2003).

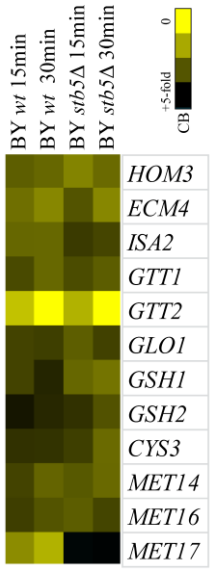

Figure 6: Sulfur cluster of BY*wt* and BY*stb5*Δ under acute mercury treatment. Fold inductions are graphically visualized via TreeView; CB – color bar;

One striking finding was the lack of *MET17* induction in *stb5*Δ after 15 and 30min mercury treatment in contrast to *wt* (Figure 6). Met17 catalyses the incorporation of sulfide into O-acetylhomoserine to form homocysteine, which is a key precursor in the biosynthesis of the sulfur-containing amino acids cysteine (one of the main components of glutathione) and methionine (Thomas and Surdin-Kerjan, 1997). Missing *MET17* transcription in *stb5*Δ might therefore explain the enhanced induction of GSH biosynthesis resulting from defective GSH leading to intracellular Hg^{2+} accumulation and increased oxidative stress in the mutant. Alternatively, homocysteine might directly function as a chelating-agent in the primary defense against toxic mercury ions and a defective biosynthesis might therefore also increase oxidative stress.

Additionally, hexose transport (*HXK1*, *HXK2*, *HXT1*, *HXT2*, and *HXT4*) which has been shown to contribute to metal uptake in yeast (Liu *et al.*, 2004), was transiently up-regulated in *stb5*Δ after 15min mercury stress but repressed in *wt* (Figure 5A). Since hexose transporters have been suggested to be down-regulated under surplus metals to restrict unspecific metal uptake (Jin *et al.*, 2008), continued hexose/metal transport in the mutant might therefore transiently increase intracellular oxidative stress. A strong indication for enhanced oxidative activities in the mutant was the significant up-regulation of chromatin remodeling processes involved in replicative cell aging (*PNC1*, *RAS2*, *PUF4*, *SIR4*, *HDA1*, *GTS1*, and *SIR2*) during short-term mercury exposure in contrast to *wt* (Figure 5A). In this regard, it is well-established that progressive aging correlates with decreased intracellular levels of GSH (Tchaikovskaya *et al.*, 2005; Robillard *et al.*, 2011).

Together, these findings clearly illustrate the importance of antioxidative strategies as a first line defense against acute mercury exposure. Deletion of *STB5* appears to enhance the oxidative stress response based on delayed inhibition of hexose transport leading to putative additional mercury uptake and a lack of *MET17* transcription causing putative intracellular Hg^{2+} accumulation. Although *MET17* upstream sequence exhibits no direct binding sites for Stb5, missing *MET17* induction in the *stb5*Δ mutant points to an indirect participation of Stb5 in *MET17* regulation under acute mercury stress.

Additional stress defense strategies

After 15 to 30min Hg^{2+} treatment 6 of the overall 7 identified yeast AAD genes (*AAD3*, *AAD6*, *AAD10*, *AAD14*, *AAD15*, and *AAD16*) were induced in *wt* and *stb5*Δ (Figure 5A). Under chronic mercury stress these putative aryl-alcohol dehydrogenases were solely up-regulated in *wt* in contrast to the mutant pointing to an indirect participation of Stb5. The Yap1-dependent AAD gene set has also been noted in the transcriptional response to other metals (Haugen *et al.*, 2004; Jin *et al.*, 2008; Hosiner *et al.*, 2012 in preparation) and has been suggested to be involved in the repair of damaged lipids during stationary phase (Delneri *et al.*, 1999a; Horan *et al.*, 2006) or in the generation of supplemental energy from glucose through alcohol fermentation during oxidative stress (Delneri *et al.*, 1999). Both potential roles may account for the reduced viability (Supplemental Figure 4) of a yeast mutant deleted for all 7 AAD genes on mercury-containing solid medium, but the *de facto* function of these genes is yet unclear.

Moreover, a cluster of genes encoding chaperones and co-chaperons primarily belonging to the HSP70 family (*SSA1-4*, *SSC1*, *HSP31*, *HSP42*, *HSP60*, *HSP104*, *KAR2*, *YDJ1*, *AHA1*, *SIL1*, and *SGT2*) was observed as significantly up-regulated after 15min mercury stress in *wt* and *stb5*Δ (Figure 5A). Most of these chaperones have been described recently to be activated as a metal detoxification mechanism under As^{3+} and Cd^{2+} exposure (Hosiner *et al.*, 2012 in preparation). These scavengers appear to establish the first line of defense for targeting, refolding, and/or removal of metal- and ROS-modified proteins in close collaboration with proteins especially involved in (ubiquitin-dependent) proteolysis (*PRE2*, *PRD1*, *RPN6*, *RPN11*, *PRE6*, *PHB2*, *PUP2*, *UBX6*, *ADD37*, and *RPT5*; Figure 5A).

Adaptation of yeast cells to sustained metal stress (2h)

Sustained incubation of *wt* and *stb5*Δ in 40µM $HgCl_2$ led to a considerable transcriptional reduction of genes involved in oxidative stress, energy generation, aldehyde and sulfur metabolism, ubiquitin-dependent protein catabolism, and protein folding genes after 2h up to 24h. Furthermore, ubiquitous DNA repair genes such as *DDR48* and *RAD3* were up-regulated in the 15 and 30min population but inactivated after 2h in *wt* and *stb5*Δ. In addition, repression of ribosomal biogenesis and translation was significantly diminished after 2h (Figure 5A). This is interesting, since inhibition of these growth-related processes under stressful conditions has been reported previously and indicated to divert energy to immediate activation of other

pathways such as metal defense strategies (Warner, 1999; Gasch *et al.*, 2000; Hosiner *et al.*, 2012 in preparation). However, at the 2h time-point growth-related and detoxification processes showed reciprocal expression patterns. Together, this might indicate successfully established metal detoxification strategies at a post-translational level via antioxidants, metal chelating agents, and chaperones accommodated by catabolic and repair processes and redistribution of transcriptional energy to growth after 2h.

Moreover, we observed up-regulation of alcohol metabolism and lipid biosynthesis mainly comprising the ergosterol pathway (*ERG1-13*, *ERG20*, *ERG25-28*, *CYB5*, *NCP1*, *MCR1*, and *GRE2*; Figure 5A) after 2h up to 24h, albeit nearly 2-fold stronger in *wt* than in *stb5*Δ. Recently, the elastic properties of phospholipid monolayers have been shown to be key factors for the interactions with mercury ions leading to lipid peroxidation, disturbances in the arrangement of phospholipid moieties, and impairment of membrane function (van Ginkel and Sevanian, 1994; Broniatowski *et al.*, 2010). Ergosterol is the major component of fungal cell membranes and alterations of sterol distribution are known to influence membrane permeability, fluidity, and integrity (Lupetti *et al.*, 2002; Rodriguez *et al.*, 1985). Previous studies linked a decrease of ergosterol contents in the plasma membrane to decreased transmembrane transport activities under osmotic stress (Toh *et al.*, 2001) and increased ergosterol concentrations were reported to preserve the structural integrity of yeast membranes in stressful environmental conditions (Dickey *et al.*, 2009). And it has been demonstrated that Stb5 is a direct activator of *ERG5*, *ERG11*, and *ERG25* under oxidative stress (Larochelle *et al.*, 2006). We found *ERG5* as activated in *wt* after 2h in contrast to the mutant, in which *ERG5* was not induced until 24h. *ERG11* was up-regulated in *wt* and *stb5*Δ after 2h and *ERG25* expression was not changed at all. These findings point to regulation of *ERG5* and *ERG11* apart from Stb5 in response to mercury.

In the context of our results, we presume a consequent shift in the systemic mercury stress response from first line metal detoxification towards membrane stabilisation to ensure growth. Although *stb5*Δ also adapted to short-term mercury stress, our expression data indicated persistently increased oxidative impact of mercury in the mutant compared to *wt*. To this effect we observed continued down-regulation of hexose transport and slight up-regulation of genes involved in cell aging and cell wall organization in *stb5*Δ, whereas *wt* exhibited reciprocal expression patterns of these pathways (Figure 5A). However, a visible sign for the adaptation process of *stb5*Δ was the regulation of *TUS1*, a guanine nucleotide exchange factor (GEF) that functions to modulate Rho1 activity as part of the cell integrity signaling pathway. This factor was initially up- but under sustained mercury exposure significantly down-regulated.

Yeast expression patterns under chronic mercury exposure (24h)

After 24h mercury treatment yeast cells exhibited global transcriptional changes comprising the 4.9- to 7.5-fold number of genes compared to the early mercury stress responses (15min, 30min, and 2h). These mainly involved the same metabolic pathways as under transient

mercury exposure but partly different genes coding for proteins of antioxidant defense, catabolic and repair strategies, carbohydrate, lipid, and alcohol metabolism, as well as iron ion homeostasis, whereas protein biosynthesis and transcription from polymerase I and III promoters were repressed (Figure 5B). A certain overlap of gene expression in *wt* and *stb5*Δ was observed though the mutant showed distinct deficiencies in contrast to *wt* (Figure 7) which are indicative for the delayed growth phenotype of *stb5*Δ.

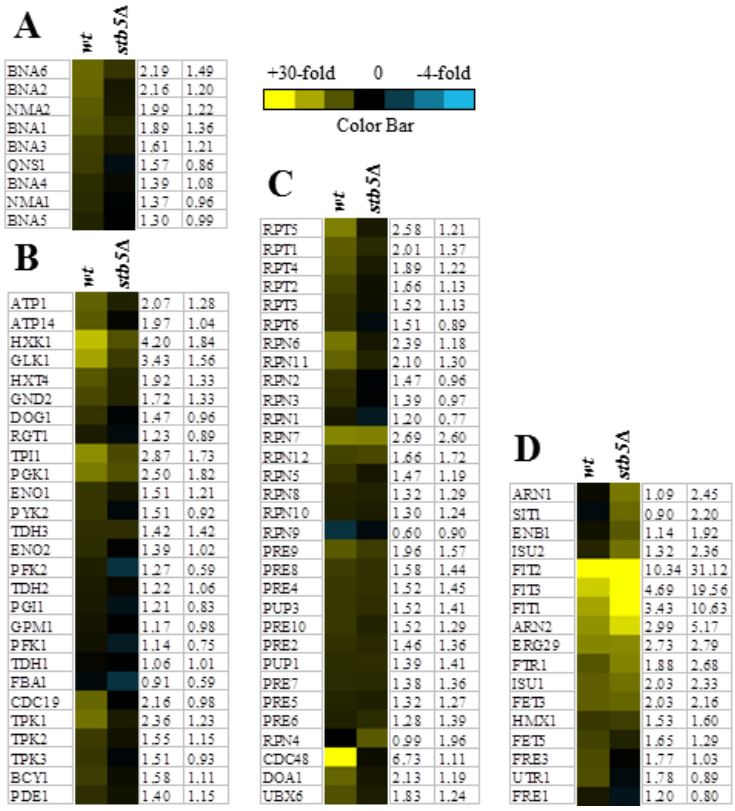

Figure 7: Striking expression distinctions of BY*wt* and BY*stb5*Δ under chronic mercury treatment. Description of the most significant transcriptional gene expression differences (> -2- and < +31-fold) between BY*wt* and BY*stb5*Δ under chronic mercury stress; fold inductions and repressions are graphically visualized via TreeView; **A)** NAD *de novo* biosynthesis; **B)** ATP synthase and glycolysis; **C)** catabolic processes; **D)** iron homeostasis;

*Decreased energy levels in stb5*Δ

Compared to *wt*, the *stb5*Δ mutant showed significantly reduced activation of aldehyde, carbohydrate, alcohol, and lipid metabolism as well as of protein catabolism (Figure 5B). In particular, we found decreased transcription of energy generating pathways in the mutant including NAD and ATP synthesis as well as glycolysis (Figure 7A and B). Nicotinamide adenine dinucleotide (NAD+) is a ubiquitous cofactor for cellular redox reactions and energy metabolism but also participates as a necessary substrate in other biological processes, including RNA metabolism (cell aging), DNA repair, or calcium-dependent signalling

pathways (Lin and Guarente, 2003). Under chronic mercury treatment NAD *de novo* biosynthesis was activated in *wt*, whereas it was nearly inactive in *stb5*Δ (Figure 7A). Similar to this effect Stb5 has previously been determined as a key element in the control of NADPH production for resistance to oxidative stress (Thorpe *et al.*, 2004; Larochelle *et al.*, 2006).

Moreover, in contrast to *wt* we observed no expression of both subunits (Atp14 of the F1 sector and Atp1 of the F0 sector) of the mitochondrial F1F0 ATP synthase in the mutant (Figure 7B). F1F0 ATP synthase is a large, evolutionarily conserved enzyme complex required for ATP synthesis (Boyer, 1997). Finally, the expression levels of genes involved in glucose metabolism (*DOG1*, *GND2*, *GLK1*, *HXK1*, *HXT4*, and *RGT1*) as well as in glycolysis (*PGI1*, *PFK1*, *PFK2*, *FBA1*, *TPI1*, *TDH1*, *TDH2*, *TDH3*, *PGK1*, *GPM1*, *ENO1*, *ENO2*, *PYK2*, and *CDC19*; Figure 7B) were significantly reduced in *stb5*Δ. Energy metabolism and glycolysis yield the high-energy compounds ATP and NADH indicative for reduced energy levels in the mutant.

In this regard, it is interesting that one main regulator of cell growth and response to nutrients and stress, the cyclic AMP-dependent protein kinase A (PKA; Toda *et al.*, 1987; Estruch, 2000; Santangelo, 2006), was nearly 2-fold up-regulated in the wild-type but inactive in the mutant. Consistent with this observation, transcription of *BCY1* that encodes the regulatory subunit of PKA and *TPK1*, *TPK2*, as well as *TPK3* coding for the catalytic PKA subunits was unaffected in *stb5*Δ. Another target of the PKA pathway with unaffected transcription in the mutant in contrast to *wt* was *PDE1*, encoding the cAMP phosphodiesterase (Figure 7B).

Together, the strongly decreased transcription of genes involved in energy generation in the mutant clearly links Stb5 to the regulation of intracellular energy production during chronic mercury exposure. Hence, we suggest that deletion of *STB5* causes an increase of oxidative stress due to the reduced levels of high-energy compounds for the antioxidative system. Accordingly, intracellular accumulation of toxic Hg^{2+} might increase and lead to enhanced cell defects. At last, these defects might account for the significantly retarded growth of *stb5*Δ compared to wild-type.

*Activation of the 20S proteasome in stb5*Δ

Another interesting effect of *STB5* deletion under chronic mercury exposure was the severely impaired induction of the ubiquitin-proteasome pathway (Figure 7C). The multi-subunit 26S proteasome consits of a 19S regulatory particle and a 20S proteolytic core and functions as a protease responsible for the non-vacuolar degradation of damaged, aberrant, or misfolded cellular proteins (Fischer *et al.*, 1994; Nussbaum *et al.*, 1998, Xie and Varshavsky, 2001). We found that especially genes of the 19S regulatory subunit with ATPase activity (*RPT1-6*), besides others (*RPN1-3*, *RPN6*, and *RPN11*) were about 1.5- to 2-fold induced in *wt*, but virtually unaffected in the *stb5*Δ mutant (Figure 7C). Further 19S subunit genes (*RPN5*, *RPN7-10*, and *RPN12*) together with 20S core genes (*PRE2*, *PRE4-10*, *PUP1*, and *PUP3*) were similarly induced in *wt* and *stb5*Δ.

Previous studies have demonstrated the pivotal role of the proteasome in the degradation of oxidatively damaged proteins but emphasized the enhanced resistance of the 20S core particle to oxidative stress in comparison with the 19S particle (Reinheckel *et al.*, 1998; Haugen *et al.*, 2004; Breusing and Grune, 2008). Recently, it has been shown that oxidative stress induces the disassembly of the ATP-/ubiquitin-dependent 26S proteasome complex. This effect was suggested to increase the capacity of the cells to remove oxidized proteins via the 20S part (Wang *et al.*, 2010). These findings might explain our data in terms of increased oxidative stress in the *stb5*Δ mutant, although it is not clear whether disassembly of the 26S proteasome is accompanied with partial down-regulation or inactivation of 19S genes.

Strikingly, degradation of oxidized proteins occurs by an ubiquitin- and ATP-independent mechanism (Shringarpure *et al.*, 2003). This appears to be consistent with our results and might explain low levels of *CDC48* transcription in the mutant. In contrast to *stb5*Δ, *CDC48*, encoding an ATPase involved in ubiquitin-mediated protein degradation, was 7-fold induced in *wt*. Additionally, interaction partners of Cdc48 such as Doa1 and Ubx6 involved in the ubiquitin pathway (Ghislain *et al.*, 1996) were both transcriptionally up-regulated in *wt* but not in *stb5*Δ (Figure 7C). As aforementioned, the wild-type grew much better under chronic mercury treatment than the mutant (Figure 3) and therefore appeared to cope better with mercury toxicity. In summary, our results indicated a minor effect of oxidative stress in *wt* than in *stb5*Δ. Alternatively, inactive expression of *CDC48* and 19S ATPases genes might result from insufficient intracellular ATP levels based on the reduced activation of ATP production in *stb5*Δ.

Expression of proteasomal subunit genes has been reported to be mediated by the TF Rpn4 (London *et al.*, 2004, Wang *et al.*, 2008), which is in turn regulated by stress response regulators such as Pdr1, Pdr3, and Yap1 (Owsianik *et al.*, 2002). Deletion of *RPN4* and *YAP1* conferred increased sensitivity to metals like Ag^{+}, As^{3+}, Cd^{2+}, Co^{2+}, Fe^{2+}, Hg^{2+}, Mn^{2+}, as well as V^{3+} (Table 2) indicating that both regulators are central to metal stress resistance. We found transcription of *RPN4* 3.5-fold induced in *stb5*Δ after 2h and 2-fold induced after 24h mercury treatment but inactive in *wt* (Figure 7C). In contrast, T Profiler analyses predicted Rpn4 regulation of metal stress after 2h and 24h in *wt* but not in *stb5*Δ (Table 1). Interestingly, Stb5 is linked to all three upstream regulators of Rpn4; *YAP1* exhibits binding sites for Stb5 in its promoter region and Pdr1 as well as Pdr3 form complexes with Stb5 for regulation of multidrug resistance genes (Akache *et al.*, 2004). Continued *RPN4* expression in the *STB5* deletion strain might therefore point to possible participation of Stb5 in the negative regulation of *RPN4*. On the other hand, enhanced oxidative stress in *stb5*Δ might increase intracellular levels of damaged proteins and therefore enhance *RPN4* expression, possibly in connection with 26S disassembly. However, why T Profiler predicted reciprocal Rpn4 participation in *wt* and *stb5*Δ is yet unclear and remains to be determined.

Siderophore transport

We observed a 2- to 3-fold stronger up-regulation of iron homeostasis genes in *stb5*Δ than in *wt* (Figure 5B). This induction affected primarily the cell wall mannoproteins (*FIT1*, *FIT2*, and *FIT3*) and, to a minor degree, members of the ARN/SIT subfamily of the major facilitator superfamily (MFS) transporters (*ARN1*, *ARN2*, *SIT1*, and *ENB1*) in addition to other iron homeostasis genes (Figure 7D). The transcriptional activators Aft1 and Aft2 regulate iron homeostasis (Yamaguchi-Iwai *et al.*, 1995; Rutherford *et al.*, 2005). This was confirmed for the 24h exposure of *stb5*Δ by phenotypic and T Profiler analyses (Table 1 and 2). Notably, whilst T Profiler predicted Aft2 for *wt* and *stb5*Δ, Aft1 was only predicted for the mutant, which might explain the considerably stronger induction of the siderophore transport genes in *stb5*Δ.

Induction of the iron regulon has been previously linked to short-term metal exposure and suggested to counteract intracellular iron depletion and/or to serve a protective role against toxic metals (Saponja and Vogel, 1996); Ward *et al.*, 2001; Stadler and Schweyen, 2002; Chen *et al.*, 2005; Pagani *et al.*, 2007). We connected this effect for the first time to chronic mercury treatment and showed that iron homeostasis is not affected under early mercury stress. Loss of *STB5* appears to increase sensitivity to mercury in yeast cells and might therefore rather indirectly enhance the expression of the siderophore iron system. Consistent with this, up-regulation of mannoproteins of the FIT family might rather function to decrease permeability of the cell wall for toxic mercury than for iron uptake (Zlotnik *et al.*, 1984; Protchenko *et al.*, 2001). Additionally, it is likely that *stb5*Δ uses mercury chelation via the ARN/SIT family with siderophores as an alternative detoxification mechanism to reduce intracellular mercury accumulation as suggested in a recent study (Hosiner *et al.*, 2012 in preparation). But these effects might also serve other protective purposes against surplus mercury. However, a *de facto* participation of the siderophore iron system in the protection against Hg^{2+} and other metals still has to be proven.

Conclusions

We investigated short- and long-term mercury stress in *S. cerevisiae* and examined the role of Stb5 under this environmental impact in comparison with *wt*. Due to its high affinity to sulfur the first targets of mercury attack are the thiol groups of cell wall and plasma membrane proteins followed by mercury uptake and intracellular accumulation leading to oxidative stress and several cell defects. Consistent with this we observed the immediate activation of genes of the cellular oxidant defense system primarily comprising the thioredoxin/glutathione pathway, besides a steady up-regulation of genes involved in vacuolar protein catabolism and carbohydrate metabolism up to 24h. In addition, yeast cells transiently induced repair and further catabolic processes especially including chaperones of the HSP70 family as a first line defense against acute mercury stress. The simultaneous down-regulation of growth-related

processes such as ribosome biogenesis and translation indicated that the limited intracellular energy required for growth was transiently diverted to the immediate transcription of stress defense and repair genes. We analyzed acute mercury stress as mediated by TFs such as the oxidative stress response regulators Yap1, Skn7, Met4, Cbf1, the Yap1 homologues Yap2, Yap4, and Yap7, the heat shock TF Hsf1, the regulators of cellular respiration Hap1 as well as Hap4, the proteasomal gene activator Rpn4, and the regulators of ribosomal biogenesis Sfp1, Fhl1 as well as Rap1.

In contrast to wild-type, the expression of *MET17*, a key-enzyme of the yeast antioxidant system, was not induced in *stb5*Δ after 15 and 30min treatment. As oxidative cell stress is well-known to correlate with aging, we assume the induction of genes involved in replicative cell aging and cell wall organization in *stb5*Δ in contrast to *wt* as an indication of increased intracellular oxidative stress based on a defective oxidant defense system in the mutant. Moreover, we showed up-regulation of hexose transport in the mutant compared to wt, which might lead to increased unspecific mercury uptake additionally contributing to intracellular Hg^{2+} accumulation. One final indication for an enhanced early stress defense response in *stb5*Δ was the strengthened down-regulation of translation compared to *wt*.

After 2h *wt* and *stb5*Δ, albeit to lower levels than *wt*, partly adapted to sustained mercury exposure. We showed considerable transcriptional reduction of oxidative stress response, catabolic, repair, chaperone, and energy generating genes along with reduced repression of growth-related processes. According to the decreased gene expression response we simultaneously detected a decrease of involved regulators to Yap1, Yap7, Hap1, Rpn4, Rap1, Fhl1, and Sfp1. In addition, expression of genes involved in alcohol and lipid metabolism, mainly comprising ergosterol biosynthesis, was up-regulated which is indicative for fermentation and membrane stabilisation to ensure structural integrity and growth. However, continued induction of cell aging genes and repression of hexose transport along with the sustained activity of the oxidative stress response regulators Yap2 and Skn7 proved enhanced intracellular oxidative stress caused by Hg^{2+} in the *STB5* deletion strain.

Following sustained mercury stress up to 2h we saw an extensive increase of expression of stress defense genes and regulators in *wt* and *stb5*Δ under chronic mercury stress (24h). In addition, we verified the participation of further putative TFs such as Aft1/2, Mal33, and Put3. However, compared to *wt*, *stb5*Δ exhibited considerably lower gene expression levels of several homeostatic pathways such as aldehyde, carbohydrate, alcohol, and lipid metabolism as well as of protein catabolism. The most striking ones included NAD and ATP synthesis, as well as glycolysis indicative for reduced energy levels in the *STB5* deletion strain. This effect most likely contributed to the retarded growth of the mutant in comparison with *wt*. Moreover, these findings were important taking into account that NAD biosynthesis provides essential cofactors for cellular redox reactions possibly accounting for strengthened oxidative stress in *stb5*Δ. We draw some support of this idea from the reduced transcriptional activation of 19S ATPase genes of the 26S ubiquitin-proteasome in the mutant and up-regulation of *CDC48* in *wt*. In accordance to these data and consistent with literature, we proposed ATP- and ubiquitin-

independent degradation of oxidized proteins via the oxidatively more resistant 20S core particle in *stb5*Δ in contrast to normal ATP- and ubiquitin-dependent protein degradation in *wt*. Finally, we suggest a considerably stronger induction of cell wall mannoproteins of the FIT family and siderophore iron transporters of the ARN/SIT family to serve additional protective roles against the increased toxicity of Hg^{2+} in *STB5* deletion compared to *wt* cells.

Taken together, we provide evidence for the influence of Stb5 on *MET17* induction, on cell wall organization, replicative cell aging, and hexose transport in response to early mercury stress and on intracellular energy levels, 20S proteasomal degradation, and the siderophore iron system under chronic mercury exposition. These findings prove no direct participation of Stb5 in the involved pathways but indicate this regulator as important in the yeast defense against acute and chronic mercury stress.

Material and Methods

Yeast Strains and Oligonucleotides – BY-4741 and BY*stb5*Δ, and diverse EUROSCARF disruptants (Table 1) and the following oligonucleotides were used in this study: Disruption of *STB5* was carried out with a KanR disruption cassette amplified with the primers FwdSTB5: 5´AATGAATTCTGTGGTAATGTGTACGACGATTTCAAC-3´ and RevSTB5: 5´AATGTCT AGATCATACAAGTTTATCAACCCAAGAG-3´. BY-4741 and BY*stb5*Δ were grown on standard YPD for two days at 30°C. Single colonies were resuspended in 10µl H_2O and broken up by heat shock for 1min in the microwave. Crashed cells were centrifuged (3.5k rpm, 5min), aliquotted into two equal amounts, and PCR-verification of *STB5* disruption was performed using the primer pairs Stb5-up / Stb5-in and Stb5-up/ KanR (Stb5-up: 5´CGCAGGGAATA TAACGAC-3´, Stb5-in: 5´GAGGTCGA TGCTCCACTG-3´, and KanR: 5´AACAGGAATCG AATGCAACC-3´).

Cloning Strategies – To insert *STB5* into the centromeric vector YCp111 the gene was PCR amplified using *STB5* primers with EcoRI/XbaI restriction sites and chromosomal BY-4741 DNA as template (Table 2). The strain BY*stb5*Δ+YCp111-*STB5* was generated by ligation of YCp111 with the restriction enzymes digested PCR products and subsequent transformation of the construct into competent BY*stb5*Δ strain.

Complementation, Toxicity Assays, Adaption Analysis – Complementation of *STB5* deletion was evidenced by incubating over-night cultures (*S. cerevisiae* BY-4741, BY*stb5*Δ, and BY*stb5*Δ+YCp111-*STB5*) in liquid YPD (OD_{600}~0,15) at 30°C and spotting them on metal-containing solid YPD ($AlCl_3$, $AgNO_3$, $AsCl_3$, $CdCl_2$, $CoCl_2$, $CuSO_4$, $FeCl_3$, $HgCl_2$, $MnCl_2$, $NiSO_4$, $Pb(NO_3)_2$, VCl_3, $ZnCl_2$) in 10-fold dilutions. Yeast growth was scored after 24h. Toxicity assays were performed with BY-4741 and BY*stb5*Δ over-night cultures in $HgCl_2$-containing liquid YPD (OD_{600}~0, 15), and OD_{600} was measured after 0h, 2h, 4h, 6h, 8h, 10h,

12h, and 24h. For adaptation analysis cells were recultivated in fresh Hg-containing YPD (OD_{600}~0, 15) after 12h and incubated for another 12h at 30°C monitoring OD_{600} every 4h.

Phenotypic Screening **–** Over-night cultures of BY-4741 and EUROSCARF disruptants were diluted in liquid YPD and grown from OD_{600}~0.15 to OD_{600}~0.8 at 30°C. The exponentially growing yeast cells were then spotted in 10-fold dilutions onto solid YPD containing increasing concentrations of dissolved metal ions ($AgNO_3$, $AsCl_3$, $CdCl_2$, $CoCl_2$, $CuSO_4$, $HgCl_2$, $MnCl_2$, $NiSO_4$, VCl_3, and $ZnCl_2$), as well as on YPD control plates lacking metal ions. All plates were incubated for 48 at 30°C, and the yeast spots were visually scored to determine growth restriction.

Preparation of Yeast RNA – Overnight cultures (BY-4741, BY*stb5*Δ) were grown in fresh YPD from OD_{600}~0, 15 to OD_{600}~0, 8 and stressed with 40µM $HgCl_2$. After 15min, 30min, 2h, and ~24h incubation at 30°C, both untreated and treated cells were harvested, and cells were immediately washed in ice-cold DEPC-H_2O, reharvested and frozen at -80°C. Total RNA was prepared by extraction with hot acidic phenol strictly according to Ausubel *et al.* (1997) with the only difference that three instead of one chloroform extractions were performed following phenol extraction. RNA was quantified by spectrophotometry at 260/280nm.

RNA Methods – Fluorescently labelled cDNA was synthesized from 15µg of total RNA by oligo dT-primed polymerization using 200 U Superscript II (Invitrogen, Carlsbad, CA) and Cy3-CTP or Cy5-CTP (GE Healthcare, Waukesha, WI). Labelled cDNAs were pooled and RNA was hydrolyzed for 20min in 10N NaOH at 65°C, neutralized with 5M acetic acid, and purified by the Cy Scribe GFX purification kit (GE Healthcare). Microarrays (obtained from Microarray Centre Toronto, Ontario, CAN) containing PCR fragments of 6144 predicted *S. cerevisiae* ORFs spotted in duplicates were used for expression profiling. Hybridization was performed for 14-18h in DigEasyHyb solution (Roche Diagnostics, Basel, Switzerland) with 0,1mg/ml salmon sperm DNA (Sigma, St Louis, MO) as a carrier solution at 37°C. After hybridization, microarrays were washed three times in 1×SSC, and 0,1% SDS at 50°C for 10min, followed by a 1min in 1×SSC and 0,1%×SSC at RT and a 5min 500rpm spin to dryness. All microarray experiments were performed in duplicate including the necessary dye swap.

Microarray Reading and Transcriptome Data Analysis – Microarrays were scanned using an Axon GenePix 4000B scanner (Molecular Devices, Sunnyvale, CA). The image data were quantified using the GenePix Pro4.1 software (Molecular Devices). Raw data are available under the ArrayExpress (http://www.ebi.ac.uk/arrayexpress/) accession no. E-MEXP-2991. The data preprocessing as well as the tests for differential expression have been performed using Bioconductor software packages (http://www.bioconductor.org), particular the limma package (Smyth, 2004). Spots in the raw data files with weights above Zero were considered for further normalization and analyses steps after removal of estimated background signals (Yang *et al.*, 2003; Smyth *et al.*, 2005; Ritchie *et al.*, 2007; Silver *et al.*, 2009).

In a second evaluation step, clustering algorithms using the cluster3 software were performed to find groups of genes with similar expression profiles (Eisen *et al.*, 1998; Nadon and Shoemaker, 2002; http://rana.stanford.edu/software). The clustering results were obtained by conducting K-means clustering and visualized by TreeView (Saldanha, 2004; http://jtreeview.sourceforge.net). Significant associations to gene ontology (GO)-terms were obtained by the GO-Term Finder on the Saccharomyces Genome Database (SGD) to identify genetic pathways or families of genes that are co-regulated (http://www.yeastgenome.org/cgi-bin/GO/goTermFinder.pl). Based on their regulatory associations with transcription factors, the differentially expressed genes by a factor greater/minor than 2 were further analyzed using the YEASTRACT repository (Yeast Search for Transcriptional Regulators And Consensus Tracking; http://www.yeastract.com/; (Teixeira *et al.*, 2006), which presently contains 48333 regulatory associations between transcription factors and genes based on more than 1200 bibliographic references (Abdulrehman *et al.*, 2011). One final search was performed with a tool developed to scan for potential TFBS (Transcription Factor Binding Sites) on promoter regions in *S. cerevisiae* (Gerber *et al.*, 2010).

Supplemental Figures

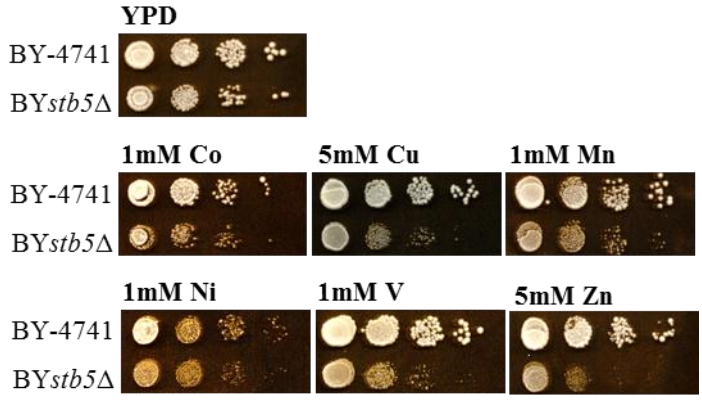

Supplemental Figure 1. Growth assays with *stb5*Δ mutants. Serial 10-fold dilutions of BY-4741 and BY*stb5*Δ cells were spotted onto metal-containing YPD plates (as indicated in the figure) and scored after 48h.

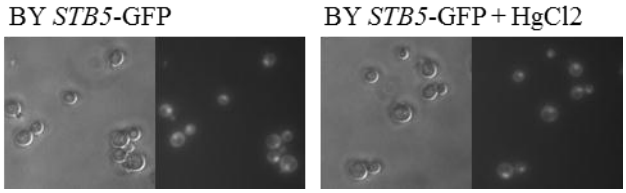

Supplemental Figure 2. Subcellular localization of *STB5*-GFP. Yeast cells carrying a *STB5*-GFP genomic fusion gene were grown to exponential phase and exposed to 50µM $HgCl_2$ for 30 min. GFP-fluorescence images were taken from cells without fixation.

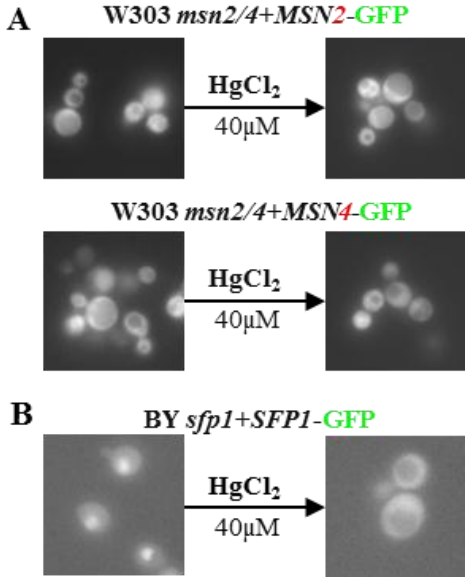

Supplemental Figure 3: Subcellular localization of *MSN2-, MSN4-* and *SFP1*-GFP upon mercury stress: A) W303 *msn2msn4* cells transformed with *pADH1-MSN2*-GFP and *pADH1*-MSN4-GFP and **B)** EY *sfp1* cells carrying an *SFP1*-GFP genomic fusion gene were grown to exponential phase and exposed to 40µM $HgCl_2$ for 30 min. GFP-fluorescence images were taken from cells without fixation.

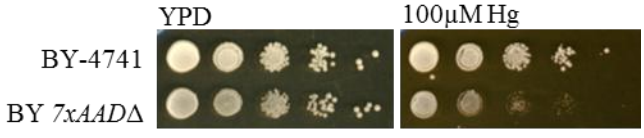

Supplemental Figure 4. Growth assay with *7xAADΔ* mutant. Serial 10-fold dilutions of *wt* and *7xAADΔ* (*AAD3*, *AAD4*, *AAD6*, *AAD10*, *AAD14*, *AAD15*, *AAD16*) cells were spotted onto solid YPD medium supplemented with 100µM mercury chloride and scored after 48h.

References

1. Abdulrehman, D., et al., YEASTRACT: providing a programmatic access to curated transcriptional regulatory associations in *Saccharomyces cerevisiae* through a web services interface. Nucleic Acids Res. 39(Database issue): p. D136-40.
2. Akache, B., et al., Complex interplay among regulators of drug resistance genes in *Saccharomyces cerevisiae*. J Biol Chem, 2004. 279(27): p. 27855-60.
3. Akache, B. and B. Turcotte, New regulators of drug sensitivity in the family of yeast zinc cluster proteins. J Biol Chem, 2002. 277(24): p. 21254-60.
4. Allen, P., S.Y. Min, and W.M. Keong, Acute effects of mercuric chloride on intracellular GSH levels and mercury distribution in the fish *Oreochromis aureus*. Bull Environ Contam Toxicol, 1988. 40(2): p. 178-84.
5. Al-Saleh, I. and A.A. Al-Sedairi, Mercury (Hg) burden in children: the impact of dental amalgam. Sci Total Environ. 409(16): p. 3003-15.
6. Ballatori, N., Transport of toxic metals by molecular mimicry. Environ Health Perspect, 2002. 110 Suppl 5: p. 689-94.
7. Barbier, O., et al., Effect of heavy metals on, and handling by, the kidney. Nephron Physiol, 2005. 99(4): p. p105-10.
8. Boyer, P.D., The ATP synthase--a splendid molecular machine. Annu Rev Biochem, 1997. 66: p. 717-49.
9. Brambila, E., et al., Effect of mercury vapor exposure on metallothionein and glutathione s-transferase gene expression in the kidney of nonpregnant, pregnant, and neonatal rats. J Toxicol Environ Health A, 2002. 65(17): p. 1273-88.
10. Breusing, N., and T. Grune, Regulation of proteasome-mediated protein degradation during oxidative stress and aging. Biol Chem, 2008. 389(3): p. 203-9.
11. Broniatowski, M., et al., Grazing incidence diffraction and X-ray reflectivity studies of the interactions of inorganic mercury salts with membrane lipids in Langmuir monolayers at the air/water interface. J Phys Chem B. 114(29): p. 9474-84.
12. Buckell, M., D. Hunter, and et al., Chronic mercury poisoning. Br J Ind Med, 1946. 3: p. 55-63.
13. Chen, H., et al., Nickel decreases cellular iron level and converts cytosolic aconitase to iron-regulatory protein 1 in A549 cells. Toxicol Appl Pharmacol, 2005. 206(3): p. 275-87.
14. Choy, C.A., et al., The influence of depth on mercury levels in pelagic fishes and their prey. Proc Natl Acad Sci U S A, 2009. 106(33): p. 13865-9.
15. Clarkson, T.W. and L. Magos, The toxicology of mercury and its chemical compounds. Crit Rev Toxicol, 2006. 36(8): p. 609-62.
16. Clifton, J.C., 2nd, Mercury exposure and public health. Pediatr Clin North Am, 2007. 54(2): p. 237-69, viii.
17. Cukrov, N., et al., A recent history of metal accumulation in the sediments of Rijeka harbor, Adriatic Sea, Croatia. Mar Pollut Bull. 62(1): p. 154-67.

18. Delneri, D., et al., Disruption of seven hypothetical aryl alcohol dehydrogenase genes from *Saccharomyces cerevisiae* and construction of a multiple knock-out strain. Yeast, 1999a. 15(15): p. 1681-9.
19. Delneri, D., D.C. Gardner, and S.G. Oliver, Analysis of the seven-member AAD gene set demonstrates that genetic redundancy in yeast may be more apparent than real. Genetics, 1999b. 153(4): p. 1591-600.
20. DeRisi, J., et al., Genome microarray analysis of transcriptional activation in multidrug resistance yeast mutants. FEBS Lett, 2000. 470(2): p. 156-60.
21. Dickey, A.N., W.S. Yim, and R. Faller, Using ergosterol to mitigate the deleterious effects of ethanol on bilayer structure. J Phys Chem B, 2009. 113(8): p. 2388-97.
22. Dormer, U.H., et al., Cadmium-inducible expression of the yeast *GSH1* gene requires a functional sulfur-amino acid regulatory network. J Biol Chem, 2000. 275(42): p. 32611-6.
23. Eisen, M.B., et al., Cluster analysis and display of genome-wide expression patterns. Proc Natl Acad Sci U S A, 1998. 95(25): p. 14863-8.
24. Estruch, F., Stress-controlled transcription factors, stress-induced genes and stress tolerance in budding yeast. FEMS Microbiol Rev, 2000. 24(4): p. 469-86.
25. Fardeau, V., et al., The central role of *PDR1* in the foundation of yeast drug resistance. J Biol Chem, 2007. 282(7): p. 5063-74.
26. Ferguson, S.B., et al., Protein kinase A regulates constitutive expression of small heat-shock genes in an Msn2/4p-independent and Hsf1p-dependent manner in *Saccharomyces cerevisiae*. Genetics, 2005. 169(3): p. 1203-14.
27. Fischer, M., et al., The 26S proteasome of the yeast *Saccharomyces cerevisiae*. FEBS Lett, 1994. 355(1): p. 69-75.
28. Fujimura, M., et al., Methylmercury induces neuropathological changes with tau hyperphosphorylation mainly through the activation of the c-jun-N-terminal kinase pathway in the cerebral cortex, but not in the hippocampus of the mouse brain. Neurotoxicology, 2009. 30(6): p. 1000-7.
28. Gasch, A.P., et al., Genomic expression programs in the response of yeast cells to environmental changes. Mol Biol Cell, 2000. 11(12): p. 4241-57.
30. Gerber, S., et al., Graphical analysis and experimental evaluation of *Saccharomyces cerevisiae PTRK1|2* and *PBMH1|2* promoter region. Genome Inform. 22: p. 11-20.
31. Ghislain, M., et al., Cdc48p interacts with Ufd3p, a WD repeat protein required for ubiquitin-mediated proteolysis in *Saccharomyces cerevisiae*. EMBO J, 1996. 15(18): p. 4884-99.
32. Gounalaki, N. and G. Thireos, Yap1p, a yeast transcriptional activator that mediates multidrug resistance, regulates the metabolic stress response. EMBO J, 1994. 13(17): p. 4036-41.
33. Grant, C.M., et al., Glutathione and catalase provide overlapping defenses for protection against hydrogen peroxide in the yeast *Saccharomyces cerevisiae*. Biochem Biophys Res Commun, 1998. 253(3): p. 893-8.
34. Gueldry, O., et al., Ycf1p-dependent Hg(II) detoxification in *Saccharomyces cerevisiae*. Eur J Biochem, 2003. 270(11): p. 2486-96.

35. Hansen, J.M., H. Zhang, and D.P. Jones, Differential oxidation of thioredoxin-1, thioredoxin-2, and glutathione by metal ions. Free Radic Biol Med, 2006. 40(1): p. 138-45.
36. Harbison, C.T., et al., Transcriptional regulatory code of a eukaryotic genome. Nature, 2004. 431(7004): p. 99-104.
37. Haugen, A.C., et al., Integrating phenotypic and expression profiles to map arsenic-response networks. Genome Biol, 2004. 5(12): p. R95.
38. Horan, S., I. Bourges, and B. Meunier, Transcriptional response to nitrosative stress in *Saccharomyces cerevisiae*. Yeast, 2006. 23(7): p. 519-35.
39. Hosiner, D., et al., Arsenic toxicity to *Saccharomyces cerevisiae* is a consequence of inhibition of the TORC1 kinase combined with a chronic stress response. Mol Biol Cell, 2009. 20(3): p. 1048-57.
40. Jan, A.T., A. Ali, and Q. Haq, Glutathione as an antioxidant in inorganic mercury induced nephrotoxicity. J Postgrad Med. 57(1): p. 72-7.
41. Jin, Y.H., et al., Global transcriptome and deletome profiles of yeast exposed to transition metals. PLoS Genet, 2008. 4(4): p. e1000053.
42. Jungwirth, H. and K. Kuchler, Yeast ABC transporters-- a tale of sex, stress, drugs and aging. FEBS Lett, 2006. 580(4): p. 1131-8.
43. Jungwirth, H., et al., Diazaborine resistance in yeast involves the efflux pumps Ycf1p and Flr1p and is enhanced by a gain-of-function allele of gene *YAP1*. Eur J Biochem, 2000. 267(15): p. 4809-16.
44. Kaplan, J.G., Action of Non-Penetrating Heavy Metals on the Catalase Activity of Yeast Cells. Nature, 1965. 205: p. 76-7.
45. Kasten, M.M. and D.J.Stillman, Identification of the *Saccharomyces cerevisiae* genes *STB1-STB5* encoding Sin3p binding proteins. Mol Gen Genet, 1997. 256(4): p. 376-86.
46. Larochelle, M., et al., Oxidative stress-activated zinc cluster protein Stb5 has dual activator/repressor functions required for pentose phosphate pathway regulation and NADPH production. Mol Cell Biol, 2006. 26(17): p. 6690-701.
47. Liang, Y.X., et al., Psychological effects of low exposure to mercury vapor: application of a computer-administered neurobehavioral evaluation system. Environ Res, 1993. 60(2): p. 320-7.
48. Lin, S.J. and L. Guarente, Nicotinamide adenine dinucleotide, a metabolic regulator of transcription, longevity and disease. Curr Opin Cell Biol, 2003. 15(2): p. 241-6.
49. Liu, J., et al., Genomic analysis of the rat lung following elemental mercury vapor exposure. Toxicol Sci, 2003. 74(1): p. 174-81.
50. Liu, Z., et al., Arsenic trioxide uptake by hexose permeases in *Saccharomyces cerevisiae*. J Biol Chem, 2004. 279(17): p. 17312-8.
51. London, M.K., et al., Regulatory mechanisms controlling biogenesis of ubiquitin and the proteasome. FEBS Lett, 2004. 567(2-3): p. 259-64.
52. Lucau-Danila, A., et al., Early expression of yeast genes affected by chemical stress. Mol Cell Biol, 2005. 25(5): p. 1860-8.
53. Lupetti, A., et al., Molecular basis of resistance to azole antifungals. Trends Mol Med, 2002. 8(2): p. 76-81.

54. Lushchak, V.I., Environmentally induced oxidative stress in aquatic animals. Aquat Toxicol. 101(1): p. 13-30.
55. MacPherson, S., M. Larochelle, and B. Turcotte, A fungal family of transcriptional regulators: the zinc cluster proteins. Microbiol Mol Biol Rev, 2006. 70(3): p. 583-604.
56. Maranzana, P., [Observations on delayed sequellae of occupational hydrargyrism in hat-makers]. Riv Infort Mal Prof, 1952. 39(6): p. 1017-25.
57. Marion, R.M., et al., Sfp1 is a stress- and nutrient-sensitive regulator of ribosomal protein gene expression. Proc Natl Acad Sci U S A, 2004. 101(40): p. 14315-22.
58. Mieiro, C.L., et al., Antioxidant system breakdown in brain of feral golden grey mullet (*Liza aurata*) as an effect of mercury exposure. Ecotoxicology. 19(6): p. 1034-45.
59. Moen, B., B. Hollund, and T. Riise, Neurological symptoms among dental assistants: a cross-sectional study. J Occup Med Toxicol, 2008. 3: p. 10.
60. Montgomery, K.S., et al., Chronic, low-dose prenatal exposure to methylmercury impairs motor and mnemonic function in adult C57/B6 mice. Behav Brain Res, 2008. 191(1): p. 55-61.
61. Mountain, H.A., A.S. Bystrom, and C. Korch, The general amino acid control regulates *MET4*, which encodes a methionine-pathway-specific transcriptional activator of *Saccharomyces cerevisiae*. Mol Microbiol, 1993. 9(1): p. 221-3.
62. Moye-Rowley, W.S., Transcriptional control of multidrug resistance in the yeast *Saccharomyces*. Prog Nucleic Acid Res Mol Biol, 2003. 73: p. 251-79.
63. Murray, A.D. and D.K. Kidby, Sub-cellular location of mercury in yeast grown in the presence of mercuric chloride. J Gen Microbiol, 1975. 86(1): p. 66-74.
64. Nadon, R. and J. Shoemaker, Statistical issues with microarrays: processing and analysis. Trends Genet, 2002. 18(5): p. 265-71.
65. Natarajan, K., et al., Transcriptional profiling shows that Gcn4p is a master regulator of gene expression during amino acid starvation in yeast. Mol Cell Biol, 2001. 21(13): p. 4347-68.
66. Ngim, C.H., et al., Chronic neurobehavioural effects of elemental mercury in dentists. Br J Ind Med, 1992. 49(11): p. 782-90.
67. Nies, D.H., Microbial heavy-metal resistance. Appl Microbiol Biotechnol, 1999. 51(6): p. 730-50.
68. Nussbaum, A.K., et al., Cleavage motifs of the yeast 20S proteasome beta subunits deduced from digests of enolase 1. Proc Natl Acad Sci U S A, 1998. 95(21): p. 12504-9.
69. Ono, B., H. Ohue, and F. Ishihara, Role of cell wall in *Saccharomyces cerevisiae* mutants resistant to Hg2+. J Bacteriol, 1988. 170(12): p. 5877-82.
70. Owsianik, G., Balzi, l.L., Ghislain, M., Control of 26S proteasome expression by transcription factors regulating multidrug resistance in *Saccharomyces cerevisiae*. Mol Microbiol., 2002. 43(5): p. 1295-308.
71. Pacyna, E.G., et al., Mercury emissions to the atmosphere from anthropogenic sources in Europe in 2000 and their scenarios until 2020. Sci Total Environ, 2006. 370(1): p. 147-56.
72. Pagani, M.A., et al., Disruption of iron homeostasis in *Saccharomyces cerevisiae* by high zinc levels: a genome-wide study. Mol Microbiol, 2007. 65(2): p. 521-37.

73. Pathak, S.K. and M.K. Bhowmik, The chronic toxicity of inorganic mercury in goats: clinical signs, toxicopathological changes and residual concentrations. Vet Res Commun, 1998. 22(2): p. 131-8.
74. Prévéral. S., et al., Metal(loid)s and radionuclides cytotoxicity in *Saccharomyces cerevisiae*. Role of *YCF1*, glutathione and effect of buthionine sulfoximine. Biochimie, 2006. 88(11): p. 1651-63.
75. Protchenko, O., et al., Three cell wall mannoproteins facilitate the uptake of iron in *Saccharomyces cerevisiae*. J Biol Chem, 2001. 276(52): p. 49244-50.
76. Reinheckel, T., et al., Comparative resistance of the 20S and 26S proteasome to oxidative stress. Biochem J, 1998. 335(3): p. 637-42.
77. Ritchie, M.E., et al., A comparison of background correction methods for two-colour microarrays. Bioinformatics, 2007. 23(20): p. 2700-7.
78. Robillard, J.M., et al., Glutathione restores the mechanism of synaptic plasticity in aged mice to that of the adult. PLoS One, 2011. 6(5): p. 20676.
79. Rodriguez, R.J., et al., Multiple functions for sterols in *Saccharomyces cerevisiae*. Biochim Biophys Acta, 1985. 837(3): p. 336-43.
80. Rutherford, J.C., et al., Activation of the iron regulon by the yeast Aft1/Aft2 transcription factors depends on mitochondrial but not cytosolic iron-sulfur protein biogenesis. J Biol Chem, 2005. 280(11): p. 10135-40.
81. Saldanha, A.J., Java Treeview--extensible visualization of microarray data. Bioinformatics, 2004. 20(17): p. 3246-8.
82. Santangelo, G.M., Glucose signaling in *Saccharomyces cerevisiae*. Microbiol Mol Biol Rev, 2006. 70(1): p. 253-82.
83. Saponja, J.A. and H.J. Vogel, Metal-ion binding properties of the transferrins: a vanadium-51 NMR study. J Inorg Biochem, 1996. 62(4): p. 253-70.
84. Shringarpure, R., et al., Ubiquitin conjugation is not required for the degradation of oxidized proteins by proteasome. J Biol Chem, 2003. 278(1): p. 311-8.
85. Silver, J.D., M.E. Ritchie, and G.K. Smyth, Microarray background correction: maximum likelihood estimation for the normal-exponential convolution. Biostatistics, 2009. 10(2): p. 352-63.
86. Smyth, G.K., Linear models and empirical bayes methods for assessing differential expression in microarray experiments. Stat Appl Genet Mol Biol, 2004. 3: p. Article3.
87. Smyth, G.K., J. Michaud, and H.S. Scott, Use of within-array replicate spots for assessing differential expression in microarray experiments. Bioinformatics, 2005. 21(9): p. 2067-75.
88. Stadler, J.A. and R.J. Schweyen, The yeast iron regulon is induced upon cobalt stress and crucial for cobalt tolerance. J Biol Chem, 2002. 277(42): p. 39649-54.
89. Stohs, S.J. and D. Bagchi, Oxidative mechanisms in the toxicity of metal ions. Free Radic Biol Med, 1995. 18(2): p. 321-36.
90. Sugawara, N., et al., Decreased hepatobiliary secretion of inorganic mercury, its deposition and toxicity in the Eisai hyperbilirubinemic rat with no hepatic canalicular organic anion transporter. Toxicology, 1998. 126(1): p. 23-31.

91. Szczypka, M.S., et al., A yeast metal resistance protein similar to human cystic fibrosis transmembrane conductance regulator (CFTR) and multidrug resistance-associated protein. J Biol Chem, 1994. 269(36): p. 22853-7.
92. Tchaikovskaya, T., et al., Glutathione S-transferase hGSTM3 neurodegeneration: relationship to Alzheimer's disease. Mech Ageing Dev, 2005. 126(2): p. 309-15.
93. Tedeschi, L.G., The Minamata disease. Am J Forensic Med Pathol, 1982. 3(4): p. 335-8.
94. Teixeira, M.C., et al., The YEASTRACT database: a tool for the analysis of transcription regulatory associations in *Saccharomyces cerevisiae*. Nucleic Acids Res, 2006. 34(Database issue): p. D446-51.
95. Thomas, D. and Y. Surdin-Kerjan, Metabolism of sulfur amino acids in *Saccharomyces cerevisiae*. Microbiol Mol Biol Rev, 1997. 61(4): p. 503-32.
96. Thorpe, G.W., et al., Cells have distinct mechanisms to maintain protection against different reactive oxygen species: oxidative-stress-response genes. Proc Natl Acad Sci U S A, 2004. 101(17): p. 6564-9.
97. Toda, T., et al., Three different genes in *S. cerevisiae* encode the catalytic subunits of the cAMP-dependent protein kinase. Cell, 1987. 50(2): p. 277-87.
98. Toh, T.H., et al., Implications of *FPS1* deletion and membrane ergosterol content for glycerol efflux from *Saccharomyces cerevisiae*. FEMS Yeast Res, 2001. 1(3): p. 205-11.
99. Valko, M., H. Morris, and M.T. Cronin, Metals, toxicity and oxidative stress. Curr Med Chem, 2005. 12(10): p. 1161-208.
100. Vallee, B.L. and D.D. Ulmer, Biochemical effects of mercury, cadmium, and lead. Annu Rev Biochem, 1972. 41(10): p. 91-128.
101. van Ginkel, G. and A. Sevanian, Lipid peroxidation-induced membrane structural alterations. Methods Enzymol, 1994. 233: p. 273-88.
102. Verlecar, X.N., K.B. Jena, and G.B. Chainy, Modulation of antioxidant defences in digestive gland of *Perna viridis* (L.), on mercury exposures. Chemosphere, 2008. 71(10): p. 1977-85.
103. Wade, J.T., D.B. Hall, and K. Struhl, The transcription factor Ifh1 is a key regulator of yeast ribosomal protein genes. Nature, 2004. 432(7020): p. 1054-8.
104. Waldron, H.A., Did the Mad Hatter have mercury poisoning? Br Med J (Clin Res Ed), 1983. 287(6409): p. 1961.
105. Wang, X., et al., Disruption of Rpn4-induced proteasome expression in *Saccharomyces cerevisiae* reduces cell viability under stressed conditions. Genetics, 2008. 180(4): p. 1945-53.
106. Wang, X., et al., Regulation of the 26S proteasome complex during oxidative stress. Sci Signal, 2010. 3(151): ra88.
107. Ward, R.J., et al., Aluminium toxicity and iron homeostasis. J Inorg Biochem, 2001. 87(1-2): p. 9-14.
108. Warner, J.R., The economics of ribosome biosynthesis in yeast. Trends Biochem Sci, 1999. 24(11): p. 437-440.
109. Westwater, J., et al., The adaptive response of *Saccharomyces cerevisiae* to mercury exposure. Yeast, 2002. 19(3): p. 233-9.

110. Wheeler, G.L., et al., Coupling of the transcriptional regulation of glutathione biosynthesis to the availability of glutathione and methionine via the Met4 and Yap1 transcription factors. J Biol Chem, 2003. 278(50): p. 49920-8.
111. Wolf, M.B. and J.W. Baynes, Cadmium and mercury cause an oxidative stress-induced endothelial dysfunction. Biometals, 2007. 20(1): p. 73-81.
112. Xie, Y. and A.Varshavsky, *RPN4* is a ligand, substrate, and transcriptional regulator of the 26S proteasome: a negative feedback circuit. Proc Natl Acad Sci U S A, 2001. 98(6): p. 3056-61.
113. Yamaguchi-Iwai, Y., et al., *AFT1*: a mediator of iron regulated transcriptional control in *Saccharomyces cerevisiae*. EMBO J, 1995. 14(6): p. 1231-9.
114. Yang, H., et al., A segmental nearest neighbour normalization and gene identification method gives superior results for DNA-array analysis. Proc Natl Acad Sci U S A, 2003. 100(3): p. 1122-7.
115. Yorifuji, T., et al., What has methylmercury in umbilical cords told us? - Minamata disease. Sci Total Environ, 2009. 408(2): p. 272-6.
116. Zalups, R.K., Molecular interactions with mercury in the kidney. Pharmacol Rev, 2000a. 52(1): p. 113-43.
117. Zalups, R.K. and J. Koropatnick, Temporal changes in metallothionein gene transcription in rat kidney and liver: relationship to content of mercury and metallothionein protein. J Pharmacol Exp Ther, 2000b. 295(1): p. 74-82.
118. Zhang, S. and S.A. Crow, Jr., Toxic effects of Ag(I) and Hg(II) on *Candida albicans* and *C. maltosa*: a flow cytometric evaluation. Appl Environ Microbiol, 2001. 67(9): p. 4030-5.
119. Zlotnik, H., et al., *Saccharomyces cerevisiae* mannoproteins form an external cell wall layer that determines wall porosity. J Bacteriol, 1984. 159(3): p. 1018-26.

2.4 Pun1 is a metal ion-inducible, calcineurin/Crz1p-regulated plasma membrane protein required for cell wall integrity

Dagmar Hosiner[1], Gerhard Sponder[1], Anton Graschopf[1], Siegfried Reipert[2], Rudolf J. Schweyen[1]†, Christoph Schüller[3], and Markus Aleschko[1a]

[1]Department of Microbiology, Immunobiology and Genetics, Max F. Perutz Laboratories, University of Vienna, A-1030 Vienna, Austria

[2]Department of Molecular Cell Biology, Max F. Perutz Laboratories, University of Vienna, A-1030 Vienna, Austria

[3]Department of Biochemistry and Cell Biology, Max F. Perutz Laboratories, University of Vienna, A-1030 Vienna, Austria

[a] Corresponding author

† Deceased February 15, 2009

The author's contribution

Dagmar Hosiner	- conceived the study, toxicity assays, phenotypic analyses, northern blot analyses, writing
Gerhard Sponder	- membrane fractionation, chemical crosslink, writing
Anton Graschopf	- conceived the study, intracellular $AsCl_3$ measurement, zymolyase sensitivity assays, advices, writing
Siegfried Reipert	- electron microscopy
Rudolf J. Schweyen	- financer, advices
Christoph Schüller	- writing, advices
Markus Aleschko	- correspondence, conceived the study, fluorescence microscopy, co-immunoprecipitation, blue native electrophoresis, writing

Published in: Biochimica et Biophysica Acta 2011 Apr; 1808(4):1108-19.

Contents lists available at ScienceDirect

Biochimica et Biophysica Acta

journal homepage: www.elsevier.com/locate/bbamem

Pun1p is a metal ion-inducible, calcineurin/Crz1p-regulated plasma membrane protein required for cell wall integrity

Dagmar Hosiner [a], Gerhard Sponder [a], Anton Graschopf [a], Siegfried Reipert [b], Rudolf J. Schweyen [a,1], Christoph Schüller [c], Markus Aleschko [a,□]

[a] Department of Microbiology, Immunobiology and Genetics, Max F. Perutz Laboratories, University of Vienna, A-1030 Vienna, Austria
[b] Department of Molecular Cell Biology, Max F. Perutz Laboratories, University of Vienna, A-1030 Vienna, Austria
[c] Department of Biochemistry and Cell Biology, Max F. Perutz Laboratories, University of Vienna, A-1030 Vienna, Austria

ARTICLEINFO

Article history:
Received 20 September 2010
Received in revised form 22 December 2010
Accepted 3 January 2011
Available online 9 January 2011

Keywords:
Cell wall
Plasma membrane
Metal ion stress
Calcineurin/Crz1p
Oligomerization

ABSTRACT

Under conditions of environmental stress, the plasma membrane is involved in several regulatory processes to promote cell survival, like maintenance of signaling pathways, cell wall organization and intracellular ion homeostasis. PUN1 encodes a plasma membrane protein localizing to the ergosterol-rich membrane compartment occupied also by the arginine permease Can1. We found that the PUN1 (YLR414c) gene is transcriptionally induced upon metal ion stress. Northern blot analysis of the transcriptional regulation of PUN1 showed that the calcium dependent transcription factor Crz1p is required for PUN1 induction upon heavy metal stress. Here we report that mutants deleted for PUN1 exhibit increased metal ion sensitivity and morphological abnormalities. Microscopical and ultrastructural observations revealed a severe cell wall defect of pun1Δ mutants. By using chemical cross-linking, Blue native electrophoresis, and co-immunoprecipitation we found that Pun1p forms homo-oligomeric protein complexes. We propose that Pun1p is a stress-regulated factor required for cell wall integrity, thereby expanding the functional significance of lateral plasma membrane compartments.

1. Introduction

The plasma membrane is involved in many cellular processes ensuring adaptation to changed environmental conditions. These include maintenance of intracellular ion homeostasis, regulation of signaling pathways, morphogenesis and cell wall biogenesis.

Studies on the plasma membrane provide strong evidence for a highly regulated structure and presence of discrete domains, like lipid rafts in higher eukaryotes as well as eisosomes and the membrane compartment of the arginine permease Can1 (MCC), being ergosterol-rich plasma membrane invaginations, in yeast [1]. Although their actual function still remains to be determined, these domains were shown to be involved in cell signaling [2] and endocytic protein turnover [3,4].

An important aspect associated with the survival of environmental stress situations, like osmotic or heat stress [5], is the adjustment of ion fluxes across the plasma membrane. Transporters, exchangers and channels, embedded in a highly flexible membrane system, allow an accurate adaptation of the cellular ion homeostasis to changing environmental conditions [6]. Consequently, tightly regulated processes for ion uptake through the plasma membrane, distribution to the appropriate subcellular compartments, as well as detoxification mechanisms are essential for cell survival.

In spite of their potential toxicity at higher concentrations, a number of transition metals e.g. manganese, cadmium, cobalt, zinc, and iron are important trace elements in humans and other organisms. The transport mechanisms and the regulation and function of involved proteins, the biological effects of some of these metals, their toxicity, as well as the respective regulatory mechanisms are not yet completely understood [7–10].

In search of genes involved in cellular adaptation to metal ion stress conditions, we found the PUN1 (YLR414c) gene as being significantly induced upon metal ion stress. PUN1 encodes a plasma membrane MCC protein which was recently shown to be induced during nitrogen starvation stress and involved in filamentous growth [11].

Surprisingly, Pun1p shares structural similarities with mammalian claudins, the major constituents of plasma membrane tight junctions [12], in particular a tetraspan topology and the highly conserved claudin family signature G-L-W-x-x-C-x(8-10)-C within the first extracellular loop (Interpro IPR017974).

Abbreviations: MCC, membrane compartment occupied by Can1; ICP-MS, inductively coupled plasma mass spectrometry; DIC, differential interference contrast; TEM, transmission electron microscope; HOG, high osmolarity glycerol; o-PDM, o-phenylenedimaleimide; D, digitonin; TX, Triton X-100; DM, n-Dodecyl-β-D-maltoside; Co-IP, Co-Immunoprecipitation

□ Corresponding author. Dr. Bohr-Gasse 9, A-1030 Vienna, Austria. Tel.: +43 1 4277 54618; fax: +43 1 4277 9546.
E-mail address: markus.aleschko@univie.ac.at (M. Aleschko).
[1] Deceased February 15, 2009.

0005-2736/$ – see front matter © 2011 Elsevier B.V. All rights reserved. doi:10.1016/j.bbamem.2011.01.002

In addition to Can1p and Pun1p, seven other proteins are known to be integral components of the MCC. Among them, the uracil permease Fur4p, the tryptophan/tyrosin permease Tat2p, and the tetraspan proteins Sur7p, Nce102p, Fmp45p, Fhn1p, and Ynl194cp, all five of unknown function [4,13]. Besides Fmp45p and Ynl194cp [14], Pun1p is a third S. cerevisiae paralog of Sur7p. Interestingly, all four proteins contain a cysteine motif similar to the claudin signature in their first extracellular loop, but only for Pun1p it is perfectly conserved [15].

Thus, the clustering of tetraspan proteins in MCC compartments raises the challenging question if these proteins and their common domains share evolutionary conserved structural and functional properties.

2. Materials and methods

2.1. Yeast strains, media and culture conditions

Saccharomyces cerevisiae strains were grown at 28 °C in liquid YPD medium (yeast extract/peptone/dextrose), on solid YPD in serial 10-fold dilution steps or in standard SD medium (0.67% yeast nitrogen base, 2% glucose, and amino acids as required). Escherichia coli strain DH10b (Invitrogen, Lofer, Austria) was cultivated at 37 °C in Luria–Bertani (LB) medium supplemented with 100 pg/ml ampicillin when appropriate. Media were supplemented with various metal ion salts when indicated. Yeast strains BY4741 (acc. no. Y00000), W303 (acc. no. 20000A) and FY1679 (acc. no. 10000 M) provided by Euroscarf (Frankfurt, Germany) were used as wild-type. Mutant derivatives of BY4741 used in this study were also provided by Euroscarf. These were BYhog1A, BYcrz1A, BYrlm1A, BYste12A, BYsko1A, and BYdig1A. Corresponding genes were completely deleted and replaced by the geneticin resistance module KanMX4. Strain W303msn2/4A was described previously [16]. Strain BY4741 bearing the chromosomal PUN1-GFP fusion was obtained from the yeast GFP-tagged collection [17]. The haploid deletion strain MApun1A was constructed from parental strain FY1679. According to the one step replacement protocol [18] the PUN1 ORF was deleted by homologous recombination with a HIS5 disruption cassette amplified from plasmid pSG634 with the primers PUN1-delfor: 5′-TTCGCTAGGAGCACTTATATTAGCCATTGTT-GCATGCGCAGGATCCGTACGCTG-CAGGTCGAC-3′ and PUN1-delrev: 5′-GACGGTGGGCCTCGATCTCACGCTACACCT-CGAATGAAATTCAGTAGGCCACTAGTGGATCTG-3′. Verification of correct gene replacement was performed by analytical PCR using primers PUN1-up: 5′-AAATCGGGCGTACTATCAGCCA-AGC-3′, PUN1-in: 5′-AAACACGAACCTATACTGACTAATAGG-3′, and HIS-in: 5′-TCTACAAAAGCCCTCCTACCCATG-3′.

2.2. Plasmid constructs

To express PUN1 from its endogenous promoter, the entire ORF and its flanking regions including 450 nt upstream of the ATG and 175 nt downstream of the stop codon, were PCR-amplified from FY1679 genomic DNA using the forward primer PUN1-fwd: 5′-TAGAGCTCAACTGTCACAGCCTCCCAC-TTGACC-3′ and reverse primer PUN1-rev: 5′-ATGTCGACAAGAAGATCA-TGCAACATCACC-3′. The PCR product was cloned via its introduced restriction sites SacI and SalI (underlined) into the centromeric vector YCplac22 [19], thereby creating the vector YCp-PUN1. To generate C-terminally triple HA-tagged Pun1p expressed via the strong MET25 promoter, the PUN1 coding sequence was PCR-amplified using the oligonucleotide primers PUN1-SpeI: 5′-AAACACTAGTTC-GAAGGACGCTATAAGCATGAGG-3′ and PUN1-SalI: 5′TTTCGTCGAC-AAATCAATGGTTTTTCCTCAATTGG-3′, and cloned via the SpeI and SalI restriction sites (underlined) into the multicopy vector YEpM351HA [20]. For expression of C-terminally triple HA-tagged Pun1p under the control of its endogenous promoter, PUN1 was PCR-amplified from FY1679 genomic DNA using the primer pair PUN1- fwd and PUN1-SalI. The PCR product was cloned via the SacI and SalI restriction sites into plasmid YEp351HA [21] and then subcloned together with the HA tag into plasmid YCplac33 [19], thereby creating the construct YCp-PUN1-HA. To generate the centromeric plasmid pUG35-PUN1-GFP expressing C-terminally GFP-tagged Pun1p under the control of the MET25 promoter, the PUN1 coding sequence was PCR-amplified using the oligonucleotide primers PUN1-SpeI (see above) and PUN1-EcoRI: 5′-TTTCAGAATTCAATCAATGGTT-TTTCCTCAATTGG-3′ and cloned into the SpeI- and EcoRI-digested vector pUG35 [22].

2.3. Intracellular AsCl3 measurement

Strains FY1679 and MApun1A carrying the empty plasmid YEpM351HA and MApun1A overexpressing C-terminally HA-tagged PUN1 from plasmid YEpM-PUN1-HA (MApun1A(PUN1)^{n}) were adjusted to an OD600 = 0.5 and grown in SD medium and SD medium supplemented with 250 pM AsCl3 for 6 h at 28 °C. Cells were collected and washed twice with Fluka highly pure deionized water (Sigma-Aldrich), $_{OD600}$ and the dry weight were defined and the total intracellular As^{3+} concentration of whole cells (pg As^{3+}/g cells) was measured by inductively coupled plasma mass spectrometry (ICP-MS, ARC Seibersdorf Research GmbH, Austria).

2.4. Fluorescence microscopy

Yeast cells used for analysis of GFP fusion proteins and for cell wall staining were grown to early log phase. Fluorescence microscopy was used to detect GFP and fluorescent dyes and differential interference contrast (DIC) optics were used to observe cell morphology. For Aniline Blue staining cells were washed with distilled water and incubated in 0.05% Aniline Blue for 5 min. For chitin staining washed cells were incubated in 1 mg/ml Calcofluor White for 5 min, washed twice and then observed. Concanavalin A–FITC staining was carried out by incubating washed cells in 0.1 mg/ml concanavalin A–FITC in 10 mM sodium phosphate buffer, pH 7.2, 150 mM NaCl for 10 min. For Filipin staining of plasma membrane ergosterol cells were washed with 50 mM potassium phosphate buffer, pH 5.5, stained with 5 pg/ml Filipin for 5 min and washed twice in the same buffer. Aniline Blue, Calcofluor White, concanavalin A–FITC, and Filipin were purchased from Sigma-Aldrich (Schnelldorf, Germany).

Fluorescence was visualized in living cells without fixation. Images were captured with equivalent exposures using a Zeiss Axioplan 2 fluorescence microscope with an AxioCam MRc5 CCD camera using AxioVision 4.8.1 software (Carl Zeiss, Oberkochen, Germany). Grayscale images were processed with Photoshop CS3 (Adobe, San Jose, CA).

2.5. Electron microscopy

FY1679 wild-type and MApun1A cells bearing the empty plasmid YCplac22, as well as MApun1A cells expressing Pun1p from plasmid YCp-PUN1 were grown in YPD to log phase (OD600 = 1). For cryofixation, cell pellets were introduced to flat sample holders of an EMPACT high-pressure freezer (LEICA Microsystems, Austria). Flat specimen holders were placed in a sample holder pod and tightly sealed. The samples were frozen as described previously for specimens of mammalian tissues [23]. Following freezing, the flat specimen holders were transferred under liquid nitrogen to an automatic freeze substitution unit (AFS; LEICA Microsystems). Freeze-substitution was performed as described elsewhere [24]. Thin sections were cut with an Ultracut S ultramicrotome (LEICA Microsystems), mounted on copper grids with Formvar support film, counterstained with uranyl acetate and lead citrate and examined at 80 kV in a JEOL JEM-1210 electron microscope. Images were acquired using a digital camera (Morada) for the wide-angle port of the TEM and analySIS FIVE software (Soft Image System).

2.6. Zymolyase sensitivity assay

FY1679 wild-type and MApun1A cells were grown to early log phase in YPD at 28 °C. Cells were harvested, washed, and diluted to an equal $_{OD600}$ value in 10 mM Tris/Cl pH 7.5 supplemented with 0, 30 or 100 pg/ml zymolyase 20T (Seikagaku Corporation, Tokyo, Japan). Cells were incubated at 28 °C and the optical density was monitored photometrically at indicated time points by the use of a HITACHI U-2000 photometer.

For immunoblotting experiments, early log phase cells were washed, concentrated by centrifugation (OD600 = 10), resuspended in 10 mM Tris/Cl pH 7.5 and treated for 30 min with identical zymolyase concentrations as described above. Equal amounts of supernatants were subjected to SDS-PAGE and immunodetected with an antibody directed against cytoplasmic hexokinase 1 (Hxk1), which was released due to cell lysis.

2.7. Yeast cell extracts and immunoblotting

Cells were harvested and washed with distilled water. For lysis, equal cell amounts were incubated in 2 N NaOH and 1.25% [3-mercaptoethanol for 10 min on ice. Proteins were precipitated with TCA (28% final concentration) for 15 min. Subsequent washings of the precipitate were performed using 90% acetone. Protein extracts were dissolved by boiling in SDS-loading buffer, separated on a 12% SDS-polyacrylamide gel, transferred to a PVDF membrane, and immunodetected.

The antibodies used in this study were mouse anti-HA (laboratory stock), mouse anti-GFP (Roche, Vienna, Austria), rabbit anti-Hxk1p (Biotrend, Cologne, Germany), rabbit anti-Pdr5p (generous gift of Karl Kuchler), mouse anti-Prc1p (Invitrogen), mouse anti-Por1p (Molecular Probes, Eugene, Oregon) and horseradish peroxidase-conjugated goat anti-mouse IgG and goat anti-rabbit IgG (Promega, Mannheim, Germany). Immunoblotting was performed in TBS-TWEEN plus 2.5% dry milk with the desired antibodies. The proteins were visualized by use of the SuperSignal West Pico system (Pierce, Rockford, Illinois).

2.8. Northern blot analysis

Overnight cultures (BY4741 wild-type, BYhog1A, BYcrz1A, BYrlm1A, BYste12A, BYsko1A, BYdig1A, W303 wild-type, and W303msn2/4A) were grown in fresh YPD from OD600 = 0.15 to OD600 = 1.0 and then incubated with metal ions (MnCl2, AgNO3, HgCl2, CdCl2, AsCl3, NaCl; concentrations as indicated in the figures) for 30 min at 28 °C. Cells were harvested and total RNA was extracted as described previously [25]. Total RNA (20 pg) was separated on a formaldehyde gel; RNA was blotted onto a hybond membrane over night and UV-crosslinked. Probes were generated by PCR from chromosomal DNA using oligonucleotide primers PUN1-Nfwd: 5^1-GGAGCACTTATATTAGCCATTGTTGCATGCGCGTCGACAACC-3^1 and PUN1-Nrev: 5^1-GATGACGGTGGGCCTCGATCTCACGCTACACC-CCACTAGTGGATC-3^1, as well as ACT1-fwd: 5^1-ACCAAGAGAGGTA-TCTTGACTTTACG-3^1 and ACT1-rev: 5^1-GACATCGACATCACACTTC-ATGATGG3^1. Radioactive labeling was performed with ((X-^{32}P) dATP by random primed DNA labeling in the course of PCR. Blots were analyzed with an Amersham Biosciences Typhoon 8600 phosphor imaging system. Quantification of PUN1 levels relative to ACT1 was performed with ImageQuant 5.1 software (Molecular Dynamics).

2.9. Membrane fractionation

Yeast strains FY1679 expressing C-terminally HA-tagged Pun1p from plasmid YEpM-PUN1-HA and BY4741 expressing chromosomally GFP-tagged Pun1p either bearing the empty plasmid YCplac33 or coexpressing C-terminally HA-tagged Pun1p from plasmid YCp-PUN1-HA were grown in SD medium at 28 °C to mid-log phase. The washed cell pellet was resuspended in solution A (0.1 M Tris/SO4 pH 9.4; 10 mM DTT) and incubated for 10 min at 28 °C with shaking. Cells were spheroplasted and homogenized as described [21]. The membrane pellet was resuspended in TEDG buffer (10 mM Tris/Cl pH 7.5; 0.2 mM EDTA; 0.2 mM DTT; 20% glycerol) and gently layered on top of discontinuous sucrose gradients (25/30/35/40/45/50/60% and 30/43/53% sucrose in TED buffer (10 mM Tris/Cl pH 7.5; 0.2 mM EDTA; 0.2 mM DTT)). The gradients were centrifuged in a SW40Ti rotor for 2 h at 100,000g. Interphase fractions were collected, diluted fourfold with ice cold water, and again centrifuged at 30,000g for 20 min. The pellet was resuspended in buffer T (10 mM Tris/Cl pH 7.4), and the protein concentration was determined using Bio-Rad protein assay reagent according to the manufacturer's instructions.

2.10. Chemical cross-linking

Equal protein amounts (10 pg) of the 43% sucrose membrane fraction were supplemented with 20 mM Hepes buffer (pH 7.5) and the cysteine-specific cross-linking reagent ortho-phenyldimaleimide (o-PDM, Sigma-Aldrich) at increasing concentrations (0, 0.3, 3, 30, and 300 pM) in a total reaction volume of 50 pl. Probes were incubated for 15 min on ice, and the reaction was quenched by adding 5 pl of 100 mM N-ethylmaleimic acid (10 min on ice). Samples were supplemented with SDS-loading buffer, heated (5 min, 65 °C) and loaded on a 12% SDS-polyacrylamide gel, followed by immunodetection against HA-tagged Pun1p.

2.11. Blue native electrophoresis

Equal protein amounts (30 pg) of the same sucrose membrane fraction used for chemical cross-linking were supplemented with 50 pl extraction buffer (750 mM aminocaproic acid; 50 mM Bis–tris/Cl pH 7.0) and with digitonin (D), Triton X-100 (TX) or n-Dodecyl-[3-D-maltoside (DM) at final concentrations indicated in the figure. After incubation on ice for 30 min, the samples were centrifuged at 45,000g for 30 min, and the supernatant was supplemented with a 0.25 volume of sample buffer (500 mM aminocaproic acid, 5% Serva blue G). Solubilized proteins were analyzed by BN-PAGE on a 5–18% linear polyacrylamide gradient [26]. Proteins were transferred to a PVDF membrane followed by immunodetection against HA-tagged Pun1p. The calibration standards (Amersham) used in the BN-PAGE were bovine thyroglobulin (669 kDa), horse spleen apoferritin (440 kDa), bovine liver catalase (232 kDa), bovine heart lactate dehydrogenase (140 kDa) and bovine serum albumin monomer (67 kDa).

2.12. Co-immunoprecipitation

Membrane fractions (43% sucrose, 100 pg total protein) of strain BY4741 expressing chromosomally GFP-tagged Pun1p, either coexpressing HA-tagged Pun1p from plasmid YCp-PUN1-HA or bearing the empty plasmid YCplac33, were resuspended in 10 mM Tris/Cl pH 7.4 and membrane proteins were solubilized by addition of TX to a final concentration of 0.1% and incubation for 30 min on ice. Samples were centrifuged at 43,000g for 30 min at 4 °C to remove nonsolubilized membrane debris. One hundred microliters of Protein A Dynabeads (Invitrogen) was washed with 10 mM Tris/Cl, pH 7.4 containing 0.1% TX. Coating of the beads was performed with a mouse anti-HA (laboratory stock) or mouse anti-GFP (Roche) antibody in the same buffer for 1 h at 4 °C under rotation. Antibody coated beads were washed twice and incubated with the clarified supernatant for 1 h at 4 °C under gentle rotation. After the binding reaction, the supernatant was removed, and the beads were washed three times with the same buffer mentioned above. Proteins were eluted from the beads by heating for 5 min at 80 °C in SDS sample buffer. The supernatants and the elution fractions were analyzed by SDS-PAGE and Western blotting was performed as described above.

3. Results

3.1. PUN1 is induced under heavy metal treatment of yeast cells

The transcriptional regulation of PUN1 in response to heavy metals was investigated by Northern blot analysis. To induce metal ion specific expression of PUN1, cells were treated with different concentrations of MnCl2, AgNO3, HgCl2, CdCl2, AsCl3, and NaCl prior to total RNA extraction. Compared to unstressed control cells, treatment with 1 or 2 mM MnCl2 increased PUN1 transcript level by a factor of 1.7 and 5.0, respectively. Treatment with 100 pM AgNO3 raised the PUN1 mRNA about 3-fold whereas 50 pM HgCl2 and 10 pM CdCl2 doubled the expression relative to control cells (Fig. 1, left panel). In contrast, treatment with 500 pM AsCl3 or 500 mM NaCl did not significantly change PUN1 transcript level (Fig. 1, right panel).

3.2. Deletion of PUN1 changes sensitivity to metal ions

For investigation of PUN1 mediated phenotypic effects, the gene was deleted in strain FY1679 resulting in strain MApun1A (see Materials and methods). Both mutant strain MApun1A and its isogenic wild-type FY1679 were grown in YPD and YPD containing 1 mM MnCl2, 1.5 mM AsCl3, 1 mM NiSO4, and 25 mM CaCl2 at 28 °C. The growth rate of strain MApun1A was slightly decreased even without metal ions (Fig. 2A). The addition of manganese, arsenic, nickel, and calcium significantly reduced growth of the MApun1A mutant. Notably, in the presence of calcium pun1A cells reached a higher density than wild-type cells after 24 h (Fig. 2A). Other metal ions tested, like Al^{3+}, Hg^{2+}, Na^{+}, or Cd^{2+} similarly reduced growth of the mutant strain (data not shown). To confirm that the mutant phenotype was caused by deletion of PUN1, the gene was reintroduced into the pun1A mutant strain. Expressing PUN1 from the centromeric plasmid YCplac22 in MApun1A cells restored growth on YPD plates supplemented with metal ions (Fig. 2B).

Because pun1A mutant cells exhibited increased sensitivity to several metal ions and not only to those causing transcriptional induction of PUN1, these data rather suggest a more general defect in maintaining ion homeostasis and not a specific transport defect. Therefore, we determined the total intracellular As^{3+} concentration in wild-type, pun1A, and YEpM351-PUN1 overexpressing cells after treatment of cells in liquid medium containing AsCl3, one of the ions which did not cause transcriptional induction of PUN1. The cells were treated for 6 h with 250 pM AsCl3 and prepared for ICP-MS analysis (see Materials and methods). Cells were washed and $_{OD600}$ and the

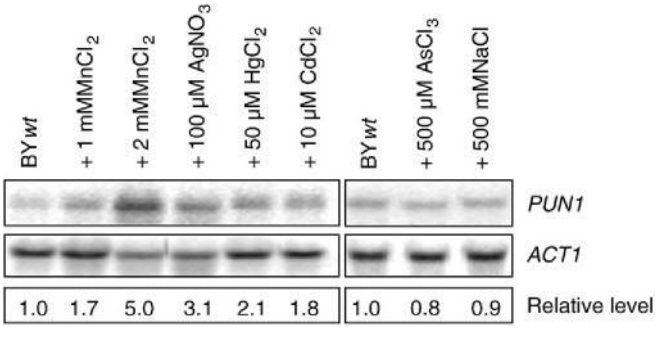

Fig. 1. Metal ion stress-dependent expression of PUN1. Induction of PUN1 by metal ion stress. Logarithmically grown BY4741 wild-type cells were induced by different concentrations of metal ions for 30 min as indicated in the figure. RNA samples were separated on a formaldehyde gel, blotted and incubated with radio labeled probes against PUN1 and ACT1, used as a loading control. Intensities of Northern blot signals were quantified by ImageQuant 5.1 software and normalized to untreated cells and the actin control.

dry weight were used as a standard to calculate the total intracellular As^{3+} concentration. As shown in Fig. 2C, pun1A cells incorporated 5.7 times more As^{3+} than wild-type cells and about 3.5 times more than PUN1 overexpressing cells, supporting our idea of an increased ion permeability of pun1A cells.

3.3. Subcellular localization of Pun1p

To further characterize the mode of function of Pun1p, the subcellular localization of the protein was determined by fluorescence microscopy, using C-terminally GFP-tagged Pun1p. Fluorescence was visualized in living cells without fixation in wild-type cells harboring pUG35-PUN1-GFP growing in early exponential phase. Fluorescence of GFP-tagged Pun1p appeared in punctate patches at the cell periphery (Fig. 3). Previously Pun1p was found to colocalize with Sur7p [15], a plasma membrane protein localized to so called MCC compartments, ergosterol-rich domains involved in turnover regulation of transport proteins [4]. To confirm MCC localization of Pun1p, the same strain was treated with Filipin, a fluorescent polyene antibiotic which stains ergosterol (Fig. 3, false colored red). Indeed, fluorescence microscopy clearly revealed colocalization of Pun1p-GFP and MCC patches.

3.4. Stress induced accumulation of Pun1p at the plasma membrane

To determine the subcellular localization of Pun1p upon metal or osmotic stress, we used a strain with the chromosomally GFP-tagged gene. Interestingly, fluorescence of the chromosomally tagged version was hardly detectable when cells were grown under standard conditions (Fig. 4A, panel a and f). The signal significantly increased when cells were stressed for 60 and 120 min with 200 mM CaCl2 or 2 mM MnCl2 (Fig. 4A, panel b, c, g, and h). This corresponds to PUN1 transcriptional activation shown above (Fig. 1). Incubation of cells with 0.8 M NaCl did not significantly increase the fluorescence signal (panel d and i), thus excluding osmotic stress as a trigger. Furthermore, treatment of cells with 1 mM AsCl3 also failed to intensify fluorescence (panel e and j). These observations were also confirmed by detection of Pun1p-GFP in crude extracts after treatment of the same strain with metal ions for 2 h (Fig. 4B).

3.5. Transcriptional regulation of PUN1 upon metal ion stress

PUN1 expression has been reported to be dependent on the high osmotic response and cell wall integrity pathways in Congo red and zymolyase treated cells [27,28]. In these studies putative interaction motifs upstream of the PUN1 coding sequence were predicted, indicating the probability for participation of other signaling pathways in gene regulation. As has been shown previously, PUN1 is also regulated via the calcineurin dependent signaling pathway [29] and therefore might be dependent on the transcriptional activator Crz1p.

We investigated the influence of candidate factors on ion-mediated induction of PUN1 by Northern blot analysis (Fig. 4C). Transcript levels of PUN1 of cells treated with 2 mM MnCl2 were compared to unstressed cells. We examined PUN1 levels in cells deleted for HOG1, a protein kinase involved in osmoregulation [30] and in mutants lacking the stress-responsive transcription factors CRZ1, RLM1, SKO1, and MSN2/4 [31], as well as the mating/filamentous growth regulating factors STE12 and DIG1 [32]. Deletion of the calcineurin dependent transcription factor CRZ1 significantly impeded activation of PUN1 transcription (Fig. 4C, red boxes), indicating that manganese stress causes CRZ1 activation. However, the absence of CRZ1 did not interfere with the basal expression level of the gene (Fig. 4C, lanes 1 and 7). Cells depleted for HOG1 showed a reduced activation of PUN1 expression by a factor of 2 when stressed with MnCl2 (lanes 5 and 6), whereas the absence of RLM1 caused an increased induction of PUN1 by the same rate (lane 10). None of the

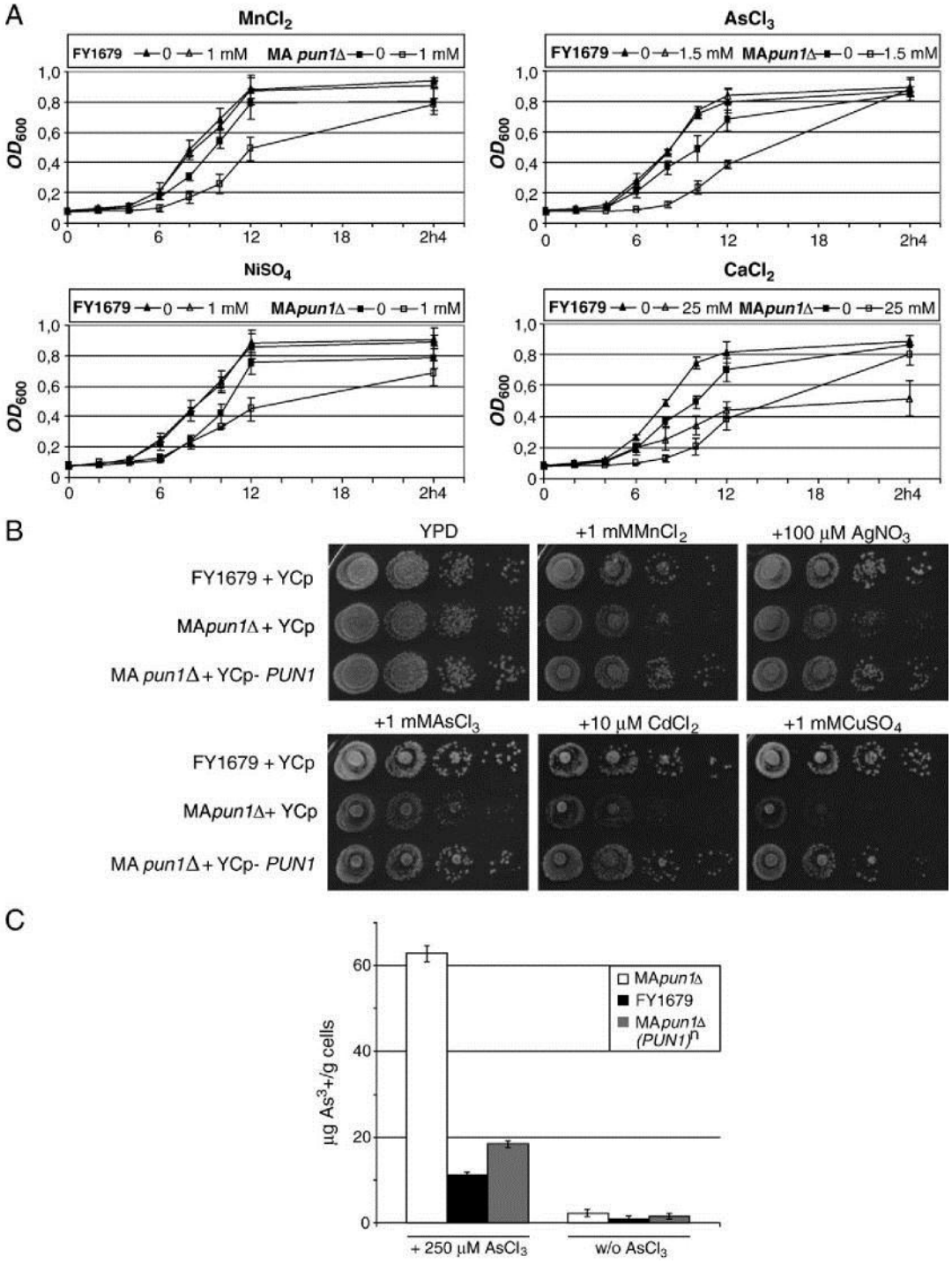

Fig. 2. Complementation and phenotyping of the pun1 deletion. A. Strains FY1679 wild-type and MApun1A were grown in YPD and YPD supplemented with 1 mM MnCl2, 1.5 mM AsCl3, 1 mM NiSO4, and 25 mM CaCl2 at 28 °C for 24 h under shaking. Growth was followed by measuring $_{OD600}$. Growth curves shown represent an average of three individual measurements. MApun1A cells exhibited increased metal ion sensitivity compared to their isogenic wild-type. B. Complementation of the pun1A growth phenotype. Serial 10-fold dilutions of strains FY1679, carrying the empty plasmid YCplac22 and MApun1A carrying the empty plasmid or expressing PUN1 under the control of its endogenous promoter (YCpPUN1), were spotted on YPD plates with and without metal ions (concentrations as indicated in the figure), and incubated at 28 °C for 48 h. Plasmid-based expression of PUN1 restored metal ion sensitivity of pun1A mutant cells. C. Measurement of intracellular AsCl3 concentration. Strains FY1679 and MApun1Δ carrying the empty plasmid YEpM351HA and MApun1A overexpressing C-terminally HA-tagged PUN1 from plasmid YEpM-PUN1-HA (MApun1A(PUN1)^n) were grown in SD medium containing 250 µM AsCl3 and SD medium (w/o AsCl3) for 6 h at 28 °C. Cells were washed, $_{OD600}$ and dry weight were defined and the total intracellular As^{3+} concentration of whole cells (µg As^{3+}/g cells) was determined by ICP-MS (ARC Seibersdorf research GmbH, Austria). Values shown represent an average of three individual measurements. Absence of PUN1 caused a highly increased intracellular As^{3+} concentration.

other factors provided evidence for a direct influence on PUN1 gene transcription when the cells were stressed with MnCl2. Similar expression data were obtained with HgCl2 and AgNO3 treated cells (data not shown).

3.6. Deletion of PUN1 affects yeast cell wall composition

Reduced growth of pun1A cells even in rich medium and the microscopic observation that mutant cells tended to be smaller and

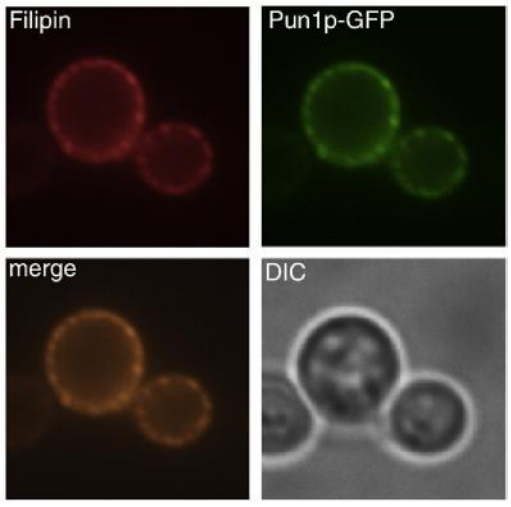

Fig. 3. Subcellular localization of Pun1p. Plasma membrane ergosterol patches colocalize with Pun1p-GFP. Logarithmically grown FY1679 cells expressing C-terminally GFPtagged Pun1p from plasmid pUG35-PUN1-GFP were treated with Filipin, which stains plasma membrane ergosterol (false colored red). The merged images demonstrate the high degree of overlap of the ergosterol patches and Pun1p-GFP. DIC, differential interference contrast.

more rounded shaped than wild-type cells pointed to a modified cell wall structure. The severe sensitivity exhibited by the MApun1A strain to metal ion treatment could be directly connected to ion transport or might be caused from changes of the cell wall composition. In addition, PUN1 was shown to be induced upon cell wall damage [33] and has promoter elements involved in regulation of cell wall integrity [27]. Therefore, we examined the cell wall morphology of the MApun1A strain in more detail. Principal cell wall constituents were stained by treatment with different dyes (Fig. 5A). Examination of cells stained with Aniline Blue and concanavalin A–FITC, fluorescent dyes binding to cell wall 1,3-β-D-glucan and mannoproteins, respectively, revealed that pun1A cells exhibited significantly weaker fluorescence compared to wild-type cells, indicating a reduced amount of these cell wall components (Fig. 5A, upper and middle panel). Analysis of cells treated with Calcofluor White, a fluorochromic dye that binds to chitin, showed normal chitin localization in the neck region of budding cells, although fluorescence again was less intense in pun1A cells (Fig. 5A, lower panel), probably due to a generally reduced cell wall layer.

Furthermore, we monitored the sensitivity to zymolyase, an enzyme which specifically hydrolyzes 1,3-β-D-glucosidic linkages in yeast cell wall 1,3-β-D-glucans. Cells were identically grown, washed in Tris-buffer and incubated with 0, 30 and 100 μg/ml zymolyase T-20. Measurement of the optical density clearly showed rapid lysis of cells deleted for PUN1, whereas wild-type cells underwent only a slight reduction in their optical density (Fig. 5B, upper panel), indicating an abnormal cell wall 1,3-β-D-glucan content of pun1A cells. Over-expression of Pun1p resulted in lysis rates comparable to wild-type (data not shown). To confirm rapid lysis of pun1A cells, we also determined the amount of released cytoplasmic hexokinase 1 (Hxk1p) after zymolyase treatment. Equal cell amounts of both strains were treated for 30 min with identical zymolyase concentrations as used for optical density measurements. After a clarifying spin, the supernatants were subjected to SDS-PAGE and immunodetected with an antibody directed against Hxk1p. Indeed, pun1A cells released much more Hxk1p (Fig. 5B, middle panel), whereas both strains exhibited comparable intracellular Hxk1p levels, as shown by immunodetection of TCA precipitates of whole cells (Fig. 5B, lower panel).

Additionally, high resolution electron microscopic analysis of the cell wall ultrastructure of wild-type and pun1A cells indicated a modified cell wall composition of the mutant strain. MApun1A cells exhibited a dramatically reduced β-glucan layer (Fig. 5C, panel c and d). Furthermore, also the outer mannoprotein layer showed an aberrant composition and appeared to be less compact than in the wild-type. These changes likely caused the increased sensitivity to zymolyase (Fig. 5B). Importantly, complementation of pun1A with plasmid YCp-PUN1 completely restored the cell wall defect (Fig. 5C, panel e and f). Taken together, these findings clearly indicate an involvement of Pun1p in correct cell wall composition.

3.7. Pun1p builds high molecular weight complexes

Pun1p and claudins of higher eukaryotes share structural similarities, especially four predicted transmembrane domains and the conserved cysteine motif G-L-W-x-x-C-x(8-10)-C within the first extracellular loop. Although their molecular architecture is currently unknown, mammalian claudins were shown to form homo-oligomers [34].

To test the oligomerization capacity of Pun1p, sucrose membrane fractions of HA-tagged Pun1p were prepared and analyzed by chemical cross-linking, SDS-PAGE, and immunoblotting against the HA epitope of Pun1p. The addition of increasing concentrations of the cysteine-specific cross-linking reagent o-phenylenedimaleimide (o-PDM) produced complexes corresponding to putative dimers, tetramers, and hexamers of the protein (Fig. 6A, black arrows). Furthermore, small amounts of dimers and tetramers were also observed in the absence of o-PDM (first lane), implying a robust protein interaction. Interestingly, signals appeared as double bands, suggesting possible protein modifications.

Additionally, identical membrane fractions were analyzed by Blue native electrophoresis for the formation of high molecular weight complexes. Pun1p-HA was solubilized with different concentrations of the detergents digitonin (D), Triton X-100 (TX), and n-Dodecyl-β-D-maltoside (DM) and detected by immunoblotting against HA. As shown in Fig. 6B, higher-order oligomers appeared, corresponding to di-, tetra-, hexa-, octa-, deca-, and dodecamers of the 35 kDa protein (indicated by arrowheads). Interestingly, we also detected a possible Pun1p-HA containing super-complex of unknown composition (solid asterisk). To our knowledge, these results demonstrate for the first time oligomeric complexes of a MCC protein.

To test for self-interaction of Pun1p, we performed Co-Immunoprecipitation (Co-IP) experiments. Sucrose membrane fractions of strain BY4741 expressing chromosomally GFP-tagged Pun1p, either coexpressing HA-tagged Pun1p from plasmid YCp-PUN1-HA or bearing the empty plasmid YCplac33, were solubilized and incubated with anti-HA serum-coated or anti-GFP serum-coated beads. Upon coexpression of GFP- and HA-tagged Pun1p, both proteins were detected in the anti-HA and anti-GFP immunoprecipitate (Fig. 6C, elution fractions, blot area 1 and 3). In the control experiments using

Fig. 4. Induction of PUN1 upon metal stress. A. Yeast strain BY4741, bearing a chromosomal PUN1-GFP fusion, was stressed with various metal ions as indicated in liquid YDP for 1 h (a–e) and 2 h (f–j) at 28 °C. Pun1p-GFP was highly induced upon exposure to 200 mM CaCl2 and 2 mM MnCl2. GFP-fluorescence and corresponding DIC images were obtained from living cells without fixation. B. The identical strain as shown in Fig. 4A was grown in YPD or treated with various metal ions as indicated for 2 h at 28 °C. Cells were collected and washed and total protein of whole cells was precipitated with TCA. Proteins were separated by SDS-PAGE and immunoblotted against GFP and Hexokinase-1 (Hxk1), used as a loading control. Western blot results clearly confirmed metal ion-induced expression of Pun1p-GFP. C. Influence of upstream regulatory elements on metal ion-induced transcription. Wild-type cells and mutants deleted for HOG1, CRZ1, RLM1, STE12, SKO1, DIG1, and MSN2/4 were analyzed by Northern blot for MnCl2 induced expression of PUN1. Red boxes highlight absent induction of PUN1 in strain BYcrz1A compared to the wild-type.

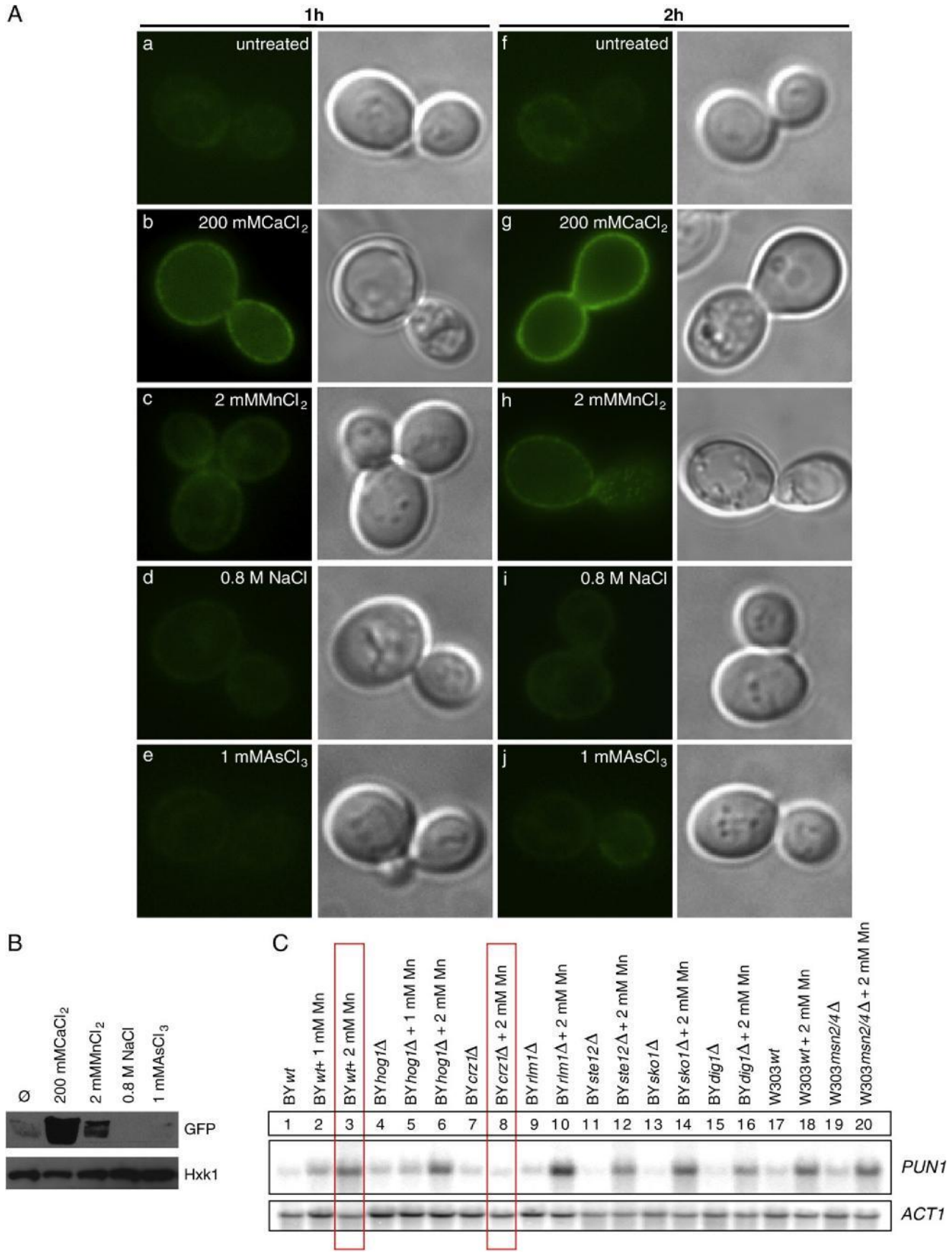
A
1h
2h
a untreated
b 200 mMCaCl2
c 2 mMMnCl2
d 0.8 M NaCl
e 1 mMAsCl3
f untreated
g 200 mMCaCl2
h 2 mMMnCl2
i 0.8 M NaCl
j 1 mMAsCl3
B
Ø
200 mMCaCl2
2 mMMnCl2
0.8 M NaCl
1 mMAsCl3
GFP
Hxk1
C
BY wt
BY wt+ 1 mM Mn
BY wt+ 2 mM Mn
BY hog1Δ
BY hog1Δ + 1 mM Mn
BY hog1Δ + 2 mM Mn
BY crz1Δ
BY crz1Δ + 2 mM Mn
BY rlm1Δ
BY rlm1Δ + 2 mM Mn
BY ste12Δ
BY ste12Δ + 2 mM Mn
BY sko1Δ
BY sko1Δ + 2 mM Mn
BY dig1Δ
BY dig1Δ + 2 mM Mn
W303 wt
W303 wt + 2 mM Mn
W303 msn2/4Δ
W303 msn2/4Δ + 2 mM Mn
1 2 3 4 5 6 7 8 9 10 11 12 13 14 15 16 17 18 19 20
PUN1
ACT1

membranes from cells expressing only GFP-tagged Pun1p, the protein was found exclusively unbound after incubation with HA-coated beads (Fig. 6C, supernatant fraction, blot area 2) as well as bound to GFPcoated beads (Fig. 6C, elution fraction, blot area 4). These results confirm self-interaction of Pun1p and suggest the protein complexes detected after cross-linking and Blue native electrophoresis to represent homo-oligomers of Pun1p.

4. Discussion

In this study we show that Pun1p is a calcineurin/Crz1p-regulated, metal ion stress-induced protein involved in correct cell wall organization, and a component of high molecular weight protein complexes. Pun1p has a tetraspan topology and contains the highly conserved claudin family signature G-L-W-x-x-C-x(8-10)-C within the first extracellular loop (www.uniprot.org/uniprot/Q06991). Furthermore, Pun1p belongs to a group of nine integral membrane proteins known to be localized to the ergosterol-rich MCC, a plasma membrane compartment found to be involved in endocytic regulation of transport proteins [4].

4.1. Deletion of PUN1 causes metal ion sensitivity

We found a strong induction of PUN1 transcription upon heavy metal treatment, whereas the pun1A strain exhibited a basic growth reduction and a pronounced sensitivity to several metal ions, not only to those causing transcriptional induction of PUN1. This led us to the suggestion that the growth defect in response to metal stress was caused by a general rather than a specific defect in ion homeostasis and that Pun1p may be directly involved in metal detoxification. To support this idea, we determined the total intracellular As^{3+} concentration of mutant cells compared to the wild-type and cells overexpressing PUN1 after AsCl3 treatment. Although the cellular concentration of As^{3+} was 5.7 times increased in pun1A cells compared to the wild-type, the multicopy expression of PUN1 did not confer As^{3+}-resistance but only restored the As^{3+} content of the mutant to a level slightly increased compared to wild-type cells. Therefore, Pun1p is probably not directly involved in metal ion detoxification and the metal ion sensitivity of pun1Δ cells might rather be a consequence of a primary defect in maintaining intracellular ion homeostasis.

4.2. Crz1p mediates PUN1 expression upon metal ion stress

In a genome wide study, regulation of PUN1 expression was found to be dependent on the calmodulin/calcineurin signaling pathway [29]. To follow induction of PUN1 in vivo, we microscopically investigated chromosomally GFP-tagged Pun1p and found fluorescence to be significantly induced upon Ca^{2+} and Mn^{2+} exposure. This gave us the first hint that Crz1p, the major effector of calmodulin/calcineurin-regulated gene expression in yeast [29], might be involved in the PUN1 regulation.

Computational promoter analyses of genes induced upon cell wall stress revealed enrichment of certain motifs some of which also residing in the upstream region of PUN1 [27,33]. Here we show that Crz1p is crucial for transcriptional activation in response to Mn^{2+}, Ag^{3+}, and Hg^{2+} but not for basal gene expression. The metal ion-induced expression of PUN1 was also slightly decreased in a hog1A strain, but the level of reduction suggests that the HOG-pathway might be not directly linked to PUN1 gene expression, when metal ions are the cause of cellular stress. Additionally, deletion of RLM1 slightly increased PUN1 expression.

Based on these findings, induction of PUN1 upon ion stress can be partly explained. Ca^{2+} activates the calcineurin/Crz1p pathway, thereby directing Crz1p to the CDRE motif in the promoter region of PUN1. This seems to be a plausible step since this pathway was shown

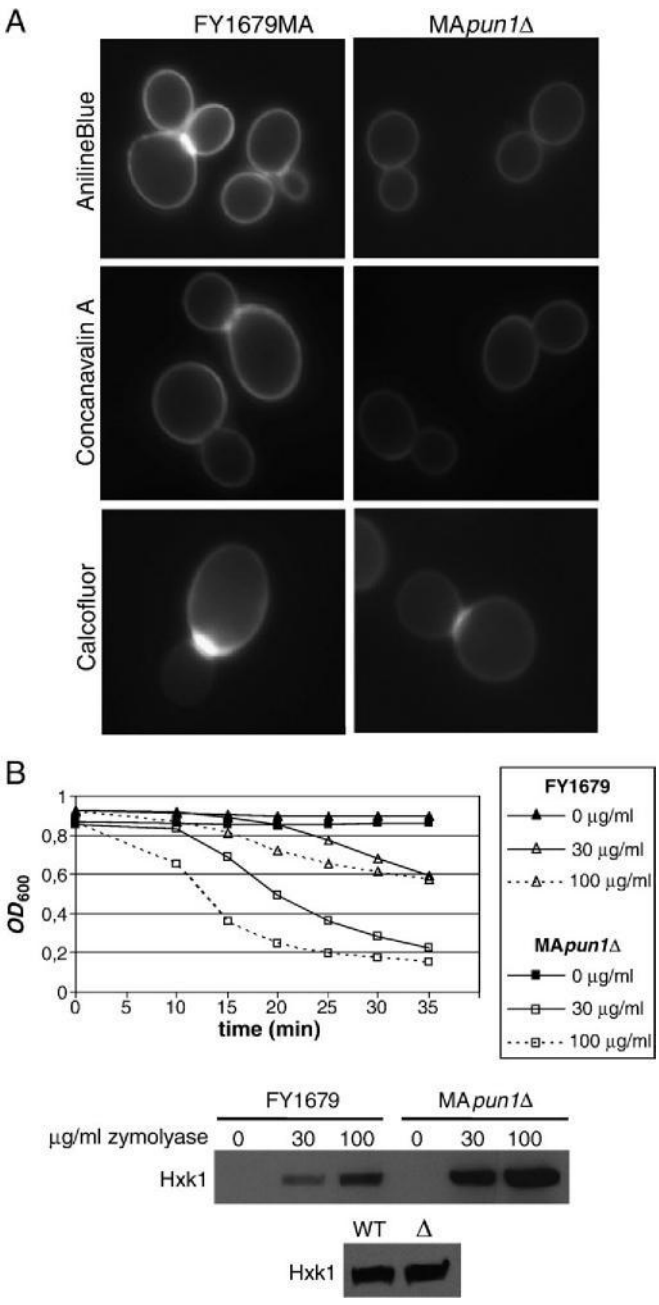

Fig. 5. Modified cell wall composition of pun1Δ mutant cells. A. Staining of cell wall components. FY1679 wild-type and MApun1A cells were treated as indicated with Aniline Blue, concanavalin A–FITC, and Calcofluor White, staining cell wall 1,3-β-D-glucan, mannoproteins, and chitin, respectively. Fluorescence microscopy revealed reduced fluorescence of pun1A cells. B. Treatment with zymolyase. FY1679 wild-type and MApun1A cells were grown logarithmically in YPD medium, diluted to an equal OD600 value and treated with 0, 30, or 100 µg/ml zymolyase 20T. At time points indicated in the figure, OD600 was determined (upper panel). Equal amounts of FY1679 wild-type and MApun1A cells were treated for 30 min with identical zymolyase concentrations as used before. After centrifugation, equal amounts of the supernatant were immunodetected for cytoplasmic hexokinase 1 (Hxk1p), representing Hxk1p release caused by cell lysis (middle panel). Intracellular Hxk1p levels of both strains were compared by immunodetection after TCA precipitation of equal cell amounts (lower panel). C. Electron microscopic images of strains FY1679 wild-type (a-b), MApun1A (c and d), and MApun1A expressing PUN1 from plasmid YCp-PUN1. Principal cell wall constituents (GL and MP) and the plasma membrane (PM) are indicated. Images b, d, and f correspond to white frames in images a, c, and e, respectively. Plasmid-based expression of PUN1 restored the defective cell wall composition of MApun1A cells. PM, plasma membrane; GL, β-glucan layer; MP, mannoprotein layer. Black bars, 100 nm.

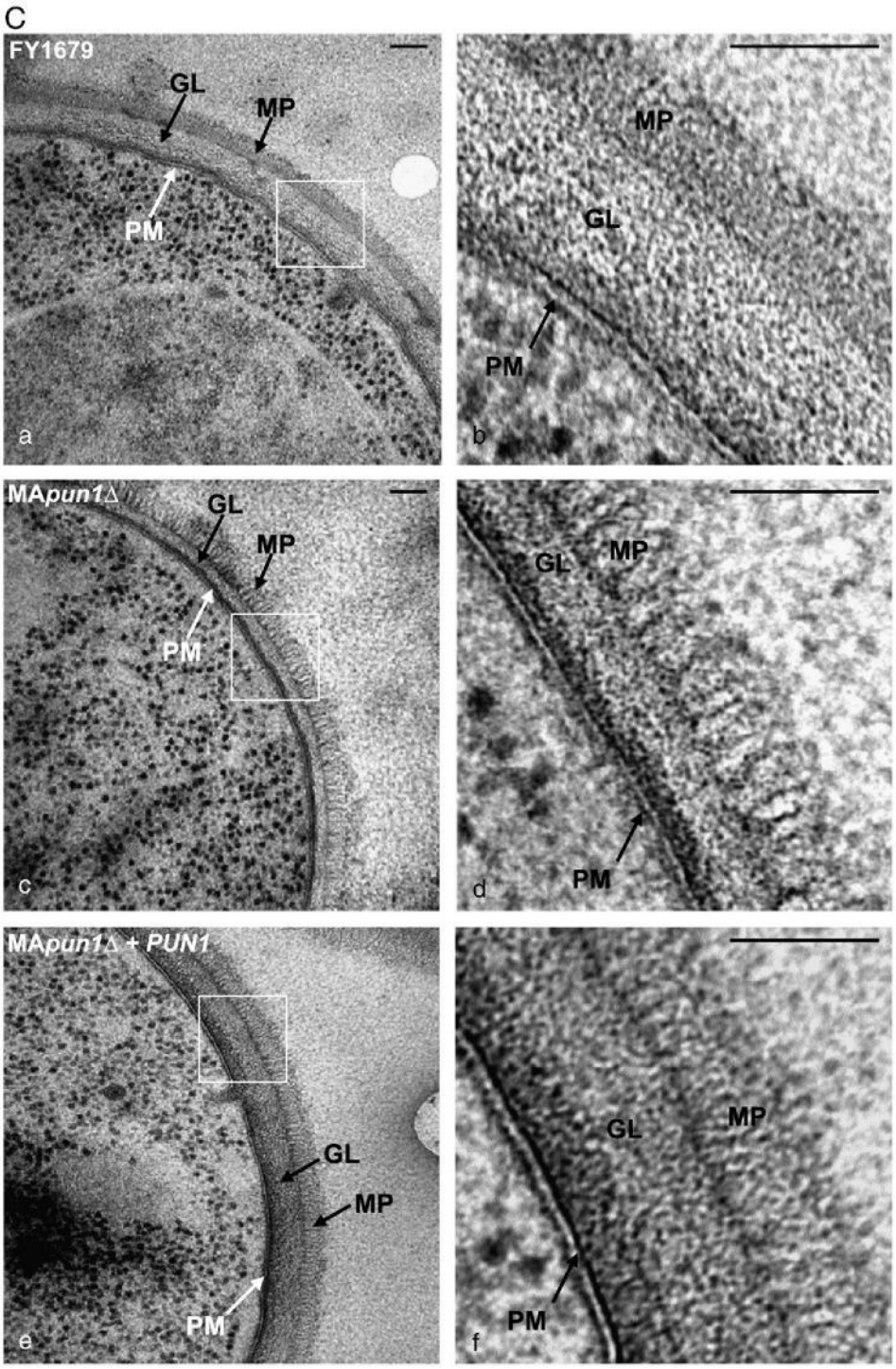

Fig. 5 (continued).

to confer high tolerance to ion stress [35]. Nevertheless, a direct regulatory interaction between Crz1p and PUN1 still has to be proven. Mn^{2+} has been known to be able to replace Ca^{2+} in the activation of calmodulin [36,37], thereby likely inducing the expression of PUN1 by mimicking the function of Ca^{2+}. Induction of PUN1 by other metal ions can be explained by raising the intracellular Ca^{2+} level. This was previously shown for mammalian cells in presence of Cd^{2+} [38] and Hg^{2+} [39], and in yeast under conditions of Mg^{2+} deprivation [40]. Although we do not have evidence of a direct interaction between Crz1p and the PUN1 promoter, we suggest that the calcineurin/Crz1p pathway is the major inducer of PUN1 upon metal ion stress.

4.3. Pun1p is required for a normal cell wall composition

Fluorescence microscopy presented here revealed a subcellular localization of Pun1p in the ergosterol-rich plasma membrane MCC, consistent with previous results showing colocalization of Pun1p with Sur7p, which also localizes to the MCC [15]. Besides reduced growth in

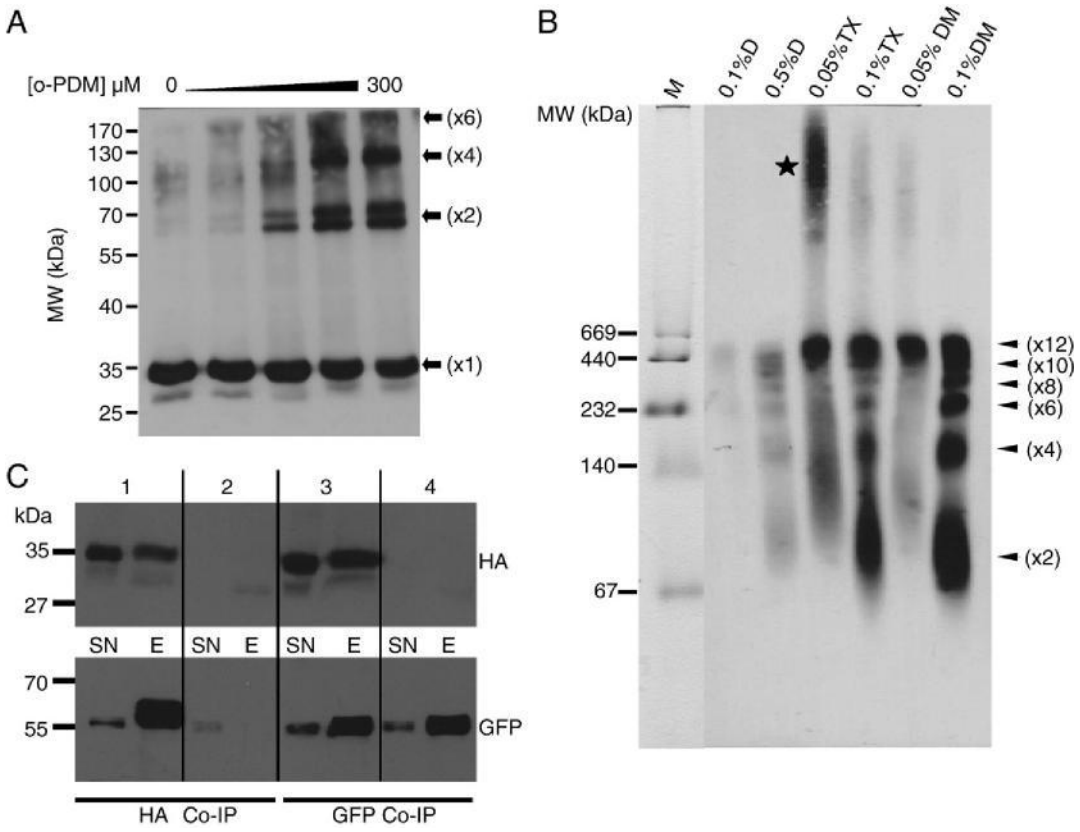

Fig. 6.Oligomerization of Pun1p. A. Chemical cross-linking of Pun1p-HA. Membranes of FY1679 cells expressing plasmid YEpM-PUN1-HA were separated by ultracentrifugation on a discontinuous sucrose gradient (see Materials and methods). Equal amounts of the membrane extract were treated with increasing concentrations (0–300 µM) of the cross-linking reagent o-PDM. Proteins were separated by SDS-PAGE and immunoblotted against the HA epitope. Black arrows point to the Pun1p-HA monomer and higher-order oligomers (dimer to hexamer from bottom to top). o-PDM, o-phenylenedimaleimide. B. Blue native electrophoresis of Pun1p-HA. Equal amounts of the same membrane fraction used for chemical cross-linking were solubilized with the indicated detergents, applied to a native gradient gel and immunoblotted against the HA epitope. Arrowheads indicate putative oligomeric states of Pun1p-HA (dimer to dodecamer from bottom to top). Solid asterisk indicates an undefined protein complex containing Pun1p-HA. D, digitonin; TX, Triton X-100; DM, n-Dodecyl-R-D-maltoside; M, protein ladder. C. Co-immunoprecipitation (Co-IP) of Pun1p. Membrane fractions of strain BY4741 expressing chromosomally GFP-tagged Pun1p, either coexpressing HA-tagged Pun1p from plasmid YCp-PUN1-HA (lanes in blot area 1 and 3) or bearing the empty plasmid YCplac33 (lanes in blot area 2 and 4), were solubilized using 0.1% TX and incubated with anti-HA serum-coated (HA Co-IP) or anti-GFP serum-coated (GFP Co-IP) beads for 1 h at 4 °C. Unbound (supernatant, SN) and bound (elution, E) fractions were separated by SDS-PAGE and analyzed by immunoblotting with antibodies directed against HA (upper panel) or GFP (lower panel).

metal ion containing media, deletion of PUN1 also caused a morphological phenotype. Mutant cells appeared smaller than wild-type cells and were more rounded shaped. This was the first evidence that pun1A cells may suffer from cell wall damage. To further investigate this aspect, principal cell wall components, namely 1,3-R-D-glucan, mannoproteins, and chitin, were stained with specific dyes and analyzed by fluorescence microscopy. Indeed, MApun1A cells displayed weaker fluorescence compared to the wild-type, suggesting a reduced amount of these cell wall components. Furthermore, zymolyase treatment caused much faster lysis of pun1A cells compared to the wild-type, thereby confirming microscopical observations.

Finally, an aberrant cell wall structure was also observed by ultrastructural comparison of wild-type and pun1A cells. Electron microscopy revealed a drastically reduced R-glucan layer within pun1A cell walls and an outer mannoprotein layer of a less compact composition compared to the wild-type, together explaining the zymolyase sensitivity of mutant cells. This cell wall insufficiency is probably also the primary cause of the increased metal ion sensitivity of strain MApun1A, although changed plasma membrane permeability cannot be excluded.

By comparison of these results with previous findings, evidence for involvement of Pun1p in cell wall assembly is growing. PUN1 was shown to be induced in five individual cell wall mutants (gas1A, mnn9A, fks1A, knr4A, and kre6A) together with 78 other genes, combined in a so called “cell wall compensatory-dependent gene cluster” [33], and we found induced expression of PUN1 in absence of the cell wall integrity transcription factor RLM1, which regulates Hog1p-dependent PUN1 expression in response to cell wall damage [27,28]. Furthermore, the calmodulin/calcineurin pathway was shown to be responsible to induce genes involved in cell wall integrity [41]. Interestingly, a recent study identified PUN1 to be induced upon nitrogen starvation by the filamentous growth factor Mss11p and to be involved in pseudohyphal growth [11]. Facing the fact that filamentous growth is regulated by the cell wall integrity pathway and the cell wall itself [42], this suggests that absent filamentous growth in pun1A cells is primarily caused by a cell wall defect.

4.4. Pun1p forms higher-order oligomeric protein complexes

Since claudins of higher eukaryotes were found to oligomerize [34] and share structural similarities with Pun1p, the possibility of oligomerization of Pun1p was investigated. By using Blue native electrophoresis, chemical cross-linking with the cysteine-specific crosslinker o-PDM, and Co-IP experiments, we could demonstrate the presence of different oligomeric Pun1p complexes and confirmed self-interaction of Pun1p. Since the claudin domain within the first extracellular loop contains two cysteine residues and was shown to be

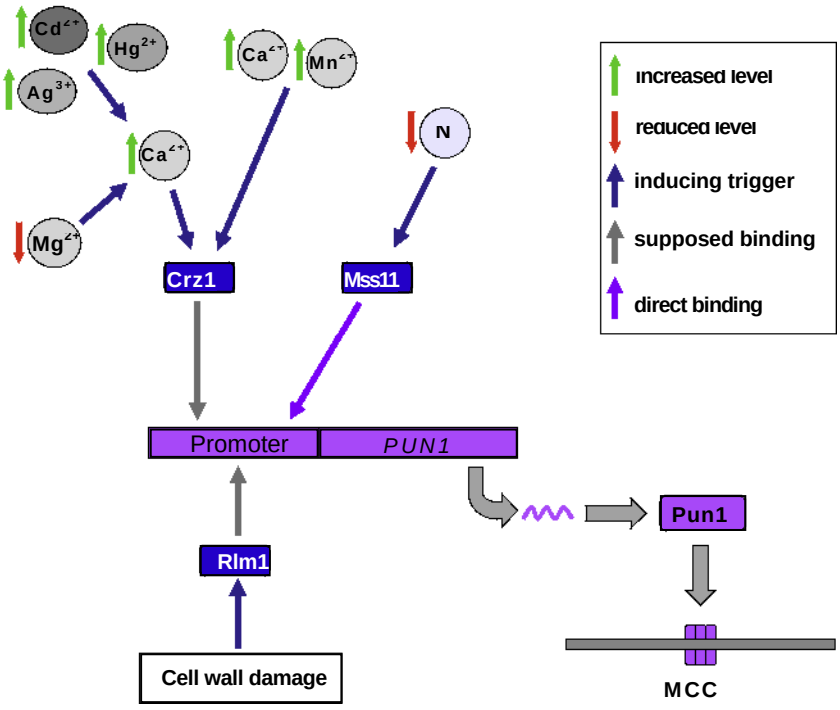

Fig. 7. Comprehensive model of transcriptional induction of PUN1 upon different stress conditions.

involved in cell–cell contact formation in higher eukaryotes [431, we hypothesize that this conserved domain is involved in protein oligomerization by forming disulfide bonds. Interestingly, Pun1p appeared as a double band pattern, suggesting possible protein modifications. Sequence analysis using the ScanProsite program (http://ca.expasy.org/prosite/) indeed identified potential sites of protein modification, among them possible myristoylation, glycosylation, and phosphorylation sites of protein kinase C, the first component of the cell wall integrity signaling pathway discovered [61.

5. Conclusions

Data presented here support a model of Pun1p as being a stress-responsive protein involved in cell wall integrity, regulated by different signaling pathways dependent on the cause of cellular stress (Fig. 7). This idea is supported by a number of predicted regulatory motifs present within its promoter region [271. Interestingly, also other proteins involved in cell wall formation were shown to be coordinately regulated, like the 1,3-β-D-glucan synthase subunit Fks2p, which is regulated by the cell wall integrity and calcineurin/Crz1p pathway [331.

Besides Sur7p [151, Pun1p is the second tetraspan protein localized in the MCC responsible for correct cell wall organization. So far, it is not clear how Pun1p contributes to cell wall integrity, especially under conditions of environmental stress. By oligomerization Pun1p may function as a scaffold for cell wall assembly or for recruitment of cell wall building proteins. Interestingly, in a recent genome wide study the 1,3-β-D-glucan synthase subunit Fks1p was found in a complex with Pil1p [441, a component of eisosomes [31, being sub-cortical protein assemblies which show overlapping localization with MCCs. Alternatively, absence of Pun1p may interfere with stress signaling and thereby cause disturbed cell wall integrity and adaptation to stress conditions.

Finally, mammalian claudins regulate paracellular ion transport between epithelial cells by the formation of charge-selective channels, and the charged residues in their first extracellular loop are believed to represent a selectivity filter [451. Interestingly, Pun1p also contains a series of charged residues in its first loop. However, yeast is a single cellular organism without paracellular transport and currently we do not have evidence that Pun1p is involved in any form of ion transport. Nonetheless, results presented in this study relate the plasma membrane MCC with cell wall integrity and metal ion stress.

Acknowledgements

We wish to dedicate this work to Rudolf J. Schweyen, who passed away in 2009, and recognize his contribution in form of experimental advice and fruitful discussions. We also thank Kristina Djinovic-Carugo for critically reading the manuscript and general support, Mirjana Iliev for excellent technical assistance, and Karl Kuchler for sharing the antiserum against Pdr5p. This work was supported by the Austrian Science Fund (P19966-B12 to C.S. and P18004 to R.J.S.).

References

[11 V. Stradalova, W. Stahlschmidt, G. Grossmann, M. Blazikova, R. Rachel, W. Tanner, J. Malinsky, Furrow-like invaginations of the yeast plasma membrane correspond to membrane compartment of Can1, J. Cell Sci. 122 (2009) 2887–2894.
[21 K. Simons, D. Toomre, Lipid rafts and signal transduction, Nat. reviews 1 (2000) 31–39.
[31 T.C. Walther, J.H. Brickner, P.S. Aguilar, S. Bernales, C. Pantoja, P. Walter, Eisosomes mark static sites of endocytosis, Nature 439 (2006) 998–1003.
[41 G. Grossmann, J. Malinsky, W. Stahlschmidt, M. Loibl, I. Weig-Meckl, W.B. Frommer, M. Opekarova, W. Tanner, Plasma membrane microdomains regulate turnover of transport proteins in yeast, J. Cell Biol. 183 (2008) 1075–1088.
[51 S. Hohmann, Osmotic stress signaling and osmoadaptation in yeasts, Microbiol. Mol. Biol. Rev. 66 (2002) 300–372.
[61 D.E. Levin, Cell wall integrity signaling in Saccharomyces cerevisiae, Microbiol. Mol. Biol. Rev. 69 (2005) 262–291.
[71 A. Van Ho, D.M. Ward, J. Kaplan, Transition metal transport in yeast, Annu. Rev. Microbiol. 56 (2002) 237–261.
[81 D. Radisky, J. Kaplan, Regulation of transition metal transport across the yeast plasma membrane, J. Biol. Chem. 274 (1999) 4481–4484.
[91 D.J. Eide, The molecular biology of metal ion transport in Saccharomyces cerevisiae, Annu. Rev. Nutr. 18 (1998) 441–469.
[101 N. Nelson, Metal ion transporters and homeostasis, EMBO J. 18 (1999) 4361–4371.

[111 T. Xu, C.A. Shively, R. Jin, M.J. Eckwahl, C.J. Dobry, Q. Song, A. Kumar, A profile of differentially abundant proteins at the yeast cell periphery during pseudohyphal growth, The Journal of biological chemistry 285 15476–15488.

[121 K. Morita, M. Furuse, K. Fujimoto, S. Tsukita, Claudin multigene family encoding four-transmembrane domain protein components of tight junction strands, Proc. Natl Acad. Sci. USA 96 (1999) 511–516.

[131 F.J. Alvarez, L.M. Douglas, J.B. Konopka, Sterol-rich plasma membrane domains in fungi, Eukaryot. Cell 6 (2007) 755–763.

[141 P. Sivadon, M.F. Peypouquet, F. Doignon, M. Aigle, M. Crouzet, Cloning of the multicopy suppressor gene SUR7: evidence for a functional relationship between the yeast actin-binding protein Rvs167 and a putative membranous protein, Yeast (Chichester, England) 13 (1997) 747–761.

[151 F.J. Alvarez, L.M. Douglas, A. Rosebrock, J.B. Konopka, The Sur7 protein regulates plasma membrane organization and prevents intracellular cell wall growth in Candida albicans, Mol. Biol. Cell 19 (2008) 5214–5225.

[161 W. Gorner, E. Durchschlag, M.T. Martinez-Pastor, F. Estruch, G. Ammerer, B. Hamilton, H. Ruis, C. Schuller, Nuclear localization of the C2H2 zinc finger protein Msn2p is regulated by stress and protein kinase A activity, Genes Dev. 12 (1998) 586–597.

[171 W.K. Huh, J.V. Falvo, L.C. Gerke, A.S. Carroll, R.W. Howson, J.S. Weissman, E.K. O'Shea, Global analysis of protein localization in budding yeast, Nature 425 (2003) 686–691.

[181 A. Wach, A. Brachat, R. Pohlmann, P. Philippsen, New heterologous modules for classical or PCR-based gene disruptions in Saccharomyces cerevisiae, Yeast 10 (1994) 1793–1808.

[191 R.D. Gietz, A. Sugino, New yeast-Escherichia coli shuttle vectors constructed with in vitro mutagenized yeast genes lacking six-base pair restriction sites, Gene 74 (1988) 527–534.

[201 M. Wachek, M.C. Aichinger, J.A. Stadler, R.J. Schweyen, A. Graschopf, Oligomerization of the Mg^{2+}-transport proteins Alr1p and Alr2p in yeast plasma membrane, FEBS J. 273 (2006) 4236–4249.

[211 A. Graschopf, J.A. Stadler, M.K. Hoellerer, S. Eder, M. Sieghardt, S.D. Kohlwein, R.J. Schweyen, The yeast plasma membrane protein Alr1 controls Mg^{2+} homeostasis and is subject to Mg^{2+}-dependent control of its synthesis and degradation, J. Biol. Chem. 276 (2001) 16216–16222.

[221 R.K. Niedenthal, L. Riles, M. Johnston, J.H. Hegemann, Green fluorescent protein as a marker for gene expression and subcellular localization in budding yeast, Yeast 12 (1996) 773–786.

[231 S. Reipert, I. Fischer, G. Wiche, High-pressure freezing of epithelial cells on sapphire coverslips, J. Microsc. 213 (2004) 81–85.

[241 S. Reipert, G. Wiche, High-pressure freezing and low-temperature fixation of cell monolayers grown on sapphire coverslips, Meth. Cell Biol. 88 (2008) 165–180.

[251 M.A. Collart, S. Oliviero, Preparation of yeast RNA, Current protocols in molecular biology / edited by Frederick M. Ausubel ... [et al Chapter 13 (2001) Unit13 12.

[261 H. Schagger, W.A. Cramer, G. von Jagow, Analysis of molecular masses and oligomeric states of protein complexes by blue native electrophoresis and isolation of membrane protein complexes by two-dimensional native electrophoresis, Anal. Biochem. 217 (1994) 220–230.

[271 J.M. Rodriguez-Pena, R.M. Perez-Diaz, S. Alvarez, C. Bermejo, R. Garcia, C. Santiago, C. Nombela, J. Arroyo, The 'yeast cell wall chip'—a tool to analyze the regulation of cell wall biogenesis in Saccharomyces cerevisiae, Microbiology 151 (2005) 2241–2249.

[281 R. Garcia, J.M. Rodriguez-Pena, C. Bermejo, C. Nombela, J. Arroyo, The high osmotic response and cell wall integrity pathways cooperate to regulate transcriptional responses to zymolyase-induced cell wall stress in Saccharomyces cerevisiae, J. Biol. Chem. 284 (2009) 10901–10911.

[291 H. Yoshimoto, K. Saltsman, A.P. Gasch, H.X. Li, N. Ogawa, D. Botstein, P.O. Brown, M.S. Cyert, Genome-wide analysis of gene expression regulated by the calcineurin/Crz1p signaling pathway in Saccharomyces cerevisiae, J. Biol. Chem. 277 (2002) 31079–31088.

[301 J.L. Brewster, T. de Valoir, N.D. Dwyer, E. Winter, M.C. Gustin, An osmosensing signal transduction pathway in yeast, Science 259 (1993) 1760–1763.

[311 M.T. Martinez-Pastor, G. Marchler, C. Schuller, A. Marchler-Bauer, H. Ruis, F. Estruch, The Saccharomyces cerevisiae zinc finger proteins Msn2p and Msn4p are required for transcriptional induction through the stress response element (STRE), EMBO J. 15 (1996) 2227–2235.

[321 S. Chou, S. Lane, H. Liu, Regulation of mating and filamentation genes by two distinct Ste12 complexes in Saccharomyces cerevisiae, Mol. Cell. Biol. 26 (2006) 4794–4805.

[331 A. Lagorce, N.C. Hauser, D. Labourdette, C. Rodriguez, H. Martin-Yken, J. Arroyo, J.D. Hoheisel, J. Francois, Genome-wide analysis of the response to cell wall mutations in the yeast Saccharomyces cerevisiae, J. Biol. Chem. 278 (2003) 20345–20357.

[341 L.L. Mitic, V.M. Unger, J.M. Anderson, Expression, solubilization, and biochemical characterization of the tight junction transmembrane protein claudin-4, Protein Sci. 12 (2003) 218–227.

[351 I. Mendoza, F.J. Quintero, R.A. Bressan, P.M. Hasegawa, J.M. Pardo, Activated calcineurin confers high tolerance to ion stress and alters the budding pattern and cell morphology of yeast cells, J. Biol. Chem. 271 (1996) 23061–23067.

[361 D.J. Wolff, P.G. Poirier, C.O. Brostrom, M.A. Brostrom, Divalent cation binding properties of bovine brain Ca^{2+}-dependent regulator protein, J. Biol. Chem. 252 (1977) 4108–4117.

[371 A. Mork, A. Geisler, Calmodulin-dependent adenylate cyclase activity in rat cerebral cortex: effects of divalent cations, forskolin and isoprenaline, Arch. Int. Physiol. Biochim. 97 (1989) 259–271.

[381 D. Beyersmann, S. Hechtenberg, Cadmium, gene regulation, and cellular signaling in mammalian cells, Toxicol. Appl. Pharmacol. 144 (1997) 247–261.

[391 X.X. Tan, C. Tang, A.F. Castoldi, L. Manzo, L.G. Costa, Effects of inorganic and organic mercury on intracellular calcium levels in rat T lymphocytes, J. Toxicol. Environ. Health 38 (1993) 159–170.

[401 G. Wiesenberger, K. Steinleitner, R. Malli, W.F. Graier, J. Vormann, R.J. Schweyen, J.A. Stadler, Mg^{2+} deprivation elicits rapid Ca^{2+} uptake and activates Ca^{2+}/calcineurin signaling in Saccharomyces cerevisiae, Eukaryot. Cell 6 (2007) 592–599.

[411 P. Garrett-Engele, B. Moilanen, M.S. Cyert, Calcineurin, the Ca^{2+}/calmodulin-dependent protein phosphatase, is essential in yeast mutants with cell integrity defects and in mutants that lack a functional vacuolar H(+)-ATPase, Mol. Cell. Biol. 15 (1995) 4103–4114.

[421 B. Birkaya, A. Maddi, J. Joshi, S.J. Free, P.J. Cullen, Role of the cell wall integrity and filamentous growth mitogen-activated protein kinase pathways in cell wall remodeling during filamentous growth, Eukaryot. Cell 8 (2009) 1118–1133.

[431 L. Cukierman, L. Meertens, C. Bertaux, F. Kajumo, T. Dragic, Residues in a highly conserved claudin-1 motif are required for hepatitis C virus entry and mediate the formation of cell–cell contacts, J. Virol. 83 (2009) 5477–5484.

[441 A.C. Gavin, M. Bosche, R. Krause, P. Grandi, M. Marzioch, A. Bauer, J. Schultz, J.M. Rick, A.M. Michon, C.M. Cruciat, M. Remor, C. Hofert, M. Schelder, M. Brajenovic, H. Ruffner, A. Merino, K. Klein, M. Hudak, D. Dickson, T. Rudi, V. Gnau, A. Bauch, S. Bastuck, B. Huhse, C. Leutwein, M.A. Heurtier, R.R. Copley, A. Edelmann, E. Querfurth, V. Rybin, G. Drewes, M. Raida, T. Bouwmeester, P. Bork, B. Seraphin, B. Kuster, G. Neubauer, G. Superti-Furga, Functional organization of the yeast proteome by systematic analysis of protein complexes, Nature 415 (2002) 141–147.

[451 O.R. Colegio, C.M. Van Itallie, H.J. McCrea, C. Rahner, J.M. Anderson, Claudins create charge-selective channels in the paracellular pathway between epithelial cells, Am. J. Physiol. Cell Physiol. 283 (2002) C142–C147.

3. DISCUSSION

One primary mechanism how microorganisms cope with environmental stress is transcriptional regulation of regulons involved in the cellular defense response. DNA microarray analysis constitutes a powerful method to simultaneously evaluate quantitative measurements for the expression of thousands of genes (Schena *et al.* 1995; Lashkari *et al.* 1997; Cheung *et al.* 1999; Figure 5). Over the last decades a number of studies have described the toxic effects of metals and the cellular defense mechanisms against metal toxicity (Wysocki and Tamas, 2010). But still several questions remain open especially concerning the cellular targets of metal toxicity, distinct metal detoxification mechanisms, and the respective regulatory associations. To gain new scientific insights regarding these questions, the study presented here investigated genome-wide transcriptional profiles which were generated in response to metal stress in the yeast *Saccharomyces cerevisiae*. In total ten metals were selected for analysis based on their health threatening effects on humans.

3.1 Metal stress response in *Saccharomyces cerevisiae* - major findings

The primary analysis of this thesis investigated the early gene expression changes of *S. cerevisiae* cells in response to ten biologically relevant metals with cadmium as the most toxic one, followed by mercury, silver, arsenic, cobalt, aluminium, vanadium, nickel, manganese, and zinc. In the corresponding manuscript entitled "Transcript profiling analysis of acute metal stress response of *Saccharomyces cerevisiae*" we mainly focused on a comparative global view of the metal stress responses and the respective regulatory associations. Three continuative yeast studies were derived from interesting findings of the aforementioned manuscript and examined specific effects of arsenic, mercury, and manganese in more detail. The following summarizes the major findings of these four manuscripts:

3.1.1 Comparative gene expression analysis upon acute metal stress

- Metal exposure generally causes oxidative stress in *S. cerevisiae* cells. Accordingly, we showed that the transcriptional response upon acute metal stress is activation of metal-specific oxidative defense pathways and protein degradation mechanisms and

enlarged the scope of involved metals compared to previous studies. We also proved that there is no common detoxification pathway against metals in yeast.

- We indicated induction of chaperone complex activities upon $Cd^{2+}$and As^{3+} and chelation of Co^{2+}, Mn^{2+}, Ni^{2+}, and Zn^{2+} via iron siderophores and chelation of Hg^{2+} and Mn^{2+} via histidine (His) and arginine (Arg) and/or His/Arg-rich proteins as additional metal detoxification mechanisms.
- Moreover, we devised a schematic model of transcriptional adaptation of yeast cells to sustained metal treatment.
- Finally, we detected distinct metal clusters (e.g. Ag^{+}, As^{3+}, Cd^{2+}, and Hg^{2+}) evoking similar metal defense strategies with shared regulatory associations.

3.1.2 Analysis of regulators involved in the arsenic stress response

- We showed that in response to arsenic the TF Sfp1 dissociates from RP gene promoters, accumulates in the cytoplasm, and thereby leads to repression of RP gene expression.
- We detected that arsenic, similar to rapamycin, causes repression of TORC1 kinase activity resulting in dephosphorylation of its direct downstream target Sch9 and most likely also of Sfp1.
- Additionally, we proved that also mercury and nickel lead to repression of Sfp1-regulated RP genes and Sch9 dephosphorylation indicating a more general role of Sfp1 and Sch9 in response to metal stress.
- At last, we illustrated that arsenic exposure induces the subsequent transition of the generally PKA-regulated TFs Msn2 and Msn4 from cytoplasm into the nucleus and activation of target genes apart from PKA activity.

3.1.3 Transcriptional consequences of *STB5* deletion during mercury stress

- We provided evidence for sensitivity of an *STB5* deletion strain to metal stress.
- We generated transcription patterns of short- (15min, 30min, and 2h) and long- (24h) term mercury and demonstrated changes of yeast cells during adaptation to mercury treatment.

- In response to acute mercury stress we observed an enhanced oxidative stress response in *stb5*Δ which we indicated to be due to loss of *MET17* transcription.
- We detected considerably retarded growth of *stb5*Δ during chronic mercury treatment based on reduced intracellular energy levels in the mutant.

3.1.4 Characterization of Pun1 participation under manganese stress

- We proved Crz1-dependent transcriptional induction of *S. cerevisiae PUN1* upon Mn^{2+}, Ag^{2+}, Hg^{2+}, and Cd^{2+}.
- We showed that Pun1 builds higher order oligomeric complexes and accumulates in MCC (membrane compartment of the arginine permease Can1) invaginations in the yeast plasma membrane in response to metal treatment.
- Finally, we found that the *pun1*Δ mutant is sensitive to metal ions and exhibits a severe cell wall defect based on abnormal formation of cell wall components like 1,3-β-D-glucan, mannoproteins, and chitin. Although we did not spot the *de facto* function of Pun1, we indicate Pun1 to obtain an important role in the maintenance of cell wall integrity especially during specific metal stress conditions.

3.2 Metal stress response in *Saccharomyces cerevisiae* – in more detail

3.2.1 Comparative gene expression analysis upon acute metal stress

3.2.1.1 *Metal detoxification pathways*

Aiming at the investigation of early defense strategies against metal stress, we generated transcriptional stress responses of *S. cerevisiae* cells treated with low to medium doses of the aforementioned metals for a short period of only 30min. We revealed a total of 1023 genes comprising 16.5% of the entire yeast genome that were significantly differentially expressed. According to annotation of these genes to significant GO terms we showed that the early metal stress response primarily focuses on the activation of metal-specific oxidative defense and protein catabolic processes possibly to prevent intracellular accumulation of toxic metals and damaged proteins. We detected expression of antioxidative genes upon Ag^{+}, As^{3+}, Cd^{2+},

Hg^{2+}, Mn^{2+}, Ni^{2+}, V^{3+}, and Zn^{2+} stress and expression of protein degradation pathways upon Al^{3+}, Ag^{+}, As^{3+}, Cd^{2+}, Hg^{2+}, Mn^{2+}, and Ni^{2+} stress. Under Cd^{2+} and As^{3+} stress we detected induction of chaperone complex genes as an additional protein catabolic and rescue process, respectively. Therefore, in comparison to earlier findings (Wysocki and Tamas, 2010) we confirmed and extended the spectrum of influence of several metals on distinct defense pathways in yeast (Figure 7).

Based on significant induction of corresponding genes, we assumed chelation of Co^{2+}, Mn^{2+}, Ni^{2+}, and Zn^{2+} via the siderophore iron transport and chelation of Hg^{2+} and Mn^{2+} via amino acids such as His and/or Arg -rich proteins as additional metal detoxification mechanisms. Previous studies linked increased iron uptake to a protective strategy against metal stress via outpacing of toxic metals (Stadler and Schweyen, 2002; Ruotolo *et al.*, 2008). In accordance we found significant induction of high-affinity iron uptake genes such as *FET3* and *FTR1* in response to the above-mentioned metals. We suggested the simultaneous activation of siderophore iron genes of the FIT and ARN family as a further protective effect in terms of metal uptake restriction via Co/Mn/Ni/Zn/siderophore chelation (Figure 7). Extracellular complex formation with siderophores has been reported previously for vanadium in *Pseudomonas aeruginosa* (Baysse *et al.*, 2000). Increased levels of histidine in the medium and the vacuole, respectively, have been determined to decrease toxicity of Cu^{2+}, Co^{2+}, and Ni^{2+}. Although the exact mechanism of vacuolar sequestration is unknown, complex formation of metal ions with histidine has been suggested to prevent interaction of toxic metals with physiologically important proteins (Pearce and Sherman, 1999; Farcasanu *et al.*, 2005). To this effect we indicate enhanced histidine and arginine biosynthesis upon Hg^{2+} and Mn^{2} treatment as a similar detoxification strategy (Figure 7). However, the definite role of siderophore, His, and Arg gene induction in the yeast metal defense needs to be proven.

Together, our findings partly substantiated previous metal-stress studies (Vido *et al.*, 2001; Jin *et al.*, 2008; Wysocki and Tamas, 2010) and expanded the range of detoxification processes in response to a number of metals (Figure 7). We further proved that although distinct gene/homeostatic overlaps exist between transcriptional metal stress responses, each particular metal ion generates its individual gene expression profile. Accordingly, there is no generic metal detoxification gene/pathway against general metal stress in yeast *S. cerevisiae*.

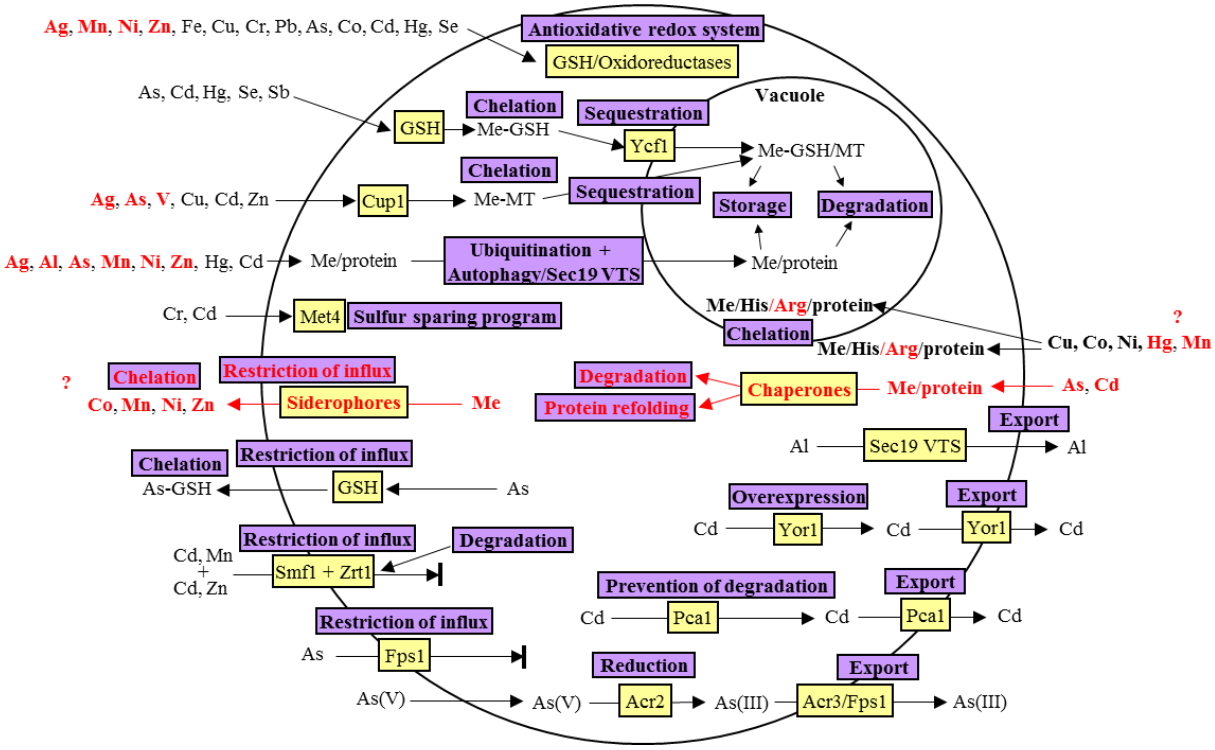

Figure 7: Metal detoxification strategies in *S. cerevisiae*. For detailed explanation of assured metal defense mechanisms see text in introduction (chapter 1.4). (Parts of) defense pathways highlighted in red illustrate findings detected and indicated, respectively, in this study. For detailed interpretation of the latter pathways see text above;

3.2.1.2 *Adaptation of yeast cells to sustained metal stress*

Consistent with previous reports (Warner, 1999; Gasch *et al.*, 2000; Wu *et al.*, 2002) we demonstrated growth-related processes like ribosomal biogenesis and translation as the most commonly repressed pathways in the yeast response to Ag^{+}, As^{3+}, Cd^{2+}, Hg^{2+}, Mn^{2+}, and Ni^{2+} treatment. Ribosome biogenesis has been shown as one major consumer of cellular energy (Li *et al.*, 1999). This substantiated the suggestion that among the vital functions gene expression with high energy consumption such as protein synthesis is reduced to divert the limited cellular energy to immediate metal detoxification under acute metal stress (30min). Comparing our data set to the 2h stress data set (Jin *et al.*, 2008) we detected transcriptional reactivation of growth-related homeostatic pathways and reduced induction of metal detoxification processes. The ability to continue growth might be due to successfully established metal detoxification on a post-translational protein level and to the redistribution of transcriptionally needed energy to metabolic growth processes. However, although these observations support the indication of adaptation of yeast cells to sustained metal stress

(Figure 8), there is so far no direct evidence for adaptation based on a consistent experimental setup including acute, sustained, and chronic metal stress. Hence, we investigated the mercury stress response of yeast cells in this respect (we will refer to this analysis in chapter 3.2.3).

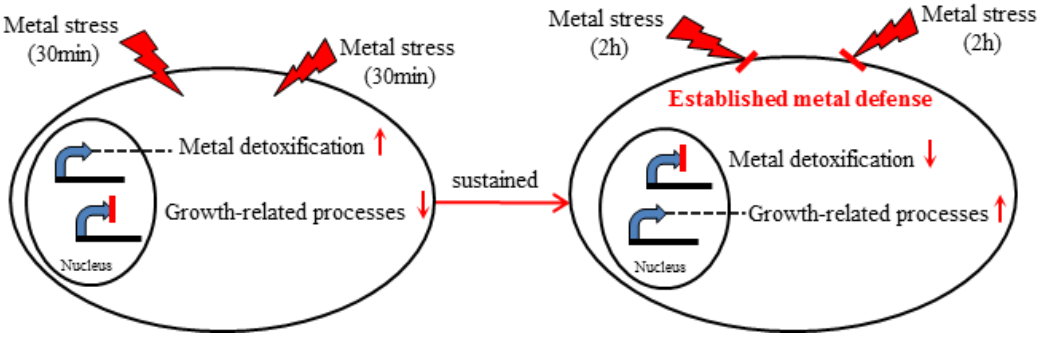

Figure 8: Schematic model of adaptation to sustained metal stress. In response to acute metal stress (30min) transcription of growth-related processes is inhibited (↓) to divert energy to the transcription of metal detoxification pathways (↑). According to sustained metal stress (2h) metal defense pathways are established on a post-translational protein level and transcription of metal detoxification pathways is deactivated (↓), whereas growth-related processes are reactivated (↑).

3.2.1.3 *Regulatory associations*

Intensive analyses for similarities between the particular expression profiles resulted in distinct metal-ion stress clusters generating stress responses with shared defense mechanisms and regulatory associations (Figure 9). In this context we specified Ag^{+}, As^{3+}, Cd^{2+}, and Hg^{2+} as forming the largest cluster primarily by evoking transcriptional induction of the glutathione/thioredoxin system and vacuolar protein catabolism. Based on T Profiler analyses these pathways are regulated by the oxidative stress response TF Yap1 and Yap1 homologues such as Yap7 and Cad1/Yap2, the stress response activators Msn2 and Msn4, the proteasomal degradation mediator Rpn4 as well as the heat shock TF Hsf1. Moreover, we indicated participation of Met4 mediating the sulfur amino acid pathway especially under Cd^{2+}, and Ag^{+} stress. In addition to T Profiler analysis, we detected the TF Hot1 as significantly differentially expressed upon Ag^{+}, Cd^{2+}, and Hg^{2+}. *HOT1* encodes a regulator required for the transient induction of the glycerol biosynthetic genes *GPD1* and *GPP2*. Interestingly, this cluster shared the most gene expression overlaps with other metals indicating a rather general systemic stress response for highly toxic metals. On the other hand, less toxic metals such as aluminum, vanadium, and manganese generated rather individual expression patterns.

Hg^{2+} and Mn^{2+} formed a smaller cluster which we assumed to involve the regulators Gcn4 and Gln3 in nitrogen/amino acid biosynthesis. We detected the activator of proline utilization Put3 in response to Ni^{2+}, Mn^{2+}, Co^{2+}, and V^{3+} and the three subunits of the HIR nucleosome assembly complex involved in regulation of histone gene transcription, Hir1, Hir2, and Hir3, solely upon Mn^{2+}. Though, the concrete function of these TFs under metal stress is yet unclear. Finally, we detected another cluster comprising As^{3+}, Cd^{2+}, Hg^{2+}, Ag^{+}, Ni^{2+}, and V^{3+} with the predicted TFs Fhl1 and Sfp1 involved in the regulation of ribosomal protein transcription and Rap1, a repressor/activator-protein with a role in diverse processes.

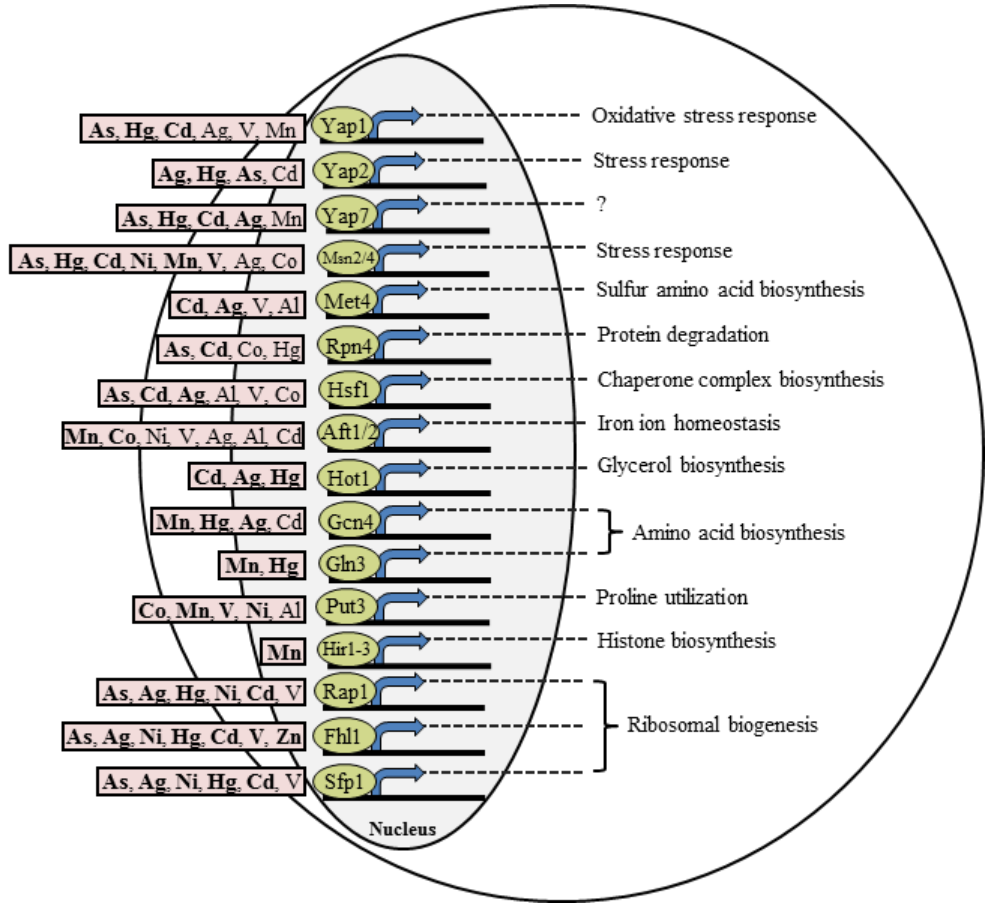

Figure 9. Transcriptional regulators of *S. cerevisiae* under acute metal stress. Predicted TFs under acute metal stress by T Profiler; metals in bold are implicated as highly significant stressors for the respective TFs; for interpretation see text.

In summary, some of the above mentioned TFs like Yap1, Cad1/Yap2, Msn2, Msn4, Rpn4, Met4, Hsf1, Fhl1, Sfp1, or Aft1 have already been linked to metal stress (Stadler *et al.*, 2002; Haugen *et al.*, 2004; Thorsen *et al.*, 2007). But we additionally linked distinct TFs to yet not described metal stress responses. This applied for instance to Cad1/Yap2 which has been involved in the response to cadmium and arsenic (Lesuisse and Labbe, 1995; Haugen *et al.*,

2004) but not to silver and mercury as indicated in this study. Others such as Yap7, Hot1, Gcn4, Gln3, Put3 and Hir1-3 were for the first time detected in the context of metal stress.

3.2.2 Analysis of regulators involved in the arsenic stress response

Subsequent to the observed significant down-regulation of ribosomal protein (RP) and ribosome biogenesis (Ribi) genes and the intensive induction of stress response (SR) genes especially upon arsenic treatment (see chapter 3.2; Supplemental Figure 1), we determined the respective regulatory associations. Here we provided evidence that the Target Of Rapamycin (TOR) pathway acts in concert with the protein kinase A (PKA) pathway not only to regulate cell growth and responses to nutrients (Wullschleger *et al.*, 2006; Santangelo, 2006), but also to regulate the yeast response to metal stress. In particular, we analyzed the regulatory effects of TORC1 and PKA on their downstream effectors Sfp1, Sch9, Msn2, and Msn4.

3.2.2.1 *Repression of RP genes via inhibition of Sfp1*

Sfp1 and Sch9 are stress- and nutrient-sensitive regulators of RP gene expression in yeast (Jorgensen *et al.*, 2004; Marion *et al.*, 2004; Urban *et al.*, 2007). Recently, Sfp1 was predicted to contribute to global repression of RP genes in response to arsenic stress (Haugen *et al.*, 2004; Thorsen *et al.*, 2007). We verified this by comparison of transcript profiles of wild-type cells with *sfp1*Δ mutants, who almost completely failed to down-regulate RP genes, and therefore substantiated a central role of Sfp1 in the repression of RP gene transcription under arsenic stress. In addition, we provided evidence for inhibition of Sfp1 by arsenic following Sfp1 phosphorylation via in-gel phosphoprotein staining and Sfp1 localization via endogenously GFP-tagged Sfp1. We showed that upon arsenic treatment Sfp1 phosphorylation was decreased and followed by dissociation from its nuclear RP gene promoters and accumulation in the cytosol, thereby preventing RP gene expression (Figure 10). This effect was likewise observed under mercury and nickel stress suggesting a more general role of Sfp1 in response to metal exposure. Sfp1-dependent RP gene repression has further been delineated under rapamycin exposure and other stresses and has been shown to be due to the inhibition of TORC1 activity by these stress impacts, which consequently affected inhibition and cytoplasmic accumulation of its downstream target Sfp1 (Jorgensen *et al.*, 2002; Marion *et al.*, 2004). Hence, our findings strongly indicated similar regulatory effects of arsenic and rapamycin.

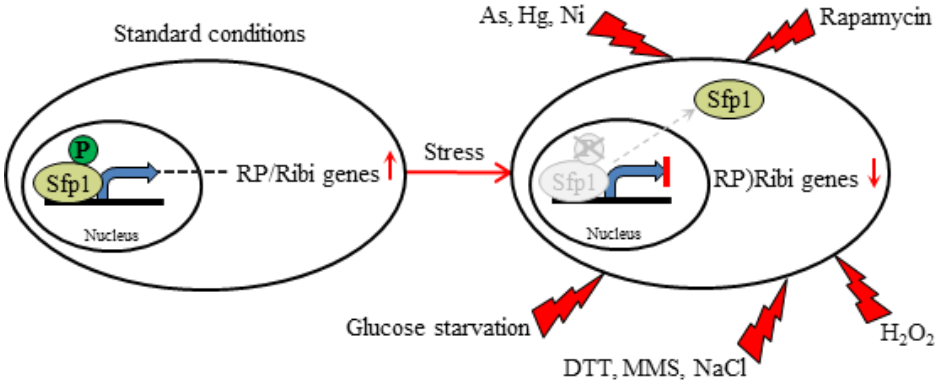

Figure 10. Repression of RP gene expression upon stress via Sfp1 inactivation. See text for details.

3.2.2.2 *Arsenic inhibits TORC1 kinase*

We showed that in regard to RP and Ribi gene repression and SR gene induction transcript profiles generated upon arsenic stress resemble those of rapamycin stress (Hardwick *et al.*, 1999). This implicated the Target of rapamycin (TOR) pathway as a putative arsenic target. Phenotypic analyses on plates supplemented with arsenic revealed reduced growth of mutants lacking full Tor1 function and therefore substantiated the need of TORC1 kinase activity to acquire arsenic tolerance. Strikingly, in contrast to Tor1 mutants, deletion of *SFP1* conferred resistance to arsenic, whereas overexpression of *SFP1* reduced resistance. These findings indicated a yet unknown function of Tor1 in response to arsenic stress apart from regulation of Sfp1.

However, similar to rapamycin treatment, we showed inhibition of TORC1 kinase under arsenic exposure by determination of the phosphorylation status of Sch9, which is as a *bona fide* TORC1 substrate (Urban *et al.*, 2007). Both Sfp1 and Sch9 regulate RP/Ribi gene expression and seem to function in parallel pathways (Fingerman *et al.*, 2003; Jorgensen *et al.*, 2004). We showed that arsenic and other toxic metals such as mercury and nickel lead to rapid dephosphorylation of Sch9. Thus, the upstream signalling components of TORC1 triggered by these metals are still unknown. We additionally confirmed the TORC1-dependent activity of Sch9 by demonstrating increased sensitivity of cells lacking Sch9 to arsenic exposure. On the other hand, we found enhanced arsenic tolerance of TORC1-independent Sch9 mutants (Urban *et al.*, 2007), which supports the aforementioned

assumption of a separate function of Tor1. We concluded that Sfp1 similar to Sch9 is likewise a direct TORC1 target, although direct proof of this was still lacking (Figure 11).

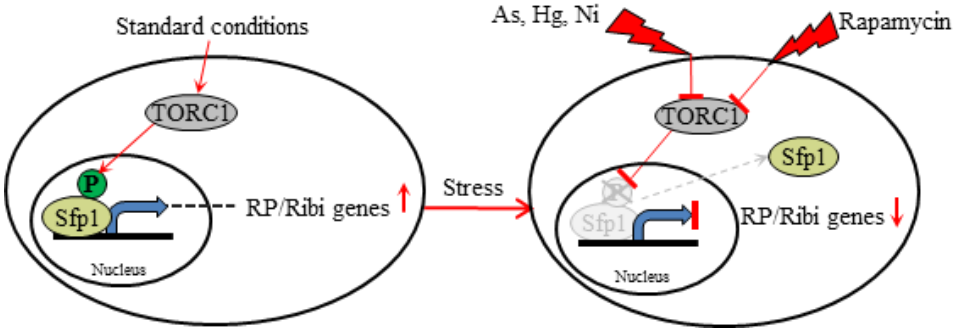

Figure 11. Hypothetic regulation of Sfp1 by TORC1 under metal ion and rapamycin stress. Toxic metals such as As, Hg, and Ni as well as rapamycin inhibit TORC1 kinase leading to dephosphorylation of Sfp1. Sfp1 dissociates from RP/Ribi gene promoters, accumulates in cytoplasm and causes repression of RP/Ribi gene expression.

3.2.2.3 *Activation of stress response genes via Msn2 and Msn4*

Based on the above mentioned comparison of expression profiles upon arsenic and rapamycin treatment we detected an activated cluster of SR genes, besides bulk repression of RP genes. Here we identified the partially redundant stress-responsive TFs Msn2 and Msn4 as the main regulators of the yeast stress response upon arsenic (Figure 12). Both TFs have been implicated in the transcriptional response to arsenic previously (Haugen *et al.*, 2004; Thorsen *et al.*, 2007). We substantiated the central role of Msn2 and Msn4 under arsenic stress via analysis of transcript profiles of an *msn2*Δ*msn4*Δ double mutant and GFP-localization of Msn2/4. We provided evidence for significant reduction of Msn2/4-dependent stress-related genes in an *msn2*Δ*msn4*Δ double deletion strain indicating that these genes are direct Msn2/4 targets. And we showed activation of Msn2/4 by metal stress as both Msn2- and Msn4-GFP rapidly translocated from cytoplasm to the nucleus to activate target genes in response to arsenic and other toxic metals (see also Supplemental Figure 2).

Msn2/4 activity involves the TOR and PKA pathway (Smith *et al.*, 1998; Beck and Hall, 1999). We found indications for sustained PKA activity, which appears to be advantageous during arsenic exposure: 1) Mutants lacking the PKA regulatory subunit (*bcy1*Δ) showed constitutively high PKA activity and increased resistance to arsenic. High PKA activity prevents hyperactivation of Msn2/4 (Durchschlag *et al.*, 2004). Bcy1 is predominantly

localized in the nucleus under optimal growth conditions but is associated to the catalytic part of PKA in cytosol under stress conditions to inactivate PKA (Toda *et al.*, 1987; Griffioen *et al.*, 2000). 2) We observed a striking growth reduction of yeast cells in response to arsenic treatment related to Msn2/4 activity; in fact, *msn2*Δ*msn4*Δ double mutants showed enhanced tolerance, whereas *MSN2* and *MSN4* overexpression slightly increased sensitivity to arsenic. Moreover, we demonstrated participation of PKA apart from its function as regulator of Msn2/4; *msn2/4*Δ mutants additionally lacking the catalytic activity of PKA (*tpk1/2/3*Δ *msn2/4*Δ) showed slightly increased sensitivity to arsenic. Together, we proved Msn2/4 activity under chronic arsenic stress despite sustained PKA activity (Figure 12). This indicated activation of Msn2/4 apart from PKA.

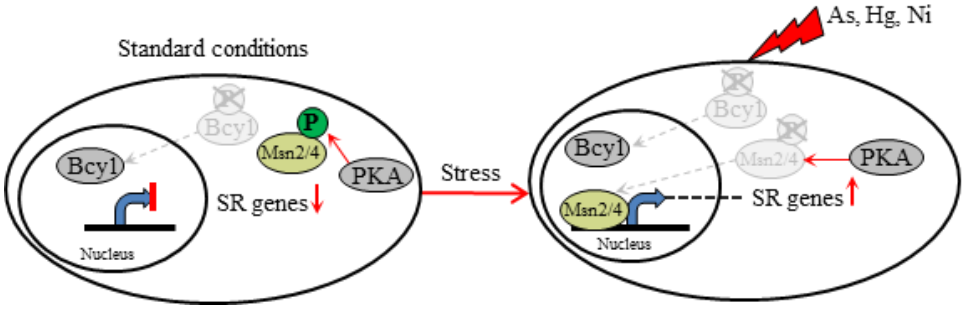

Figure 12. Induction of SR gene expression upon metal stress via Msn2/4 activation. See text for details.

Strikingly, we detected that deletion of *MSN2/*4 completely alleviated the arsenic sensitivity of *tor1*Δ mutants. In line with a previous study implicating TORC1 as a negative regulator of Msn2/4 (Beck and Hall, 1999) we concluded that even if PKA activity levels remain high under excess arsenic, TORC1 activity plays the major regulatory role of RP and SR gene expression. It appears as if chronic stress response is detrimental for yeast growth. This might be due to enhanced energy consumption for transcriptional processes, which generates an energy lack for reactivation of growth, finally driving yeast cells into stationary phase. RP and SR gene expression are indirectly coupled. Consistently, a recent metal stress study illustrated that copper and arsenic at higher concentrations lead to significant down-regulation of ribosome biogenesis and activation of SR genes and genes involved in energy generation as opposed to other metals and arsenic at lower concentrations (Jin *et al.*, 2008). In this regard, we assume that reactivation of growth under sustained moderate metal stress is a consequence of successfully established defense pathways on a posttranslational level (chapter 3.2.1.2). On

the other hand, sustained arsenic exposure leads to induction of stress response and growth inhibition (Jin *et al.*, 2008).

3.2.2.4 *Modified model of signaling pathways under arsenic stress*

When we initially proposed our model for arsenic stress in 2009, some dubieties especially regarding the mechanism by which arsenic inhibits TORC1, the question whether Sfp1 is a direct TORC1 target, *tor1*Δ sensitivity in connection with *sfp1*Δ resistance to arsenic, and the exact role of Sch9 downstream activity remained unclear. Today, in the light of new findings concerning this subject we have partly solved these inconsistencies and present a modified schematic model (Figure 13):

Under optimal growth conditions Sfp1 activates RP/Ribi gene expression in the nucleus, whereas transcription of SR genes is down-regulated and Msn2/4 are localized in the cytoplasm. Strikingly, RP/Ribi gene transcription appears to regulate dephosphorylation of Sch9 by TORC1 in a yet not well understood negative-feedback mechanism (Lempiäinen *et al.*, 2009). Possibly this process is connected to further regulators of RP/Ribi gene transcription such as Fhl1, Ifh1, Stb3, Dot6, and Tod6 (Martin *et al.*, 2004; Wade *et al.*, 2004; Wei and Zheng, 2009; Huber *et al.*, 2011). The *de facto* functional consequences of Sch9 dephosphorylation are yet unclear. However, we provided evidence that arsenic and other toxic metals like mercury and nickel also lead to TORC1-dependent dephosphorylation of Sch9, most likely with different functional consequences. Moreover, we suggested that the same metals inhibit TORC1 activity leading to dissociation of Sfp1 from RP/Ribi gene promoters, Sfp1 accumulation in the cytoplasm, and RP/Ribi gene repression. Consistent with these findings a follow-up study revealed that Sfp1 as Sch9 is a direct TORC1 target by means of direct *in vitro* phosphorylation of Sfp1 by TORC1 kinase upon rapamycin treatment (Lempiäinen *et al.*, 2009). It was further suggested that TORC1 acts directly in the nucleus in complex with Sfp1 and is rapidly exported to the cytoplasm under rapamycin exposure (Li *et al.*, 2006; Lempiäinen *et al.*, 2009). Whether this is also true for treatment with metal ions, remains to be examined.

Recently, Mtl1, a member of the cell wall integrity (CWI) pathway, has been indicated as a cell-surface sensor for oxidative stress and has been shown to inhibit Tor1 and Ras2 activity under oxidative stress (Vilella *et al.*, 2005; Petkova *et al.*, 2010). These authors especially indicated Msn2 as a putative target of Mtl1 based on the down-regulation of a cluster of

Msn2-dependent genes in the absence of Mtl1 (Petkova *et al.*, 2010). Since metal exposure in yeast cells generates oxidative stress, Mtl1 might also act as a trigger of TORC1 inhibition in response to arsenic. However, TORC1-dependent dephosphorylation of Sch9 as shown in this study might provide the link to the activation of Msn2/4 in a separate pathway apart from RP/Ribi gene repression. Interestingly, Sch9 regulates Bcy1 via the Mitogen Activated Protein Kinase 1 (MAPK1) and was shown to reduce PKA activity under rapamycin treatment (Urban *et al.*, 2007; Soulard *et al.*, 2010; Zhang *et al.*, 2011). However, the PKA target genes Msn2/4 were not activated by this pathway (Soulard *et al.*, 2010) pointing to a different Msn2/4 activation mechanism in response to rapamycin.

As Sch9 has been reported to dephosphorylate the protein kinase Rim15 involved in Msn2/4 regulation as well (Wanke *et al.*, 2008), we implicate Rim15 as an alternative activator of Msn2/4 under arsenic stress. Rim15 dephosphorylation leads to accumulation of active Rim15 in the nucleus and activation of Msn2/4-dependent SR gene expression (Fabrizio *et al.*, 2001; Swinnen *et al.*, 2006; Wanke *et al.*, 2008; Wei *et al.*, 2008). Notably, these findings fit perfectly to the phenotypes of *mtl1*Δ, *tor1*Δ, and *sch9*Δ mutants conferring increased sensitivity to rapamycin (Petkova *et al.*, 2010) and arsenic (this study), respectively, whereas overproduction of *SCH9*, *bcy1*Δ, as well as *msn2*Δ/*msn4*Δ mutants showed increased resistance to arsenic. In this context, a *rim15*Δ mutant might also exhibit increased sensitivity to arsenic as it is part of the Mtl1/Tor1/Sch9 pathway that prevents growth reduction of yeast cells via inhibition of Msn2/4 activity. Thus, the aforementioned discrepancy of the apparently contradictory roles of Tor1 and Sfp1 under arsenic treatment might not be seen in the context of TORC1 dephosphorylation of Sfp1 but of Sch9 in a separate pathway. Accordingly, as a consequence of missing Sch9 dephosphorylation activation of Msn2/4 is inhibited; this inhibition leads to increased resistance to arsenic. Again several details of these pathways like the definite cellular localization of Sch9 or the exact mechanism of Msn2/4 activation remain unclear. Further studies are therefore required to unravel all open questions concerning the genetic interactions of all signalling components involved in the yeast response to arsenic stress.

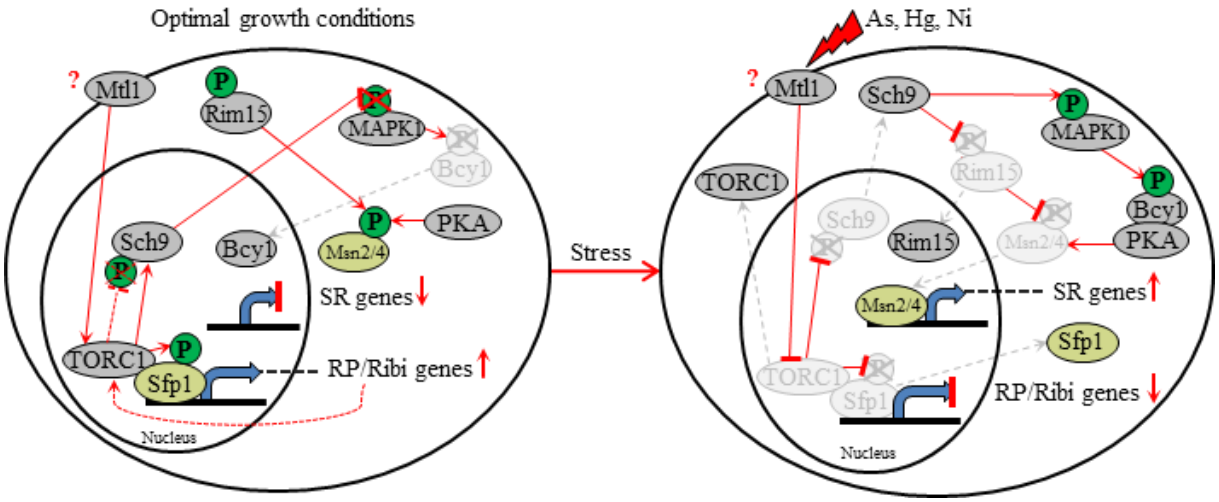

Figure 13. Schematic model of signaling components for RP/Ribi gene repression and SR gene induction under arsenic stress. For interpretation see text.

3.2.3 Transcriptional consequences of *STB5* deletion during mercury stress

3.2.3.1 *Stb5 is involved in metal stress defense*

The aforementioned comparative metal stress analyses (chapter 3.2.1) revealed the expression of *STB5* encoding a transcriptional regulator involved in oxidative stress as significantly up-regulated in the presence of As^{3+} and Cd^{2+}. In following growth assays on solid medium we observed sensitivity of an *STB5* deletion strain upon metal ions such as As^{3+}, Cd^{2+}, Co^{2+}, Cu^{2+}, Hg^{2+}, Mn^{2+}, Ni^{2+}, V^{3+}, and Zn^{2+}. In additional growth assays in liquid medium we detected considerably retarded growth of *stb5*Δ under chronic mercury exposure compared to *wt*. We thereby provided evidence for participation of Stb5 in the adaptation process of yeast cells to metal stress. To investigate the role of Stb5 in the systemic metal defense on a transcriptional level, we applied mercury as representative toxic metal and examined acute (15 and 30min), sustained (2h), and chronic mercury stress (24h) in wild-type and *stb5*Δ mutant cells by cDNA microarray technique. During mercury treatment we localized Stb5 as permanently present in the nucleus.

3.2.3.2 *Transcriptional and regulatory changes during adaptation to mercury stress*

We for the first time followed the transcriptional and regulatory changes of yeast wild-type cells during mercury treatment; a graphical overview of our results is presented below (Figure 14 and 15). Due to the fact that mercury causes oxidative stress (Valko *et al.*, 2005) we demonstrated immediate induction of the glutathione/thioredoxin antioxidant system and chaperones of the HSP70 family as the first line defense of yeast cells against acute mercury stress (15min and 30min). Additionally, yeast cells induced transcription of genes involved in protein catabolism, energy generation, and aldehyde as well as carbohydrate metabolism. We defined that these pathways are mainly regulated by stress response activators such as Yap1, Skn7, Met4, Cbf1, the Yap1 homologues Yap2, Yap4, and Yap7, the heat shock TF Hsf1, the regulators of cellular respiration Hap1 as well as Hap4, and the proteasomal gene activator Rpn4. Strikingly, based on GO annotations of the observed activators involved in the mercury defense, the expression of their target genes appears to exclusively occur from polymerase II promoters, whereas transcription from polymerase I and III promoters was inhibited. Consistent with previous findings (Warner *et al.*, 1999; Gasch *et al.*, 2000; Wu *et al.*, 2002; Hosiner *et al.*, 2009; Hosiner *et al.*, 2012 in preparation) we further detected repression of growth-related processes like ribosome biogenesis and translation, most likely to divert the limited intracellular energy to the immediate transcriptional activation of mercury defense pathways. We assumed the TFs Sfp1, Fhl1, and Rap1 to mediate this "energy saving strategy".

Upon up to 2h sustained mercury stress we found partial adaptation of yeast cells to the toxic environmental situation (Hosiner *et al.*, 2012 in preparation). Consequently, expression of oxidative stress defense, glutathione and aldehyde metabolism, catabolic as well as repair genes along with repression of growth-related processes was reduced. Simultaneously, we observed a reduction of involved regulators (Figure 14) and interpreted these findings in terms of successfully established metal defense strategies on a post-translational level followed by redistribution of cellular energy to growth. As another strong indication for this assumption we showed significant up-regulation of lipid and alcohol metabolism mainly comprising ergosterol synthesis and hexose transport. According to recent studies (Lupetti *et al.*, 2002; Dickey *et al.*, 2009) these processes increase membrane integrity and ensure growth.

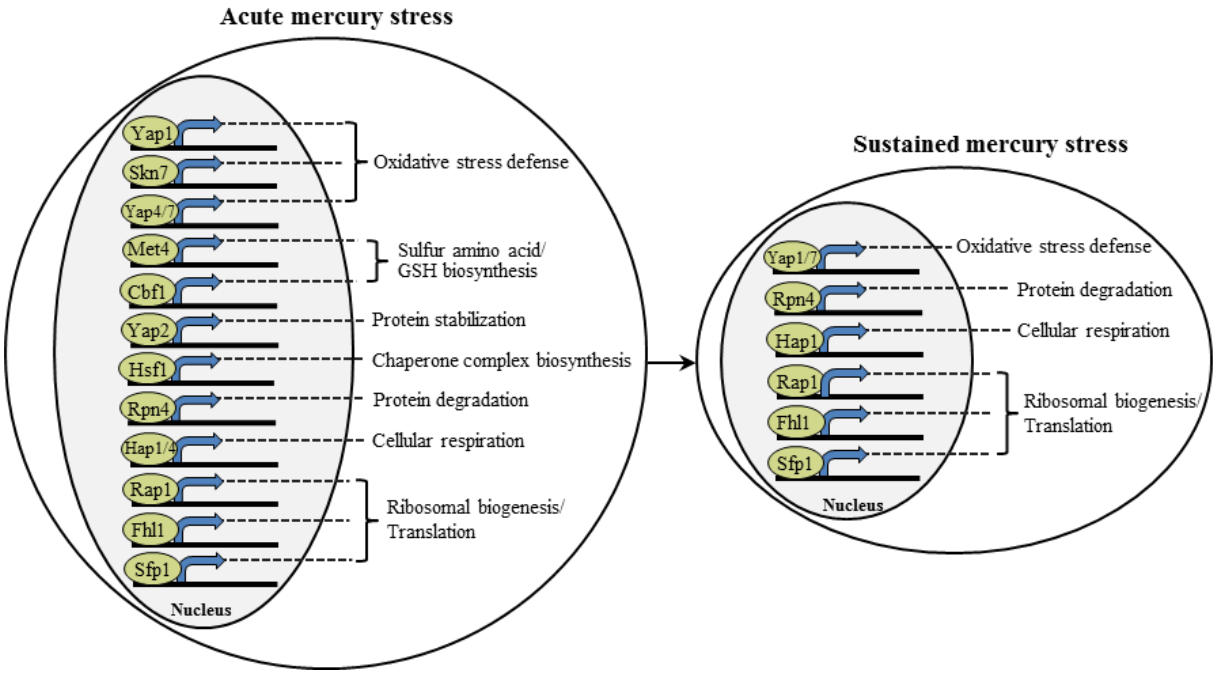

Figure 14. Adaptation of *S. cerevisiae* to short-term mercury stress. Expression changes of yeast wild-type cells during adaptation to mercury stress and the respectively involved regulators are illustrated in this figure. For explanation see text.

Interestingly, we found more extensive expression patterns in *wt* and *stb5*Δ under chronic (24h) compared to short-term mercury treatment. These mostly comprised the same metabolic pathways as upon the adaptation process but included many additional genes. Additionally, we detected significant reactivation of stress defense genes and respective regulators as well as the induction of Aft1/2-dependent siderochrome transport and further protein catabolic processes such as for instance proteolysis via the 26S proteasome (Figure 15). Further regulators predicted by T Profiler included the maltose fermentation regulatory protein Mal33 and the regulator of proline catabolism Put3, which mediates the utilization of proline as nitrogen source under poor nitrogen availability (Huang and Brandriss, 2000). We proposed participation of Put3 for in response to treatment of yeast cells with other metals like nickel, manganese, cobalt, and vanadium in a recent study (Hosiner *et al.*, 2012 in preparation). These results point to nitrogen deprivation under metal stress. Then again, TFs such as Skn7, Yap2, Yap4, Yap7, and Hap4 appeared to function under acute but not under chronic mercury stress. Together, we suggest sustained adaptation of yeast cells to long-term mercury treatment at the cost of increased metabolic effort to support degradation of damaged proteins, nutrient supply, to sustain growth despite reduced protein biosynthesis. However, these

suppositions were solely based on transcriptional changes of yeast cells and remain to be substantiated on a proteomic level.

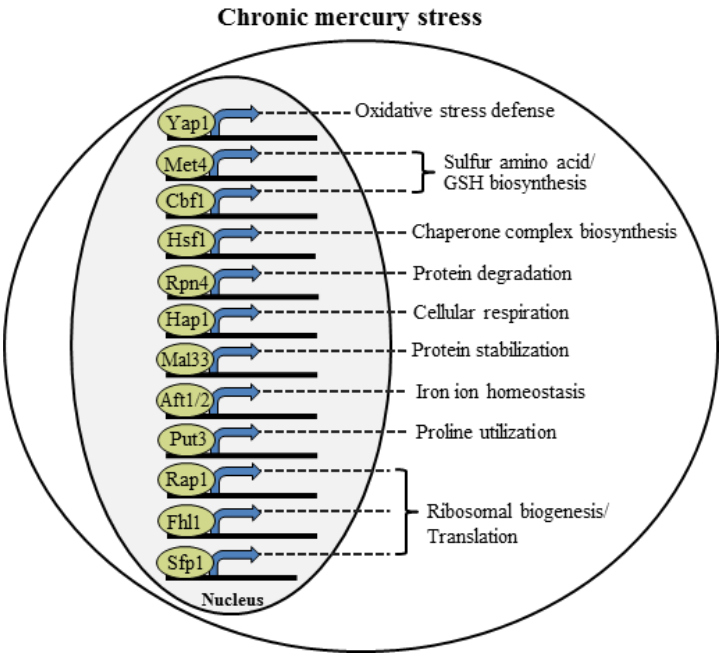

Figure 15. Adaptation of *S. cerevisiae* to long-term mercury stress. Expression changes of yeast wild-type cells during adaptation to mercury stress and the respectively involved regulators are illustrated in this figure. For explanation see text

3.2.3.3 *Deletion of STB5 leads to an enhanced early oxidative stress response*

We provided clear indications for an enhanced early oxidative stress response in the *STB5* deletion strain under acute mercury stress. Primarily, we detected loss of *MET17* transcription and up-regulation of hexose transport in *stb5*Δ. Met17 is a key enzyme of the sulfur/methionine metabolism. It catalyzes the synthesis of homocysteine, a main component of glutathione, which plays a central role in the yeast defense against toxic metal ions and oxidative stress (Thomas *et al.*, 1997). Thus, we indicated that missing *MET17* transcription might lead to impaired detoxification and cellular accumulation of mercury ions, thereby indirectly causing oxidative stress. On the other hand, hexose transport has been suggested to contribute to unspecific metal uptake (Jin *et al.*, 2008) and consequently might lead to increased intracellular Hg^{2+} accumulation. Both effects eventually point to elevated oxidative stress in the mutant. Additional simultaneous induction of cell wall organization and cell aging genes in *stb5*Δ cells substantiated this idea especially in light of the well-established correlation between progressive cell aging and severe intracellular oxidative stress

(Tchaikovskaya *et al.*, 2005; Robillard *et al.*, 2011). Although we did not prove direct participation of Stb5 in the observed deficiencies of *stb5*Δ cells in response to short-term mercury stress, our results are in line with a study which implicated Stb5 as central in the oxidative stress response (Larochelle *et al.*, 2006).

3.2.3.4 *Stb5Δ exhibits decreased energy levels under chronic mercury exposure*

We also characterized Stb5 to participate in the regulation of energy and cofactor production for the oxidative stress defense during adaptation of yeast cells to chronic mercury exposure and again supposed increased oxidative stress in *stb5*Δ. In this regard we showed that the *STB5* deletion strain exhibited significantly retarded growth in comparison with the wild-type strain, but adapted to mercury toxicity despite a severe handicap. We assumed that this handicap was primarily due to a considerably reduced expression of genes involved in energy metabolism (e.g. NAD *de novo* and ATP biosynthesis as well as glucose metabolism). We again verified no direct participation of Stb5, but our results were consistent with findings, linking Stb5 to NADPH production during oxidative stress (Larochelle *et al.*, 2006). In addition, reduced expression of further homeostatic processes such as aldehyde, carbohydrate, alcohol, and lipid metabolism as well as of protein catabolism in *stb5*Δ compared to *wt* most likely contributed to the retarded growth phenotype of the mutant.

As a result of reduced intracellular levels of high-energy compounds for the oxidative stress defense in the *STB5* deletion strain we indicated an increase of oxidative impact. It has been reported previously that oxidized proteins are degraded by an ubiquitin- and ATP-independent mechanism (Shringarpure *et al.*, 2003). Accordingly, it has been proven that the disassembly of the ATP-/ubiquitin-dependent 26S proteasome into the 19S and the 20S particle under oxidative stress leads to an increased cellular protein degradation capacity via the oxidatively more resistant ATP-/ubiquitin-independent 20S proteasome (Reinheckel *et al.*, 1998; Breusing and Grune, 2008; Wang *et al.*, 2010). To this effect we found sustained activity of the oxidative stress response regulators Skn7 and Yap2 in *stb5*Δ and especially showed transcriptional activation genes encoding the 20S core particle of the 26S proteasome. On the other hand, transcription of both, 19S and 20S proteasome genes, as well as *CDC48*, encoding an ATPase involved in ubiquitin-dependent protein degradation, was significantly up-regulated in *wt* indicative for a minor oxidative impact of Hg^{2+} in *wt*.

Finally in addition to previous metal studies (Saponja and Vogel, 1996; Ward *et al.*, 2001; Stadler and Schweyen, 2002; Chen *et al.*, 2005; Pagani *et al.*, 2007b), we showed activation of Aft1/2-dependent iron regulon genes in response to chronic mercury stress. We especially found genes coding for cell wall mannoproteins of the FIT family and siderophore transporters of the ARN/SIT family as significantly stronger induced in *stb5*Δ than in *wt*. Although we provided no direct evidence, we suggested these iron homeostasis genes to serve additional protective functions against metal stress. Since mannoproteins have been shown to determine cell wall porosity (Zlotnik *et al.*, 1984), we indicated the increased expression of mannoprotein genes to decrease cell wall permeability for toxic Hg^{2+} ions. On the other hand, in a recent study (Hosiner *et al.*, 2012 in preparation) we assumed chelation of siderophores with metals as an additional detoxification strategy to prevent their uptake and also linked this mechanism to chronic Hg^{2+} stress.

Summarized, this manuscript presented evidence for an important role of Stb5 in the regulation of metal stress defense in *S. cerevisiae* and provided a number of indirect effects of Stb5 under acute and chronic mercury exposure in yeast cells. However, the actual molecular function of this regulator under metal stress remains to be shown.

3.2.4 Characterization of the plasma membrane protein Pun1 under metal stress

According to the significant transcriptional up-regulation of *PUN1* (*YLR414C*), encoding an uncharacterized membrane protein, in response to manganese and silver stress (as observed in the primal metal stress analysis; Supplemental Figure 4), we investigated Pun1 function as a putative metal transporter.

3.2.4.1 *Pun1 participates in the adaptation to metal stress*

Using northern blot analysis we also detected *PUN1* expression upon mercury and cadmium exposure, besides manganese and silver stress. But we proved effective participation of Pun1 in the yeast metal defense via phenotyping the *pun1*Δ mutant on plates and in liquid medium supplemented with different metals. Accordingly, we demonstrated decreased growth of *pun1*Δ under manganese, silver, calcium, arsenic, cadmium, nickel, copper, and aluminium (see also Supplemental Figure 5). Reintroduction of *PUN1* into *pun1*Δ restored this growth defect. However, sensitivity of *pun1*Δ to a broader range of metals than those inducing

transcriptional *PUN1* activation pointed to a more general defect in maintenance of ion permeability rather than to a specific transport defect. This assumption was supported by an intracellular determination of total As^{3+} concentration, which revealed significantly higher As^{3+} incorporation in *pun1*Δ mutants than in wild-type and *PUN1* overexpressing cells.

3.2.4.2 *Pun1 builds oligomeric complexes in punctate plasma membrane patches*

Via subcellular localization of GFP-tagged Pun1 we provided evidence that Pun1 functions in punctate patches in the plasma membrane and accumulates in these regions in response to Mn^{2+} and Ca^{2+}. This was consistent with our microarray and northern blot analyses and with a previous study describing colocalization of Pun1 with the plasma membrane protein Sur7 within MCC (membrane compartment of the arginine permease Can1) invaginations (Alvarez *et al.,* 2009). In addition, seven further proteins of mostly unknown function are known to localize to MCCs (Grossmann *et al.,* 2008; Alvarez *et al.,* 2009). MCC compartments are ergosterol-rich domains involved in turnover regulation of transport proteins, but their actual function is still unknown (Grossmann *et al.,* 2008). One possibility might be that the aforementioned proteins act in connection with ergosterol contents to regulate membrane permeability. This assumption is in line with the fact that fluctuating ergosterol concentrations influence transmembrane transport activities and the structural integrity of yeast membranes under stressful environmental conditions (Toh *et al.,* 2001; Lupetti *et al.,* 2002; Dickey *et al.,* 2009).

Notably, we found that *PUN1* comprises a tetraspan topology and a highly conserved claudin family signature G-L-W-x-x-C-x(8-10)-C within the first extracellular loop. Mammalian claudins are known to create charge-selective pores by forming homo-oligomers (Mitic *et al.,* 2003). Based on the structural similarities of Pun1 with claudins, we proved the oligomerization capacity of Pun1 via accurate analysis of membrane fractions via chemical cross-linking, Blue native electrophoresis, and Co-immunoprecipitation. At last we detected that Pun1 indeed forms higher-order homo-oligomers related to mammalian claudins and demonstrated Pun1 self-interaction, most probably by forming disulfide bonds between the cysteine residues in the first extracellular loop. Another similarity to mammalian claudins represented a series of charged residues in the first loop of Pun1. In mammalians these are believed to serve as a selective filter of the claudin-built channel for regulation of paracellular ion transport (Colegio *et al.,* 2002). Even though yeast is a single cellular organism without paracellular transport, these findings further supported our indication regarding an important

role of Pun1 in the regulation of ion permeability through the plasma membrane under conditions of metal stress.

3.2.4.3 *Crz1 is the key mediator of PUN1 induction under metal stress*

Based on previous reports describing Pun1 involvement in cell wall stress and the determination of putative interaction motifs in the upstream region of *PUN1* (Garrett-Engele *et al.,* 1995; Yoshimoto *et al.,* 2002; Garcia *et al.*, 2004; Rodriguez-Pena *et al.,* 2005; Garcia *et al.,* 2009), we observed the involvement of different signalling pathways in *PUN1* regulation under metal stress. By conducting northern blot analyses we showed that the calcineurin-responsive transcriptional activator Crz1 is crucial for *PUN1* induction upon certain metal ions such as Mn^{2+}, Ag^{2+}, Hg^{2+}, and Cd^{2+} (see also Supplemental Figure 6). Further, we demonstrated the additional participation of Hog1 and Rlm1 in *PUN1* induction upon Hg^{2+} and Cd^{2+} exposure, but not upon Mn^{2+} and Ag^{2+} (Supplemental Figure 6); Hog1 constitutes the mitogen-activated protein kinase involved in osmoregulation, whereas Rlm1 is a component of the protein kinase C-mediated MAP kinase pathway involved in the maintenance of cell integrity. Hog1-dependent *PUN1* activation has been shown previously to occur under cell wall stress (Rodriguez-Pena *et al.,* 2005). An explanation for our findings might therefore be that Crz1 is the key regulator of *PUN1* induction under metal stress, albeit with different upstream signaling pathways in response to different metal ions.

The Ca^{2+}/calmodulin/calcineurin pathway in yeast is required to maintain normal cell wall and cell integrity (Garrett-Engele *et al.*, 1995). Consistent with the fact that this pathway has been detected to confer tolerance to excess Ca^{2+} and Mn^{2+} (Farcasanu *et al.*, 1995; Stathopoulos and Cyert, 1997), we proposed this signalling pathway as very probable for induction of *PUN1* under Ca^{2+}, Mn^{2+}, and Ag^{+} treatment. Mn^{2+} has been shown to replace Ca^{2+} in the induction of calmodulin (Mork and Geisler, 1989) which might also apply to Ag^{+}. Calmodulin in turn activates the phosphatase calcineurin, which dephosphorylates Crz1 (Matheos *et al.*, 1997). Accordingly, Crz1 translocates to the nucleus (Matheos *et al.*, 1997) and might bind to the CDRE (calcineurin-dependent response element) motif in the *PUN1* promoter region leading to *PUN1* induction (Figure 16). However, a direct interaction between both factors still has to be verified.

On the other hand, Hg^{2+}, Cd^{2+}, and Al^{3+} have been detected to alter intracellular Ca^{2+} homeostasis (Tan *et al.*, 1993; Beyersmann and Hechtenberg, 1997; Zheng *et al.*, 2007; Li *et*

al., 2011). In this regard, Crz1-dependent *PUN1* induction upon these metals might occur through elevated intracellular Ca^{2+} levels and/or under cooperation with further TFs such as Hog1 and Rlm1 (Figure 16). This might also explain the sensitivity of *pun1*Δ mutants to Al^{3+} (Supplemental Figure 5). It is of note that Hog1 has been shown to contribute to metalloid tolerance by mediating restriction of arsenite- and antimonite-uptake via the glycerol channel Fps1 (Thorsen *et al.*, 2006). In this regard, it appears likely that Hog1 might also be involved in the regulation of ion permeability by activating *PUN1* in response to metals like Hg^{2+}, Cd^{2+}, and Al^{3+}. Though, the exact mechanism is yet unclear. However, the previously reported induction of *PUN1* via the Slt2 kinase/Rlm1 signalling pathway upon cell wall stress (Watanabe *et al.*, 1995; Jung *et al.*, 2002; Rodríguez-Peña *et al.*, 2005) points to simultaneous participation of several signal transduction pathways. A situation of dual control has for instance been described for *FKS2* encoding the alternative 1,3-*β*-glucan synthase subunit, which is dependent upon both Rlm1 and Crz1 (Jung and Levin, 1999; Lagorce *et al.*, 2003). In conclusion we assumed that in case of Hg^{2+}, Cd^{2+}, and Al^{3+} stress a triple control mechanism might be necessary for *PUN1* induction. But how the exact control of these pathways is governed still needs to be clarified.

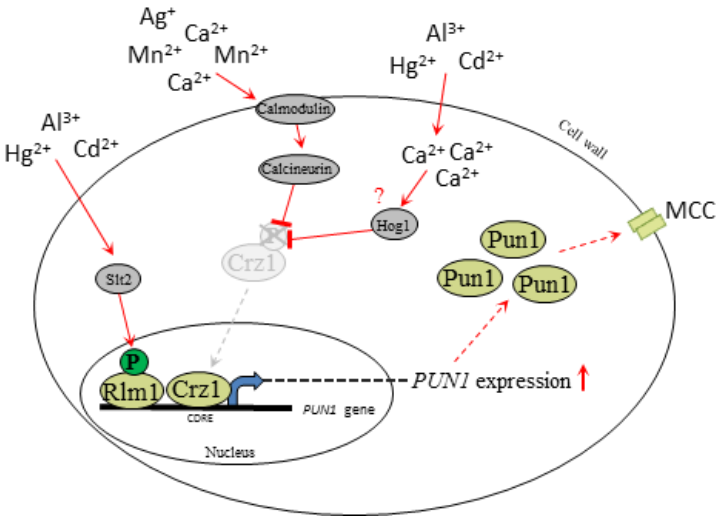

Figure 16. Schematic model of *PUN1* induction under metal stress. For interpretation see text.

3.2.4.4 *Pun1 is required for correct cell wall composition*

Strikingly, we detected that the *pun1*Δ mutant exhibited modified cell morphology in terms of reduced cell size and rounder cell shape compared to wild-type. To this effect we suggested a severe cell wall defect of *pun1*Δ cells. We effectively confirmed an abnormal formation of

cell wall components like 1,3-β-D-glucan, mannoproteins, and chitin in *pun1*Δ by using staining methods, zymolyase assays, and electron microscopy in comparison with wild-type: 1) Staining of these cell wall components in *pun1*Δ revealed weaker fluorescence; 2) Zymolyase treatment showed significantly accelerated cell lyses of *pun1*Δ cells, whilst *PUN1* overexpression in the mutant compensated this effect and even re-established a normal cell morphology compared to *pun1*Δ; 3) Electron microscopy illustrated a dramatically reduced β-glucan layer and a less compact composition of the outer mannoprotein layer within *pun1*Δ cell walls. Moreover, we identified potential sites for protein modification in Pun1 including phosphorylation sites of protein kinase C (PKC), which is a main component of the cell wall integrity signalling pathway (Levin, 2005). The latter findings were in line with our regulatory results of *PUN1* activation.

Taken together, our results pointed to an essential role of Pun1 in cell wall assembly, the maintenance of cell wall integrity, and the regulation of cell wall permeability during stressful environmental impacts such as metal stress. However, it is yet unclear how Pun1 contributes to these metabolic processes and additional work will be necessary to decipher the *de facto* function of Pun1 in rich medium as well as in response to metal stress.

3.4 Conclusions and Outlook

One might compare metal homeostasis with an enormous puzzle. Even though genomic and proteomic screens perpetually provide new insights into metabolic pathways of metal toxicity and detoxification mechanisms, science has only just begun to assemble some small pieces of this puzzle of how organisms effectively cope with toxic concentrations of metal ions. For each type of metal ion that enters a cell, a strictly regulated system of transport and detoxification pathways is activated in relation to the organisms´ environment. The results of our metal stress studies also helped to put some pieces of the puzzle into the right place especially in regard to assigning specific detoxification mechanisms to distinct metal stress conditions, to deciphering dedicated regulatory coherences under metal stress, to itemizing the metabolic changes during adaptation to metal stress, and to the participation of Pun1 and Stb5 in metal stress. However, a number of questions still remain open. Of particular importance will be a systematic study of the highly sophisticated cross-regulations of innumerable transcriptional as well as posttranslational regulators involved in metal toxicity and detoxification processes.

Ideker and his colleagues envision that one day systems-biology algorithms will be developed that enable biologists to perform routine network screens to define novel models of regulation, to identify evolutionary conserved pathways, or to interrogate regulatory circuits responding to the entire spectrum of drugs and human diseases (Ideker *et al.*, 2002).

We are looking forward to this scenario!

4. APPENDIX

4.1 References

Adle DJ, Sinani D, Kim H, Lee J. **A cadmium-transporting P_{1B}-type ATPase in yeast *Saccharomyces cerevisiae*.** J Biol Chem. 2007; 282(2):947-955.

Adle DJ, Lee J. **Expressional control of a cadmium-transporting P_{1B}-type ATPase by a metal sensing degradation signal.** J Biol Chem. 2008; 283(46):31460-31468.

Adle DJ, Wei W, Smith N, Bies JJ, Lee J. **Cadmium-mediated rescue from ER-associated degradation induces expression of its exporter.** Proc Natl Acad Sci U S A. 2009; 106(25):10189-10194.

Aguilar-Barajas E, Díaz-Pérez C, Ramírez-Díaz MI, Riveros-Rosas H, Cervantes C. **Bacterial transport of sulfate, molybdate, and related oxyanions.** Biometals. 2011; 24(4):687-707.

Ahmad S, Kitchin KT, Cullen WR. **Arsenic species that cause release of iron from ferritin and generation of activated oxygen.** Arch Biochem Biophys. 2000; 382(2):195-202.

Ali MA, Ashraf M, Athar HR. **Influence of nickel stress on growth and some important physiological/biochemical attributes in some diverse canola (*Brassica napus* L.) cultivars.** J Hazard Mater. 2009; 172(2-3):964-969.

Al-Saleh I, Al-Sedairi AA. **Mercury (Hg) burden in children: The impact of dental amalgam.** Sci Total Environ. 2011; 409(16):3003-3015.

Alvarez FJ, Douglas LM, Konopka JB. **The Sur7 protein resides in punctate membrane subdomains and mediates spatial regulation of cell wall synthesis in *Candida albicans*.** Commun Integr Biol. 2009; 2(2):76-77.

Aschner M, Aschner JL. **Manganese neurotoxicity: cellular effects and blood-brain barrier transport.** Neurosci Biobehav Rev. 1991; 15(3):333-340.

Au C, Benedetto A, Aschner M**. Manganese transport in eukaryotes: the role of *DMT1*.** Neurotoxicology. 2008; 29(4):569-576.

Aubrecht J, Narla RK, Ghosh P, Stanek J, Uckun FM. **Molecular genotoxicity profiles of apoptosis-inducing vanadocene complexes.** Toxicol Appl Pharmacol. 1999; 154(3):228-235.

Ayed-Boussema I, Abassi H, Bouaziz C, Hlima WB, Ayed Y, Bacha H. **Antioxidative and antigenotoxic effect of vitamin E against patulin cytotoxicity and genotoxicity in HepG2 cells.** Environ Toxicol. 2011; doi: 10.1002/tox.20720. [Epub ahead of print]

Ballatori N. **Transport of toxic metals by molecular mimicry.** Environ Health. 2002; 110(5):689-694.

Banerjee S, Flores-Rozas H. **Cadmium inhibits mismatch repair by blocking the ATPase activity of the *MSH2-MSH6* complex.** Nucleic Acids Res. 2005; 33(4):1410-1419.

Barbier O, Jacquillet G, Tauc M, Cougnon M, Poujeol P. **Effect of heavy metals on, and handling by, the kidney.** Nephron Physiol. 2005; 99(4):105-110.

Basun H, Forssell LG, Wetterberg L, Winbald B. **Metals and trace elements in plasma and cerebrospinal fluid in normal aging and Alzheimer´s disease.** J Neural Transm Park Dis Dement Sect. 1991; 3(4):231-258.

Baysse C, De Vos D, Naudet Y, Vandermonde A, Ochsner U, et al. **Vanadium interferes with siderophore-mediated iron uptake in *Pseudomonas aeruginosa*.** Microbiology. 2000; 146(10):2425-2434.

Beck T, Hall MN. **The TOR signalling pathway controls nuclear localization of nutrient-regulated transcription factors.** Nature. 1999; 402(6762):689-692.

Begley TJ, Rosenbach AS, Ideker T, Samson LD. **Damage recovery pathways in *Saccharomyces cerevisiae* revealed by genomic phenotyping and interactome mapping.** Mol Cancer Res. 2002; 1(2):103-112.

Benini S, Ciurli S, Nolting HF, Mangani S. **X-ray absorption spectroscopy study of native and phenylphosphorodiamidate-inhibited *Bacillus pasteurii* urease.** Eur J Biochem. 1996; 239(1):61-66.

Beyersmann D, Hechtenberg S. **Cadmium, gene regulation, and cellular signalling in mammalian cells.** Toxicol Appl Pharmacol. 1997; 144(2):247-261.

Beyersmann D, Hartwig A. **Carcinogenic metal compounds: recent insight into molecular and cellular mechanisms.** Arch Toxicol. 2008; 82:493-512.

Bhattacharjee H, Carbrey J, Rosen BP, Mukhopadhyay R. **Drug uptake and pharmacological modulation of drug sensitivity in leukemia by AQP9.** Biochem Biophys Res Commun. 2004; 322(3):836-841.

Blaha D, Arous S, Blériot C, Dorel C, Mandrand-Berthelot MA, Rodrigue A. **The *Escherichia coli* metallo-regulator RcnR represses rcnA and rcnR transcription through binding on a shared operator site: Insights into regulatory specificity towards nickel and cobalt.** Biochimie. 2011; 93(3):434-439.

Bolin CM, Basha R, Cox D, Zawia NH, Maloney B, Lahiri DK, Cardozo-Pelaez F. **Exposure to lead and the developmental origin of oxidative DNA damage in the aging brain.** FASEB J. 2006; 20(6):788-790.

Bouganim N, David J, Wysocki R, Ramotar D. **Yap1 overproduction restores arsenite resistance to the ABC transporter deficient mutant *ycf1* by activating *ACR3* expression.** Biochem Cell Biol. 2001; 79(4):441-448.

Breusing N, Grune T. **Regulation of proteasome-mediated protein degradation during oxidative stress and aging.** Biol Chem. 2008; 389(3):203-209.

Broday L, Peng W, Kuo MH, Salnikow K, Zoroddu M, Costa M. **Nickel compounds are novel inhibitors of histone H4 acetylation.** Cancer Res. 2000; 60(2):238-241.

Bun-ya M, Shikata K, Nakade S, Yompakdee C, Harashima S, Oshima Y. **Two new genes, *PHO86* and *PHO87*, involved in inorganic phosphate uptake in *Saccharomyces cerevisiae*.** Curr Genet. 1996; 29(4):344-351.

Carroll S, Wood EJ. **Exposure of human keratinocytes and fibroblasts in vitro to nickel sulphate ions induces synthesis of stress proteins Hsp72 and Hsp90.** Acta Derm Venereol. 2000; 80(2):94-97.

Castelain M. **Globalisation and allergy.** Eur J Dermatol. 2011. [Epub ahead of print]

Causton HC, Ren B, Koh SS, Harbison CT, Kanin E, Jennings EG, Lee TI, True HL, Lander ES, Young RA. **Remodeling of yeast genome expression in response to environmental changes.** Mol Biol Cell. 2001; 12(2):323-337.

Chatziargyriou V, Dailianis S. **The role of selenium-dependent glutathione peroxidase (Se-GPx) against oxidative and genotoxic effects of mercury in haemocytes of mussel *Mytilus galloprovincialis* (Lmk.).** Toxicol In Vitro. 2010; 24(5):1363-1372.

Chavan H, Oruganti M, Krishnamurthy P. **The ATP-binding cassette transporter ABCB6 is induced by arsenic and protects against arsenic cytotoxicity.** Toxicol Sci. 2011; 120(2):519-528.

Chen F, Shi X. **Intracellular signal transduction of cells in response to carcinogenic metals.** Crit Rev Oncol Hematol. 2002; 42:105-121.

Chen H, Davidson T, Singleton S, Garrick MD, Costa M. **Nickel decreases cellular iron level and converts cytosolic aconitase to iron-regulatory protein 1 in A549 cells.** Toxicol Appl Pharmacol. 2005; 206(3):275-287.

Chen H, Ke Q, Kluz T, Yan Y, Costa M. **Nickel ions increase histone H3 lysine 9 dimethylation and induce transgene silencing.** Mol Cell Biol. 2006; 26(10):3728-3737.

Chen H, Giri NC, Zhang R, Yamane K, Zhang Y, Maroney M, Costa M. **Nickel ions inhibit histone demethylase JMJD1A and DNA repair enzyme ABH2 by replacing the ferrous iron in the catalytic centers.** J Biol Chem. 2010; 285(10):7374-7383.

Cheung V, Morley M, Aguilar F, Massimi A, Kucherlapati R, G C. **Making and reading microarrays.** Nat Genet; 1999; 21:15–9.

Chiancone E, Ceci P, Ilari A, Ribacchi F, Stefanini S. **Iron and proteins for iron storage and detoxification.** Biometals. 2004; 17(3):197-202.

Chrestensen CA, Starke DW, Mieyal JJ. **Acute cadmium exposure inactivates thioltransferase (Glutaredoxin), inhibits intracellular reduction of protein-glutathionyl-mixed disulfides, and initiates apoptosis.** J Biol Chem. 2000; 275(34):26556-26565.

Cobbett C, Goldsbrough P. **Phytochelatins and metallothioneins: roles in heavy metal detoxification and homeostasis.** Annu Rev Plant Biol. 2002; 53:159-182.

Colangelo EP, Guerinot ML. **The essential basic helix-loop-helix protein Fit1 is required for the iron deficiency response.** Plant Cell. 2004; 16(12):3400-3412.

Colegio OR, Van Itallie CM, McCrea HJ, Rahner C, Anderson JM. **Claudins create charge-selective channels in the paracellular pathway between epithelial cells.** Am J Physiol Cell Physiol. 2002; 283(1):142-47.

Conrad ME, Umbreit JN, Moore EG. **Iron absorption and transport.** Am J Med Sci. 1999; 318(4):213-229.

Cornett CR, Markesbery WR, Ehmann WD. **Imbalances of trace elements related to oxidative damage in Alzheimer´s disease brain.** Neuro Toxicology 1998; 19(3):339-346.

Costa M, Sutherland JE, Peng W, Salnikow K, Broday L, Kluz T. **Molecular biology of nickel carcinogenesis.** Mol Cell Biochem. 2001; 222(1-2):205-211.

Crans DC, Zhang B, Gaidamauskas E, Keramidas AD, Willsky GR, Roberts CR. **Is vanadate reduced by thiols under biological conditions? Changing the redox potential of V(V)/V(IV) by complexation in aqueous solution.** Inorg Chem. 2010; 49(9):4245-4256.

Culotta VC, Howard WR, Liu XF. ***CRS5* encodes a metallothionein-like protein in *Saccharomyces cerevisiae*.** J Biol Chem. 1994; 269(41):25295-25302.

Dally H, Hartwig A. **Induction and repair inhibition of oxidative DNA damage by nickel(II) and cadmium(II) in mammalian cells.** Carcinogenesis. 1997; 18(5):1021-1026.

Dancis A, Yuan DS, Haile D, Askwith C, Eide D, Moehle C, Kaplan J, Klausner RD. **Molecular characterization of a copper transport protein in *S. cerevisiae*: an unexpected role for copper in iron transport.** Cell. 1994; 76(2):393-402.

Dandrea T, Hellmold H, Jonsson C, Zhivotovsky B, Hofer T, Warngard L, Cotgreave I. **The transcriptosomal response of human A549 lung cells to a hydrogen peroxide-generating system: relationship to DNA damage, cell cycle arrest, and caspase activation.** Free Radic. Biol. Med. 2004; 36(7):881-896.

Davletova S, Schlauch K, Coutu J, Mittler R. **The zinc-finger protein Zat12 plays a central role in reactive oxygen and abiotic stress signaling in *Arabidopsis*.** Plant Physiol. 2005; 139(2):847-856.

Delaunay A, Isnard AD, Toledano MB. **H_2O_2 sensing through oxidation of the Yap1 transcription factor.** EMBO J. 2000; 19(19):5157-5166.

Dickey AN, Yim WS, Faller R. **Using ergosterol to mitigate the deleterious effects of ethanol on bilayer structure.** J Phys Chem B. 2009; 113(8):2388-2397.

Dix DR, Bridgham JT, Broderius MA, Byersdorfer CA, Eide DJ. **The *FET4* gene encodes the low affinity Fe(II) transport protein of *Saccharomyces cerevisiae*.** J Biol Chem. 1994; 269(42):26092-26099.

Dizdaroglu M, Jaruga P, Birincioglu M, Rodriguez H. **Free radical-induced damage to DNA: mechanisms and measurement.** Free Radic Biol Med. 2002; 32(11):1102-15.

Dormer UH, Westwater J, Stephen DW, Jamieson DJ. **Oxidant regulation of the *Saccharomyces cerevisiae GSH1* gene.** Biochim Biophys Acta. 2002; 1576(1-2):23-29.

Dürr G, Strayle J, Plemper R, Elbs S, Klee SK, Catty P, Wolf DH, Rudolph HK. **The medial-Golgi ion pump Pmr1 supplies the yeast secretory pathway with Ca^{2+} and Mn^{2+} required for glycosylation, sorting, and endoplasmic reticulum-associated protein degradation.** Mol Biol Cell. 1998; 9(5):1149-1162.

Durchschlag E, Reiter W, Ammerer G, Schüller C. **Nuclear localization destabilizes the stress-regulated transcription factor Msn2.** J Biol Chem. 2004; 279(53):55425-55432.

Dziadkowiec D, Krasowska A, Liebner A, Sigler K. **Protective role of mitochondrial superoxide dismutase against high osmolarity, heat and metalloid stress in *Saccharomyces cerevisiae*.** Folia Microbiol (Praha). 2007; 52(2):120-126.

Ecker DJ, Butt TR, Sternberg EJ, Neeper MP, Debouck C, Gorman JA, Crooke ST. **Yeast metallothionein function in metal ion detoxification.** J Biol Chem. 1986; 261(36):16895-16900.

Eguez L, Chung YS, Kuchibhatla A, Paidhungat M, Garrett S. **Yeast Mn^{2+} transporter, Smf1p, is regulated by ubiquitin-dependent vacuolar protein sorting.** Genetics. 2004; 167(1):107-117.

Ercal N, Gurer-Orhan H, Aykin-Burns N. **Toxic metals and oxidative stress part I: mechanisms involved in metal-induced oxidative damage.** Curr Top Med Chem. 2001; 1(6):529-539.

Ertekin MV, Tekin SB, Erdogan F, Karslioglu I, Gepdiremen A, Sezen O, Balci E, Gündogdu C. **The effect of zinc sulphate in the prevention of radiation-induced dermatitis.** J Radiat Res (Tokyo). 2004; 45(4):543-548.

Ezaki B, Gardner RC, Ezaki Y, Kondo H, Matsumoto H. **Protective roles of two aluminum (Al)-induced genes, *HSP150* and *SED1* of *Saccharomyces cerevisiae*, in Al and oxidative stresses.** FEMS Microbiol Lett. 1998; 159(1):99-105.

Ezaki B, Sasaki K, Matsumoto H, Nakashima S. **Functions of two genes in aluminium (Al) stress resistance: repression of oxidative damage by the *AtBCB* gene and promotion of efflux of Al ions by the *NtGDI1*gene.** J Exp Bot. 2005; 56(420):2661-2671.

Fabrizio P, Pozza F, Pletcher SD, Gendron CM, Longo VD. **Regulation of longevity and stress resistance by Sch9 in yeast.** Science. 2001; 292(5515):288-290.

Farcasanu IC, Hirata D, Tsuchiya E, Nishiyama F, Miyakawa T. **Protein phosphatase 2B of *Saccharomyces cerevisiae* is required for tolerance to manganese, in blocking the entry of ions into the cells.** Eur J Biochem. 1995; 232(3):712-717.

Farcasanu IC, Mizunuma M, Nishiyama F, Miyakawa T. **Role of L-histidine in conferring tolerance to Ni^{2+} in *Sacchromyces cerevisiae* cells.** Biosci Biotechnol Biochem. 2005; 69(12):2343-2348.

Fauchon M, Lagniel G, Aude JC, Lombardia L, Soularue P, Petat C, Marguerie G, Sentenac A, Werner M, Labarre J. **Sulfur sparing in the yeast proteome in response to sulfur demand.** Mol Cell. 2002; 9(4):713-723.

Ferguson SB, Anderson ES, Harshaw RB, Thate T, Craig NL, Nelson HCM. **Protein kinase A regulates constitutive expression of small heat shock genes in an Msn2/4p-independent and Hsf1p-dependent manner in *Saccharomyces cerevisiae*.** Genetics. 2004; 169:1203-1214.

Figueiredo-Pereira ME, Yakushin S, Cohen G. **Disruption of the intracellular sulfhydryl homeostasis by cadmium-induced oxidative stress leads to protein thiolation and ubiquitination in neuronal cells**. JBC. 1998; 273:12703-12709.

Fingerman I, Nagaraj V, Norris D, Vershon AK. **Sfp1 plays a key role in yeast ribosome biogenesis.** Eukaryot Cell. 2003; 2(5):1061-1068.

Finley JW. **Manganese absorption and retention by young women is associated with serum ferritin concentration.** Am J Clin Nutr. 1999; 70(1):37-43.

Fitsanakis VA, Zhang N, Garcia S, Aschner M. **Manganese (Mn) and iron (Fe): Interdependency of transport and regulation.** Neurotox Res. 2009; 18(2):124-131.

Flora SJ. **Arsenic-induced oxidative stress and its reversibility.** Free Radic Biol Med. 2011; 51(2):257-281.

Forte G, Petrucci F, Bocca B. **Metal allergens of growing significance: epidemiology, immunotoxicology, strategies for testing and prevention.** Inflamm Allergy Drug Targets. 2008; 7(3):145-162.

Fraga CG. **Relevance, essentiality and toxicity of trace elements in human health.** Mol Aspects Med. 2005; 26(4-5):235-244.

Freitas M, Gomes A, Porto G, Fernandes E. **Nickel induces oxidative burst, NF-κB activation and interleukin-8 production in human neutrophils.** J Biol Inorg Chem. 2010; 15(8):1275-1283.

Fulle S, Di Donna S, Puglielli C, Pietrangelo T, Beccafico S, Bellomo R, Protasi F, Fanò G. **Age-dependent imbalance of the antioxidative system in human satellite cells.** Exp Gerontol. 2005; 40(3):189-197.

Furuchi T, Hwang GW, Naganuma A. **Overexpression of the ubiquitin-conjugating enzyme Cdc34 confers resistance to methylmercury in *Saccharomyces cerevisiae*.** Mol Pharmacol. 2002; 61(4):738-741.

Furukawa J, Yamaji N, Wang H, Mitani N, Murata Y, Sato K, Katsuhara M, Takeda K, Ma JF. **An aluminum-activated citrate transporter in barley.** Plant Cell Physiol. 2007; 48(8):1081-1091.

Furuse M, Fujita K, Hiiragi T, Fujimoto K, Tsukita S. **Claudin-1 and -2: novel integral membrane proteins localizing at tight junctions with no sequence similarity to occludin.** J Cell Biol. 1998; 141(7):1539-1550.

Gachot B, Tauc M, Morat L, Poujeol P. **Zinc uptake by proximal cells isolated from rabbit kidney: effects of cysteine and histidine.** Pflugers Arch. 1991; 419(6):583-587.

García R, Bermejo C, Grau C, Pérez R, Rodríguez-Peña JM, Francois J, Nombela C, Arroyo J. **The global transcriptional response to transient cell wall damage in *Saccharomyces cerevisiae* and its regulation by the cell integrity signaling pathway.** J Biol Chem. 2004; 279(15):15183-15195.

García R, Rodríguez-Peña JM, Bermejo C, Nombela C, Arroyo J. **The high osmotic response and cell wall integrity pathways cooperate to regulate transcriptional responses to zymolyase-induced cell wall stress in *Saccharomyces cerevisiae*.** J Biol Chem. 2009; 284(16):10901-10911.

Garrett-Engele P, Moilanen B, Cyert MS. **Calcineurin, the Ca^{2+}/calmodulin-dependent protein phosphatase, is essential in yeast mutants with cell integrity defects and in mutants that lack a functional vacuolar $H(^{+})$-ATPase.** Mol Cell Biol. 1995; 15(8):4103-4114.

Gasch AP, Spellman PT, Kao CM, Cermel-Harel O, Eisen MB, Storz G, Botstein D, Brown PO. **Genomic expression programs in the response of yeast cells to environmental changes.** Mol. Cell. Biol. 2000; 11:4241-4267.

Ghosh M, Shen J, Rosen BP. **Pathways of As(III) detoxification in *Saccharomyces cerevisiae*.** Proc Natl Acad Sci U S A. 1999; 96(9):5001-5006.

Gitan RS, Eide DJ. **Zinc-regulated ubiquitin conjugation signals endocytosis of the yeast *ZRT1* zinc transporter.** Biochem J. 2000; 346(2):329-336.

Gitan RS, Shababi M, Kramer M, Eide DJ. **A cytosolic domain of the yeast Zrt1 zinc transporter is required for its post-translational inactivation in response to zinc and cadmium.** J Biol Chem. 2003; 278(41):39558-39564.

Gounalaki N and Thireos G. **Yap1p, a yeast transcriptional activator that mediates multidrug resistance, regulates the metabolic stress response.** EMBO J. 1994; 13:4036-4041.

Grant CM, Perrone G, Dawes IW. **Glutathione and catalase provide overlapping defenses for protection against hydrogen peroxide in the yeast *Saccharomyces cerevisiae*.** Biochem Biophys Res Commun. 1998; 253(3):893-898.

Grant CM. **Role of the glutathione/glutaredoxin and thioredoxin systems in yeast growth and response to stress conditions.** Mol Microbiol. 2001; 39(3):533-541.

Graschopf A, Stadler JA, Hoellerer MK, Eder S, Sieghardt M, Kohlwein SD, Schweyen RJ. **The yeast plasma membrane protein Alr1 controls Mg^{2+} homeostasis and is subject to Mg^{2+}-dependent control of its synthesis and degradation.** J Biol Chem. 2001; 276(19):16216-16222.

Grass G, Fricke B, Nies DH. **Control of expression of a periplasmic nickel efflux pump by periplasmic nickel concentrations.** Biometals. 2005; 18(4):437-448.

Greetham D, Grant CM. **Antioxidant activity of the yeast mitochondrial one-Cys peroxiredoxin is dependent on thioredoxin reductase and glutathione in vivo.** Mol Cell Biol. 2009; 29(11):3229-3240.

Greetham D, Vickerstaff J, Shenton D, Perrone GG, Dawes IW, Grant CM. **Thioredoxins function as deglutathionylase enzymes in the yeast *Saccharomyces cerevisiae*.** BMC Biochem. 2010; 11:3.

Griffioen G, Anghileri P, Imre E, Baroni MD, Ruis H. **Nutritional control of nucleocytoplasmic localization of cAMP-dependent protein kinase catalytic and regulatory subunits in *Saccharomyces cerevisiae*.** J Biol Chem. 2000; 275(2):1449-1456.

Gross C, Kelleher M, Iyer VR, Brown PO, Winge DR. **Identification of the copper regulon in *Saccharomyces cerevisiae* by DNA microarrays.** J Biol Chem. 2000; 275(41):32310-32316.

Grossmann G, Malinsky J, Stahlschmidt W, Loibl M, Weig-Meckl I, Frommer WB, Opekarová M, Tanner W. **Plasma membrane microdomains regulate turnover of transport proteins in yeast.** J Cell Biol. 2008; 183(6):1075-1088.

Gueldry O, Lazard M, Delort F, Dauplais M, Grigoras I, Blanquet S, Plateau P. **Ycf1p-dependent Hg(II) detoxification in *Saccharomyces cerevisiae*.** Eur J Biochem. 2003; 270(11):2486-2496.

Gunshin H, Mackenzie B, Berger UV, Gunshin Y, Romero MF, Boron WF, Nussberger S, Gollan JL, Hediger MA. **Cloning and characterization of a mammalian proton-coupled metal-ion transporter.** Nature. 1997; 388(6641):482-488.

Hall JL. **Cellular mechanisms for heavy metal detoxification and tolerance.** J Exp Bot. 2002; 53(366):1-11.

Halliwell B, Gutteridge JM. **Oxygen toxicity, oxygen radicals, transition metals and disease.** Biochem J. 1984; 219(1):1-14.

Han YH, Kim SH, Kim SZ, Park WH. **Apoptosis in arsenic trioxide-treated Calu-6 lung cells is correlated with the depletion of GSH levels rather than the changes of ROS levels.** J Cell Biochem. 2008; 104(3):862-878.

Han SG, Castranova V, Vallyathan V. **Heat shock protein 70 as an indicator of early lung injury caused by exposure to arsenic.** Mol Cell Biochem. 2005; 277(1-2):153-164.

Han Y, Zhang W, Zhang B, Zhang S, Wang W, Ming F. **One novel mitochondrial citrate synthase from *Oryza sativa* L. can enhance aluminum tolerance in transgenic tobacco.** Mol Biotechnol. 2009; 42(3):299-305.

Hansen JM, Zhang H, Jones DP. **Differential oxidation of thioredoxin-1, thioredoxin-2, and glutathione by metal ions.** Free Radic Biol Med. 2006; 40(1):138-145.

Hara M, Fujinaga M, Kuboi T. **Metal binding by citrus dehydrin with histidine-rich domains.** J Exp Bot. 2005; 56(420):2695-2703.

Hardwick JS, Kuruvilla FG, Tong JK, Shamji AF, Schreiber SL**. Rapamycin-modulated transcription defines the subset of nutrient-sensitive signaling pathways directly controlled by the Tor proteins.** Proc. Natl. Acad. Sci. USA. 1999; 96:14866–14870.

Hartwig A. **Zinc finger proteins as potential targets for toxic metal ions: differential effects on structure and function.** Antioxid Redox Signal. 2001; 3(4):625-634.

Hassinen VH, Tervahauta AI, Schat H, Kärenlampi SO. **Plant metallothioneins--metal chelators with ROS scavenging activity?** Plant Biol (Stuttg). 2011; 13(2):225-232.

Haugen AC, Kelley R, Collins JB, Tucker CJ, Deng C, Afshari CA, Brown JM, Ideker T, Van Houten B. **Integrating phenotypic and expression profiles to map arsenic-response networks.** Genome Biol. 2004; 5(12):R95.

Hosiner D, Lempiäinen H, Reiter W, Urban J, Loewith R, Ammerer G, Schweyen R, Shore D, Schüller C. **Arsenic toxicity to *Saccharomyces cerevisiae* is a consequence of inhibition of the TORC1 kinase combined with a chronic stress response.** Mol Biol Cell. 2009; 20(3):1048-1057.

Huang HL, Brandriss MC. **The regulator of the yeast proline utilization pathway is differentially phosphorylated in response to the quality of the nitrogen source.** Mol Cell Biol. 2000; 20(3):892-899.

Huber A, French SL, Tekotte H, Yerlikaya S, Stahl M, Perepelkina MP, Tyers M, Rougemont J, Beyer AL, Loewith R. **Sch9 regulates ribosome biogenesis via Stb3, Dot6 and Tod6 and the histone deacetylase complex RPD3L.** EMBO J. 2011; 30(15):3052-3064.

Hussain T, Shukla GS, Chandra SV. **Effects of cadmium on superoxide dismutase and lipid peroxidation in liver and kidney of growing rats. In vivo and in vitro studies**. Pharmacol Toxicol. 1987; 60:355-358.

Hwang GW, Furuchi T, Naganuma A. **The ubiquitin-conjugating enzymes, Ubc4 and Cdc34, mediate cadmium resistance in budding yeast through different mechanisms.** Life Sci. 2008; 82(23-24):1182-1185.

Ideker T, Thorsson V, Ranish JA, Christmas R, Buhler J, Eng JK, Bumgarner R, Goodlett DR, Aebersold R, Hood L. **Integrated genomic and proteomic analyses of a systematically perturbed metabolic network.** Science. 2001; 292(5518):929-934.

Ideker T, Ozier O, Schwikowski B, Siegel AF. **Discovering regulatory and signalling circuits in molecular interaction networks.** Bioinformatics. 2002; 18(Suppl 1):S233-240.

Iida H, Nakamura H, Ono T, Okumura MS, Anraku Y. ***MID1*, a novel *Saccharomyces cerevisiae* gene encoding a plasma membrane protein, is required for Ca^{2+} influx and mating.** Mol Cell Biol. 1994; 14(12):8259-8271.

Ivison SM, Wang C, Himmel ME, Sheridan J, Delano J, Mayer ML, Yao Y, Kifayet A, Steiner TS. **Oxidative stress enhances IL-8 and inhibits CCL20 production from intestinal epithelial cells in response to bacterial flagellin.** Am J Physiol Gastrointest Liver Physiol. 2010; 299(3):G733-741.

Jan AT, Ali A, Haq Q. **Glutathione as an antioxidant in inorganic mercury induced nephrotoxicity.** J Postgrad Med. 2011; 57(1):72-77.

Jensen LT, Howard WR, Strain JJ, Winge DR, Culotta VC. **Enhanced effectiveness of copper ion buffering by *CUP1* metallothionein compared with *CRS5* metallothionein in *Saccharomyces cerevisiae*.** J Biol Chem. 1996; 271(31):18514-18519.

Jensen LT, Ajua-Alemanji M, Culotta VC. **The *Saccharomyces cerevisiae* high affinity phosphate transporter encoded by *PHO84* also functions in manganese homeostasis.** J Biol Chem. 2003; 278(43):42036-42040.

Jensen LT, Carroll MC, Hall MD, Harvey CJ, Beese SE, Culotta VC. **Down-regulation of a manganese transporter in the face of metal toxicity.** Mol Biol Cell. 2009; 20(12):2810-2819.

Jin YH, Clark AB, Slebos RJ, Al-Refai H, Taylor JA, Kunkel TA, Resnick MA, Gordenin DA. **Cadmium is a mutagen that acts by inhibiting mismatch repair.** Nat Genet. 2003; 34(3):326-329.

Jin YH, Dunlap PE, McBride SJ, Al-Refai H, Bushel PR, Freedman JH. **Global transcriptome and deletome profiles of yeast exposed to transition metals.** PLoS Genet. 2008; 4(4):e1000053.

Jorgensen P, Nishikawa JL, Breitkreutz BJ, Tyers M**. Systematic identification of pathways that couple cell growth and division in yeast.** Science. 2002; 297:395-400.

Jorgensen P, Rupes I, Sharom JR, Schneper L, Broach JR, Tyers M. **A dynamic transcriptional network communicates growth potential to ribosome synthesis and critical cell size.** Genes Dev. 2004; 18(20):2491-2505.

Jomova K, Valko M. **Advances in metal-induced oxidative stress and human disease.** Toxicology. 2011; 283(2-3):65-87.

Jung US, Levin DE. **Genome-wide analysis of gene expression regulated by the yeast cell wall integrity signalling pathway.** Mol Microbiol. 1999; 34(5):1049-1057.

Jung US, Sobering AK, Romeo MJ, Levin DE. **Regulation of the yeast Rlm1 transcription factor by the Mpk1 cell wall integrity MAP kinase.** Mol Microbiol. 2002; 46(3):781-789.

Kaluarachchi H, Chan Chung KC, Zamble DB. **Microbial nickel proteins.** Nat Prod Rep. 2010; 27(5):681-694.

Kanik-Ennulat C, Neff N. **Vanadate-resistant mutants of *Saccharomyces cerevisiae* show alterations in protein phosphorylation and growth control.** Mol Cell Biol. 1990; 10(3):898-909.

Karaczyn AA, Golebiowski F, Kasprzak KS. **Ni(II) affects ubiquitination of core histones H2B and H2A.** Exp Cell Res. 2006; 312(17):3252-3259.

Kasprzak KS. **Possible role of oxidative damage in metal-induced carcinogenesis.** Cancer Invest. 1995; 13(4):411-430.

Kasprzak KS, Sunderman FW Jr, Salnikow K. **Nickel carcinogenesis.** Mutat Res. 2003; 533(1-2):67-97.

Ke Q, Davidson T, Chen H, Kluz T, Costa M. **Alterations of histone modifications and transgene silencing by nickel chloride.** Carcinogenesis. 2006; 27(7):1481-1488.

Keen CL, Ensunsa JL, Watson MH, et al. **Nutritional aspects of manganese from experimental studies.** Neurotoxicology. 1999; 20(2-3):213-223.

Kennett EC, Rees MD, Malle E, Hammer A, Whitelock JM, Davies MJ. **Peroxynitrite modifies the structure and function of the extracellular matrix proteoglycan perlecan by reaction with both the protein core and the heparan sulfate chains.** Free Radic Biol Med. 2010; 49(2):282-293.

Kern AL, Bonatto D, Dias JF, Yoneama ML, Brendel M, Pêgas Henriques JA. **The function of Alr1p of *Saccharomyces cerevisiae* in cadmium detoxification: insights from phylogenetic studies and particle-induced X-ray emission.** Biometals. 2005; 18(1):31-41.

Khan H, Khan MF, Asim-ur-Rehman, Jan SU, Ullah N. **The protective role of glutathione in silver induced toxicity in blood components.** Pak J Pharm Sci. 2011; 24(2):123-128.

Khanna S, Lakhera PC, Khandelwal S. **Interplay of early biochemical manifestations by cadmium insult in sertoli-germ coculture: An in vitro study.** Toxicology. 2011; 287(1-3):46-53.

Klein C, Struhl K. **Protein kinase A mediates growth-regulated expression of yeast ribosomal protein genes by modulating *RAP1* transcriptional activity.** Mol. Cell. Biol. 1994; 14: 1920-1928.

Klein M, Mamnun YM, Eggmann T, Schüller C, Wolfger H, Martinoia E, Kuchler K. **The ATP-binding cassette (ABC) transporter Bpt1p mediates vacuolar sequestration of glutathione conjugates in yeast.** FEBS Lett. 2002; 520(1-3):63-67.

Korshunova YO, Eide D, Clark WG, Guerinot ML, Pakrasi HB. **The *IRT1* protein from *Arabidopsis thaliana* is a metal transporter with a broad substrate range.** Plant Mol Biol. 1999; 40(1):37-44.

Lafaye A, Junot C, Pereira Y, Lagniel G, Tabet JC, Ezan E, Labarre J. **Combined proteome and metabolite-profiling analyses reveal surprising insights into yeast sulfur metabolism.** J Biol Chem. 2005; 280(26):24723-24730.

La Fontaine S, Mercer JF. **Trafficking of the copper-ATPases, ATP7A and ATP7B: role in copper homeostasis.** Arch Biochem Biophys. 2007; 463(2):149-167.

Lagorce A, Hauser NC, Labourdette D, Rodriguez C, Martin-Yken H, Arroyo J, Hoheisel JD, François J. **Genome-wide analysis of the response to cell wall mutations in the *yeast Saccharomyces cerevisiae*.** J Biol Chem. 2003; 278(22):20345-20357.

Larochelle M, Drouin S, Robert F, Turcotte B. **Oxidative stress-activated zinc cluster protein Stb5 has dual activator/repressor functions required for pentose phosphate pathway regulation and NADPH production.** Mol Cell Biol. 2006; 26(17):6690-6701.

Lashkari D, DeRisi J, McCusker J, Namath A, Gentile C, Hwang S, Brown P, Davis R. **Yeast microarrays for genome wide parallel genetic and gene expression analysis**. Proc Natl Acad Sci USA, 1997; 94(24):13057–1306.

Lau WT, Howson RW, Malkus P, Schekman R, O'Shea EK. **Pho86p, an endoplasmic reticulum (ER) resident protein in *Saccharomyces cerevisiae*, is required for ER exit of the high-affinity phosphate transporter Pho84p.** Proc Natl Acad Sci U S A. 2000; 97(3):1107-1112.

Lazard M, Ha-Duong NT, Mounié S, Perrin R, Plateau P, Blanquet S. **Selenodiglutathione uptake by the *Saccharomyces cerevisiae* vacuolar ATP-binding cassette transporter Ycf1p.** FEBS J. 2011; 278(21):4112-4121.

Ledwidge R, Patel B, Dong A, Fiedler D, Falkowski M, Zelikova J, Summers AO, Pai EF, Miller SM. **NmerA, the metal binding domain of mercuric ion reductase, removes Hg^{2+} from proteins, delivers it to the catalytic core, and protects cells under glutathione-depleted conditions.** Biochemistry. 2005; 44(34):11402-11416.

Lee J, Godon C, Lagniel G, Spector D, Garin J, Labarre J, Toledano MB. **Yap1 and Skn7 control two specialized oxidative stress response regulons in yeast.** J Biol Chem. 1999; 274(23):16040-16046.

Lee YW, Klein CB, Kargacin B, Salnikow K, Kitahara J, Dowjat K, Zhitkovich A, Christie NT, Costa M. **Carcinogenic nickel silences gene expression by chromatin condensation and DNA methylation: a new model for epigenetic carcinogens.** Mol Cell Biol. 1995; 15(5):2547-2557.

Lempiäinen H, Uotila A, Urban J, Dohnal I, Ammerer G, Loewith R, Shore D. **Sfp1 interaction with TORC1 and Mrs6 reveals feedback regulation on TOR signaling.** Mol Cell. 2009; 33(6):704-716.

Leonard S, Gannett PM, Rojanasakul Y, Schwegler-Berry D, Castranova V, Vallyathan V, Shi X. **Cobalt-mediated generation of reactive oxygen species and its possible mechanism.** J Inorg Biochem. 1998; 70(3-4):239-244.

Leonard SS, Harris GK, Shi X. **Metal-induced oxidative stress and signal transduction.** Free Radic Biol Med. 2004; 37(12):1921-1942.

Lesuisse E, Labbe P. **Effects of cadmium and of *YAP1* and *CAD1/YAP2* genes on iron metabolism in the yeast *Saccharomyces cerevisiae*.** Microbiology. 1995; 141(11):2937-2943.

Levin DE. **Cell wall integrity signaling in *Saccharomyces cerevisiae*.** Microbiol Mol Biol Rev. 2005; 69(2):262-291.

Li B, Nierras CR, Warner JR. **Transcriptional elements involved in the repression of ribosomal protein synthesis.** Mol Cell Biol. 1999 Aug;19(8):5393-5404.

Li H, Tsang CK, Watkins M, Bertram PG, Zheng XF. **Nutrient regulates Tor1 nuclear localization and association with rDNA promoter.** Nature. 2006; 442(7106):1058-1061.

Li X, Qian J, Wang C, Zheng K, Ye L, Fu Y, Han N, Bian H, Pan J, Wang J, Zhu M. **Regulating cytoplasmic calcium homeostasis can reduce aluminum toxicity in yeast.** PLoS One. 2011; 6(6):e21148.

Li ZS, Szczypka M, Lu YP, Thiele DJ, Rea PA. **The yeast cadmium factor protein (*YCF1*) is a vacuolar glutathione S-conjugate pump.** J Biol Chem. 1996; 271(11):6509-6517.

Li ZS, Lu YP, Zhen RG, Szczypka M, Thiele DJ, Rea PA. **A new pathway for vacuolar cadmium sequestration in *Saccharomyces cerevisiae*: *YCF1*-catalyzed transport of bis(glutathionato) cadmium.** Proc Natl Acad Sci U S A. 1997; 94(1):42-47.

Liu SX, Davidson MM, Tang X, Walker WF, Athar M, Ivanov V, Hei TK. **Mitochondrial damage mediates genotoxicity of arsenic in mammalian cells.** Cancer Res. 2005; 65(8):3236-3242.

Liu Z, Shen J, Carbrey JM, Mukhopadhyay R, Agre P, Rosen BP. **Arsenite transport by mammalian aquaglyceroporins AQP7 and AQP9.** Proc Natl Acad Sci U S A. 2002; 99(9):6053-6058.

Liu Z, Boles E, Rosen BP. **Arsenic trioxide uptake by hexose permeases in *Saccharomyces cerevisiae*.** J Biol Chem. 2004; 279(17):17312-17318.

Long Y, Li Q, Li J, Cui Z. **Molecular analysis, developmental function and heavy metal-induced expression of *ABCC5* in zebrafish.** Comp Biochem Physiol B Biochem Mol Biol. 2011; 158(1):46-55.

Lorico A, Bertola A, Baum C, Fodstad O, Rappa G. **Role of the Multidrug Resistance Protein 1 in protection from heavy metal oxyanions: investigations in vitro and in *MRP1*-deficient mice.** Biochem Biophys Res Commun. 2002; 291(3):617-622.

Lucau-Danila A, Lelandais G, Kozovska Z, Tanty V, Delaveau T, Devaux F, Jacq C. **Early expression of yeast genes affected by chemical stress.** Mol Cell Biol. 2005; 25(5):1860-1868.

Lupetti A, Danesi R, Campa M, Del Tacca M, Kelly S. **Molecular basis of resistance to azole antifungals.** Trends Mol Med. 2002; 8(2):76-81.

Lynn S, Gurr JR, Lai HT, Jan KY. **NADH oxidase activation is involved in arsenite-induced oxidative DNA damage in human vascular smooth muscle cells.** Circ Res. 2000; 86(5):514-519.

Ma JF, Ryan PR, Delhaize E. **Aluminium tolerance in plants and the complexing role of organic acids.** Trends Plant Sci. 2001; 6(6):273-278.

Macara IG, Kustin K, Cantley LC Jr. **Glutathione reduces cytoplasmic vanadate. Mechanism and physiological implications.** Biochim Biophys Acta. 1980; 629(1):95-106.

MacDiarmid CW, Gardner RC. **Overexpression of the *Saccharomyces cerevisiae* magnesium transport system confers resistance to aluminum ion.** J Biol Chem. 1998; 273(3):1727-1732.

MacDiarmid CW, Gaither LA, Eide D. **Zinc transporters that regulate vacuolar zinc storage in *Saccharomyces cerevisiae*.** EMBO J. 2000; 19(12):2845-2855.

Maciaszczyk-Dziubinska E, Migdal I, Migocka M, Bocer T, Wysocki R. **The yeast aquaglyceroporin Fps1p is a bidirectional arsenite channel.** FEBS Lett. 2010; 584(4):726-732.

Mackenzie B, Hediger MA. **SLC11 family of H^+-coupled metal-ion transporters NRAMP1 and DMT1.** Pflugers Arch. 2004; 447(5):571-579.

Mager W and De Kruijff A. **Stress-induced transcriptional activation.** Microbiol. rev. 1995; 59(3):506–531.

Mahanty SK, Khaware R, Ansari S, Gupta P, Prasad R. **Vanadate-resistant mutants of *Candida albicans* show alterations in phosphate uptake.** FEMS Microbiol Lett. 1991; 68(2):163-166.

Marion RM, Regev A, Segal E, Barash Y, Koller D, Friedman N, O'Shea EK. **Sfp1 is a stress- and nutrient-sensitive regulator of ribosomal protein gene expression.** Proc Natl Acad Sci U S A. 2004; 101(40):14315-14322.

Martin DE, Soulard A, Hall MN. **TOR regulates ribosomal protein expression via PKA and the forkhead transcription factor *FHL1*.** Cell. 2004; 119:969-979.

Martínez-Pastor MT, Marchler G, Schüller C, Marchler-Bauer A, Ruis H, Estruch F. **The *Saccharomyces cerevisiae* zinc finger proteins Msn2p and Msn4p are required for transcriptional induction through the stress response element (STRE).** EMBO J. 1996; 15(9):2227-2235.

Matheos DP, Kingsbury TJ, Ahsan US, Cunningham KW. **Tcn1p/Crz1p, a calcineurin-dependent transcription factor that differentially regulates gene expression in *Saccharomyces cerevisiae*.** Genes Dev. 1997; 11(24):3445-3458.

Menezes RA, Amaral C, Delaunay A, Toledano M, Rodrigues-Pousada C. **Yap8p activation in *Saccharomyces cerevisiae* under arsenic conditions.** FEBS Lett. 2004; 566(1-3):141-146.

Meng YL, Liu Z, Rosen BP. **As(III) and Sb(III) uptake by GlpF and efflux by ArsB in *Escherichia coli*.** J Biol Chem. 2004; 279(18):18334-18341.

Mielniczki-Pereira AA, Schuch AZ, Bonatto D, Cavalcante CF, Vaitsman DS, Riger CJ, Eleutherio EC, Henriques JA. **The role of the yeast ATP-binding cassette Ycf1p in glutathione and cadmium ion homeostasis during respiratory metabolism.** Toxicol Lett. 2008; 180(1):21-27.

Milczarek R, Sokolowska E, Hallmann A, Klimek J. **The NADPH- and iron-dependent lipid peroxidation in human placental microsomes.** Mol Cell Biochem. 2007; 295(1-2):105-111.

Mitic LL, Unger VM, Anderson JM. **Expression, solubilization, and biochemical characterization of the tight junction transmembrane protein claudin-4.** Protein Sci. 2003; 12(2):218-227.

Moen B, Hollund B, Riise T. **Neurological symptoms among dental assistants: a cross-sectional study.** J Occup Med Toxicol. 2008; 3:10.

Momose Y, Iwahashi H. **Bioassay of cadmium using a DNA microarray: genome-wide expression patterns of *Saccharomyces cerevisiae* response to cadmium.** Environ Toxicol Chem. 2001; 20(10):2353-2360.

Montgomery KS, Mackey J, Thuett K, Ginestra S, Bizon JL, Abbott LC. **Chronic, low-dose prenatal exposure to methylmercury impairs motor and mnemonic function in adult C57/B6 mice.** Behav Brain Res. 2008; 191(1):55-61.

Morita K, Furuse M, Fujimoto K, Tsukita S. **Claudin multigene family encoding four-transmembrane domain protein components of tight junction strands.** Proc Natl Acad Sci U S A. 1999; 96(2):511-516.

Mørk A, Geisler A. **Calmodulin-dependent adenylate cyclase activity in rat cerebral cortex: effects of divalent cations, forskolin and isoprenaline.** Arch Int Physiol Biochim. 1989; 97(3):259-271.

Mukhopadhyay R, Shi J, Rosen BP. **Purification and characterization of Acr2p, the *Saccharomyces cerevisiae* arsenate reductase.** J Biol Chem. 2000; 275(28):21149-21157.

Mutter J, Naumann J, Sadaghiani C, Schneider R, Walach H. **Alzheimer disease: mercury as pathogenetic factor and apolipoprotein E as a moderator.** Neuro Endocrinol Lett. 2004; 25(5):331-339.

Nagy Z, Montigny C, Leverrier P, Yeh S, Goffeau A, Garrigos M, Falson P. **Role of the yeast ABC transporter Yor1p in cadmium detoxification.** Biochimie. 2006; 88(11):1665-1671.

Nash RA. **Metals in medicine.** Altern Ther Health Med. 2005; 11(4):18-25.

Natarajan K, Meyer MR, Jackson BM, Slade D, Roberts C, Hinnebusch AG, Marton MJ. **Transcriptional profiling shows that Gcn4p is a master regulator of gene expression during amino acid starvation in yeast.** Mol Cell Biol. 2001; 21(13):4347-4368.

Nelson N. **Metal ion transporters and homeostasis.** EMBO J. 1999; 18(16):4361-4371.

Nies DH. **Microbial heavy-metal resistance.** Appl Microbiol Biotechnol. 1999; 51(6):730-750.

Nies DH. **Efflux-mediated heavy metal resistance in prokaryotes.** FEMS Microbiol Rev. 2003; 27(2-3):313-339.

Nikko E, Sullivan JA, Pelham HR. **Arrestin-like proteins mediate ubiquitination and endocytosis of the yeast metal transporter Smf1.** EMBO Rep. 2008; 9(12):1216-1221.

Nilius B, Prenen J, Janssens A, Voets T, Droogmans G. **Decavanadate modulates gating of TRPM4 cation channels.** J Physiol. 2004; 560(3):753-765.

Olanow CW. **Manganese-induced parkinsonism and Parkinson's disease.** Ann N Y Acad Sci. 2004; 1012:209-223.

Owsianik G, Balzi l L, Ghislain M. **Control of 26S proteasome expression by transcription factors regulating multidrug resistance in *Saccharomyces cerevisiae*.** Mol Microbiol. 2002; 43(5):1295-1308.

Padayatty SJ, Katz A, Wang Y, Eck P, Kwon O, Lee JH, Chen S, Corpe C, Dutta A, Dutta SK, Levine M. **"Vitamin C as an antioxidant: evaluation of its role in disease prevention.".** J Am Coll Nutr. 2003; 22(1):18–35.

Pagani A, Villarreal L, Capdevila M, Atrian S. **The *Saccharomyces cerevisiae* Crs5 Metallothionein metal-binding abilities and its role in the response to zinc overload.** Mol Microbiol. 2007a; 63(1):256-269.

Pagani MA, Casamayor A, Serrano R, Atrian S, Ariño J. **Disruption of iron homeostasis in *Saccharomyces cerevisiae* by high zinc levels: a genome-wide study.** Mol Microbiol. 2007b; 65(2):521-537.

Paterson JK, Shukla S, Black CM, Tachiwada T, Garfield S, Wincovitch S, Ernst DN, Agadir A, Li X, Ambudkar SV, Szakacs G, Akiyama S, Gottesman MM. **Human ABCB6 localizes to both the outer mitochondrial membrane and the plasma membrane.** Biochemistry. 2007; 46(33):9443-9452.

Paulsen IT, Sliwinski MK, Nelissen B, Goffeau A, Saier MH Jr. **Unified inventory of established and putative transporters encoded within the complete genome of *Saccharomyces cerevisiae*.** FEBS Lett. 1998; 430(1-2):116-125.

Pearce DA, Sherman F. **Toxicity of copper, cobalt, and nickel salts is dependent on histidine metabolism in the yeast *Saccharomyces cerevisiae*.** J Bacteriol. 1999; 181(16):4774-4779. Erratum in: J Bacteriol. 1999; 181(21):6856.

Petkova MI, Pujol-Carrion N, Arroyo J, García-Cantalejo J, Angeles de la Torre-Ruiz M. **Mtl1 is required to activate general stress response through Tor1 and Ras2 inhibition under conditions of glucose starvation and oxidative stress.** J Biol Chem. 2010; 285(25):19521-19531.

Petris MJ. **The SLC31 (Ctr) copper transporter family.** Pflugers Arch. 2004; 447(5):752-755.

Piao MJ, Kang KA, Lee IK, Kim HS, Kim S, Choi JY, Choi J, Hyun JW. **Silver nanoparticles induce oxidative cell damage in human liver cells through inhibition of reduced glutathione and induction of mitochondria-involved apoptosis.** Toxicol Lett. 2011; 201(1):92-100.

Pócsi I, Prade RA, Penninckx MJ. **Glutathione, altruistic metabolite in fungi.** Adv Microb Physiol. 2004; 49:1-76.

Prévéral S, Ansoborlo E, Mari S, Vavasseur A, Forestier C. **Metal(loid)s and radionuclides cytotoxicity in *Saccharomyces cerevisiae*. Role of *YCF1*, glutathione and effect of buthionine sulfoximine.** Biochimie. 2006; 88(11):1651-1663.

Prévéral S, Gayet L, Moldes C, Hoffmann J, Mounicou S, Gruet A, Reynaud F, Lobinski R, Verbavatz JM, Vavasseur A, Forestier C. **A common highly conserved cadmium detoxification mechanism from bacteria to humans: heavy metal tolerance conferred by the ATP-binding cassette (ABC) transporter SpHMT1 requires glutathione but not metal-chelating phytochelatin peptides.** J Biol Chem. 2009; 284(8):4936-4943.

Qiu JW, Xie ZC, Wang WX. **Effects of calcium on the uptake and elimination of cadmium and zinc in Asiatic clams.** Arch Environ Contam Toxicol. 2005; 48(2):278-287.

Rainbow PS, Black WH. **Cadmium, zinc and the uptake of calcium by two crabs, *Carcinus maenas* and *Eriocheir sinensis*.** Aquat Toxicol. 2005; 72(1-2):45-65.

Ramesh G, Podila GK, Gay G, Marmeisse R, Reddy MS. **Different patterns of regulation for the copper and cadmium metallothioneins of the ectomycorrhizal fungus *Hebeloma cylindrosporum*.** Appl Environ Microbiol. 2009; 75(8):2266-2274.

Reinheckel T, Sitte N, Ullrich O, Kuckelkorn U, Davies KJ, Grune T. **Comparative resistance of the 20S and 26S proteasome to oxidative stress.** Biochem J. 1998; 335 (Pt 3):637-642.

Robillard JM, Gordon GR, Choi HB, Christie BR, Macvicar BA. **Glutathione restores the mechanism of synaptic plasticity in aged mice to that of the adult.** PLoS One. 2011; 6(5):e20676.

Rodríguez-Peña JM, Pérez-Díaz RM, Alvarez S, Bermejo C, García R, Santiago C, Nombela C, Arroyo J. **The 'yeast cell wall chip' - a tool to analyse the regulation of cell wall biogenesis in *Saccharomyces cerevisiae*.** Microbiology. 2005; 151(7):2241-2249.

Roels H, Lauwerys R, Buchet JP, et al. **Epidemiological survey among workers exposed to manganese: effects on lung, central nervous system, and some biological indices.** Am J Ind Med. 1987; 11(3):307-327.

Roess DA, Smith SM, Winter P, Zhou J, Dou P, Baruah B, Trujillo AM, Levinger NE, Yang X, Barisas BG, Crans DC. **Effects of vanadium-containing compounds on membrane lipids and on microdomains used in receptor-mediated signaling.** Chem Biodivers. 2008; 5(8):1558-1570.

Rohde JR, Cardenas ME. **The TOR pathway regulates gene expression by linking nutrient sensing to histone acetylation.** Mol. Cell. Biol. 2003; 23:629-635.

Rosen BP. **Families of arsenic transporters.** Trends Microbiol. 1999; 7(5):207-212.

Rosen BP, Tamás MJ. **Arsenic transport in prokaryotes and eukaryotic microbes.** Adv Exp Med Biol. 2010; 679:47-55.

Ruelas-Inzunza J, Páez-Osuna F, Ruiz-Fernández AC, Zamora-Arellano N. **Health risk associated to dietary intake of mercury in selected coastal areas of Mexico.** Bull Environ Contam Toxicol. 2011; 86(2):180-188.

Ruotolo R, Marchini G, Ottonello S. **Membrane transporters and protein traffic networks differentially affecting metal tolerance: a genomic phenotyping study in yeast.** Genome Biol. 2008; 9(4):R67.

Santangelo GM. **Glucose signaling in *Saccharomyces cerevisiae*.** Microbiol. Mol. Biol. Rev. 2006; 70:253–282.

Saponja JA, Vogel HJ. **Metal-ion binding properties of the transferrins: a vanadium-51 NMR study.** J Inorg Biochem. 1996; 62(4):253-270.

Sarikaya AT, Akman G, Temizkan G. **Nickel resistance in fission yeast associated with the magnesium transport system.** Mol Biotechnol. 2006; 32(2):139-146.

Sasaki T, Yamamoto Y, Ezaki B, Katsuhara M, Ahn SJ, Ryan PR, Delhaize E, Matsumoto H. **A wheat gene encoding an aluminum-activated malate transporter.** Plant J. 2004; 37(5):645-653.

Satarug S, Nishijo M, Lasker JM, Edwards RJ, Moore MR. **Kidney dysfunction and hypertension: role for cadmium, p450 and heme oxygenases?** Tohoku J Exp Med. 2006; 208(3):179-202.

Schauer K, Muller C, Carrière M, Labigne A, Cavazza C, De Reuse H. **The *Helicobacter pylori* GroES cochaperonin HspA functions as a specialized nickel chaperone and sequestration protein through its unique C-terminal extension.** J Bacteriol. 2010; 192(5):1231-1237.

Serero A, Lopes J, Nicolas A, Boiteux S. **Yeast genes involved in cadmium tolerance: Identification of DNA replication as a target of cadmium toxicity.** DNA Repair (Amst). 2008; 7(8):1262-1275.

Shekar SN, Banerjee T, Biswas A. **Hypotheses on the effect of cadmium on glutathione content of red blood corpuscles.** Twin Res Hum Genet. 2006; 9(1):73-75.

Shen R, Ma JF, Kyo M, Iwashita T. **Compartmentation of aluminium in leaves of an Al-accumulator, *Fagopyrum esculentum* Moench.** Planta. 2002; 215(3):394-398.

Schena M, Shalon D, Davis R, Brown P. **Quantitative monitoring of gene expression patterns with a complementary DNA microarray.** Science, 1995; 270(5235):467–470.

Shi H, Hudson LG, Liu KJ. **Oxidative stress and apoptosis in metal ion-induced carcinogenesis.** Free Radic Biol Med. 2004; 37(5):582-593.

Shibasaki T, Ohno I, Ishimoto F, Sakai O. **Characteristics of cadmium-induced nephrotoxicity in syrian hamsters**. Nippon Jinzo GakkaiShi. 1993; 8:913-917.

Shiraishi E, Inouhe M, Joho M, Tohoyama H. **The cadmium-resistant gene, *CAD2*, which is a mutated putative copper-transporter gene (*PCA1*), controls the intracellular cadmium-level in the yeast *S. cerevisiae*.** Curr Genet. 2000; 37(2):79-86.

Shringarpure R, Grune T, Mehlhase J, Davies KJ. **Ubiquitin conjugation is not required for the degradation of oxidized proteins by proteasome.** J Biol Chem. 2003; 278(1):311-318.

Silver S. **Bacterial resistances to toxic metal ions - a review.** Gene. 1996; 179(1):9-19.

Sirover MA, Loeb LA. **Infidelity of DNA synthesis in vitro: screening for potential metal mutagens or carcinogens.** Science. 1976; 194(4272):1434-1436.

Smith A, Ward MP, Garrett S. **Yeast PKA represses Msn2p/ Msn4p-dependent gene expression to regulate growth, stress response and glycogen accumulation.** EMBO J. 1998; 17:3556–3564.

Smith FW, Hawkesford MJ, Prosser IM, Clarkson DT. **Isolation of a cDNA from *Saccharomyces cerevisiae* that encodes a high affinity sulphate transporter at the plasma membrane.** Mol Gen Genet. 1995; 247(6):709-715.

Smith RL, Maguire ME. **Distribution of the CorA Mg^{2+} transport system in gram-negative bacteria.** J Bacteriol. 1995; 177(6):1638-1640.

Soares SS, Gutiérrez-Merino C, Aureliano M. **Mitochondria as a target for decavanadate toxicity in *Sparus aurata* heart.** Aquat Toxicol. 2007; 83(1):1-9.

Soares SS, Henao F, Aureliano M, Gutiérrez-Merino C. **Vanadate induces necrotic death in neonatal rat cardiomyocytes through mitochondrial membrane depolarization.** Chem Res Toxicol. 2008; 21(3):607-618.

Sooksa-Nguan T, Yakubov B, Kozlovskyy VI, Barkume CM, Howe KJ, Thannhauser TW, Rutzke MA, Hart JJ, Kochian LV, Rea PA, Vatamaniuk OK. ***Drosophila* ABC transporter, DmHMT-1, confers tolerance to cadmium. DmHMT-1 and its yeast homolog, SpHMT-1, are not essential for vacuolar phytochelatin sequestration.** J Biol Chem. 2009; 284(1):354-362.

Soulard A, Cremonesi A, Moes S, Schütz F, Jenö P, Hall MN. **The rapamycin-sensitive phosphoproteome reveals that TOR controls protein kinase A toward some but not all substrates.** Mol Biol Cell. 2010; 21(19):3475-3486.

Sparke LS, Gallagher JS. **Galaxies in the Universe (1 ed.).** Cambridge University Press. 2000; p.8.

Stadler JA, Schweyen RJ. **The yeast iron regulon is induced upon cobalt stress and crucial for cobalt tolerance.** J Biol Chem. 2002; 277:39649-39654.

Stathopoulos AM, Cyert MS. **Calcineurin acts through the *CRZ1*/*TCN1*-encoded transcription factor to regulate gene expression in yeast.** Genes Dev. 1997; 11(24):3432-3444.

Stearman R, Yuan DS, Yamaguchi-Iwai Y, Klausner RD, Dancis A. **A permease-oxidase complex involved in high-affinity iron uptake in yeast.** Science. 1996; 271(5255):1552-1557.

Stimpson HE, Lewis MJ, Pelham HR. **Transferrin receptor-like proteins control the degradation of a yeast metal transporter.** EMBO J. 2006; 25(4):662-672.

Stohs SJ, Bagchi D. **Oxidative mechanisms in the toxicity of metal ions.** Free Radic Biol Med. 1995; 18(2):321-336.

Supek F, Supekova L, Nelson H, Nelson N. **A yeast manganese transporter related to the macrophage protein involved in conferring resistance to mycobacteria.** Proc Natl Acad Sci U S A. 1996; 93(10):5105-5110.

Swinnen E, Wanke V, Roosen J, Smets B, Dubouloz F, Pedruzzi I, Cameroni E, De Virgilio C, Winderickx J. **Rim15 and the crossroads of nutrient signalling pathways in *Saccharomyces cerevisiae*.** Cell Div. 2006; 1:3.

Szczypka MS, Wemmie JA, Moye-Rowley WS, Thiele DJ. **A yeast metal resistance protein similar to human cystic fibrosis transmembrane conductance regulator (CFTR) and multidrug resistance-associated protein.** J Biol Chem. 1994; 269(36):22853-22857.

Tamás MJ, Wysocki R. **Mechanisms involved in metalloid transport and tolerance acquisition.** Curr Genet. 2001; 40(1):2-12.

Tan XX, Tang C, Castoldi AF, Manzo L, Costa LG. **Effects of inorganic and organic mercury on intracellular calcium levels in rat T lymphocytes.** J Toxicol Environ Health. 1993; 38(2):159-170.

Tandon SK, Prasad S, Singh S. **Chelation in metal intoxication: influence of cysteine or N-acetyl cysteine on the efficacy of 2,3-dimercaptopropane-1-sulphonate in the treatment of cadmium toxicity.** J Appl Toxicol. 2002; 22(1):67-71.

Tchaikovskaya T, Fraifeld V, Urphanishvili T, Andorfer JH, Davies P, Listowsky I. **Glutathione S-transferase hGSTM3 and ageing-associated neurodegeneration: relationship to Alzheimer's disease.** Mech Ageing Dev. 2005; 126(2):309-315.

Tennstedt P, Peisker D, Böttcher C, Trampczynska A, Clemens S. **Phytochelatin synthesis is essential for the detoxification of excess zinc and contributes significantly to the accumulation of zinc.** Plant Physiol. 2009; 149(2):938-948.

Thilakaraj R, Raghunathan K, Anishetty S, Pennathur G. **In silico identification of putative metal binding motifs.** Bioinformatics. 2007; 23(3):267-271.

Thomas D, Surdin-Kerjan Y. **Metabolism of sulfur amino acids in *Saccharomyces cerevisiae*.** Microbiol Mol Biol Rev. 1997; 61(4):503-32.

Thorpe GW, Fong CS, Alic N, Higgins VJ, Dawes IW. **Cells have distinct mechanisms to maintain protection against different reactive oxygen species: oxidative-stress-response genes.** Proc Natl Acad Sci U S A. 2004;101(17):6564-6569.

Thorsen M, Di Y, Tängemo C, Morillas M, Ahmadpour D, Van der Does C, Wagner A, Johansson E, Boman J, Posas F, Wysocki R, Tamás MJ. **The MAPK Hog1p modulates Fps1p-dependent arsenite uptake and tolerance in yeast.** Mol Biol Cell. 2006; 17(10):4400-4410.

Thorsen M, Lagniel G, Kristiansson E, Junot C, Nerman O, Labarre J, Tamás MJ. **Quantitative transcriptome, proteome, and sulfur metabolite profiling of the *Saccharomyces cerevisiae* response to arsenite.** Physiol Genomics. 2007; 30(1):35-43.

Thorsen M, Perrone GG, Kristiansson E, Traini M, Ye T, Dawes IW, Nerman O, Tamás MJ. **Genetic basis of arsenite and cadmium tolerance in *Saccharomyces cerevisiae*.** BMC Genomics. 2009; 10:105.

Toda T, Cameron S, Sass P, Zoller M, Scott JD, McMullen B, Hurwitz M, Krebs EG, Wigler M. **Cloning and characterization of *BCY1*, a locus encoding a regulatory subunit of the cyclic AMP-dependent protein kinase in *Saccharomyces cerevisiae*.** Mol Cell Biol. 1987; 7(4):1371-1377.

Toh TH, Kayingo G, van der Merwe MJ, Kilian SG, Hallsworth JE, Hohmann S, Prior BA. **Implications of *FPS1* deletion and membrane ergosterol content for glycerol efflux from *Saccharomyces cerevisiae*.** FEMS Yeast Res. 2001; 1(3):205-211.

Tohoyama H, Kadota H, Shiraishi E, Inouhe M, Joho M. **Induction for the expression of yeast metallothionein gene, *CUP1*, by cobalt.** Microbios. 2001; 104(408):99-104.

Tuszyńska S. **Ni^{2+} induces changes in the morphology of vacuoles, mitochondria and microtubules in *Paxillus involutus* cells.** New Phytol. 2006; 169(4):819-828

Urban J, Soulard A, Huber A, Lippman S, Mukhopadhyay D, Deloche O, Wanke V, Anrather D, Ammerer G, Riezman H, Broach JR, De Virgilio C, Hall MN, Loewith R. **Sch9 is a major target of TORC1 in *Saccharomyces cerevisiae*.** Mol Cell. 2007; 26(5):663-674.

Uriu-Adams JY, Keen CL. **Copper, oxidative stress, and human health.** Mol Aspects Med. 2005; 26(4-5):268-298.

Valko M, Morris H, Cronin MT. **Metals, toxicity and oxidative stress.** Curr Med Chem. 2005; 12(10):1161-1208.

Valko M, Rhodes CJ, Moncol J, Izakovic M, Mazur M. **Free radicals, metals and antioxidants in oxidative stress-induced cancer.** Chem Biol Interact. 2006; 160(1):1-40.

Vatamaniuk OK, Bucher EA, Sundaram MV, Rea PA. **CeHMT-1, a putative phytochelatin transporter, is required for cadmium tolerance in *Caenorhabditis elegans*.** J Biol Chem. 2005; 280(25):23684-23690.

Vido K, Spector D, Lagniel G, Lopez S, Toledano MB, Labarre J. **A proteome analysis of the cadmium response in *Saccharomyces cerevisiae*.** J Biol Chem. 2001; 276(11):8469-8474.

Vilella F, Herrero E, Torres J, de la Torre-Ruiz MA. **Pkc1 and the upstream elements of the cell integrity pathway in *Saccharomyces cerevisiae*, Rom2 and Mtl1, are required for cellular responses to oxidative stress.** J Biol Chem. 2005; 280(10):9149-9159.

Vogt BL, Rossman TG. **Effects of arsenite on p53, p21 and cyclin D expression in normal human fibroblasts -- a possible mechanism for arsenite's comutagenicity.** Mutat Res. 2001; 478(1-2):159-168.

Vujcic M, Shroff M, Singh KK. **Genetic determinants of mitochondrial response to arsenic in yeast *Saccharomyces cerevisiae*.** Cancer Res. 2007; 67(20):9740-9749.

Wade JT, Hall DB, Struhl K. **The transcription factor Ifh1 is a key regulator of yeast ribosomal protein genes.** Nature. 2004; 432(7020):1054-1058.

Walsh CT, Distefano MD, Moore MJ, Shewchuk LM, Verdine GL. **Molecular basis of bacterial resistance to organomercurial and inorganic mercuric salts.** FASEB J. 1988; 2(2):124-130.

Wang W, Ballatori N. **Endogenous glutathione conjugates: occurrence and biological functions.** Pharmacol Rev. 1998; 50(3):335-356.

Wang W, Pan J, Zheng K, Chen H, Shao H, Guo Y, Bian H, Han N, Wang J, Zhu M. **Ced-9 inhibits Al-induced programmed cell death and promotes Al tolerance in tobacco.** Biochem Biophys Res Commun. 2009; 383(1):141-145.

Wang X, Yen J, Kaiser P, Huang L. **Regulation of the 26S proteasome complex during oxidative stress.** Sci Signal. 2010; 3(151):ra88.

Wanke V, Cameroni E, Uotila A, Piccolis M, Urban J, Loewith R, De Virgilio C. **Caffeine extends yeast lifespan by targeting TORC1.** Mol Microbiol. 2008; 69(1):277-285.

Ward RJ, Zhang Y, Crichton RR. **Aluminium toxicity and iron homeostasis.** J Inorg Biochem. 2001; 87(1-2):9-14.

Warner JR. **The economics of ribosome biosynthesis in yeast.** Trends Biochem Sci. 1999; 24(11):437-440.

Watanabe Y, Irie K, Matsumoto K. **Yeast *RLM1* encodes a serum response factor-like protein that may function downstream of the Mpk1 (Slt2) mitogen-activated protein kinase pathway.** Mol Cell Biol. 1995; 15(10):5740-5749.

Wedler FC. **Biochemical and nutritional role of manganese: an overview.** In: Klimis-Tavantzis DJ (ed). Manganese in health and disease. Boca Raton: CRC Press, Inc. 1994; 1-37.

Wei M, Fabrizio P, Hu J, Ge H, Cheng C, Li L, Longo VD. **Life span extension by calorie restriction depends on Rim15 and transcription factors downstream of Ras/PKA, Tor, and Sch9.** PLoS Genet. 2008; 4(1):e13.

Wei Y, Zheng XF. **Sch9 partially mediates TORC1 signaling to control ribosomal RNA synthesis.** Cell Cycle. 2009; 8(24):4085-4090.

Weinlich G, Eisendle K, Hassler E, Baltaci M, Fritsch PO, Zelger B. **Metallothionein - overexpression as a highly significant prognostic factor in melanoma: a prospective study on 1270 patients.** Br J Cancer. 2006; 94(6):835-841.

Westwater J, McLaren NF, Dormer UH, Jamieson DJ. **The adaptive response of *Saccharomyces cerevisiae* to mercury exposure.** Yeast. 2002; 19(3):233-239.

Wheeler GL, Trotter EW, Dawes IW, Grant CM. **Coupling of the transcriptional regulation of glutathione biosynthesis to the availability of glutathione and methionine via the Met4 and Yap1 transcription factors.** J Biol Chem. 2003; 278(50):49920-49928.

Winge DR, Nielson KB, Gray WR, Hamer DH. **Yeast metallothionein. Sequence and metal-binding properties.** J Biol Chem. 1985; 260(27):14464-14470.

Wolf MB, Baynes JW. **Cadmium and mercury cause an oxidative stress-induced endothelial dysfunction.** Biometals. 2007; 20(1):73-81.

Wong RH, Kuo CY, Hsu ML, Wang TY, Chang PI, Wu TH, Huang S. **Increased levels of 8-hydroxy-2 -deoxyguanosine attributable to carcinogenic metal exposure among schoolchildren.** Environ Health Perspect. 2005; 113(10):1386-1390.

Wu J, Shao Y, Liu J, Chen G, Ho PC. **The medicinal use of realgar (As(4)S(4)) and its recent development as an anticancer agent.** J Ethnopharmacol. 2011; 135(3):595-602.

Wu LF, Hughes TR, Davierwala AP, Robinson MD, Stoughton R, et al. **Large-scale prediction of *Saccharomyces cerevisiae* gene function using overlapping transcriptional clusters.** Nat Genet. 2002; 31:255-265.

Wullschleger S, Loewith R, Hall MN. **TOR signaling in growth and metabolism.** Cell. 2006; 124(3):471-484.

Wurtmann EJ, Wolin SL. **RNA under attack: cellular handling of RNA damage.** Crit Rev Biochem Mol Biol. 2009; 44(1):34-49.

Wysocki R, Chéry CC, Wawrzycka D, Van Hulle M, Cornelis R, Thevelein JM, Tamás MJ. **The glycerol channel Fps1p mediates the uptake of arsenite and antimonite in *Saccharomyces cerevisiae*.** Mol Microbiol. 2001; 40(6):1391-1401.

Wysocki R, Fortier PK, Maciaszczyk E, Thorsen M, Leduc A, Odhagen A, Owsianik G, Ulaszewski S, Ramotar D, Tamás MJ. **Transcriptional activation of metalloid tolerance genes in *Saccharomyces cerevisiae* requires the AP-1-like proteins Yap1p and Yap8p.** Mol Biol Cell. 2004; 15(5):2049-2060.

Wysocki R and Tamas MJ. **How *Saccharomyces cerevisiae* copes with toxic metals and metalloids.** FEMS Microbiology Reviews, 2010; 34(6):925–951.

Xie J, Fan R, Meng Z. **Protein oxidation and DNA-protein crosslink induced by sulfur dioxide in lungs, livers, and hearts from mice.** Inhal Toxicol. 2007; 19(9):759-765.

Xie Y, Varshavsky A. ***RPN4* is a ligand, substrate, and transcriptional regulator of the 26S proteasome: a negative feedback circuit.** Proc Natl Acad Sci U S A. 2001; 98(6):3056-3061.

Yompakdee C, Ogawa N, Harashima S, Oshima Y. **A putative membrane protein, Pho88p, involved in inorganic phosphate transport in *Saccharomyces cerevisiae*.** Mol Gen Genet. 1996; 251(5):580-590.

Yorifuji T, Kashima S, Tsuda T, Harada M. **What has methylmercury in umbilical cords told us? - Minamata disease.** Sci Total Environ. 2009; 408(2):272-276.

Yoshimoto H, Saltsman K, Gasch AP, Li HX, Ogawa N, Botstein D, Brown PO, Cyert MS. **Genome-wide analysis of gene expression regulated by the calcineurin/Crz1p signaling pathway in *Saccharomyces cerevisiae*.** J Biol Chem. 2002; 277(34):31079-31088.

Yu S, Qin W, Zhuang G, Zhang X, Chen G, Liu W. **Monitoring oxidative stress and DNA damage induced by heavy metals in yeast expressing a redox-sensitive green fluorescent protein.** Curr Microbiol. 2009; 58(5):504-510.

Zeng YB, Zhang DM, Li H, Sun H. **Binding of Ni^{2+} to a histidine- and glutamine-rich protein, Hpn-like.** J Biol Inorg Chem. 2008; 13(7):1121-1131.

Zenk MH. **Heavy metal detoxification in higher plants -- a review.** Gene. 1996; 179(1):21-30.

Zhang A, Shen Y, Gao W, Dong J. **Role of Sch9 in regulating Ras-cAMP signal pathway in *Saccharomyces cerevisiae*.** FEBS Lett. 2011; 585(19):3026-3032.

Zhao G, Arosio P, Chasteen ND. **Iron(II) and hydrogen peroxide detoxification by human H-chain ferritin. An EPR spin-trapping study.** Biochemistry. 2006; 45(10):3429-3436.

Zhao H, Butler E, Rodgers J, Spizzo T, Duesterhoeft S, Eide D. **Regulation of zinc homeostasis in yeast by binding of the *ZAP1* transcriptional activator to zinc-responsive promoter elements.** J Biol Chem. 1998; 273(44):28713-28720.

Zheng K, Pan JW, Ye L, Fu Y, Peng HZ, Wan BY, Gu Q, Bian HW, Han N, Wang JH, Kang B, Pan JH, Shao HH, Wang WZ, Zhu MY. **Programmed cell death-involved aluminum toxicity in yeast alleviated by antiapoptotic members with decreased calcium signals.** Plant Physiol. 2007; 143(1):38-49.

Zlotnik H, Fernandez MP, Bowers B, Cabib E. ***Saccharomyces cerevisiae* mannoproteins form an external cell wall layer that determines wall porosity.** J Bacteriol. 1984; 159(3):1018-1026.

Zoroddu MA, Schinocca L, Kowalik-Jankowska T, Kozlowski H, Salnikow K, Costa M. **Molecular mechanisms in nickel carcinogenesis: modeling Ni(II) binding site in histone H4.** Environ Health Perspect. 2002; 110(5):719-723.

4.2 Supplemental Figures

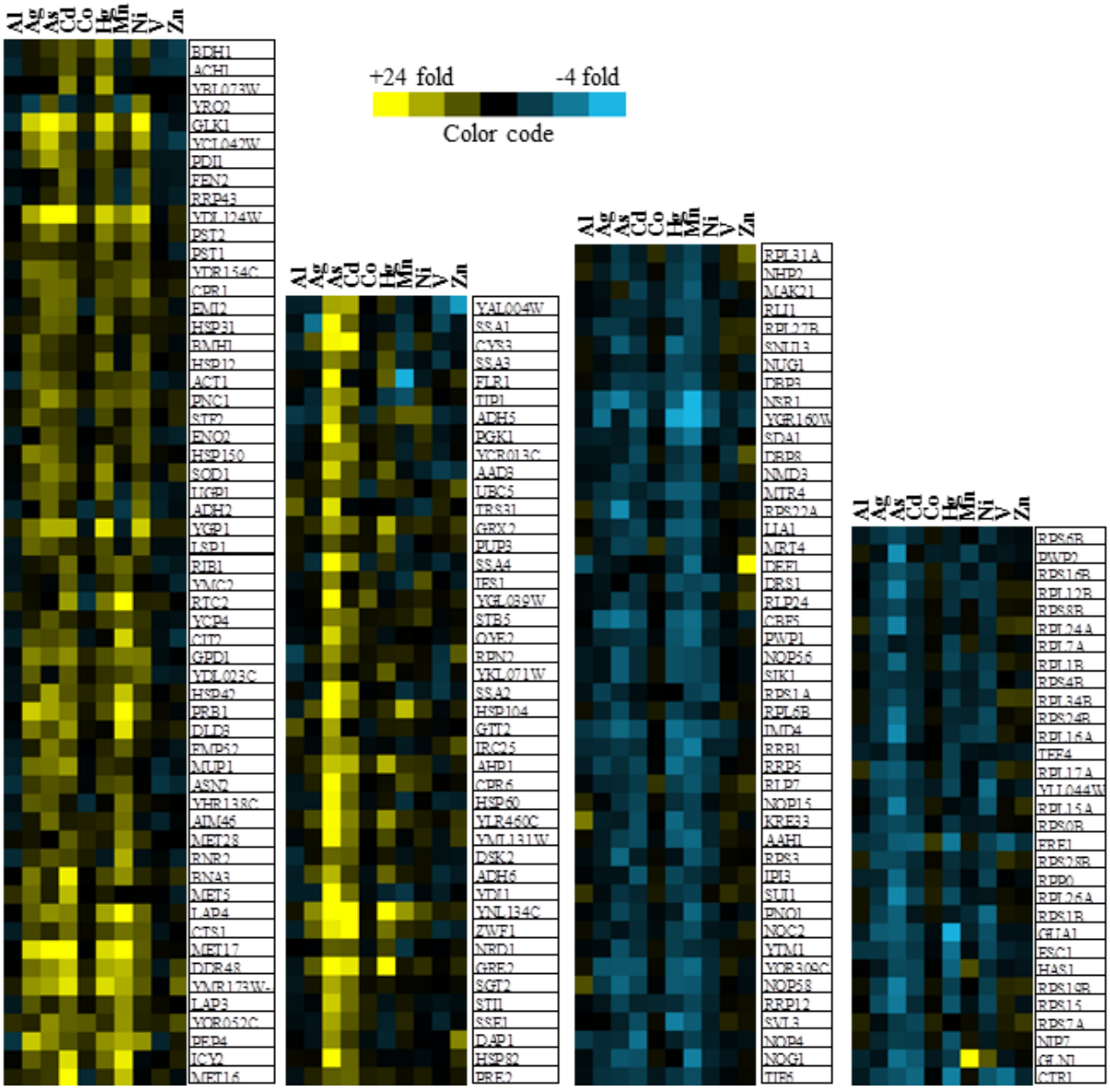

Supplemental Figure 1: Transcript profile of stress response and RP genes upon metal stress. JS018 wild-type cells were treated with 500µM $AlCl_3$, 40µM $AgNO_3$, 200µM $AsCl_3$, 2µM $CdCl_2$, 1,5mM $CoCl_2$, 30µM $HgCl_2$, 1,5mM $MnCl_2$, 1,5mM $NiSO_4$, VCl_3, and $ZnCl_2$ for 30min at 30°C. **A:** stress responsive genes, **B:** RP genes;

A

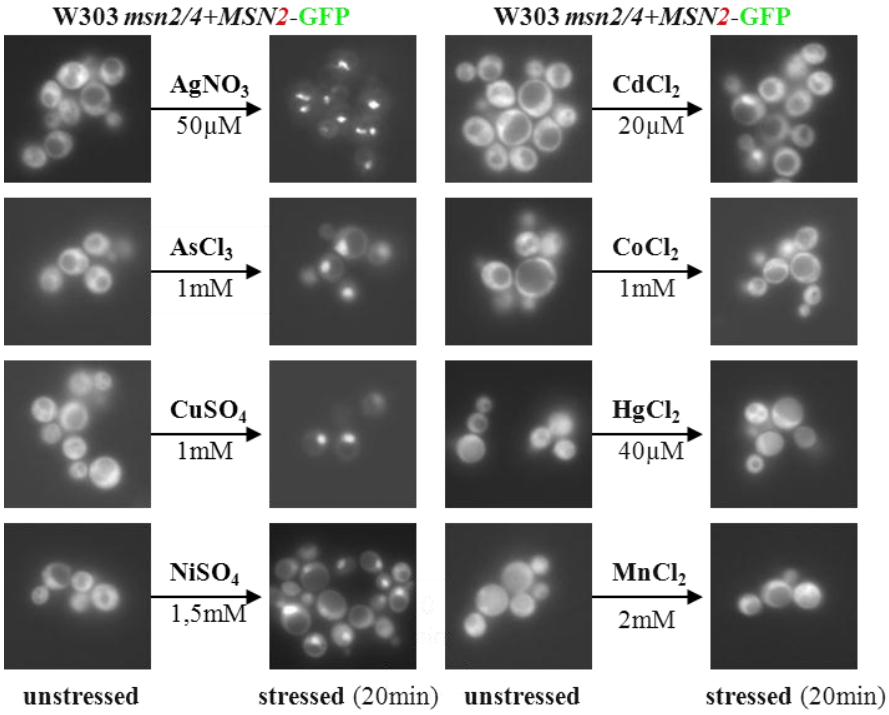

B

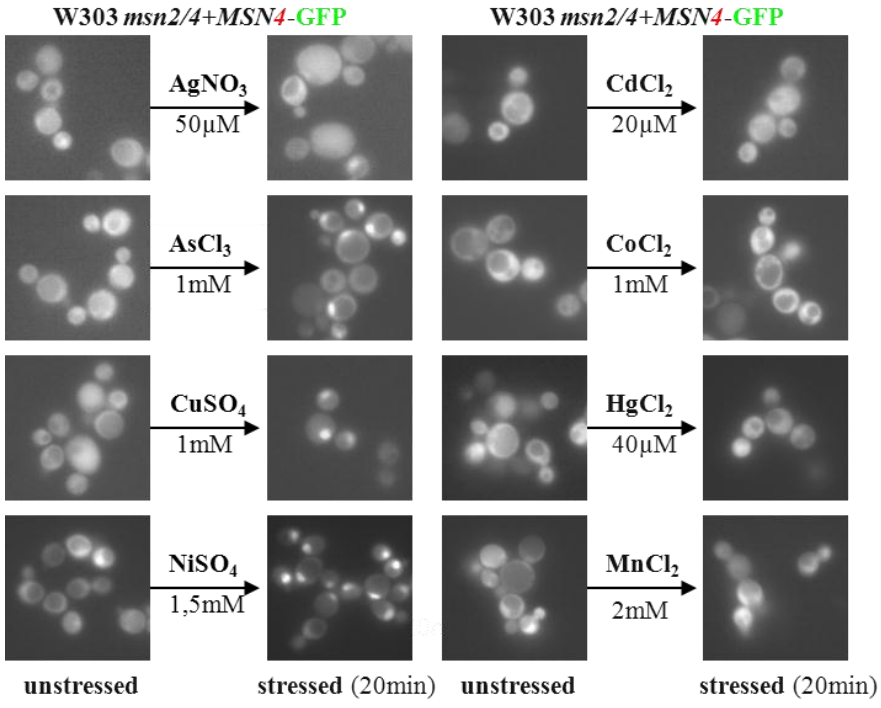

Supplemental Figure 2: Subcellular localization of Msn2p- and Msn4p-GFP upon metal stress. Stressed and unstressed W303 *msn2msn4* cells transformed with pAdh1-*MSN2*-GFP **(A)** and *pADH1-MSN4-GFP* **(B)** were grown logarithmically in synthetic medium and treated with metal ions (concentrations as indicated in the figure) for 20min at 30°C. GFP was visualized in live cells without fixation on prewarmed object slides (30°C). Images were recorded on a Zeiss Axioplan 2 fluorescence microscope with a Quantix CCD camera using Lightview software. Fluorescence microscopy was performed in collaboration with Christoph Schüller.

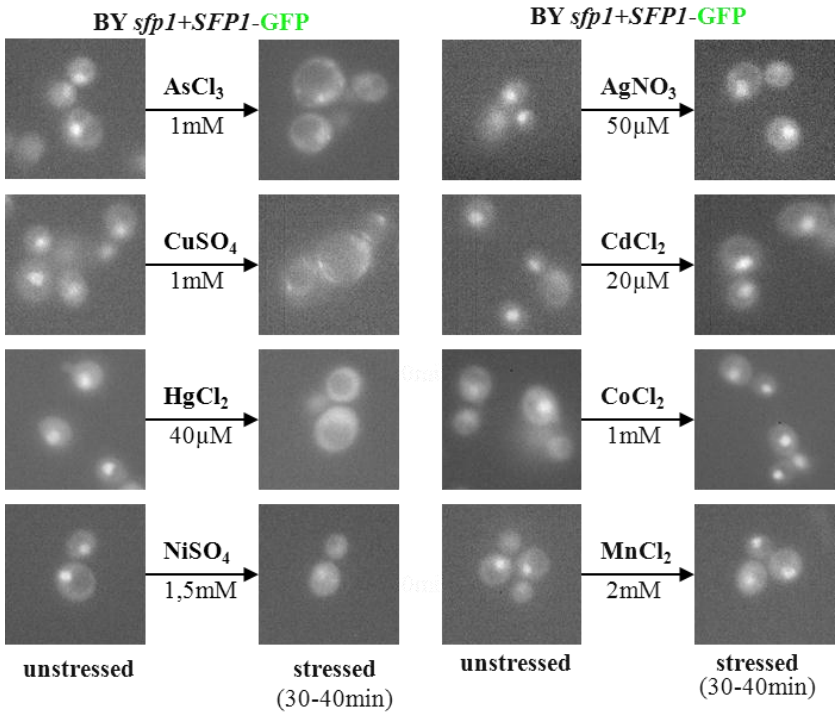

Supplemental Figure 3: Subcellular localization of Sfp1p-GFP upon metal stress. Stressed and unstressed BY *sfp1* cells, producing single C-terminal GFP-tagged proteins expressed from its chromosomal locus under the control of its native promoter (Marion *et al.*, 2004), were grown logarithmically in synthetic medium and treated with metal ions (concentrations as indicated in the figure) for 30-40min at 30°C. GFP was visualized in live cells without fixation, and images were recorded on a Zeiss Axioplan 2 fluorescence microscope with a Quantix CCD camera, using Lightview software. Fluorescence microscopy was performed in collaboration with Christoph Schüller.

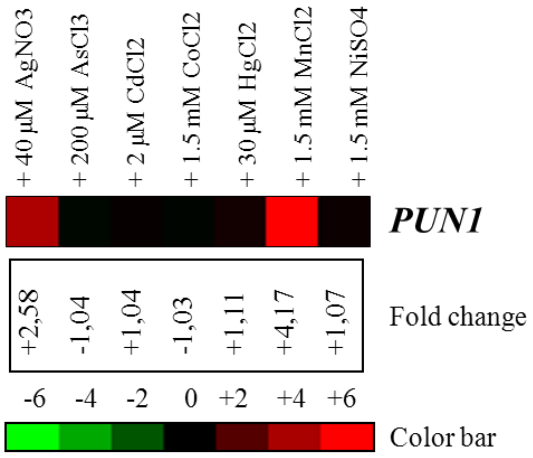

Supplemental Figure 4: Expression profile of *PUN1* upon metal stress. Transcriptional profile representing average inductions over three replicate profiles of FY-1679 grown in standard YPD medium to an OD_{600}~0,8 and stressed with metal ions for 30min;

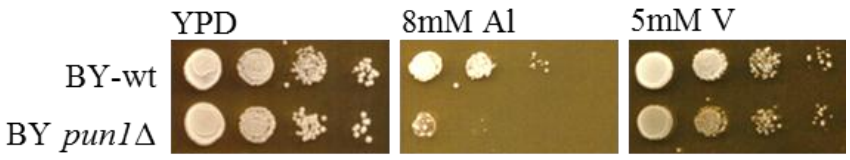

Supplemental Figure 5: Phenotypic profiling. A BY *pun1* deletion strain was tested for growth phenotypes on aluminium- and vanadium-containing medium (metal concentrations as dedicated in the figure). Serial 10-fold dilutions of overnight cultures (BY-wt, BY *pun1*) were spotted onto YPD, with and without metal ions, and plates inspected after 48-62h incubation at 30°C.

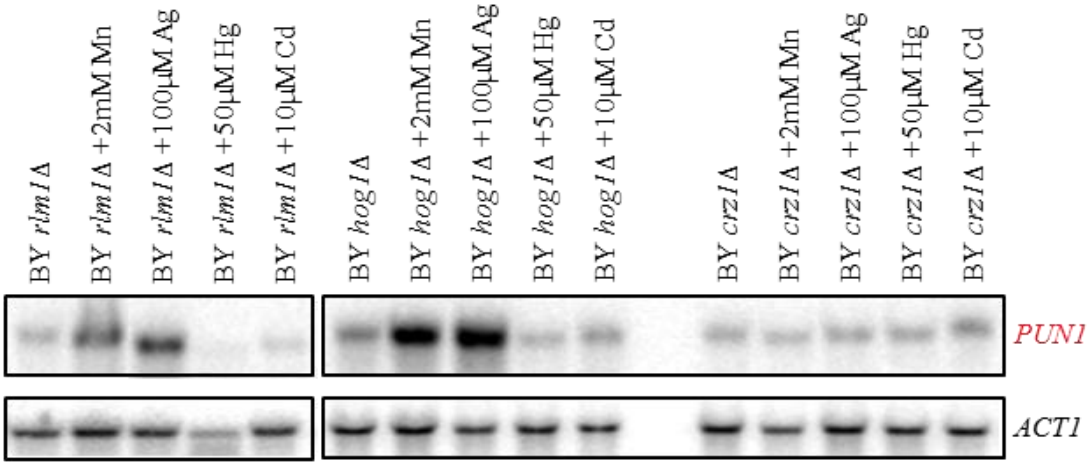

Supplemental Figure 6: Influence of Rlm1, Hog1, and Crz1 on *PUN1* induction under metal stress. Wild-type cells and mutants deleted for *RLM1*, *HOG1*, and *CRZ1* were analysed by Northern blot analysis for metal-induced induction of *PUN1*. For interpretation see text (Discussion).

4.3 Abstract

Metals are an integral part of life and the threatening influence of metal toxicity on organisms is well established today. Although biologically relevant metals operate as cofactors for a variety of enzymatic reactions and play essential structural and functional roles in the cell´s metabolism, they become toxic at higher concentrations. Physiologically non-relevant metals may already produce severe cell damage at very low doses. Over the last decades a considerable amount of studies contributed to new insights into the research of metal toxicity and cellular metal defense strategies. But still little is known about metal sensing and signalling mechanisms or about molecular details of metal defense strategies and their fundamental regulatory associations. To find answers to these issues we investigated the genome-wide transcriptional response of the baker´s yeast, *Saccharomyces cerevisiae*, following the stress conditions of silver, aluminium, arsenic, cadmium, cobalt, mercury, manganese, nickel, vanadium, and zinc.

The aim of this study was in particular to identify new genes and pathways as well as putative common transcriptional regulators participating in the cellular response to metal stress. The results have been partially published and can be summarized as follows: 1) Yeast cells respond highly specific to each metal ion and no common detoxification strategy exists for acute metal stress in principal. 2) The Target Of Rapamycin Complex 1 (TORC1) protein kinase participates in arsenic stress. 3) The transcription factor Stb5 (Yhr178w) plays an important role during the adaption of yeast cells to acute and chronic mercury treatment. 4) The hitherto scarcely characterized plasma membrane protein Pun1 (Ylr414c) participates in the maintenance of cell wall integrity upon manganese exposure.

4.3 Zusammenfassung

Schwermetalle sind ein integraler Bestandteil unseres Lebens. Biologisch relevante Metallionen, die normalerweise wichtige strukturelle und funktionelle Aufgaben im Zellstoffwechsel unzähliger Lebewesen erfüllen, können allerdings in höheren Konzentrationen zu ernsthaften Zellschädigungen führen. Toxische Metalle ohne biologische Funktion schädigen den Organismus bereits in sehr geringen Mengen. Obwohl die Wissenschaft in den letzten Jahrzehnten wichtige Erkenntnisse auf dem Gebiet der Metallforschung gewonnen hat, bleiben nach wie vor noch unzählige Fragen offen, vor allem in Bezug auf zelluläre Metallsensoren und Signaltransduktions Kaskaden als auch hinsichtlich molekularer Details variabler Verteidigungsstrategien gegen toxische Metalle und deren zugrunde liegende regulatorische Mechanismen. Um Antworten auf diese ungelösten Fragen zu erlangen, haben wir Genom-weite transkriptionelle Stressreaktionen der einzelligen eukaryontischen Bäckerhefe, *Saccharomyces cerevisiae*, auf Silber, Aluminium, Arsen, Cadmium, Kobalt, Quecksilber, Mangan, Nickel, Vanadium und Zink mit Hilfe der cDNA Mikrochip Technik untersucht.

Die Zielvorgabe dieser Arbeit war die Entdeckung einzelner Gene beziehungsweise miteinander interagierender Stoffwechselwege und deren Regulationsmechanismen, welche bisher im Zusammenhang mit Metallstress noch nicht beschrieben wurden. Die Datenanalyse ergab zahlreiche interessante Entdeckungen, die teilweise bereits publiziert wurden und wie folgt zusammengefasst werden können: 1) Jedes einzelne Metall ruft eine individuelle Stressantwort in Hefe hervor, und es gibt keine generelle Abwehrstrategie gegen physiologisch zu hohe intrazelluläre Metallkonzentrationen, obwohl bestimmte zelluläre Entgiftungsmechanismen auch gegen mehrere Metalle wirken. 2) Arsenstress inhibiert die hoch konservierte Target Of Rapamycin Complex 1 (TORC1) Protein Kinase. 3) Der Transkriptions Faktor Stb5 spielt während der Adaptierung von Hefezellen an akuten und chronischen Quecksilberstress eine wichtige Rolle. 4) Das bisher nur unzureichend charakterisierte Membranprotein Pun1 ist unter Manganstress an der Aufrechterhaltung der Zellwand Integrität beteiligt.

4.4 Acknowledgements

In the first instance, I have to thank Prof. Rudolf Schweyen for the opportunity of working in his MRS-lab and for sharing with us his passion for science.

I would like to express my gratefulness to Christoph Schüller for assuming supervision for my doctor thesis. I am indebted to Christoph for his helpful scientific as well as writing encouragements.

Special thanks go to the former colleagues Anton Graschopf, Ludmila Zotova, Markus Aleschko, Sona Svidova, Martin Piskacek, Karin Nowikovsky, and Mirjana Iliev, who provided an enjoyable and unstressed working atmosphere with several useful scientific inputs and endless humorous discussions during lunch as well as during and after work.

Finally, my deepest appreciations go to my children, Alina und Anna, who have been my anchor throughout this work, and to Peter for his love and support, particularly during completion of this study.

4.4 Curriculum Vitae

Kontakt Tel: 0650/5250678
mail: dagmar.hosiner@univie.ac.at

Mag. rer. nat. Dagmar Johanna Hosiner

Geburtsdaten	Wien, 26. Oktober 1970
Staatsbürgerschaft	Österreich
Kinder	Alina Hosiner, 18. November 1996 Anna Hosiner, 19. März 2003

Schulbildung

1977-1981	Volksschule, Steinlechnergasse, Wien
1981-1987	Gymnasium des Institutes Sacre Coeur der Erzdiözese Wien, Pressbaum (neusprachlicher Zweig)
1987-1990	Bundesgymnasium, Auf der Schmelz, Wien (naturwissenschaftlicher Zweig)
08.06.1990	Matura

Universität

1990-2004	Immatrikulation als ordentliche Hörerin der Universität Wien, Inskription der Studienrichtung Biologie, nach Bestand der 1. Diplomprüfung Inskription des Studienzweiges Mikrobiologie, Nebenfach Genetik, 1. Teil der 2. Diplomprüfung mit Auszeichnung bestanden
Okt. 2001-Okt. 2005	Diplomarbeit an der Universität Wien, Institut für Mikrobiologie und Genetik bei Prof. Rudolf Schweyen (Titel meiner Diplomarbeit: „Heavy metal response in *Saccharomyces cerevisiae*“)
25. Nov.2005	2. Teil der 2. Diplomprüfung mit Auszeichnung bestanden
Jän. 2006-April 2012	Doktorat-Studium der Naturwissenschaften (Titel meiner Dissertation: „Heavy metal attack: Stress response analyses of *Saccharomyces cerevisiae*”) Universitätsassistentin in Ausbildung an der Universität Wien, Department für Genetik /Mikrobiologie (Projektleitung: o.Univ.- Prof. Dr. Rudolf Schweyen†; in der Folge P.Doz. Dr. Christoph Schüller)

Wissenschaftliche Erfahrungen

Aug. 1993	mikrobiologisches Praktikum am Jakob-Erdheim-Institut für Pathologie und Klinische Bakteriologie des KH Lainz
April 1994-Juli 1996	eigenständige Durchführung einer medizinischen Studie über die statistische Verbreitung und die Eradikation des pathogenen Bakteriums Helicobacter pylori in der Ordination Dr. Gerhard Walcher
April-Mai 2001	immunbiologisches Praktikum in der Firma Intercell bei Dr. Wolfgang Zauner und Dr. Juliane Schalich

Lehrtätigkeit

Feb. 1994-1999	Verfassen und Vertrieb eines Skriptums für die Vorlesung „Genexpression“ am Institut für Mikrobiologie und Genetik unter der Mitwirkung von Prof. Alexander von Gabain
Okt. 2001-Jän. 2002 März 2002-Juni 2002 Okt. 2002-Jän. 2003	Tutorien am Institut für Mikrobiologie und Genetik – experimentelle Genetik I
März 2006 - Dez. 2009	Lehrtätigkeit an der Universität (Dr. Bohrgasse 9)
Dez. 2008 – Dez. 2009	Lehrtätigkeit im Vienna Open Lab (Dialog Gentechnik; Dr. Bohrgasse 3)

Weitere Berufserfahrungen

Jän. 1993-Nov. 1993	Call Centre Agent bei TAS (Telefon-Antwort-Service)
März 1994-Juli1996	Ordinationshilfe und Endoskopie-Assistentin in der Ordination Dr. Gerhard Walcher (Facharzt für Gastroenterologie und Hepatologie)
März 1997-Okt. 1998	Ordinationshilfe in der Ordination Dr. Josef Scholler (Facharzt für Gynäkologie und Geburtshilfe)
März 1996-Sept. 1996 und Nov. 2000-Feb. 2003	Assistenztätigkeit in der Steuerberatungskanzlei S+P (Dr. Gottfried Scholler und Partner)
Sept. 2005-Nov. 2005	Chauffeurin bei der Firma „Ernst Walenda GMBH“

Publikationen

Dez. 2008	Arsenic Toxicity to *Saccharomyces cerevisiae* is a Consequence of Inhibition of the TORC1 Kinase Combined with a Chronic Stress Response
Jän. 2011	Pun1 is a metal ion-inducible, calcineurin/Crz1-regulated plasma membrane protein required for cell wall integrity